Recovery of Dairy Aroma Compounds and Concentration of Dairy Solutions by Membranes

by

Boya Zhang

A thesis
presented to the University of Waterloo
in fulfillment of the
thesis requirement for the degree of
Doctor of Philosophy
in
Chemical Engineering

Waterloo, Ontario, Canada, 2018

Examining Committee Membership

The following served on the Examining Committee for this thesis. The decision of the Examining Committee is by majority vote.

External Examiner	Dr. Huu Dung Doan Professor
Supervisor	Dr. Xianshe Feng Professor
Internal Member	Dr. Eric Croiset Professor
	Dr. Boxin Zhao Associate Professor
Internal-external Member	Dr. Sigrid Peldszus Associate Professor

AUTHOR'S DECLARATION

I hereby declare that I am the sole author of this thesis. This is a true copy of the thesis, including any required final revisions, as accepted by my examiners.

I understand that my thesis may be made electronically available to the public.

Abstract

This study explores the potential of using different types of poly(ether block amide) (PEBA) membranes for recovering aroma compounds from dairy solutions and concentration of dairy products by membrane processes.

The selective recovery of eight aroma compounds from their binary and multicomponent aqueous solutions by pervaporation using PEBA 2533 membrane was studied. This membrane was proved to be effective for recovering not only hydrophobic aroma compounds but also hydrophilic ones, which were not easy to be enriched by other organophilic PV membranes. The effects of feed concentration and temperature on aroma recovery were also investigated. In addition, the coupling effect among aroma species was found to be significant in multicomponent aroma system, even if the aroma concentrations in feed were low.

The performance of PEBA 2533 for recovering aromas by batch pervaporation was evaluated, and the experimental data were analyzed with a batch pervaporation model. The maximum amounts of almost pure aroma compounds obtained in the permeate during the process were predicted. The effects of initial feed amount and membrane area on the recovery of aroma compounds from their aqueous feed solution were also simulated, and a large membrane area and/or a small initial amount of feed solution were found to be favorable to for a good aroma recovery.

Four non-volatile dairy components, that is NaCl, lactose, whey protein and milk fat, were confirmed to influence the recovery of aroma compounds from their aqueous solutions. It was found that the permeation of hydrophobic aroma could be enhanced by the presence of NaCl in the feed, but reduced by the presence of lactose, protein, and fat in the feed.

PEBA 1074 membrane for pervaporative concentration of dairy solutions was investigated by comparing the performance of PEBA 1074 with that of representative ultrafiltration, nanofiltration and reverse osmosis membranes. The PEBA 1074 membrane showed a high water permeance and a low flux decline with time during the operations. A high milk solid retention (almost 100%) was obtained, and the membrane was easily cleaned. The effects of feed solid content and transmembrane pressure on membrane filtrations were revealed using the resistance-in-series model. At a higher feed solid content and transmembrane pressure, the resistance of membrane fouling was higher, which lead to a more rapid flux decline.

Acknowledgements

Firstly, I would like to express my sincere appreciation to my supervisor Dr. Xianshe Feng, for continuously supporting me during this tough journey. On the academic level, Dr. Feng has taught me fundamentals of conducting scientific research in the membrane separation area. Under his supervision, I learned how to define a research problem, find a solution to it, and finally publish the results. He enlightened me the way of being a responsible researcher and critical thinker. On a personal level, Dr. Feng inspired me by his hardworking and passionate attitude. I appreciate all his contributions of time, ideas, and funding to make my Ph.D. experience productive and stimulating.

I would like to thank my committee members of this thesis: Dr. Eric Croiset, Dr. Huu Dung Doan (external), Dr. Sigrid Peldszus and Dr. Boxin Zhao, for their valuable suggestions, insightful questions and encouraging comments on my work.

I am also grateful for my dear colleagues in the Membrane Separation group, who have contributed immensely to my personal and professional time at University of Waterloo: Dr. Yijie Hu, Dr. Ying Zhang, Dr. Dihua Wu, Dr. Shuixiu Lai, Dr. Yifeng Huang, Dr. Miaoqing Liu, Min Guan, Kai Wu, Aoran Gao, Bo Qiu, Jingjing Zhang, Silu Chen, Xiaotong Cao, Xuezhen Wang, Abdullah Albiladi, Elnaz Halakoo, Muhammad Waqas lqbal and Yiran Wang. I appreciate the inspirational discussions and the collaborations we have over the past several years. It is lucky for me to have them in my life as great friends.

I also want to thank my other friends in Canada: Dr. Zhen Zhang, Zhuangqing Yan, Jian Xiong, Dr. Gaopeng Jiang, Dr. Kun Feng, Dr. Zhiyu Mao, Dr. Jing Fu, Dr. Jingde Li, Guihua Liu, and Dr. Ali Ghorbani Kashkooli et al, who always support and help me go through all the ups and downs.

Financial support from China Scholarship Council and Natural Sciences and Engineering Research Council of Canada is deeply acknowledged.

Lastly, I would like to thank my dearest parents, who raised me with a love of science and unconditionally supported me in all my pursuits. I can hardly imagine how my Ph.D. life would be without their love, patience and faithful support. They are the most important people in my world and I dedicate this thesis to them.

Dedication

I would like to dedicate this thesis to my beloved family.

Table of Contents

List of Figures

List of Tables

List of Symbols

P_i	Permeability coefficient, mol.m/(m^2.h.Pa)
D_i	Diffusivity coefficient, m/h
S_i	Solubility coefficient, mol/(m^2.Pa)
J_i	Permeation flux, g/m^2.h or Kg/m^2.h or L/m^2.h
X_i	Mole fraction in feed
Y_i	Mole fraction in permeate
γ_i	Activity coefficient
p_i^{sat}	Saturated vapor pressure, Pa
p^p	Permeate pressure, Pa
l	Membrane thickness, μm
A	Membrane area, m^2
α	Separation factor
β	Enrichment factor
J_0, D_0 and S_0	Preexponential factor
R	Gas constant, 8.314 J/mol. K
T	Temperature, K
E_j	Apparent activation energy, kJ/mol
E_p	Activation energy, kJ/mol
E_D	Activation energy of diffusion, kJ/mol
ΔH_S	Enthalpy change of dissolution, kJ/mol

ΔH_V	Heat of evaporation of the permeant, kJ/mol
C_i	Coupling factor
t	Operating time, h
F	Feed mass amount, g
R_r	Recovery rate of the aroma component, %
S_a	Aroma solubility in water, g aroma/g water
S_w	Water solubility in aroma, g water/g aroma
m_w	Mass of water in organic phase, g
m_o	Mass of aroma compound in water phase, g
FD	Flux decline percentage
R_s	Retention of solids, %
R_{cp}	Resistance of the concentration polarization layer, Pa.s/m
R_m	Membrane resistance, Pa.s/m
R_f	Membrane fouling resistance, Pa.s/m
R_{total}	Total resistance, Pa.s/m
VCR	Volume concentration ratio

Chapter 1

Introduction

1.1 Background

Over the past few decades, a considerably large number of aroma compounds in dairy products have been identified. Parliament and McGorrin (2000) and McGorrin (2001) provided a comprehensive review on the most potent aroma components in milk, cream, butter, cheese and other cultured dairy products. Recently, the recovery of aroma compounds from dairy products has attracted significant attention. During the processing of dairy products, some volatile aroma compounds may be lost due to evaporation or thermal degradation. Even a small loss of the aroma compounds may significantly affect the sensory quality of the products. Nowadays, artificial flavors can no longer satisfy the needs of consumers who are gradually shifting away from artificial flavors, and naturally occurring flavors are becoming increasingly popular. This is especially true for dairy aromas because it is very difficult to produce authentic flavors artificially due to the complex profile of the compounds involved. Thus, the extraction and recovery of aroma compounds from natural sources as flavoring ingredients are of particular interest to the food, pharmaceutical and cosmetic industries.

Traditionally, aroma compounds are concentrated by solvent extraction, distillation, partial condensation, and gas stripping (Baudot and Marin, 1997; Karlsson and Tragardh, 1997). Thermal processes that involve phase changes (e.g. evaporation and condensation) are often unsatisfactory for recovering heat-sensitive aroma compounds even at moderately high temperatures. Solvent extraction, on the other hand, requires the use of extracting agent, which needs to be removed from the extract subsequently. Aroma extraction with liquid solvents is

uncommon for food processing, and supercritical fluids may be used but the process is costly and other undesired components (for example, fat) are often extracted along with the aroma compounds. Gas stripping is generally ineffective for recovery of aromas with low volatilities. Pervaporation, a relatively new separation process, has attracted attention as an alternative to the conventional aroma recovery technologies. Pervaporation separation is a membrane process in which the components in a liquid mixture pass through a membrane selectively to produce a vaporous stream on the downstream side of the membrane, and the permeate vapor can be condensed and collected as a liquid. For aroma compounds recovery from aqueous solutions, organophilic membranes should be used, and the aroma compounds will permeate through the membrane preferentially over water, resulting in an aroma-enriched permeate. Comparing to the traditional aroma compound recovery methods, pervaporation has the following major advantages:

(1) No additives are needed, and thus there is no secondary contamination to the products recovered (which can be regarded as natural products);

(2) It can operate at ambient or moderate temperatures, a feature that is particularly important to prevent thermal degradation of aroma compounds;

(3) Only the permeate, which is a small fraction of the feed, undergoes phase change, and thus the energy consumption of the process is relatively low;

(4) With current organophilic membranes, many hydrophobic aroma compounds can be enriched in the permeate to an extent beyond their solubility limits, and consequently a much higher purity may be achieved in the organic phase upon phase separation of the permeate.

In spite of a great deal of research on pervaporation for aroma recovery, industrial-scale units for this application are still lacking, partially because the sensory profiles of the permeate

have not been well studied and little is known about the long-term membrane performance. Another concern is that if the feed solution contains more than one aroma compound, it is possible for the compounds to interact with each other during pervaporation (Karlsson and Tragardh, 1993; Kedem, 1989). The situation becomes more complex if the feed mixture contains other components apart from aroma compounds and water. For instance, most dairy products contain fat, protein, lactose, and salts. These non-volatile components usually do not pass through pervaporation membranes, but they may nevertheless interact with aroma compounds and affect the pervaporation behavior of aromas. Most researchers use binary aroma-water solutions to study the pervaporation process without any complicating factors, but the permeation performance with real dairy solutions do not always match the results obtained with model feeds (Kanani et al., 2003; Souchon et al., 2002). Therefore, the research on pervaporative recovery of aromas using more complex feed systems is of particular interest.

Concentration of dairy solutions is also a necessary step in producing most dairy products in the industry. It is of particular importance for producing milk powder or protein (or other nutritional components) enriched products, extending product shelf life, and reducing the weight or volume during packaging and transportation. Currently, evaporation, freeze concentration and membrane concentration (especially reverse osmosis) are the three common methods for the removal of water in the dairy industry. However, they have some weaknesses such as high energy consumption, possible degradation of nutritious components (such as proteins and vitamins) and aroma compounds during thermal treatments, and flux decline induced by membrane fouling in membrane processes. Pervaporation could be an alternative to those traditional methods considering its low energy consumption, readily achievable operating conditions and its great anti-fouling property.

Poly(ether block amide) (PEBA) is a family of copolymers, consisting of polyamide hard segments and polyether soft segments in the polymer chains. Because of their bi-phasic microstructures, the copolymers often offer many properties that are not readily available in either constituent polymer alone. PEBA not only has favorable thermal and mechanical stabilities but also good chemical resistance to acid, basic and organic solvents. On the one hand, certain PEBA polymers in general exhibit good permselectivity for high-boiling point aromas (including many dairy aroma compounds), and is also found to be more selective to water-based aroma compounds than poly(dimethyl siloxane) (PDMS) and poly(octhylmethyl siloxane) (POMS). Therefore, a more balanced dairy aroma profile in pervaporation permeate could be produced by using some PEBA membranes. On the other hand, some PEBA membranes may have good water affinity due to its high content of hydrophilic polyamide segments. PEBA 2533 was chosen in this study as a membrane material because it comprises of 80 wt.% poly(tetramethylene oxide) as the rubbery domains. PEBA membranes with a higher polyether content tend to have better organic selectivity (Djebbar et al., 1998). PEBA 1074 was selected to concentrate dairy solutions by removing water from the steam. It contains 55 wt.% polyamide crystalline domains, which accounts for the good hydrophilicity of this membrane.

1.2 Research objectives

The aim of this study was to investigate pervaporation as a method of (1) recovering aroma compounds from dairy solutions and (2) concentrating dairy solutions using PEBA membranes. The specific objectives of this project were:

(1) To determine the effects of operating conditions (i.e., feed aroma concentration and feed temperature) on the pervaporation of each aroma compound in binary aroma-water feed solutions;

(2) To compare the pervaporation behavior of representative aroma compounds in their binary (aroma-water) feed solutions and multicomponent (multiple aromas-water) feed solutions; To identify whether there were coupling interactions between permeating species and the effects of operating conditions (i.e. feed aroma concentration and feed temperature) on the coupling effects;

(3) To monitor the pervaporation behavior of aromas as a function of time during batch pervaporation;

(4) To identify the effects of non-volatile components (e.g., protein, fat, sugar, salts) in feed solutions on pervaporative recovery of dairy aromas;

(5) To investigate the potential of pervaporation for concentrating dairy products by removing water and compare its separation performance with ultrafiltration, nanofiltration and reverse osmosis membrane operations.

1.3 Thesis structure

This thesis consists of seven chapters and they are organized as follows:

Chapter 1 presents the background of this study, including an overview of the research that has been done in the field, and additional work that should be investigated further. The research objectives of this study are also presented.

Chapter 2 provides a literature review. It introduces the aims of aroma recovery and concentration of dairy products, and the recent developments of related technologies. Pervaporation, as a promising alternative to traditional techniques, was thoroughly reviewed.

The mechanism of mass transport, the membranes that can be used in pervaporation for recovering aromas and concentrating dairy products, and some factors that may influence the separation performance have been discussed.

In Chapter 3, the experimental results of pervaporation with binary model aroma-water feed solutions and multicomponent aroma-water feed solutions using PEBA 2533 membrane were presented. The effects of feed aroma concentration and temperature on permeation flux, permeability and enrichment factor were studied. In addition, the competitive permeation relationships among the aroma compounds in the multicomponent system were evaluated.

The recovery of aroma as a function of time in batch pervaporation, using binary aroma-water feed solutions, was studied in Chapter 4. The profiles of permeation fluxes, feed concentrations and accumulated masses of the permeate stream enriched in aroma compounds as a function of operating time were determined calculated based on mathematic models. The influences of initial feed amount and membrane area on the recovery of aromas were also investigated.

Chapter 5 presents the effects of non-volatile components, (e.g., NaCl, lactose, whey protein and milk fat), on the recovery of aroma compounds by pervaporation. The relationship between the hydrophobicity of aromas and the aroma permeation fluxes were determined. The fouling behavior of the PEBA membrane was also studied.

Chapter 6 provides a comparison of the performance of ultrafiltration, nanofiltration, and reverse osmosis with that of pervaporative concentration of dairy products. The permeation flux and solid retention of dairy solutions were determined, and the flux decline due to concentration polarization and membrane fouling was well studied based on resistance-in-series model. The anti-fouling and flux recovery capability of these membranes were evaluated

by cyclic operation of membrane permeation and foulant-cleaning. What's more, the effects of temperature and non-volatile dairy components on the concentration performance of pervaporation were evaluated.

Chapter 7 summarizes the general conclusions and original contributions of this research, and future work for further studies was recommended. Figure 1.1 illustrates the organization of this thesis.

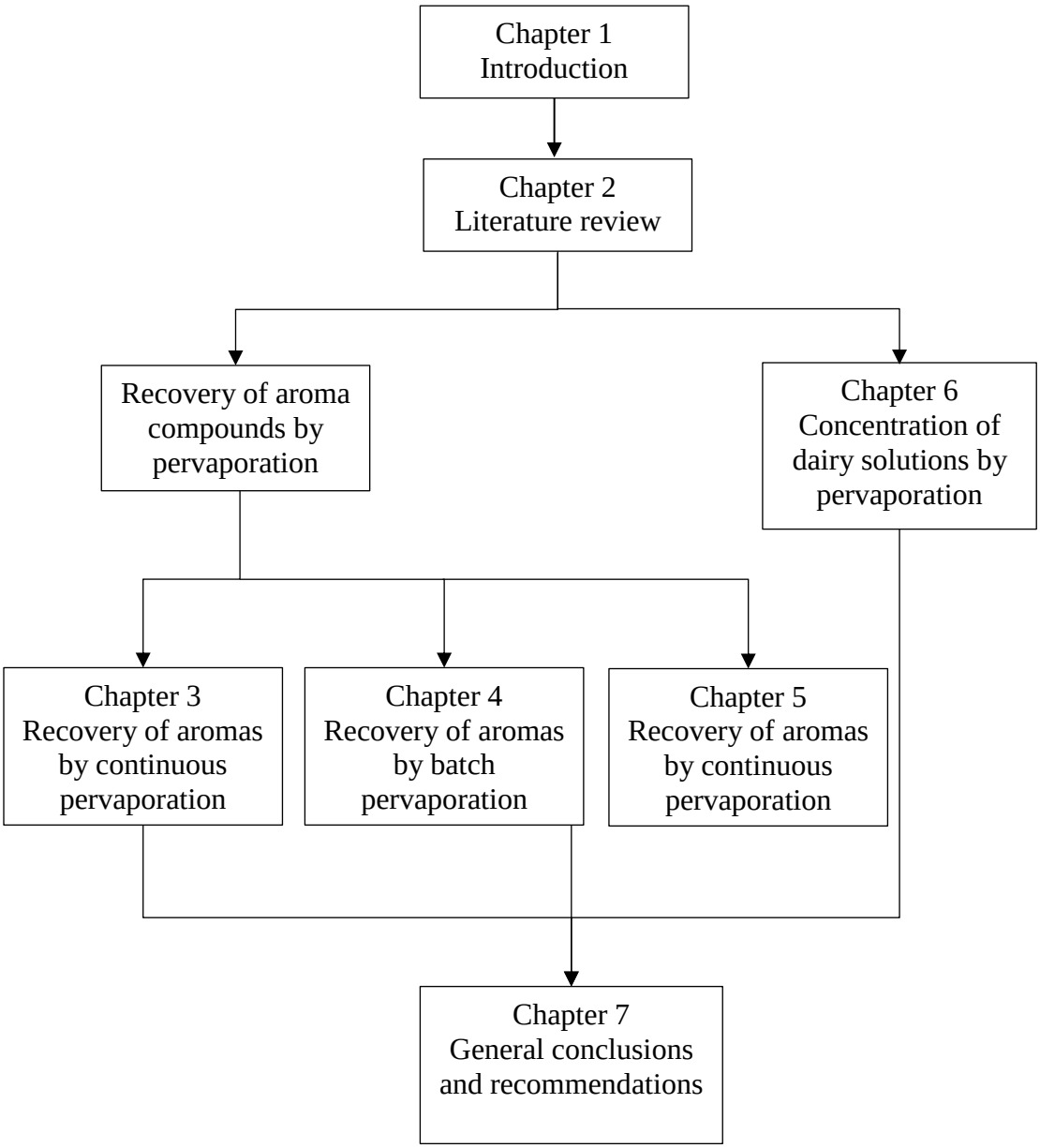

Figure 1.1 Thesis structure in terms of chapters and content relevance

Chapter 2

Literature Review

2.1 Introduction

The recovery of aromas from dairy products and their uses as natural flavors in cosmetic or food industries are attracting more and more attention due to their safe and customer-favorable properties, and there is a significant market out there. However, this area has not been well explored and developed, and development of effective techniques is of great interest from both a research and application standpoints. Dehydration and concentration of dairy compounds is another important step of producing certain dairy products. Traditional methods, such as evaporation or freeze concentration, have been well developed and used for several decades. However, there are some disadvantages with these methods, e.g., high energy consumption, degradation of dairy components, and low efficiency in treating dairy products of high concentration and high viscosity. Therefore, processes that are more energy-efficient, capable of maintaining the integrity of ingredients and feasible to treat dairy products at a high solid content are needed.

Pervaporation, a promising membrane separation method, has gained more and more attention in the areas of organic compound recovery from aqueous solutions and dehydration of organic solvents due to its high selectivity to certain species and low energy consumption. However, research work on pervaporation in treating dairy products is very limited, presumably due to the complex ingredients in dairy and the high viscosity of dairy. In this chapter, an overview of dairy aroma chemistry, aroma recovery techniques, and the methods of concentrating dairy products are presented. The principles of pervaporation and the current status of pervaporation membranes for aroma recovery are reviewed.

2.2 Mass transport mechanism of pervaporation

The usefulness of pervaporation for separation of liquid mixtures was recognized in the mid-1930s (Farber, 1935). However, it was not until the 1980s that the first industrial-scale pervaporation plant was commercialized for dehydration of ethanol when a composite membrane comprising of a thin layer of cross-linked poly(vinyl alcohol) supported on a porous polyacrylonitrile substrate was developed. This remains the primary industrial application of pervaporation today. The first reported work on pervaporation for extraction and concentration of volatile aroma compounds may be attributed to Voilley *et al.* (1990) who investigated the recovery of volatile aroma compounds (1-octene-3-ol and 2,5-dimethylpyrazine) from water, although it was strictly speaking not a pervaporation process because a microporous polypropylene membrane (pore diameter 0.2 μm, porosity 50%) was used and the aroma recovery was really based on air stripping via the microporous membrane. They later used vacuum pervaporation through non-porous PDMS membranes and zeolite-filled PDMS membranes, and the model aromas tested were expanded to include ethyl ethanoate, ethyl butanoate, and ethyl hexanoate (Lamer and Voilley, 1991; Voilley et al., 1989; Voilley et al., 1990). The vacuum pervaporation with nonporous membranes was shown to be more efficient than the membrane-based air stripping process.

Pervaporation is different from other membrane processes in that there is a phase change involved. The permeate leaving the membrane is in a vaporous state. Because of the nonporous structure of the membrane, the permeation flux is generally low. This makes pervaporation useful for certain niche applications where conventional separation processes are ineffective or the permeate products are highly value-added. It is not particularly suitable for circumstances where a high permeate throughput is required. As only a small fraction of the

feed that has permeated through the membrane undergoes a phase change from liquid to vapor, the energy needed for the vaporization of the permeate is generally not a significant issue. From an energy consumption point of view, pervaporation is especially advantageous when the concentration of the preferentially permeating species in the feed is low, which is the case for recovery of aroma compounds from dilute feed solutions and removing water from products with high content of non-water ingredients. In practice, the heat required for the vaporization of permeate during the course of permeation can simply be provided by the feed liquid in the form of sensible heat, and no heat supply directly to the membrane module is needed.

The fundamental knowledge of pervaporation and some critical aspects in pervaporation process on dairy aroma recovery will be covered in the following sections.

In pervaporation, the liquid mixture to be separated (feed) is placed in contact with a membrane and the permeated product (permeate) is removed at a low pressure from the other side. The permeate vapor can be condensed and collected as liquid. Unlike reverse osmosis, mass transport in pervaporation is not limited by the osmotic pressure of the feed, and the driving force for mass transfer through the membrane is provided by lowering the chemical potential of the permeate stream on the downstream side, which is normally achieved by applying a vacuum pump on the permeate side to maintain a permeate vapor pressure lower than the saturated vapor pressure of the feed (Garcia et al., 2008; She and Hwang, 2006a; Trifunovic and Tragardh, 2005). In industrial applications, the vacuum on the permeate side may also be partially generated by condensation of the permeate vapor. Alternatively, the driving force may be created by using a purge gas on the permeate side, and the permeate stream is subjected to an additional processing step (e.g., partial condensation) in order to separate the membrane permeated species from the sweeping gas. Vacuum pervaporation is

the most widely utilized mode of operation, while the purge gas pervaporation is of interest when the permeate can be discharged without condensation (e.g., solvent dehydration with highly water-selective membranes). For pervaporative recovery of aroma compounds and concentration of dairy products, vacuum pervaporation is more appropriate.

Unlike ultrafiltration or microfiltration where the separation is primarily based on size sieving of the permeating species, pervaporation separation is governed by the chemical nature of the macromolecules that form the membrane, the physical structure of the membrane, the physicochemical properties of the components in the feed, and the permeant-permeant and permeant-membrane interactions. This is why aroma compounds, which are bigger molecules than water, may still permeate through an organophilic membrane preferentially to become enriched in the permeate, in spite of their relatively low mobility or diffusivity in the membrane. A good affinity between the membrane and the preferably permeating species is favorable to the separation. In fact, this is the basis of using organophilic membranes for permeating aroma compounds in pervaporative recovery of aroma compounds and using hydrophilic membranes for permeating water in concentrating dairies. However, some components may cause membrane swelling, which tends to make the membrane more permeable to all components in the feed, compromising the selectivity of the membrane. In application point of view, excessive swelling of membrane should be constricted.

The mechanism of mass transport in pervaporation with nonporous membranes can be described by the solution-diffusion model. It was originally proposed by Graham (1866) to describe gas permeation through polymer membranes, and then adopted by Binning *et al.* (Binning et al., 1961) to describe pervaporation transport. According to this mechanism, pervaporative transport through a non-porous membrane consists of three sequential steps:

(1) Sorption of the permeant from the liquid feed to the membrane through the feed/membrane interface;

(2) Diffusion of the sorbed molecules in the membrane;

(3) Desorption of the permeant molecules from the membrane to the vapor phase on the downstream side.

This is shown schematically in Figure 2.1. Both the sorption and desorption steps are generally considered to be very fast and equilibria are established instantaneously on both sides of the membrane. Unlike the sorption step where selective sorption may occur due to specific affinities of the membrane to certain components in the feed (i.e., preferential sorption), the desorption step is non-selective and all permeating molecules are removed from the membrane upon arrival at the downstream side (Fleming, 1990).

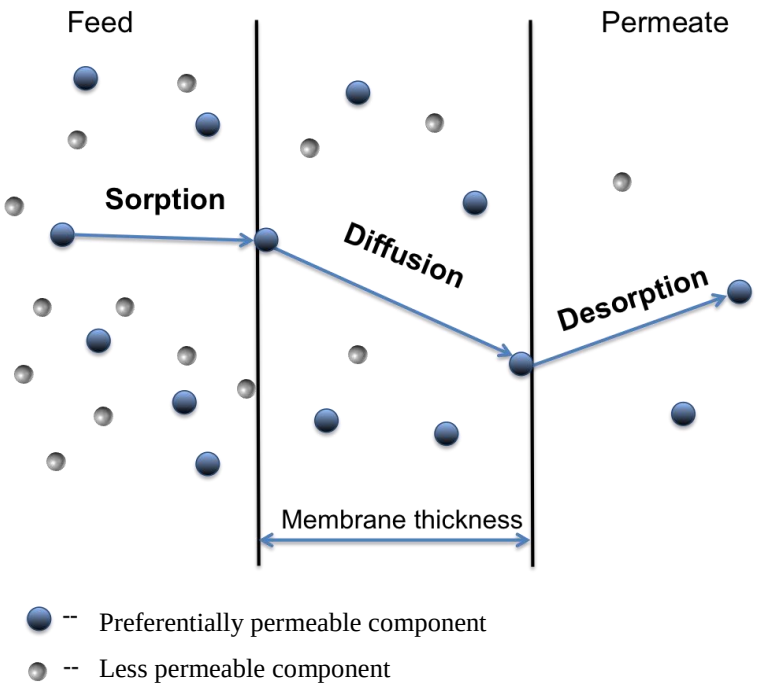

Figure 2.1 Illustration of solution-diffusion model for mass transport in pervaporation.

In general, both solubility and diffusivity of the permeant in the membrane are concentration dependent. A number of mathematical equations for mass transport have been formulated on the basis of Fick's diffusion equation using different empirical correlations of concentration dependence of the solubility and/or diffusivity. However, caution should be exercised in using the equations as they are valid only within the established range for which the relationships for diffusion and thermodynamic equilibrium are applicable. As an approximation, when the solubility and diffusivity coefficients can be treated as constant, the permeability coefficient of the membrane can be related to the solubility and diffusivity coefficients by (Feng and Huang, 1997; Shao and Huang, 2007):

$$P_i = S_i D_i \tag{2.1}$$

where P_i, S_i and D_i are the permeability, solubility and diffusivity coefficients of permeating species i, respectively. The permeability is an intrinsic property of the membrane material in relation to the permeant properties, and it is related to the permeation flux by

$$\left[\frac{P_i}{l}\right] = J_i/(X_i\gamma_i p_i^{sat} - Y_i p^p) \tag{2.2}$$

where p^{sat} and γ are the saturated vapor pressure and activity coefficient of the permeating components in the feed liquid, respectively, p^p is the permeate pressure, l is the effective thickness of the membrane, X and Y are the concentrations of the permeant (in mole fractions) in the feed and permeate, respectively. J is the permeation flux, which is the permeation rate of the permeant per unit membrane area:

$$J_i = N_i/A \tag{2.3}$$

Equation (2.2) is derived for pervaporation in analog to gas permeation through a membrane, assuming an equivalent partial pressure difference ($X_i\gamma_i p_i^{sat} - Y_i p^p$) across the membrane as the driving force for permeation. The quantity (P_i/l), which is the membrane permeability normalized by the membrane thickness, is called permeance of the membrane. It is equal to the permeation flux normalized by the transmembrane driving force. Unlike permeability coefficient P_i, which is a property of the membrane material, the permeance (P_i/l) is a property of the membrane as the membrane thickness comes into play. Thus, the membrane permeance is more relevant for practical applications, especially when asymmetric or composite membranes, whose effective thicknesses are often difficult to determine accurately, are used for increased permeation fluxes.

The permselectivity of a membrane to a pair of permeating species *i* and *j* can be measured by their permeability ratio (or permeance ratio):

$$\alpha_{ij}^0 = \frac{P_i}{P_j} = \frac{[P_i/l]}{[P_j/l]} \tag{2.4}$$

The actual degree of separation can be measured by the separation factor, defined as:

$$\alpha_{ij} = \frac{Y_i/Y_j}{X_i/X_j} \tag{2.5}$$

Obviously, the permeate composition is determined by the relative permeation rates of the permeants, that is, $Y_i = J_i/((J_i + J_j)$ and $Y_j = J_j/((J_i + J_j)$. When the permeate pressure is negligibly low as compared to the vapor pressure on the feed side, the separation factor can be related with the permselectivity by

$$\alpha_{ij} = \alpha_{ij}^0 \times \left(\frac{\gamma_i}{\gamma_j}\right) \times \left(\frac{p_i^{sat}}{p_j^{sat}}\right) \tag{2.6}$$

Equation (2.6) reveals that the separation factor is determined by three parameters. The first parameter (α_{ij}^{0}) is the membrane permselectivity, an intrinsic permeability property of the membrane material. The second parameter (γ_i/γ_j) is the ratio of activity coefficients of permeating species in the feed liquid, which is a thermodynamic property of the feed solution determined by the excess Gibbs energy of the feed liquid. The activity coefficient ratio is affected by the liquid composition and temperature; however, if the feed liquid behaves as an ideal solution (which is uncommon for most pervaporation applications), then the second parameter will become unity. The third parameter (p_i^{sat}/p_j^{sat}) reflects the effect of saturated vapor pressure of pure permeant on the separation performance. Generally speaking, all the three parameters are affected by the operating temperature. Equation (2.6) demonstrates how the membrane, the nature of the permeants, and more explicitly the operating conditions (composition and temperature) affect the separation.

For pervaporative recovery of aroma compounds from aqueous solutions, the extent of the enrichment of aroma compounds in permeate is commonly characterized by an enrichment factor (β). It is simply defined as a ratio of the aroma concentration in the permeate (Y_i) to the aroma concentration in the feed (X_i),

$$\beta = \frac{Y_i}{X_i} \tag{2.7}$$

When the aroma concentration in the feed liquid is considerably low ($X_i \ll 1$) and a high vacuum is applied on the permeate side ($p^p \to 0$), the enrichment factor can be related to the separation factor by

$$\beta = \frac{\alpha}{1 + \alpha X} \tag{2.8}$$

where X is the aroma mol fraction in the feed and α is the separation factor for aroma/water; for convenience their subscripts are removed. Equation (2.8) shows the following features: (1) when the feed aroma concentration X is sufficiently low that $\alpha X \ll 1$, then α and β will be equal numerically, and (2) when the separation factor is sufficiently high that $\alpha X \gg 1$, the enrichment factor will approach an upper limit that is equal to $(1/X)$.

For water removal to concentrate dairy products by pervaporation, the membrane selectivity to water can be characterized by its retention to solid (R_s) dissolved or suspended in the feed solution:

$$R_s = \frac{C_p}{C_f} \tag{2.9}$$

where C_p is the solid content in the permeate, C_f is the solid content in the feed.

In pervaporation, the effect of operating temperature on the separation performance is often measured by temperature dependence of permeation flux, which can usually be described by an Arrhenius type of correlation:

$$J_i = J_{0i} \exp(-\frac{E_{Ji}}{RT}) \tag{2.10}$$

where E_J is the apparent activation energy for permeation of component *i*, J_0 is a preexponential factor, R is the universal gas constant, and T is the temperature. It should be pointed out that the apparent activation energy measures the overall effects of temperature on the permeation flux, which has accounted for the effect of temperature on the driving force. As mentioned above, the activity coefficient and the saturated vapor pressure are affected by temperature as well. The apparent activation energy is not a true representation of the activation energy for

permeation in the membrane. The activation energy E_P that characterizes the temperature effect on the intrinsic permeability of the membrane should be distinguished from the apparent activation energy E_J. As mentioned earlier, the permeability coefficient (P) is a product of the diffusivity (D) and solubility (S) coefficients (Equation 2.1). Both D and S are normally dependent on temperature and their temperature dependencies can be expressed as

$$D_i = D_{0i} \exp\left(-\frac{E_{Di}}{RT}\right) \tag{2.11}$$

$$S_i = S_{0i}\exp(-\frac{\Delta H_{Si}}{RT}) \tag{2.12}$$

where E_D and ΔH_S are the activation energy of diffusion and the enthalpy change of dissolution of the permeant in the membrane, respectively, and D_0 and S_0 are their preexponential factors. As such, the following relation results:

$$P_i = P_{0i}\exp(-\frac{E_{Pi}}{RT}) \tag{2.13}$$

where E_P is the activation energy of permeation, which is a combination of the activation energy of diffusion and the enthalpy change of dissolution of the permeant in the membrane (i.e., $E_P = E_D + \Delta H$), and P_0 is the preexponential factor for the permeability coefficient ($P_0 = D_0 S_0$). Rearranging Equations (2.2) and (2.13),

$$\left[\frac{P_i}{l}\right] = \frac{J_i}{(X_i\gamma_i p_i^{sat} - Y_i p^p)} = \left[\frac{P_{0i}}{l}\right] \exp\left(-\frac{E_{Pi}}{RT}\right) \tag{2.14}$$

Thus, the activation energy E_P can be evaluated from the temperature dependence of membrane permeance $\left[\frac{P_i}{l}\right]$ (which is equal to the permeation flux normalized by the driving force for permeation). Plotting $\ln\left[\frac{P_i}{l}\right]$ vs 1/T will yield a straight line with a slope from which the E_P can

be determined. On the other hand, since the permeate pressure in pervaporation is generally low, the driving force for permeation is largely determined by the equilibrium vapor pressure. As a first approximation, if the saturated vapor pressure (p^{sat}) of a liquid follows the Clausius-Clapeyron equation and the temperature dependence of activity coefficient of the permeant is insignificant, then the activation energy E_P will be equal to the apparent activation energy minus the heat of evaporation of the permeant (Feng and Huang, 1997):

$$E_P = E_J - \Delta H_V \tag{2.15}$$

where ΔH_V is the heat of evaporation of the permeant. Because evaluating the apparent activation energy E_J from the ln$J$ vs 1/T data is much simpler than evaluating the activation energy for permeation E_P from the $\ln\left[\frac{P_i}{l}\right]$ vs 1/T data, especially when the permeate pressure is not accurately known, a simple yet useful approach of estimating E_P is to subtract the heat of evaporation ΔH_V from the apparent activation energy E_J. This also explicitly shows how the enthalpy change due to the phase change in pervaporation influences the permeation behavior.

For pervaporative recovery of aroma compounds, the separation performance is often measured in terms of permeation flux and separation factor (or aroma enrichment factor), which have accounted for the effects of operating conditions (feed composition and temperature) on the separation.

2.3 Dairy aroma compounds

Dairy aroma composition has been studied for decades. A number of volatile compounds are identified as aroma contributors to various dairy products including milk, cultured dairy product, and cheese. This section provides a brief summary of major aroma compounds

associated with raw milk, butter, buttermilk, yogurt, and different types of cheeses. Their key aroma compounds are summarized in Table 2.1.

Milk

The aroma is an important attribute of milk because it impacts consumer preference and acceptance. High-quality fresh milk provides a bland but distinctive aroma with an enjoyable mouth-feel. The bland aroma of milk is attributed to the mixture of multiple aroma compounds at their threshold concentrations (Nursten, 1997). As a beverage, milk is consumed after pasteurization, during which process heat-generated compounds may be formed and can alter the original milk aroma profile. Under mild pasteurization conditions, the aroma of raw milk remains the same. However, high-temperature pasteurization can produce a cooked aroma along with ketone-like taste (Parliment and McGorrin, 2000).

Butter

Butter is produced by isolating butter fat from cream or milk. Fresh sweet cream is the major source of butter production in the USA (Parliment and McGorrin, 2000). Fresh sweet cream butter has similar characteristic to milk fat, which is preferable, and lacks cultured aroma. Diacetyl, δ-decalactone, butyric acid, and C_{10}-C_{12} lactones are important contributors to butter aroma (Nursten, 1997). Major aroma constituents of heated butter come from lactones, unsaturated aldehydes and ketones (Parliment and McGorrin, 2000).

Buttermilk

Buttermilk is produced by lactic acid bacteria based fermentation of skim milk or whole milk, or as a byproduct of butter manufacture. The aroma of fresh sweet cream buttermilk is sweet and buttery. In contrast to fresh buttermilk, stored buttermilk has (E,Z)-2,6-nonadienol

as the major aroma contributor along with increased potency in other aromas already known in fresh butter milk (Nursten, 1997).

Yogurt

Yogurt aroma is characterized as delicate and not intense. The preparation of yogurt involves culturing of *Streptococcus thermophiles* and *Lactobacillus bulgaricus* in milk. Its aroma is attributed to both the existing volatile compounds in milk and consequent metabolites produced by lactic acid bacteria (Routray and Mishra, 2011). Numerous aroma compounds are found in yogurt. It was reported that the carbonyl compounds (including ethyl butanoate, ethyl hexanoate, diacetyl, acetone, and 2-heptanoate) are mainly responsible for preferable aroma flavors in yogurt (Cheng, 2010).

Cheese

The consumption of cheese can date back to the beginning of human history. Nowadays, it has been estimated that thousands of cheese types are available all over the world. The aroma of cheese comes from the interaction of inoculating bacteria, enzymes from milk and rennet, associating lipases, and the secondary flora. The starting culture, processing of the cheese, and the secondary flora define the cheese variety (Urbach, 1997).

Camembert cheese, a type of French cheese, is characterized with soft and buttery texture and a salty butter taste. Its major aroma contributors include 2,3-butanedoine, 3-methylbutanol, methional, 1-octen-3-one, 1-octen-3-ol, 2-undecanone, δ-decalactone, butyric, and hexanoic acids (McGorrin, 2001).

Goat cheese is often recognized with a strong typical aroma, which comes from the lipid fraction. An analysis of the aroma compounds in goat cheese showed that the potent aroma

flavors are branched fatty acids, while butanoic, hexanoic, octanoic, nonanoic, and decanoic acids are less abundant (Urbach, 1997).

Cheddar cheese tastes sweet, buttery, and walnut-like. In its aroma composition, the most potent volatile compounds are 2-butanone, 2,3-butanedione, ethyl butanoate, and 3-hydroxy-2-butanone (Parliment and McGorrin, 2000). It was found that lipid derived aldehydes, methyl ketones, and esters are the major aroma bearers.

Table 2.1 Key aroma compounds in dairy products.

Dairy Product	Compounds	Ref.
Milk		
Raw milk	Ethyl hexanoate, ethyl butyrate, dimethylsulfone, nonanal, 1-octen-3-ol, indole, 2-butanone, 2-hexanone, 2-pentanone, Hexanal, methyldisulphide	(Parliment and McGorrin, 2000; Toso et al., 2002)
Pasteurized milk	Dimethyl sulfone, hexanal, nonanal, 1-octen-3-ol, indole	(Parliment and McGorrin, 2000)
Butter		
Fresh sweet cream butter	δ-Decalactone, 1-hexen-3-one, δ-dodecalactone, 1-octen-3-one, skatole (3-me indole), (Z)-6-dodeceno-γ-lactone	(Nursten, 1997; Parliment and McGorrin, 2000)
Heated butter	δ-Decalactone, skatole, methional, δ-dodecalactone, furaneol, 1-octen-3-one, 1-hexen-3-one, *cis*-2-nonenal, *trans*, *trans*-2,4-decadienal, *trans*-4,5-epoxy-*trans*-2-decenal, γ-octalactone	(Nursten, 1997; Parliment and McGorrin, 2000)
Buttermilk		
Fresh sweet cream buttermilk	γ-Decalactone, δ-decalactone, δ-octalactone, γ-octalactone, vanillin, 2,3-butanedione	(Nursten, 1997)
Stored sour cream buttermilk	δ-Decalactone, (*E*,*Z*)-2,6-nonadienol, 4,5-epoxy-(*E*)-2-decenal. 3-methyl indole, vanillin, γ-octalactone, γ-nonalactone, (*E*)-2-undecenal, methional	(Parliment and McGorrin, 2000)
Yogurt	Acetaldehyde, acetone, 2-butanone, diacetyl, hexanal, acetoin, heptanal, nonanal, 2-heptanone, ethyl butanoate, ethyl hexanoate, hexanoic acid, ethanol, 1-pentanol, ethyl acetate, acetic acid	(Cheng, 2010; Parliment and McGorrin, 2000; Routray and Mishra, 2011)
Cheese		
Camembert cheese	3-Methylbutanal, methional, 2-undecanone, 2,3-butanedione, 2-heptanol, 2-nonanol	(McGorrin, 2001)
Goat cheese	Methional, 4-ehyl octanoic acid, 3-methyl butanoic acid, phenylethanol, nonanoic acid,	(Urbach, 1997)
Cheddar cheese	Methional, 3-methylbutanal, 1-octen-3-one, butanoic acid, ethyl butyrate, hexanoic acid, 5-ethyl-4-hydroxy-2-methyl-2 *H*-furan-3-one, diacetyl	(Parliment and McGorrin, 2000)

2.4 Traditional methods of aroma compounds recovery

During industrial processing of dairy products, a large number of aroma compounds may be lost through evaporation or degradation due to the high operating temperature used. Heat treatment, however, is inevitable since raw milk has to be pasteurized before it is used to produce other dairy products. The changes in the aroma composition are in many cases unwanted. In order to minimize or avoid such changes and losses, many techniques are applied in industry or in lab scale. The following are four most commonly used methods.

2.4.1 Distillation or evaporation

Distillation or evaporation is a dominant aroma recovery method in food industry. Feed components can be separated based on their relative volatilities. If one component is much more volatile than the others, then the volatile component will be easily separated using distillation (Karlsson and Tragardh, 1997). In other words, good candidates for aroma recovery by distillation are food products in which all the important aroma compounds are more volatile than water, and have similar volatiles to each other. However, dairy products have a very complex aroma compound profile. Some important aroma compounds, such as acetic acid (Thujssen, 1970), are similar to or less volatile than water, so it is hard to recover them from water by distillation only.

Distillation has the advantage of being a well-established and well-understood technique. Its major limitations are thermal damage and high energy consumption. In the food industry, high temperatures may damage aromas. The thermal damage can be avoided by carrying out distillation or evaporation at a reduced pressure, which enables the mixture to boil at a lower

temperature, typically in the range 40-100 °C (Karlsson and Tragardh, 1997). High energy input is needed in thermal process in order to provide the latent heat of evaporation.

2.4.2 Gas stripping

Gas stripping involves contacting an aroma feed liquid with an inert gas (e.g., nitrogen or air), so that the volatile aroma compounds are transferred from the liquid feed to the gas phase. Therefore, gas stripping is often effective only for aroma compounds with high volatilities. In gas stripping, a good contact between the liquid and the gas is needed, and the process may be carried out in a packed tower, batch sparged aerator or bubble column (Ribeiro Jr et al., 2004). The gas stripping should be followed by a condenser working at low temperatures in order to collect the aroma vapors from the inert gas (Karlsson and Tragardh, 1997). In practice, however, it is difficult to operate condensers at very low temperatures necessary to condense all the aromas, especially if the partial pressures of the aromas in the gas strip are low. In such a case, a wet scrubber may be used for treatment of the vent gases (Karlsson and Tragardh, 1997).

Gas stripping as an traditional recovery method is often used in industry along with distillation or partial condensation (Karlsson and Tragardh, 1997). Recently, some new processes combining gas stripping and other recovery methods were studied. For example, Ribeiro Jr. *et al*. (Ribeiro Jr et al., 2004) applied gas stripping in a bubble column to extract esters, and then concentrated the aromas by vapor permeation using a PDMS membrane. In their tests, a multi-stage condensation system comprising of four traps in series was employed to collect the permeate, and a recovery rate as high as 98% was observed.

2.4.3 Solvent extraction

Conventional extraction with organic solvents has been widely used to recover aroma compounds from natural sources. Organic solvent extraction is advantageous over distillation when a water-free aroma extract is needed (Schultz and Randall, 1970). However, this method has such drawbacks as low selectivity, high energy costs, and possible residue of organic solvent in the product when the boiling point of the solvent is close to that of aroma compound (Schultz and Randall, 1970). Therefore, this method is not commonly used in food processing (Karlsson and Tragardh, 1997).

An alternative to traditional solvent extraction is membrane-based solvent extraction, which couples solvent extraction with a membrane contactor where the membrane acts as an interface between the feed and the solvent. Compared to conventional solvent extraction, the membrane contactors have many advantages. The density difference between solvent and aroma feed is no longer necessary, which leads to a greater choice of solvents. The process is easy to operate, and no agitation and mixing are needed. However, there is a drawback when using a membrane because it creates additional resistance that hinders diffusion from one phase to another, thus slowing down the separation (Pierre et al., 2001). Using hollow fiber modules can help overcome this problem by offering large surface area per volume (Bocquet et al., 2006).

2.5 Pervaporation as a promising alternative technique for recovery of dairy aromas

The separation performance of pervaporation for aroma recovery depends on the following factors: the nature (chemical structure and physicochemical properties) of the aroma compounds, the properties (material and morphology) of the membrane, the feed composition

and other operating conditions, which will be discussed later. Most of the work reported in the literature deals with dilute aqueous solutions containing model aroma compounds, mainly binary water-organic mixtures and, to a lesser extent, dilute aqueous solutions of multiple dairy aroma components. When multiple aroma compounds are present in the feed, the permeation of one aroma compound may be affected by the presence of the other aromas due to the coupling effects among the permeating species caused by the permeant-permeant interactions. However, this effect is often negligible in highly diluted solutions (Peng and Liu, 2003; She and Hwang, 2006b; Shepherd et al., 2002). Almost all the aroma compounds have bigger molecular sizes than water, and the diffusivity aspect involved in pervaporation is unfavorable to the enrichment of aroma compounds on the permeate side. Thus, the membrane needs to have a good affinity to the aroma compounds in order to compensate for the unfavorable diffusivity selectivity. In other words, the solubility aspect involved in pervaporation should be exploited to achieve the desired separation. As such, organophilic membranes are appropriate for pervaporative recovery of the aroma compounds from aqueous solutions.

2.5.1 Aroma compounds recovery by pervaporation in lab-scale

Among the thousands of dairy aroma compounds identified, over 30 aroma compounds have been used for research on pervaporative recovery. They are listed in Table 2.2, along with their sensory attributes and boiling points. In general, all aroma compounds present in dairy products are at very low concentrations, and the sensory aroma of a product is given by a combination of the odors from all the compounds. It may be pointed out that the aroma composition can be different, depending on the feedstock of the animal, grazing or silage, and the processing and storage conditions of the products as well. Real dairy solutions often contain more than one aroma compounds, and their concentration profile determines their overall

smells and tastes. In addition, proteins, fats and sugars are present in dairy products, and these substances may potentially affect the separation performance due to the interaction between the substances and aroma compounds. Thus, model feed solutions containing single or multiple aroma compounds are extensively used in pervaporation research.

Based on a literature survey, the top 10 most widely used aroma compounds in pervaporation research are presented in Figure 2.2. Three ester compounds (i.e., ethyl acetate, ethyl butanoate and ethyl hexanoate) are on the top of the list, which is not surprising because they are also common aromas in fruit and vegetable juices. This does not mean the esters are more dominant than other aromas in dairy products. To get a general idea about the magnitude of enrichment factor that can be achieved by pervaporation, the range of selectivity for pervaporative recovery of some dairy aroma compounds with current membranes are presented in Figure 2.3 (Bai et al., 2008, 2007; Baudot et al., 1999; Baudot and Marin, 1999; Baudot and Matin, 1996; Boddeker et al., 1997; Bowen et al., 2003; Djebbar et al., 1998; Dong et al., 2012; Huang et al., 2002; Isci et al., 2006; Jiraratananon et al., 2002; Kanani et al., 2003; Kujawa et al., 2015; Lamer et al., 1994; Li et al., 2015; Martinez et al., 2011; Mishima and Nakagawa, 2002; Mohammadi et al., 2008; Nguyen et al., 2000; Overington et al., 2008; Pereira et al., 2005, 2002; Raisi and Aroujalian, 2011; Rajagopalan et al., 1994; Rossi et al., 2017; Sampranpiboon et al., 2000a, 2000b; Schafer et al., 2004; She and Hwang, 2006b; Shepherd et al., 2002; Slater, 1997; Song et al., 2004; Song and Lee, 2005; Tanaka et al., 2010; Tian and Jiang, 2008; Wu et al., 2012, 2011; Zhu et al., 2005; Zou et al., 2018). A general rule of thumb is that aroma compounds with higher hydrophobicity tend to be separated more effectively by pervaporation using organophilic membrane (Baudot and Marin, 1997).

Table 2.2 Dairy aroma compounds studied for pervaporative recovery

Aroma compounds	Formula	Odor	Molecular weight (g/mol)	Boiling point (°C)
Esters				
Methyl acetate	$C_3H_6O_2$	Fragrant	74	57
Ethyl acetate	$C_4H_8O_2$	Sweet	88	77
Ethyl propionate	$C_5H_{10}O_2$	Pineapple-like	102	99
Ethyl butanoate	$C_6H_{12}O_2$	Pineapple-like	116	120
Ethyl hexanoate	$C_8H_{16}O_2$	Pineapple-like	144	228
Ethyl octanoate	$C_{10}H_{20}O_3$	Fruity	172	207
Propyl acetate	$C_5H_{10}O_2$	Fruity, pear-like	102	102
Butyl acetate	$C_6H_{12}O_2$	Banana/apple-like	116	127
Ketones				
2-Heptanone	$C_7H_{14}O$	Banana-like	114	151
2-Nonanone	$C_9H_{18}O$	Fruity	142	192
Diacetyl	$C_4H_6O_2$	Buttery	86	88
2-Butanone	C_4H_8O	Butterscotch-like	72	80
3-Octanone	$C_8H_{16}O$	Grassy	128	167
Acids				
Acetic acid	$C_2H_4O_2$	Sour, pungent	60	118
Butanoic acid	$C_4H_8O_2$	Obnoxious	88	164
Hexanoic acid	$C_6H_{12}O_2$	Goaty	116	206
Octanoic acid	$C_8H_{16}O_2$	Irritating	144	240
Propionic acid	$C_3H_6O_2$	Slightly rancid	74	141
Heptanoic acid	$C_7H_{14}O_2$	Rancid	130	223
Alcohols				
1-Octen-3-ol	$C_8H_{16}O$	Mushroom-like	128	84
1-hexanol	$C_6H_{14}O$	Acoholic	102	155
Aldehydes				
Hexanal	$C_6H_{12}O$	Green	100	130
Phenylacetaldehyde	C_8H_8O	Sweet, rose	120	195
Acetaldehyde	C_2H_4O	Etherial	44	20
3-Methylbutanal	$C_5H_{10}O$	Green, malty	86	91
Pentanal	$C_5H_{10}O$	Pungent	86	102
Heptanal	$C_7H_{14}O$	Obnoxious	114	153
Lactones				
γ-Decalactone	$C_{10}H_{18}O_2$	Coconut-like	170	281
Sulfur compounds				
Dimethyl trisulfide	$C_2H_6S_3$	Sulfury	126	65
Methyl thiobutanoate	$C_5H_{10}OS$	Cheese-like	118	142
Aromatic compounds				
Vanillin	$C_8H_8O_3$	Vanilla	152	285

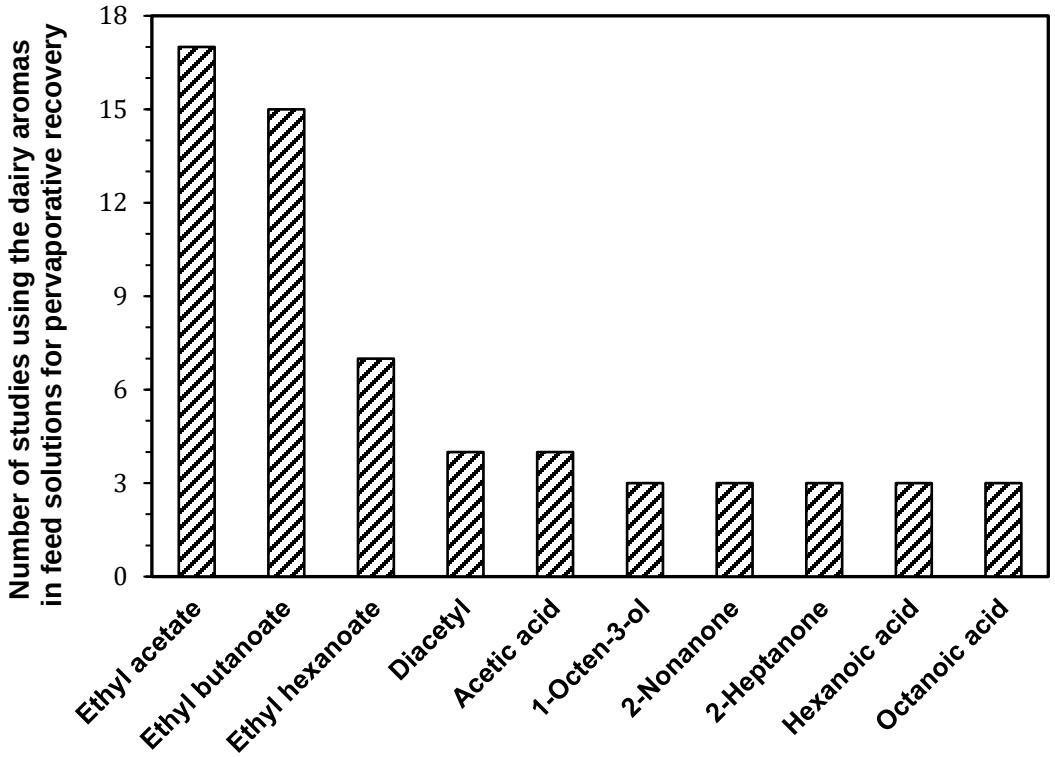

Figure 2.2 Dairy aroma compounds most widely used as model compounds in pervaporative recovery.

Ester aromas are a typical group of hydrophobic aroma molecules with relatively small molecular sizes. They are normally fruity-flavored. As shown in Figure 2.3, the membranes generally have a higher selectivity to the ester molecules than other aroma compounds. Among all the ester aromas shown, ethyl hexanoate is best concentrated by pervaporation with an enrichment factor in the range of 112-8,200, depending on the membranes used (Pereira et al., 2005; Sampranpiboon et al., 2000a). The broad range of selectivity is a result of the different membrane types and structures and different operating conditions used in the pervaporation processes. Hydrophobic alcohols (e.g., 1-octen-3-ol (Pereira et al., 2005)), aldehydes (e.g., acetaldehyde (Wu et al., 2012) and 3-methylbutanal (Kanani et al., 2003; Raisi and Aroujalian, 2011)) and ketones (e.g., 2-heptanone (Overington et al., 2008)) and diacetyl (Rajagopalan et al., 1994)) also have good selectivities in pervaporation.

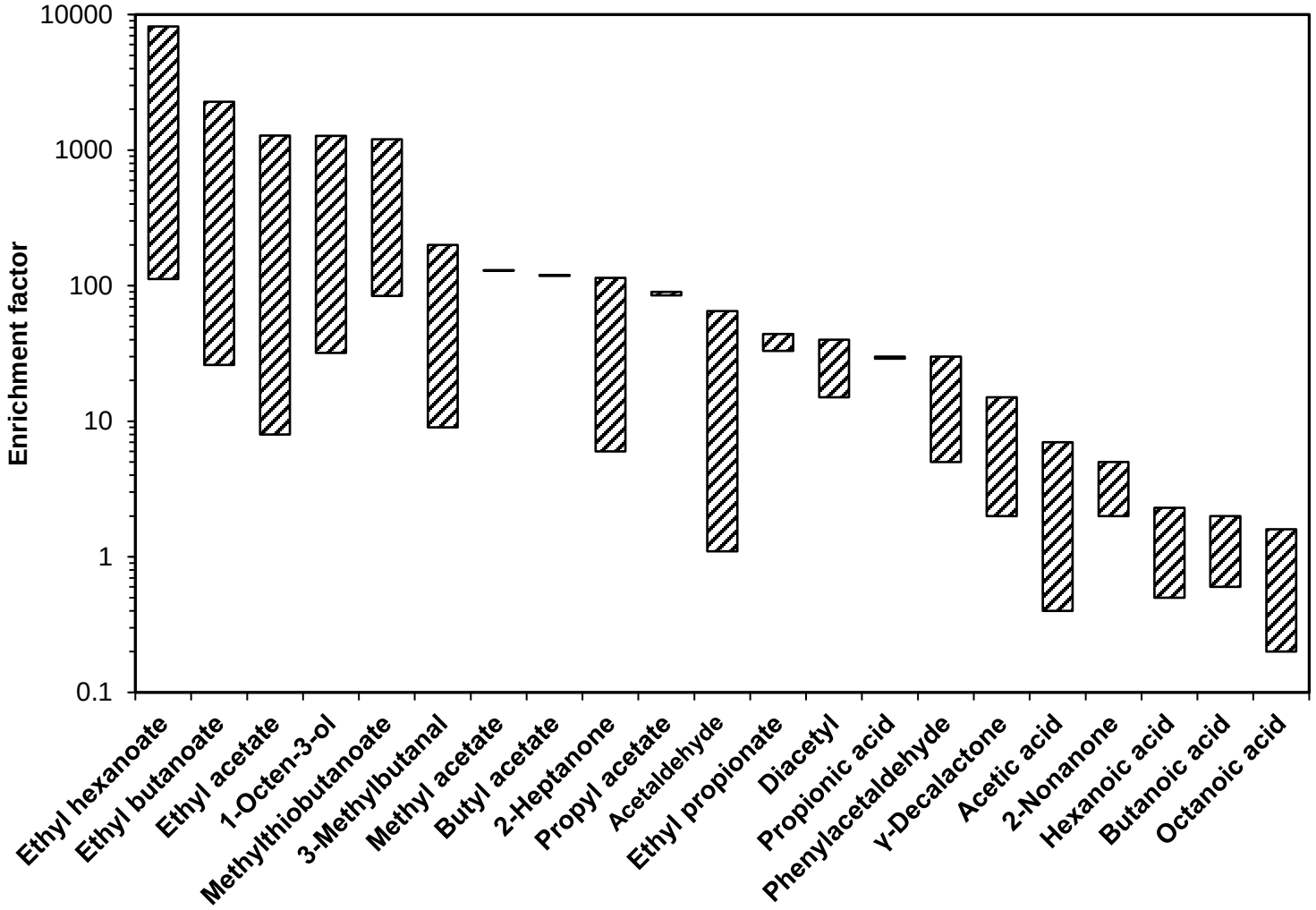

Figure 2.3 Ranges of enrichment factor for pervaporative recovery of dairy aroma compounds.

It has been observed that for a given group of aroma compounds, the aroma compounds with greater molecular weights can be better enriched by pervaporation (Overington et al., 2008). The boiling points of the aromas are also reported to affect their pervaporative recovery (Baudot et al., 1999). These observations shall not be treated as general trends in pervaporation. As mentioned above, the performance of pervaporative separation is determined by the membrane permselectivity and the driving force for permeation. Permeating molecules with bigger sizes tend to have lower mobility when diffusing through the membrane, but they usually exhibit higher solubility in the membrane. In addition, while bigger aroma molecules often have higher boiling points and thus lower saturated vapor pressures, dilute aqueous aroma solutions tend to deviates more significantly from ideal solution behavior and their activity coefficients in dilute aqueous solutions can be much greater than 1. Because of all these opposing effects, there is no guarantee that bigger aroma molecules will be better pervaporated by the membrane.

2.5.2 Membranes used for pervaporative aroma recovery

In aroma recovery by pervaporation, the separation performance is governed by the membranes used. Pervaporation membranes can be categorized on the basis of structure or nature of the selective layer of the membrane.

While dense homogeneous membranes are often used in laboratory research, composite membranes comprising of a thin selective layer supported on a microporous substrate may be used for practical applications in order to enhance the permeation flux. The membranes may be in the form of hollow fibers or flat sheets, and as such appropriate module designs should be used. Hollow fiber modules with either shell-side feed or tube-side feed are commonly used configurations. Flat sheet membranes are usually packed as plate-and-frame or spiral wound

modules. Generally hollow fiber modules have a larger membrane packing density than flat membranes. During manufacturing of flat membranes, the substrate membrane is often cast onto a nonwoven backing material, which provides additional support to the resulting composite membrane. Microporous substrates are primarily based on poly(vinylidene fluoride) (PVDF), polyacrylonitrile (PAN), polysulfone (PS) or polyetherimide (PEI) with pore sizes in the range of ultrafiltration membranes. Huang et al. (2002) have reported that the pore size and porosity of the substrate, rather than the substrate material itself, also influence the separation performance, although the top layer is more dominant. When the permeate vapor passes through a microporous substrate, the mass transport resistance can still be significant due to Knudsen diffusion (Rautenbach and Helmus, 1994).

Most of the selective surface layers in pervaporation membranes are homogeneous. To improve the separation performance, hydrophobic fillers may be incorporated into the polymer matrix, thereby enhancing the sorption selectivity and restricting membrane swelling. Zeolites (Bowen et al., 2003; Vankelecom et al., 1997), silica (Shirazi et al., 2012), activated carbon (Ji et al., 1995) and carbon black (Panek and Konieczny, 2007) have been used as the filler materials. A survey of current literature shows that PDMS is by far the most widely used rubbery material for pervaporative recovery of aroma compounds, followed by POMS and PEBA. These three materials account for about 2/3 of all the membranes used for aroma recovery by pervaporation (Figure 2.4). Ethylene propylene diene monomer (EPDM) and ethylene vinyl acetate copolymer (EVA) are also used to a lesser extent. The chemical structures of PDMS, POMS and PEBA are shown in Figure 2.5.

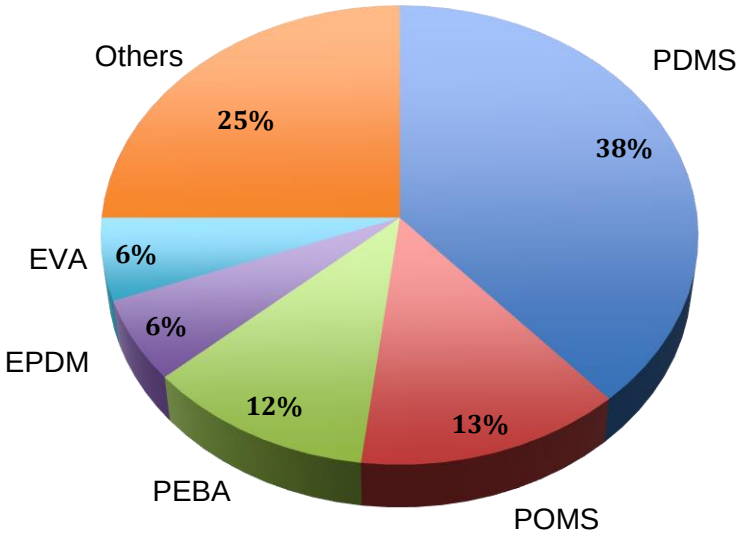

Figure 2.4 Organophilic membranes used for pervaporative recovery of dairy aroma compounds.

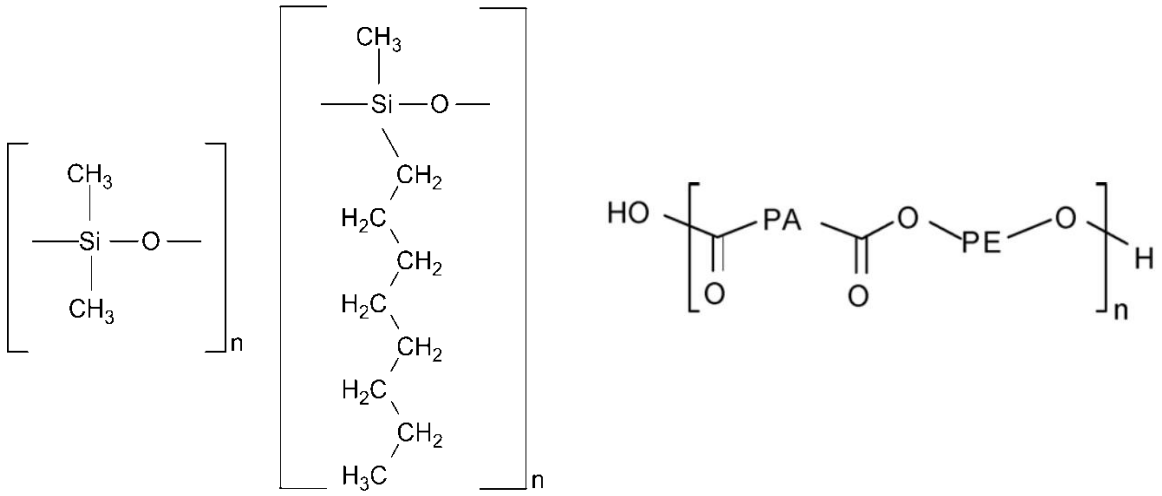

PDMS POMS PEBA

Figure 2.5 Structures of PDMS (Borjesson et al., 1996), POMS (Trifunovic and Tragardh, 2006) and PEBA (Mandal and Bhattacharya, 2006) polymers.

Poly (dimethyl siloxane) (PDMS)

Poly(dimethyl siloxane) (PDMS) is often referred to as "silicone rubber". PDMS has good mechanical and chemical properties, and can be used to fabricate supported or unsupported flat sheets. It can also be used to produce hollow fibers by coating on suitable hollow fiber substrates. There is a great deal of research on dairy aroma recovery by pervaporation using PDMS membranes. Flat sheet PDMS membranes, either standing alone or supported by a substrate, with or without hydrophobic nanofillers, have been investigated extensively.

The PDMS membranes exhibit good selectivity for aroma enrichment. For example, a separation factor of 100-250 can be achieved for the separation of ethyl acetate from water using homogeneous PDMS films (Pereira et al., 2005; Slater, 1997). When silicalite fillers are incorporated into the PDMS films, a selectivity from 100 to 1,300 can be obtained (Baudot et al., 1999; Baudot and Marin, 1999; Pereira et al., 2005). Dotremont et al. (1995) reported that the silicalites have a "reservoir" effect towards hydrophobic molecules, which enhances the membrane performance. Similar results were observed by Hennepe et al. (1991), who showed that the exclusion and tortuosity effects arising from zeolite fillers in PDMS membranes resulted in a decrease in water permeability. This is also supported by the work of Slater (1997), who compared the performance of unfilled PDMS 1060 membrane and silicalite-filled PDMS 1070 membrane for ethyl acetate separation from water under same operating conditions. At a feed concentration of 2.03% ethyl acetate and at a temperature of 50°C, the separation factor achieved with PDMS 1070 is about 2.5-fold higher than that with PDMS 1060. However, the enhanced selectivity is at the expense of significantly reduced flux. The experimental data of Slater (1997) showed that the permeation flux with PDMS 1070 membrane was only 1/3 of the flux produced with the unfilled PDMS 1060 membrane. While a simple comparison of the

fluxes between the two membranes is insufficient to conclude how the membrane permeability is affected by the silicalite fillers because of their different thicknesses, an examination of the differences in the partial fluxes of water and aroma between the two membranes revealed that the presence of the hydrophobic zeolites in PDMS 1170 not only significantly reduced the water flux, the aroma flux was also reduced.

However, the permselectivity of PDMS membranes are not always increased by incorporating silicate-fillers in the membrane. Baudot and Marin (1999; 1996) investigated the separation of methyl thiobutanoate from water under similar conditions by using both unfilled PDMS 1060 and silicalite-filled PDMS 1070 membranes. Both the selectivity and the partial permeation flux of the aroma obtained with PDMS 1070 were found to be 50% lower than those obtained with PDMS 1060 membrane. Obviously, the use of silicalite fillers is not advantageous if the aroma molecules are big enough for the zeolite to induce significant exclusion effect to the aroma compounds.

Poly(octhylmethyl siloxane) (POMS)

Poly(octhylmethyl siloxane) (POMS) is another promising organosiloxane polymer for pervaporative recovery of dairy aromas. Compared to PDMS membranes, POMS membranes usually exhibit a better selectivity, with a similar or lower aroma permeability. Sampranpiboon et al. (2000b) studied the separation of ethyl butanoate and ethyl hexanoate from aqueous solutions using PDMS and POMS membranes of the same thickness (10 μm). The POMS membrane showed better permselectivity to the aroma compounds than PDMS. However, their aroma fluxes appear to be similar. An aroma enrichment of 118-281 was obtained with the POMS membrane as compared to an enrichment of 77-234 with the PDMS membrane. In addition, both membranes showed better selectivity for separation of ethyl hexanoate from

water than ethyl butanoate/water separation. Raisi and Aroujalian (2011), who studied the separation of 3-methylbutanal from water using POMS and PDMS membranes, showed that POMS membrane is more selective to the permeation of 3-methylbutanal and a few other fruit aromas than the PDMS membrane. They also reported that the coupling effects between aroma compounds are not negligible when multiple aroma compounds are present in the feed solution.

Interestingly, Kanani et al. (2003), who also investigated pervaporation separation of 3-methylbutanal from water using PDMS and POMS membranes, reported an opposite order in the selectivities of the two membranes for enrichment of 3-methylbutanal. Under the same operating conditions, 3-methylbutanal was enriched in the permeate more significantly with PDMS membrane than the POMS membrane, and PDMS was reported to give better separation than POMS for the aldehyde. This, however, cannot be attributed to a higher selectivity of PDMS membrane because the PDMS membrane (thickness 160 μm) used was much thicker than the POMS membrane (5 μm). The observed separation performance is determined by the membrane and boundary layer effect. The mass transfer resistance of the membrane is directly related to the membrane thickness. If the liquid boundary layer effect is negligible, the use of thicker membranes will give a better separation, although the permeation flux will be compromised. The boundary layer effect should be minimized in practice in order for the membranes to work at their full potential.

Poly(ether block amide) (PEBA)

Poly(ether block amide) (PEBA) is a group of block copolymers comprising of soft polyether segments and rigid polyamide segments developed by Atofina (now Arkema Inc.). A broad range of physical properties can be acquired by changing the nature or lengths of the rigid and soft blocks (Fleshcer, 1986). PEBA represents a group of non-silicone organophilic

membranes for pervaporation. The work on PEBA membranes for dairy aroma recovery by pervaporation is listed in Table 2.3. Djebbar et al. (1998) prepared and evaluated the performance of a series of PEBA membranes (thickness ca. 100 μm) with different contents of ether segments. Their applicability for pervaporation was tested with three ester aromas, including ethyl acetate, ethyl propionate and ethyl butanoate. Both the aroma permeation flux and enrichment factors were increased with an increase in the content of polyether segments in the copolymer. However, among the PEBA membranes tested, the one with the best performance showed a similar enrichment factor as PDMS membrane (thickness ca. 500 μm) when the feed was a saturated aqueous solution of ethyl acetate (8.4 wt.%), propionate (2 wt.%) or butyrate (0.6 wt.%) at 30 °C. The permeability of the aromas in the PEBA membranes is lower than in the PDMS membrane, which is understandable in view of the generally high diffusivities in PDMS matrix due to the extraordinary flexibility of polymer chains arising from their siloxane linkages.

PEBA membranes appear to be advantageous over PDMS for the recovery of high-boiling hydrophobic aroma compounds. An enrichment factor up to 1205 has been reported (Baudot et al., 1996) for extracting methyl thiobutanoate (normal boiling point 142 °C,) from water using a PEBA 40 membrane (thickness 70 μm). Compared to a silicalite-filled PDMS 1070 membrane (thickness 30 μm), the partial flux of methyl thiobutanoate through PEBA 40 was 2- to 4-fold higher, while the water flux was still lower. At 30 °C and 15 ppm of methyl thiobutanoate in the feed, the permeability coefficient of the aroma in PEBA 40 is 4 times that in PDMS 1070, whereas water permeability coefficient in PEBA 40 is only 40% of the water permeability in PDMS 1070. This clearly demonstrates the excellent pervaporation performance of the PEBA membranes. In a subsequent study, Baudot and Marin (1999) also

compared the performance of the PEBA 40 membrane with the silicalite-free PDMS 1060 membrane. While both membranes had similar permeabilities to the thioester, the PEBA 40 membrane was much less permeable to water.

For rather hydrophilic and low-boiling aromas such as diacetyl (normal boiling point 88°C), both PEBA 40 and PDMS 1070 membranes showed similar selectivities (Baudot et al., 1996). With PEBA 40 membrane, the sorption is more dominating than diffusion as far as the mass transport is concerned. Consequently, this membrane favors permeation of non-polar and bulky permeant (e.g., thioesters), but it is not very competitive to selective permeation of such smaller and more polar molecules as diacetyl.

Mujiburohman and Feng (2007a) prepared a PEBA membrane using Pebax 2533 for pervaporative separation of propyl propionate from water. This copolymer has a high content of polyether segments (86 wt.% of polytetramethyleneoxide), with polyamide-12 being the hard segments. It was found that the permselectivity of the membrane was mainly derived from its excellent sorption selectivity. The diffusivity of propyl propionate through the membrane from its dilute aqueous solutions was affected exponentially by the aroma concentration in the feed solution.

Table 2.3 Pervaporative recovery of dairy aromas by PEBA-based membranes.

Membranes [a]	Effective thickness (μm)	Feed conc. (ppm)	Temperature (°C)	Permeate pressure (Pa)	Aroma flux (g/(m^{2}h))	Separation factor	Enrichment factor	Ref.
Ethyl acetate								
PEBA (PE/PA 57.8/42.2)	100	Saturated	30	<100	301	-	10	(Djebbar et al., 1998)
PEBA (PE/PA 40/60)	100	Saturated	30	<100	40	-	8.2	(Djebbar et al., 1998)
Ethyl butanoate								
PEBA (PE/PA 89.4/10.6)	100	Saturated	30	<100	800	-	137	(Djebbar et al., 1998)
PEBA (PE/PA 84.5/15.5)	100	Saturated	30	<100	660	-	142	(Djebbar et al., 1998)
PEBA (PE/PA 73.2/26.8)	100	Saturated	30	<100	282	-	132	(Djebbar et al., 1998)
PEBA (PE/PA 57.8/42.2)	100	Saturated	30	<100	86	-	128	(Djebbar et al., 1998)
PEBA (PE/PA 40/60)	100	Saturated	30	<100	10	-	91	(Djebbar et al., 1998)
PEBA 2533	100	100-900	30-60	667	1.5-25	60-175	-	(Sampranpiboon et al. 2000)
PEBA (PE/PA 57/43)	-	200-900	25	-	-	50-130	-	(Mohammadi et al., 2008)
PEBA (PE/PA 57/43)	-	900	20-50	-	-	70-125	-	(Mohammadi et al., 2008)
Methylthiobutanoate								
PEBA 40	70	15	30	250-2,000	0.55-0.2	700-1200	-	(Baudot et al., 1999)
PEBA 40	70	15	30	190-2,000	0.3-0.14	700-1205	-	(Baudot and Matin, 1996)
Ethyl propionate								
PEBA (PE/PA 89.4/10.6)	100	Saturated	30	<100	1,180	-	40.5	(Djebbar et al., 1998)
PEBA (PE/PA 84.5/15.5)	100	Saturated	30	<100	1,000	-	42.1	(Djebbar et al., 1998)
PEBA (PE/PA 73.2/26.8)	100	Saturated	30	<100	295	-	39	(Djebbar et al., 1998)
PEBA (PE/PA 57.8/42.2)	100	Saturated	30	<100	88	-	35	(Djebbar et al., 1998)
PEBA (PE/PA 40/60)	100	Saturated	30	<100	20	-	33.5	(Djebbar et al., 1998)
Diacetyl								
PEBA 40	30	80	30, 50	220-5,000	0.019-0.087	17,18	-	(Baudot and Matin, 1996)

Table 2.3 Pervaporative recovery of dairy aromas by PEBA-based membranes (continued).

Membranes [a]	Effective thickness (μm)	Feed conc. (ppm)	Temperature (°C)	Permeate pressure (Pa)	Aroma flux ($g/(m^2h)$)	Separation factor	Enrichment factor	Ref.
Vanillin								
PEBA 40	25-140	0-7,000	15-80	-	0-25	-	-	(Boddeker et al., 1997)
PEBA 25	100	5,000	15-80	-	2-40	-	-	(Boddeker et al., 1997)

[a] The numbers referred to the contents of polyether (PE) and polyamide (PA) segments or the codes of the polymer grades. All the membranes were flat sheet membranes.

Other materials

The investigation of membranes for pervaporative recovery of dairy aromas has been extended to other materials. Ethylene propylene diene monomer (EPDM) and ethylene vinyl acetate copolymer (EVA) are two elastomer materials that have also been exploited. EPDM is a terpolymer of ethylene and propylene with ethylidene norbornene as a diene comonomer inserted in the chains. It has a strong resistance to ozone and other chemicals due to the saturated backbones (Huang et al., 2002). Several EPDM membranes with different propylene contents have been investigated to separate ethyl butanoate from water (Huang et al., 2002). An increase in the propylene content in the EPDM membrane resulted in an improved permselectivity to ethyl butanoate, but the membrane permeability was lowered due to the greater rigidity of propylene that hinders mass transport in the membrane.

Another commercially available elastomer with desirable properties for pervaporative aroma recovery is ethylene vinyl acetate copolymer (EVA). It consists of non-polar crystalline ethylene segments and polar non-crystalline vinyl acetate segments. To investigate EPDM and EVA membranes for aroma separation by pervaporation, Pereira et al. (2005) carried out a comparative pervaporation study using PDMS membranes (PDMS 1060, PDMS 1070) as a baseline. The EPDM membranes showed the best performance among the four membranes tested.

Bai et al. (2008) used a cross-linked hydroxyl-terminated polybutadiene-based polyurethaneurea (HTPB-DVB-PU) membrane for pervaporative recovery of ethyl acetate from water. The thermal resistance of the membrane was significantly enhanced by the introduction of the crosslinker. The separation factor and the total flux increased with a higher divinyl benzene content. And at a feed ethyl acetate concentration of 2.5 wt.% and 30 °C, the

membrane showed a separation factor of 655 and a total flux of 256 g/(m^2h). In addition, fluoropolymers, mainly poly(vinylidene fluoride) and its copolymers, have also been used for fabricating membranes to extract ethyl acetate by pervaporation (Tian and Jiang, 2008; Zhu et al., 2005).

Most pervaporation membranes for aroma recovery are organophilic. Surprisingly, Dong et al. (2012) prepared a hybrid membrane by incorporating a hydrophilic ionic liquid into poly(vinylidene-fluoride-co-hexafluoropropene) for separation of ethyl acetate from water. The ionic liquid used, 3-butylimidazolium tetrafluoroborate ([bmim]BF_4), is hydrophilic and miscible with water in any proportion (Huddleston et al., 2001; Sheldon and van Rantwijk, 2008) As expected, the sorption uptake of the oleophilic ethyl acetate in the membrane decreased significantly as the [bmim]BF_4 content in the membrane increased (Dong et al., 2012). However, it is intriguing that incorporating the hydrophilic ionic liquid in the organophilic polymer matrix was reported to have enhanced the membrane permselectivity to ethyl acetate. It was hypothesized that water molecules in the feed would form a hydrate with [bmim]BF_4 loaded in the membrane, which would slow down water diffusion while enhancing the diffusion of ethyl acetate in the membrane.

Bowen et al. (2003) used Ge-ZSM-5 zeolite (germanium substituted, MFI structure) membranes to separate carboxylic acids (acetic acid, propionic acid), esters (methyl acetate, ethyl acetate) and a few other organic compounds from aqueous solutions. This membrane was reported to be more hydrophobic than silicalite-1 membranes prepared by similar procedures.

2.5.3 Influence of non-volatile components and operating conditions on dairy aroma recovery by pervaporation

2.5.3.1 Influence of non-volatile dairy ingredients

The composition of real feed solutions in dairy industry is complicated. Proteins, lactose, and fats are the major components of dairy products. They can interact with both volatile and non-volatile aromas in the feed. As such the research findings with model feed solutions may not be directly applicable to industrial production (Swaisgood, 1996). Research on the interactions between aromas and the non-volatile substances is mainly conducted from a sensory perspective: the aroma level is perceived to be reduced if less aroma is released due to binding to or associating with the non-volatile components. Depending on the hydrophobicities of the aromas, a certain portion of them can be dissolved by dairy fats, which help prevent volatilization of volatile aromas (Hatchwell, 1996; Leland, 1997; de Roos, 1997). Milk proteins can bind numerous aroma compounds (Fischer and Widder, 1997; Guichard and Langourieux, 2000; Hansen and Booker, 1996; Kühn et al., 2007, 2006a). Lactose can generally bind aromas by hydrogen bonding due to its abundant hydroxyl groups, resulting in a reduction in the volatility of the aromas (Godshall, 1997; Kellam, 1998). Therefore, at a given aroma concentration in the feed solution, the presence of proteins, lactose and fats will suppress the saturated vapor pressure of the aromas, thereby lowering the driving force for pervaporative transport of the aromas through the membrane. This will compromise the effectiveness of pervaporation to extract and concentrate the aromas present in the system. One should look into this aspect in recovering dairy aromas for practical applications.

Overington et al. (2011) carried out a comprehensive study on the effects of non-volatile dairy components on aroma recovery by pervaporation using a PDMS membrane. These non-

volatile components can influence both the driving force for permeation and the mass transfer coefficient. For pervaporative recovery of esters and ketones, the milk proteins can reduce the driving forces for aroma permeation by 56-94%, and the impact seems to be more significant for long-chain and hydrophobic aroma compounds. Interestingly, they have little impact on the permeation flux of water. When both milk protein and fat are present in the feed, the separation performance for aroma recovery is affected by the protein more significantly. Similar to proteins, lactose does not have evident negative effect on water permeation, but the aroma flux and thus the enrichment factor are lowered. These trends, however, cannot be generalized because the impacts of the non-volatile substances on aroma recovery depend on the nature and magnitude of their interactions with the aromas as well as the type of membranes used. In contrast, lactose has been reported to have no effect on the permeation flux or selectivity for dairy aroma diacetyl using a PDMS-polycarbonate copolymer membrane (25 μm thick) (Rajagopalan et al., 1994) or methyl thiobutanoate using a GKSS PEBA 40 membrane (70 μm thick) (Baudot et al., 1996). In the latter case, even the addition of salts (NaCl, Na_2HPO_4, KH_2PO_4), sodium lactate and amino acids to the feed solution close to a real cultrate medium does not change the flux and enrichment factor.

2.5.3.2 Influence of feed aroma concentration

In dilute feed solutions, the permeation f1ux of an aroma usually increases almost linearly with the aroma concentration in the feed, while water flux is not significantly affected by the feed concentration (Isci et al., 2006; Jullok et al., 2013; Mishima and Nakagawa, 2000; Pereira et al., 2005; Song et al., 2004). The linear relationship can be explained using the solution-diffusion model (Kanani et al., 2003), where the diffusivity and solubility are approximately constant. Under such circumstances, the membrane selectivity measured by permeability ratio

will be independent of feed concentrations. However, if the membrane has a strong affinity to the aroma compounds (i.e., a high solubility coefficient), a considerable membrane swelling by the penetrant may occur, which will increase the diffusivities of both water and aroma in the membrane. This normally happens when the aroma concentration in the feed is over a few thousands of ppm. Sometimes, the aroma diffusivity can be affected exponentially by its concentration in the feed, resulting in a nonlinear concentration dependence of the aroma flux (Gu et al., 2013; Mujiburohman and Feng, 2007a). While membrane swelling tends to increase both the aroma and water fluxes (Feng and Huang, 1997; M Peng and Liu, 2003), the selectivity can be increased (Wu et al., 2012) or lowered (Sampranpiboon et al., 2000b) at higher feed aroma concentrations. Generally speaking, excessive membrane swelling will lower the membrane selectivity.

The effect of feed concentration on the membrane selectivity is apparently related to the aroma compounds and to the membrane. For instance, Mohammadi et al. (2008) found that with the same PEBA membrane (57 wt.% poly(tetramethylene glycol) segment and 43 wt.% polyamide 12 segments), the separation factor for ethyl butanoate enrichment increased with the ethyl butanoate concentration in the feed solution, whereas the opposite was true for the separation of isopropanol enrichment. Sampranpiboon et al. (2000b) also investigated ethyl butanoate enrichment and found that the separation factor for ethyl butanoate/water separation is roughly proportional to the feed aroma concentration when a PEBA 3533 membrane was used, and the separation factor appeared to be inversely proportional to the feed concentration when PDMS and POMS membranes were used (Sampranpiboon et al., 2000a). In addition, when multiple aromas are present in the feed, the interactions among the aromas will also

influence the permeation of individual aromas, and this is reflected by the commonly observed coupling effects.

2.5.3.3 Influence of temperature

In general, a higher feed temperature favors both partial permeation fluxes of aroma and water. As discussed above, the increase in the permeation flux is attributed to increased driving force for permeation arising from the higher vapor pressure of permeant in the feed as well as enhanced permeability (though in certain cases the permeability may decrease with temperature if the increased diffusivity due to enhanced thermal motion of polymer chains and increasingly energized penetrant is insufficient to compensate for the decrease in the solubility due to exothermic sorption). Olsson and Tragardh (1999), who studied pervaporation of several esters using a POMS membrane at different temperatures, found that the increase in aroma flux with an increase in temperature is mainly due to the increased permeability, while the increase in water flux is attributed to the increased driving force. Similar results are observed for separation of acids, esters and ketones from aqueous solutions with PDMS and POMS membranes (Baudot et al., 1996; Overington et al., 2009).

The overall temperature dependence of permeation flux can be measured by the apparent activation energy (Beaumelle et al., 1992; Overington et al., 2009), which is normally in the range of 20-60 kJ/mol (Feng and Huang, 1996). Obviously, the effect of temperature on the selectivity of pervaporation separation depends on the difference in the apparent activation energies of the permeating species (i.e., aroma and water) to be separated. If the activation energy of an aroma compound is higher than that of water, then the aroma selectivity will be increased with an increase in temperature (Mujiburohman and Feng, 2007a; Olsson et al., 2002; Sampranpiboon et al., 2000b). For aroma compounds (e.g., ethyl butanoate (Sampranpiboon

et al., 2000b), ethyl hexanoate (Sampranpiboon et al., 2000a) and ethyl acetate (Feng and Huang, 1996)) with a lower activation energy than water, their selectivity will be lower at a higher operating temperature. Even if a high temperature favors both permeation flux and selectivity, the operating temperature is still limited so as to prevent thermal degradation of the aroma compounds.

2.5.3.4 Influence of hydrodynamics of feed liquid on the upstream side

The hydrodynamic conditions of the feed solution are another important aspect in pervaporation. Since aroma compounds are to permeate through the membrane preferentially, water molecules will be built up in the liquid boundary layer near the membrane surface (Cussler, 1997; Feng and Huang, 1997; She and Hwang, 2004), which is referred to as "concentration polarization". Because of the concentration polarization, the concentration of aroma compounds that the membrane "sees" on the feed side is lower than the aroma concentration in the bulk liquid, whereas the opposite is true for water. The liquid boundary layer thus presents an additional resistance to mass transfer of aroma compounds, while it does not affect water permeation significantly for dilute solutions. For pervaporation separation of minor components from water, the boundary layer mass transfer may become dominant over the membrane itself if the hydrodynamic conditions of the feed solution are not properly controlled (Jiang et al., 1997; Lipnizki et al., 2001).

The extent of concentration polarization is determined by both the permselectivity of the membrane and the hydrodynamic conditions of the feed on the upstream side. Fluid management techniques to reduce the boundary layer thickness by promoting good mixing of the feed solution near the membrane surface are important in order to minimize concentration polarization. Thus, it is often recommended to use a relatively high turbulence on the feed side.

Generally, water flux is not strongly affected by the hydrodynamic conditions of the feed solution at low aroma concentrations because water concentration on the membrane surface is not considerably different from the water concentration in the bulk solution (She and Hwang, 2004).

2.5.3.5 Influence of permeate pressure on the downstream side

As the driving force for pervaporative transport is provided by applying vacuum on the downstream side, the permeation flux is directly affected by the permeate pressure. As expected, the lower the permeate pressure, the higher the permeation flux (Aroujalian and Raisi, 2007; Fouda et al., 1993; Olsson et al., 2001, 1999; Raisi et al., 2008). For aroma recovery, an increase in the permeate pressure will lower both the partial fluxes of aroma and water. Thus, the pervaporation selectivity is not strongly influenced by the permeate pressure as compared to the permeation flux, unless the aroma is a high boiler with a low saturated vapor pressure on the feed side. It has been shown that effect of permeate pressure on pervaporative recovery of a high-boiling-point aroma γ-decalactone (boiling point 281°C) is much more pronounced than recovery of low-boiling-point aromas (e.g., ethyl acetate and diacetyl, boiling points 77°C and 88°C, respectively) (Baudot et al., 1999). Aromas with moderate boiling points (e.g., methyl thiobutanoate) displayed an intermediate behavior; the separation factor may increase or decrease with an increase in the permeate pressure, depending on the membranes used (Baudot et al., 1999).

In industrial operations, the permeate pressure may range from several hundred to a few thousand Pascal, which is a lower vacuum than that normally used in the laboratory (Baudot et al., 1999; Pereira et al., 2006). Therefore, caution should be exercised in extrapolating bench-scale pervaporation results in process design. In addition, when hollow fiber membranes are

used, there will be a pressure buildup along the fiber length on the permeate side (especially for shell side feed configurations), which should be taken in account in module scale up. Attention should also be paid to the pumping and piping aspects for permeate withdrawal to minimize the negative effect of pressure buildup (e.g., using a large hydrodynamic diameter and minimal length) (Willemsen et al., 2004).

In aroma recovery by pervaporation, the primary energy consumption element is the vacuum pump used for permeate evacuation. Conventionally, the permeate vapor needs to be condensed under vacuum before reaching the pump inlet to avoid contamination. A new development in the vacuum pump industry is the dry vacuum pump that runs completely dry, without using any lubricant in the swept volume. They are more efficient than conventional vacuum pumps and use less energy.

2.6 Concentration of dairy products

In the processing of dairy products, one of the important processing units is the concentration of milk or other semi-finished dairy products. The concentration of dairy products is essentially the removal of water. The main objective of concentration is to produce milk powder or protein (or other nutritional components) enriched products, to reduce the weight or volume during packaging and transportation, to improve the stability and handling of the product, or to reduce water activity to lengthen the shelf life of dairy products.

Evaporation, freeze concentration and membrane concentration (especially reverse osmosis) are three common methods for concentration of dairy products.

2.6.1 Evaporation on concentrating dairy products

Evaporation is currently a major technique used for the removal of water in the dairy industry. It uses gas-liquid phase separation by heat and/or vacuum. In general, an evaporator consists of three principal elements: heat transfer, vapor-liquid separation, and vapor condensation. To save energy, many food evaporation systems use multiple-effect evaporation, in which the vapor from one effect is used as the heating medium to boil a subsequent effect at a lower temperature. This system is usually used under vacuum to sustain evaporation at a lower temperature. Evaporation has low capital cost and high concentration obtainable (>50^{o} Brix) (Sánchez et al., 2011); however, it consumes higher energy (Sánchez et al., 2011) than other concentration techniques. In addition, the thermal treatments involved may degrade nutritious components (such as proteins and vitamins) and aroma compounds, thereby compromising the dairy products quality.

2.6.2 Freeze concentration of dairy products

Freeze concentration is another concentration technique applied in dairy industry. Normally, water is separated from milk or other dairy products by crystallizing ice at low temperatures, followed by a separation step to remove ice from the concentrate. Owing to the low temperatures applied, the loss of volatile aromas and flavors and thermally sensitive components can be minimized, resulting in high quality of dairy products (Hartel, 1993). A maximum solid concentration of dairy products achieved by using freeze concentration was reported to be about 50^{o} Brix (Heldman, 2003). Best and Vasavada (1993) also reported that using suspension freeze concentration, skim milk had been concentrated up to 40 wt.% TS (total solid) and whole milk up to 44 wt.% TS. Using block freeze concentration, cheese whey

and whey proteins have been concentrated up to 35 wt.% TS and up to 6.49% (w/v), respectively (Aider et al., 2007).

Although freeze concentration shows some advantages, it does have limitation for practical use in dairy industry. For instance, its total costs (including energy, capital and cleaning) are three to four times higher than those for evaporation or reverse osmosis (van Mil and Bouman, 1990). The losses of solids are high, especially at high feed concentrations (Hartel, 1993). The high viscosity of dairy product is another limiting factor for the freeze concentration of both skim milk and whole milk. What's more, the presence of fat in dairy causes difficulty in the removal of ice from the concentrates (Sánchez et al., 2011).

2.6.3 Membrane technologies applied to concentration of dairy products

To meet the current market demand, recent developments in concentration technology in the dairy industry have focused on non-thermal technologies. Membrane processing is a pressure-driven separation technology using membranes with different pore sizes or with no pores. It is an important alternative for the clarification and concentration of dairy products because it operates at room temperature, exhibits low energy consumption, high performance, and easy scale up, and rejects a wide range of food contaminants. However, comparing to traditional membrane applications (for instance, water treatment or desalination), the concentration of fluid milk or certain dairy components is more challenging due to the high solid content and complex compositions of milk. In the past few decades, thanks to the fast development of membrane materials and membrane element configurations, almost all types of membrane processes, except for pervaporation, have been successfully used in the processing of milk and dairy products.

Microfiltration (MF), ultrafiltration (UF), nanofiltration (NF) and reverse osmosis (RO) membranes are characterized by different membrane pore sizes and thus operating pressures and mass transfer mechanisms. Table 2.4 and Figure 2.6 summarize the characteristics of these membrane processes and their applications in concentration or separation of dairy ingredients. MF membranes have relatively large pores (within the range of 0.1 to 10 μm) than other membranes, and they are mainly used to remove bacteria and associated spores from milk before pasteurization, allowing for an extended shelf-life of the product. MF is also used to separate casein from whey proteins (Hu et al., 2015), and this separation is based on the physicochemical properties of these two types of proteins. Although casein proteins themselves do not have larger molecular weights than whey proteins (the molecular weights of caseins are 12000-25000 Da and the molecular weights of whey proteins fall in 14000-900000 Da (Fox and McSweeney, 2003)), 95% of casein in milk is in the form of colloidal particles, which have a diameter ranging from 0.05 to 0.5 μm (Fox and McSweeney, 2003). These casein micelles are much larger than whey proteins and can be easily separated from whey proteins by MF.

Table 2.4 Characteristics of membrane processes applied to the concentration or separation of dairy ingredients in industry.

Membrane processes	Membrane pore size [a]	Mt cut off ranges, Da [a]	Operating pressure, MPa	Separation mechanism	Applications in dairy industry
MF	0.1-10 μm	>200,000	0.01-0.2	Size exclusion	Removal of bacteria and spores; fractionation of milk proteins
UF	1-500 nm	5,000-200,000	0.1-1.0	Size exclusion	Removal of lactose; concentration of milk protein and fat.
NF	0.1-1 nm	200-5,000	1.0-3.0	Size exclusion	Removal of monovalent salts from dairy.
RO	<0.1 nm	<200	3.0-15.0	Size exclusion, sorption and diffusion	Concentration of milk and whey.

[a] (Baker, 2012; Cheryan, 1998; Mulder, 1996)

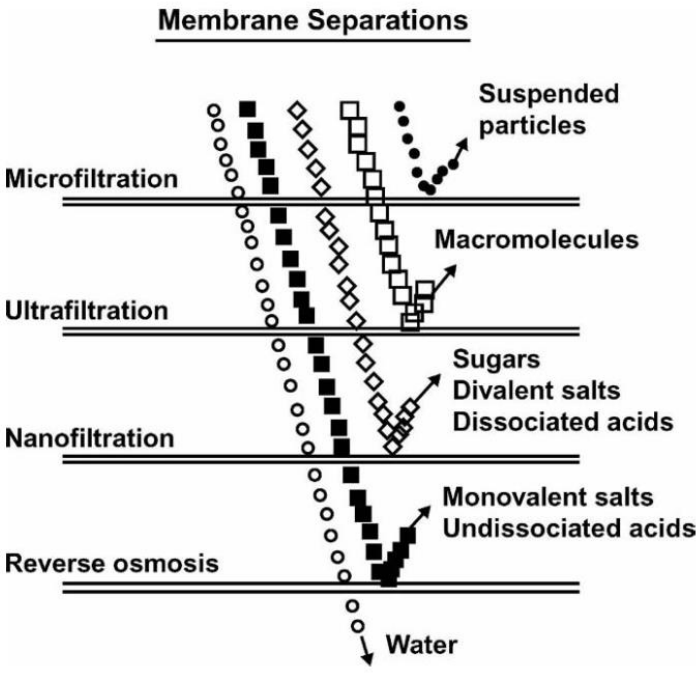

Figure 2.6 Schematic diagram of membrane separation processes (Henning et al., 2006).

UF seems to be the most widely used membrane process in dairy manufacturing. It is effective for reducing lactose in milk, allowing for manufacturing of low-lactose dairy products. Fats and proteins are retained in the retentate of the UF processes, while lactose and salts can pass through the UF membrane. UF is often coupled with NF and/or RO to produce lactose-free products. One example is a patented process for manufacturing lactose-free milk using UF, NF and RO membrane technologies (Tossavainen and Sahlstein, 2003). The pasteurized milk was ultrafiltered by UF membranes with a MWCO of 20000 Da. Then the UF permeate containing mainly lactose and minerals was filtered by NF membranes. The NF permeate, which consisted mainly of univalent minerals was further concentrated by RO. The RO retentate was later mixed with UF retentate and finally the obtained milk contained less than 0.01% of lactose. UF is also an attractive unit operation in the concentration of proteins to

make milk protein concentrate and whey protein isolate or in pre-concentration of milk before cheese making (Henning et al., 2006).

NF is a process using membranes with pores that are larger than those of RO membranes, but smaller than those of UF and MF membranes (see Table 2.4). The NF membranes can normally retain species with a molecular weight bigger than 200 Da. Therefore, it can reject lactose, protein and fat, but allow many monovalent salts (e.g., sodium and chloride) to permeate freely. The primary applications of NF in dairy industry is to concentrate dairy components and remove salts from dairy fluids. The dairy fluids include whole milk, whey (van der Horst et al., 1995), and UF permeate of milk or whey (Cuartas-Uribe et al., 2009). In desalting of dairy products, NF membranes allow monovalent sodium ions to penetrate, while retain the more nutritionally relevant divalent ions, such as calcium, zinc and magnesium (Rice et al., 2008). This approach can be used to prepare Ca and Mg enriched dairy products.

RO is a membrane technology in which the solution is pressed to transport through the membrane by applying a pressure higher than the osmotic pressure of the solution, resulting in a separation of most solutes and solvent. Since the pore sizes of reverse osmosis membranes are very small (<0.1 nm), they can retain almost all components other than the solvent (e.g., water). Therefore, strictly speaking, RO is a true de-watering technique, while MF, UF and NF can be considered as methods for simultaneously purifying, concentrating, and fractionating certain components from a fluid system. In dairy industry, RO is most applied to concentrate milk or whey, and it is more energy efficient than evaporation or other drying methods. For example, RO can be used to remove water from milk or whey before evaporation or spray drying operations, and this is more energy efficient than applying only evaporation/spray drying for water-removing. As Daufin et al. (2001) reported, 9-150 kWh energy was needed

per ton of water removed for evaporation for whey pre-concentration, while only 9 kWh/t was consumed if the evaporation step was replaced by RO. However, the concentrations of the products obtained using RO are always lower than that obtained with evaporation, the maximum concentration obtainable with RO is only around 30° Brix (Sánchez et al., 2011). The high osmotic pressure of dairy fluids and membrane fouling are two significant limiting factors that restrict the wide use of RO in dairy industry.

To summarize, even though the membrane separation technologies mentioned above are very promising, there are some challenges that limit the applications of these processes in the dairy industry. The major limiting factor is the strong flux decline caused by concentration polarization and membrane fouling. Membrane fouling refers to the gel lay formation, as well as adsorption and deposition of solute molecules on the surface of or inside the membrane. The flux decline can be very severe, especially in MF and UF; in some cases, the flux can be decreased to <5% of the pure-water flux. A gel layer may form when significant accumulation of solute molecules on the membrane surface occurs, particularly when proteins are present in the feed (Huisman et al., 2000).

2.6.4 Pervaporation as an alternative technique for concentrating dairy products

Another potential application of pervaporation is water removal from a solution, for example, solvent dehydration and desalination. In the case of solvent dehydration, the feed mixtures are normally azeotropic solutions. Traditional distillation is only able to separate the azeotrope with pure solvents with the use of entrainers, which then must be removed using an additional separation step. Pervaporation can be used to break the azeotrope, because the separation is based on selective sorption and diffusion of certain molecules through the

membranes, rather than relative volatility of the components to be separated. The widely studied solvent dehydration processes include the dehydration of alcohols (Mah et al., 2014; Wu et al., 2015; Yu et al., 2011) and acids (Chen et al., 2012). For pervaporative desalination, sea water is the most commonly studied salt solutions, and hydrophilic membranes are often used as they preferentially permeate water, producing a permeate with a high water content and a solvent-enriched retentate.

To our knowledge, pervaporation has not been applied in concentrating dairy products. Unlike other membrane processes, pervaporation requires no pressure applied to the feed side, and a much higher concentration of permeate is achieved using pervaporation than other membrane processes. More importantly, pervaporation membranes are non-porous, which means membrane pore blockage is not relevant. Therefore, the flux decline, which is the major limiting factor for other membrane processes in dairy processing, may not be very significant. The above advantages of pervaporation make it a potential alternative in concentrating dairy products, and thus it is a subject in this thesis research.

A good polymer for membranes to selectively permeate water needs to have good sorption characteristics, through interactions with water by dipole-dipole and ion-dipole actions (in the case of a polyelectrolyte) and/or hydrogen bonding (Semenova et al., 1997). Thus the membrane material that has such features is often desirable. PEBA 1074 has a high content of polyamide, which can interact with water by hydrogen bonding, and therefore PEBA 1074 is expected to be suitable for the dehydration applications.

2.7 Summary

The current state of separation methods for dairy aroma compound recovery and concentration of dairy products are reviewed. Pervaporation offers advantages of mild

processing temperature, low energy consumption and easy operation. Its potential for recovering natural aromas is apparent in view of the increasing demand for natural aroma substances.

Among the large number of dairy aroma compounds identified, only about 30 aromas have been investigated extensively for pervaporative recovery from aqueous solutions using organophilic membranes. More studies are needed to look into other dairy aromas as well. Most of the research to date on pervaporative recovery of aroma compounds has been carried out with binary aroma-water mixtures. Even though it is convenient for membrane testing and evaluation in the lab, the research findings obtained cannot be simply extrapolated to real aroma solutions that involve multiple aromas as coupling effects are likely to occur. In addition, the presence of dairy proteins, fats and lactose may also affect pervaporative recovery of aroma compounds. For a given membrane and feed aroma composition, the separation performance is affected by the operating temperature, permeate pressure and hydrodynamic conditions of the feed solution. Proper selection of operating parameters is critical for practical applications.

Considering the working mechanism of pervaporation (i.e., selective sorption and diffusion of certain molecules in the membrane), it may be used to concentrate dairy products by selectively removing water from the mixture.

Among the various membrane types, PEBA is a series of excellent materials with good selectivity to certain organics or water. A more balanced dairy aroma profile in permeate could be obtained by certain organiophilic PEBA membranes with a high content of polyether segments, comparing to other organophilic membranes. This is appealing in aroma recovery industry. In addition, hydrophilic PEBA membranes with a high content of polyether segments are likely to be favorable for dehydrating and concentrating dairy solutions.

Chapter 3

Recovery of Dairy Aroma Compounds from Aroma-Water Solutions by Pervaporation Using PEBA Membranes

3.1 Introduction

As discussed in Chapter 2, the pervaporation performance depends on the types of aroma compounds, the membranes used and the operating conditions. Organophilic membranes, particularly PEBA, PDMS and POMS, are suitable for the recovery of aroma compounds from their aqueous solutions. Although most of dairy aroma compounds are oil-based, water-based aromas cannot be ignored as they impact the dairy quality as well. PDMS and POMS membranes work well to capture oil-based aromas, but not so well for water-based aromas. PEBA copolymer comprising both organophilic ether groups and hydrophilic amide groups, has well balanced affinities to both water-based aromas and oil-based aromas. In the recovery of aromas from real dairy solutions, PEBA membranes is preferred over other polymers because a more balanced concentration profile of aromas in the permeate can be generated. PEBA 2533 is a block copolymer comprising 80 wt.% poly(tetramethylene oxide) and 20 wt.% nylon 12 (Liu et al., 2005). Its high content of polyether segment is expected to result in a good permselectivity to hydrophobic aroma compounds in dairy solutions. That is the reason why it was selected as membrane material in this study. Operating parameters are another key factor affecting aroma recovery. In order to scale up the experimental results obtained in lab for industrial applications, certain operating parameters need to be evaluated and optimized. In this study, the effects of aroma concentration in the feed and temperature, which are the two most important operating parameters, on the separation performance were studied.

Although some studies on the recovery of aroma compounds from aqueous solutions by pervaporation have been reported, most research only focused on aqueous solutions containing single aroma compound. Since real dairy solutions involve multiple aroma compounds, it is necessary to extend the pervaporation studies from binary aroma-water feed system to multicomponent feed system. However, complicated interactions often take place among the permeant and the membrane, especially for pervaporation of multicomponent mixtures. The interactions among the permeating species, which are sometimes known as "coupling effects", often change the sorption and diffusion characteristics of the permeating species through the membrane. Due to difficulty in direct measurements of the interactions quantitatively, most investigations focused on the simplest coupled transport of binary or ternary mixtures, and only a few studies have been carried out for multicomponent mixtures. Sampranpiboon et al. (2000a) found that esters fluxes were decreased when other esters were added to the dilute feed solutions. In contrast, some alcohols were observed to have higher permeabilities in their multicomponent feed systems than in their binary systems (Kanani et al., 2003; M. Peng and Liu, 2003). Therefore, another objective of this study was to investigate how the presence of an additional aroma compound affects the mass transfer of individual aroma component. The model aroma compounds used in this study were selected from six categories of representative dairy aromas: esters, ketones, aldehydes, sulfur compounds, and aromatic compounds. A literature search showed that among these aroma compounds, the pervaporative recovery of indole, nonanal, and dimethyl sulfone has not been reported.

3.2 Experiments

3.2.1 Model feed solutions

Binary (single aroma compound + water) and multicomponent (eight aroma compounds + water) feed solutions were used in this study. Eight aroma compounds, ethyl hexanoate, ethyl butanoate, 2-heptanone, diacetyl, dimethyl sulfone, indole, nonanal, and hexanoic acid, were selected as model aromas. They were selected for the uses as model aromas in this study because they are key aromas in dairy products (as seen in Table 2.1) and they represent six categories of dairy aromas. They were all of reagent grade and supplied by Sigma Aldrich. The feed solutions were prepared by mixing a predetermined amount of the aroma compound(s) and water.

3.2.2 Membrane preparation

PEBA 2533 in the form of elliptic pellets was kindly supplied by Arkema Inc.. The physical properties of PEBA 2533 is shown in Table 3.1. Flat-sheet dense membranes were prepared using the solution-casting method. At first, the PEBA pellets were dissolved in *N*, *N*-dimethyl acetamide (DMAc) (from Acros Organic Inc.) at a concentration of 15 wt.%. The polymer solution was kept at 60 °C under vigorous stirring for 24 hours to facilitate dissolution of the polymer. Then the homogeneous polymer solution was kept at 60 °C for 10 more hours to degas the bubbles trapped during the stirring. After fully degassing, the polymer solution was cast on a heated glass plate (60 °C) using a casting knife, which is in the form of a glass rod with wires at both ends to control the membrane thickness. After evaporation of the solvent in an oven at 65 °C for 48 hours, the glass plate with the membrane on the top was immersed in water, followed by detaching the membrane carefully from the glass plate in water. Finally,

the membrane was dried in an oven at 50 °C for 5 hours. The thickness of the membrane so prepared was about 25 μm.

The contact angles of the pure aroma compounds on dry PEBA 2533 membranes were measured using a contact angle meter (Cam-plus Micro, Tantec Inc.) at 22 °C. At least 10 measurements on different locations of a single membrane sample were performed, and the results presented were an average of the measured values.

The membrane sample was used for 6 months. To test the stability of the membrane, pure water fluxes of a fresh membrane and the membrane after everyday use were tested under a permeation pressure of 400 Pa and 22 °C. If pure water flux of a membrane after pervaporation test was consistent with the initial water flux of the virgin membrane, which indicates there was no change in the membrane behavior, the same membrane was used continuously in subsequent study.

Table 3.1 Chemical component and physical properties of PEBA 2533.

Name	PA[a]	PE[b]	PE content, wt%	Density, g/m^3	T_g, °C	T_m, °C
PEBA 2533	PA12	PTMO	80	20	-77	126

a. PA 12 is polyamide (nylon)12.
b. PTMO is poly(tetramethylene oxide).

3.2.3 Pervaporation procedures and gas chromatography analysis

The experimental setup for pervaporation experiments is shown in Figure 3.1. The PEBA membrane was mounted into the permeation cell with an effective membrane area of 22.05 cm^2. The feed solution was continuously circulated through the membrane cell and back into the 1000 mL feed tank, using a circulation pump, at a pressure of 1atm. Vacuum was applied on the permeate side to provide the driving force for permeation. The temperature of the feed solution was controlled using a heating mantle, a Dyna-Sense® Thermoregulatory Control

System, and a thermometer. The permeate samples were condensed in a cold trap immersed in liquid nitrogen (around -196 °C).

In order to achieve steady state operation quickly, new membranes were conditioned for 10 hours under pervaporation experiments with deionized water at 36 °C under a downstream pressure of 400 Pa achieved by a vacuum pump. Before each pervaporation run at a new feed concentration or temperature, the membrane was reconditioned by circulating the feed solution at the specific temperature for 2 hours to reach steady state. The pervaporation experiments were conducted at a feed flow rate of 1.14 L/min. When one pervaporation run was finished, the permeate sample was collected and weighed using an analytical balance. The aroma-enriched permeate sample was then diluted with deionized water for composition analysis with a Varian-3800 gas chromatography.

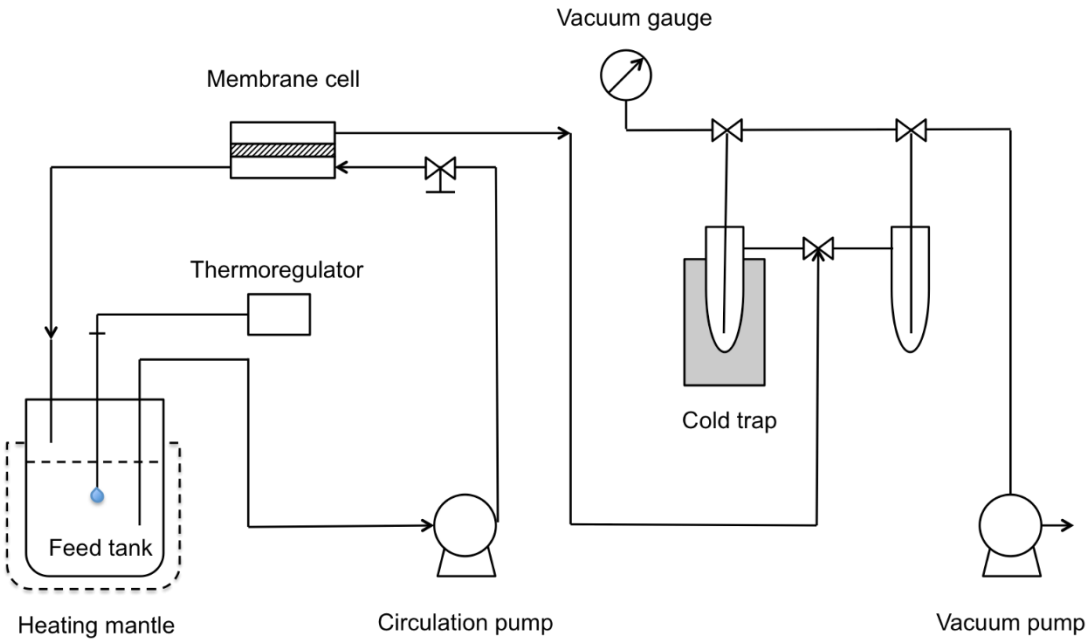

Figure 3.1 Schematic diagram of the pervaporation setup

Pervaporation performance was characterized by flux, permeability and enrichment factor. These parameters were calculated using Equations 2.3, 2.2 and 2.7, respectively. The activity

coefficients and partial pressures of aromas and water (Appendix A Table A.1 and A.2) were estimated using Aspen plus V8.0 based on UNIQUAC equation. Unfortunately, the membrane permeability of dimethyl sulfone was not calculated due to lack of the thermodynamic data. The feed and permeate composition were analyzed by a Varian-3800 gas chromatography (GC) equipped with a FID detector and an Agilent CP-Sil 5 CB capillary column (60 m long, 0.32 mm inside diameter, 0.45 mm outside diameter, 1.00 μm film thickness). The GC operating conditions were: the injector temperature 250 °C, the FID detector temperature 300 °C, and the oven temperature was set to be 80 °C for 1 min and then increased to 250 °C at 20 °C/min. The carrier gas (helium) flow rate was 2 mL/min, with a makeup flow rate of 27 mL/min. The flow rates of H_2 and O_2 were 30 and 300 mL/min, respectively. The sample injection was in split mode; the split ratio was 30: 1. Each sample was measured three times.

The pervaporation data reported was an average of three measurements, and the average experimental error was estimated to be 10 %.

3.3 Results and discussion

3.3.1 Effects of feed concentration on pervaporative recovery of aromas

The effects of feed aroma concentration on the recovery of aromas from water were investigated at 36 °C using binary (one aroma + water) feed mixtures. The aroma concentration ranges were selected based on the aroma composition in real dairy products (Nursten, 1997; Parliment and McGorrin, 2000; Toso et al., 2002) and the aroma solubility in water. Table 3.2 lists the physicochemical properties of the aroma compounds. Since the pervaporation experiments were carried out at dilute concentrations, total permeation fluxes (which were not presented) were close to water permeation fluxes.

Table 3.2 Physical properties of the model aroma compounds.

Aroma compounds	Formula	MW [a], g/mol	BP [b], °C	log *P* [c]	Aroma contact angle on PEBA 2533, deg.	Molar volume, cm^3/mol	S_a [c] at 25 °C, g aroma/g water
Esters							
Ethyl hexanoate	$C_8H_{16}O_2$	144	228	2.759	39	166	4.60×10^{-4} (Pereira et al., 2005)
Ethyl butanoate	$C_6H_{12}O_2$	116	120	1.705	40	132	5.75×10^{-3} (Pereira et al., 2005)
Ketones							
2-Heptanone	$C_7H_{14}O$	114	151	1.822	42	143	4.30×10^{-3} (Kirk and Othmer, 1981)
Diacetyl	$C_4H_6O_2$	86	88	-1.976	63	87	2.50×10^{-1} (Yalkowsky et al., 2010)
Acid							
Hexanoic acid	$C_6H_{12}O_2$	116	206	1.807	63	125	1.08×10^{-2} (Yalkowsky et al., 2010)
Aldehyde							
Nonanal	$C_9H_{18}O$	142	191	3.171	52	172	9.6×10^{-5} (Yalkowsky et al., 2010)
Sulfur compound							
Dimethyl sulfone	$C_8H_{16}O_2$	144	240	-3.587	- [e]		Miscible (Yalkowsky et al., 2010)
Aromatic compound							
Indole	C_8H_7N	117	253	2.06	- [e]	100	1.90×10^{-3} (Yalkowsky et al., 2010)

a. Molecular weight.
b. Boiling point
c. Aroma solubility in water.
d. The chemicals are in solid form at room temperature, therefore their contact angle data are not available

The eight model aroma compounds came from six categories of chemicals. Due to the differences in the structures and physical properties of these aromas, different permeation behavior of the aromas through the PEBA membrane was expected. Table 3.3 shows the aroma permeation fluxes at a feed aroma concentration of 50 ppm and 36 °C, and the two determining factors of aroma flux: the equilibrium partial vapor pressure in feed (permeation driving force) and membrane permeabilities of the aromas. It can be seen that for the compounds tested, two esters (ethyl butanoate and ethyl hexanoate) and 2-heptanone (which is the longer-chain ketone of the two ketones) had higher permeation fluxes and enrichment factors than other aromas, and this is followed by nonanal, dimethyl sulfone, diacetyl, hexanoic acid and indole. This sequence agrees with the sequence of the partial vapor pressures of these aromas, in spite of the different permeabilities of the aromas (Table 3.3). This indicates that higher driving force caused esters and ketones to have higher fluxes and larger enrichment factors than the other aroma compounds. In other word, an aroma compound with a high partial vapor pressure tends to have a high permeation flux.

Table 3.3 Permeation fluxes partial vapor pressure in feed, membrane permeabilities and enrichment factors of aromas at a feed concentration of 50 ppm for each aroma, 36 °C and a permeate pressure of 400 Pa.

	Partial flux, $g/(m^2.h)$	Enrichment factor	Partial vapor pressure in feed, Pa	Permeability, 10^{-8} $mol.m/(m^2.h.Pa)$
Ethyl butanoate	1.52	152.82	26.69	1.66
2-heptanone	1.33	138.6	5.6	6.95
Ethyl hexanoate	1.18	144	24.63	1.39
Nonanal	0.73	73.65	12.89	1.81
Dimethyl sulfone	0.25	25.43	-	-
Diacetyl	0.18	18.24	1.06	4.89
Hexanoic acid	0.1	10.43	0.07	47.63
Indole	0.07	7.34	0.05	39.42

Figure 3.2 shows the permeation fluxes of aroma compounds as a function of the feed aroma concentrations. It can be observed that the partial fluxes of all the aroma compounds (except for indole) increased with an increase in the aroma concentration in feed, while permeation flux of indole remained almost constant. The increased aroma flux is partly due to the increase in the feed-side partial pressure of the aroma on the feed side (see Appendix A), and thus the driving force for aroma permeation also increased. For 2-heptanone-water permeation, membrane swelling may also contribute to the enhancement of 2-heptanone flux, which will be illustrated in Figure 3.6 and Figure 3.7. In an infinite dilute solution, if the organic concentration varies in a small range, the activity coefficient may be considered constant and the polymeric membrane swelling sometimes was considered negligible (Martinez et al., 2013). Therefore, the membrane permeability to aroma compounds did not change significantly. However, in the relatively large aroma concentration range in this study, it is interesting to note from Figure 3.3 that the intrinsic permeability of the eight aromas in the membrane was not always constant: the permeabilities of 2-heptanone, ethyl butanoate and ethyl hexanoate increased with an increase in their concentrations, which also contributed to the increased permeation flux. On the contrary, the permeabilities of diacetyl and hexanoic acid decreased at higher feed aroma concentrations, and the permeability of nonanal was almost constant within the small concentration range studied in this work (10-50 ppm). Therefore, for the permeation of diacetyl, hexanoic acid and nonanal, it was their increased partial pressures on feed side that caused their permeation fluxes to increase with the feed aroma concentration. In addition, as the concentration of indole increased from 50 to 900 ppm, the increase in permeation driving force of indole was compensated by the reduction in its permeability, which resulted in an almost constant flux.

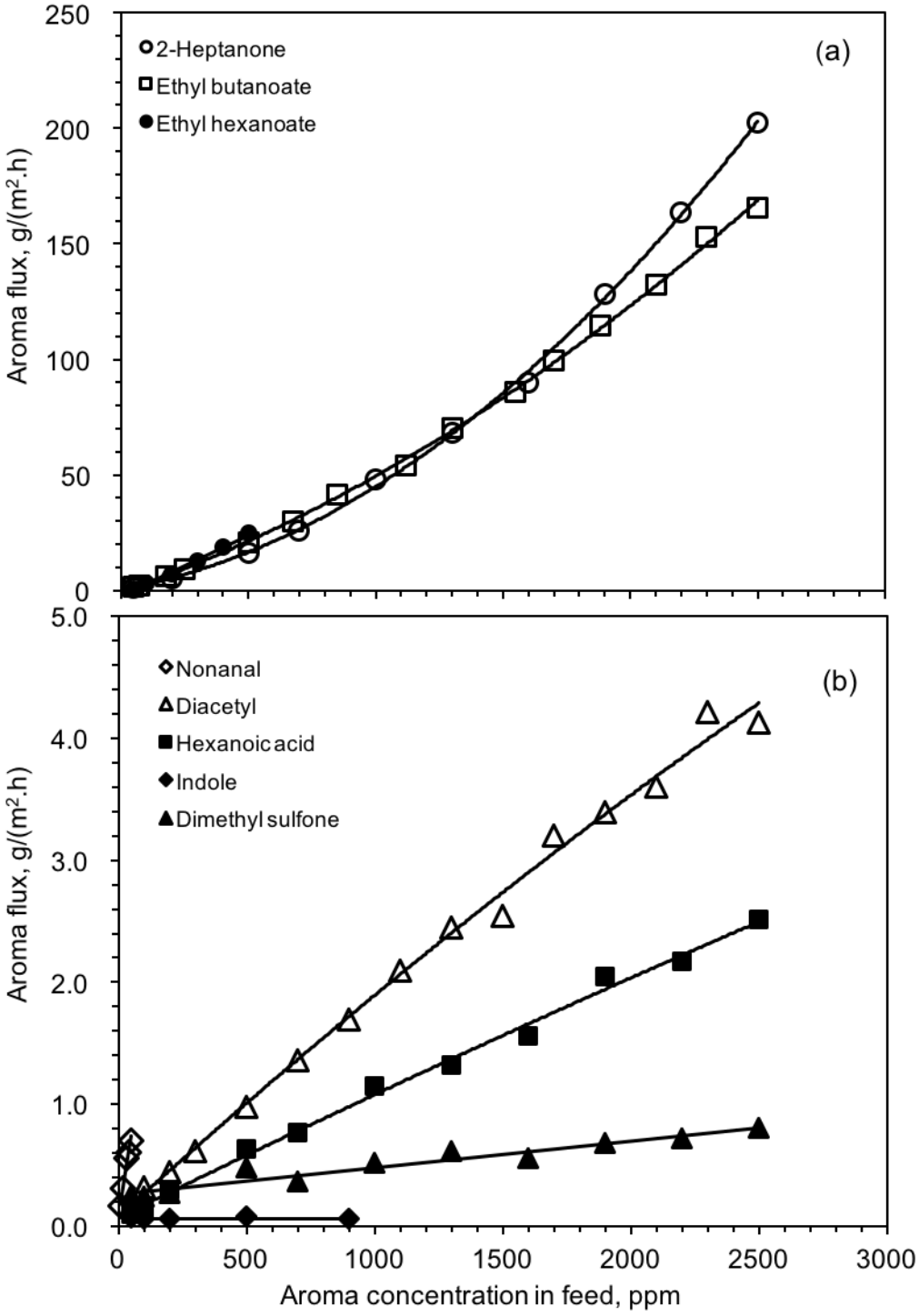

Figure 3.2 Effect of aroma concentration in binary feed solution (aroma + water) on the flux of (a) 2-heptanone, ethyl butanoate and ethyl hexanoate; (b) nonanal, diacetyl, hexanoic acid, indole and dimethyl sulfone. Temperature 36 °C, and permeate pressure 400 Pa.

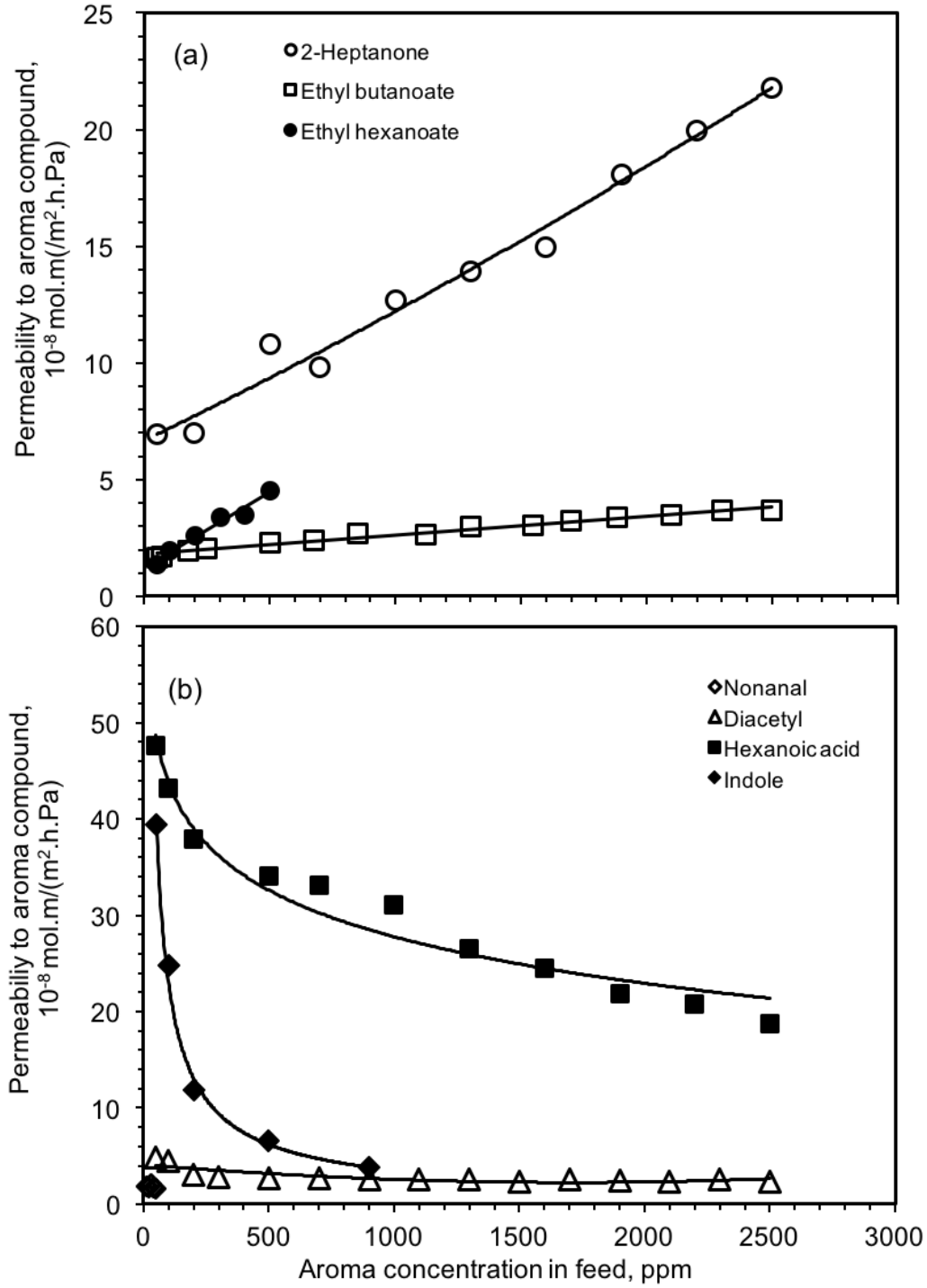

Figure 3.3 Aroma permeability in the membrane for pervaporation of binary aroma + water solutions. (a) 2-heptanone, ethyl butanoate and ethyl hexanoate; (b) nonanal, diacetyl, hexanoic acid and indole. Temperature 36 °C, and permeate pressure 400 Pa.

According to the solution-diffusion model, the permeability coefficient is equal to the product of the solubility coefficient and the diffusion coefficient. In general, in dilute organic-water mixture, the feed concentration does not significantly affect the solubility coefficient of organic component (Lamer et al., 1994; Trifunovic and Tragardh, 2003). The diffusion coefficient of a permeant in a polymer is generally concentration-dependent. Some studies suggested using linear and exponential (Brun et al., 1985; Mujiburohman and Feng, 2007b; Rautenbach and Albrecht, 1985) correlations to describe the concentration dependency of the diffusivity. Normally, the diffusivity increases with an increase in feed concentration. In our study, the increase in the permeabilities for ethyl butanoate, ethyl hexanoate and 2-heptanone is possibly due to their increasing diffusivities in the membrane. Trifunovic et al. (2006) also found that the diffusivities of highly hydrophobic organic compounds, e.g., esters and ketones with large molecular weights, increased when their feed concentration increased. For the other four aromas, the reduction in the their permeability may be caused by the clustering effect between aroma compounds and water due to their proton donating power (Trifunovic and Tragardh, 2006). At a higher aroma concentration in feed, more clusters of the molecules may form, which may not significantly affect the aroma solubility in the membrane but may decrease the aroma diffusivity in the membrane.

To better understand the root cause for concentration dependencies of aroma fluxes, the driving force and the membrane permeability were considered separately. The increase in aroma fluxes as feed aroma concentration increased was attributed to the increase in the driving force for aroma permeation and/or membrane permeabilities. Figure 3.4 compares the contributions of this two factors to the enhancement in aroma flux. In Figure 3.4, J is aroma flux, DF is the driving force for aroma permeation, P is the permeability to aroma, subscripts

$_h$ and $_l$ represent a relatively high feed concentration (50 ppm for nonanal, 500 ppm for the other aromas) and the lowest feed concentration used in this study (10 ppm for nonanal, 50 ppm for the other aromas). The ratio of J_h/J_l represents the increase in aroma flux when the aroma concentration increased, DF_h/DF_l and P_h/P_l represent the corresponding increases in permeation driving force and permeability to aroma, respectively. It can be seen that when feed aroma concentration increased from 50 ppm to 500 ppm (or from 10 ppm to 50 ppm for nonanal), there was a 7-10 fold increase in the driving force for aroma permeation, while the membrane permeabilities to ethyl hexanoate, ethyl butanoate and 2-heptanone only increased by 1.3-2.6 folds, while membrane permeabilities to other aromas decreased. This indicates that the driving force for aroma permeation contributed more than membrane permeability to the increased aroma flux with an increase in the feed aroma concentration.

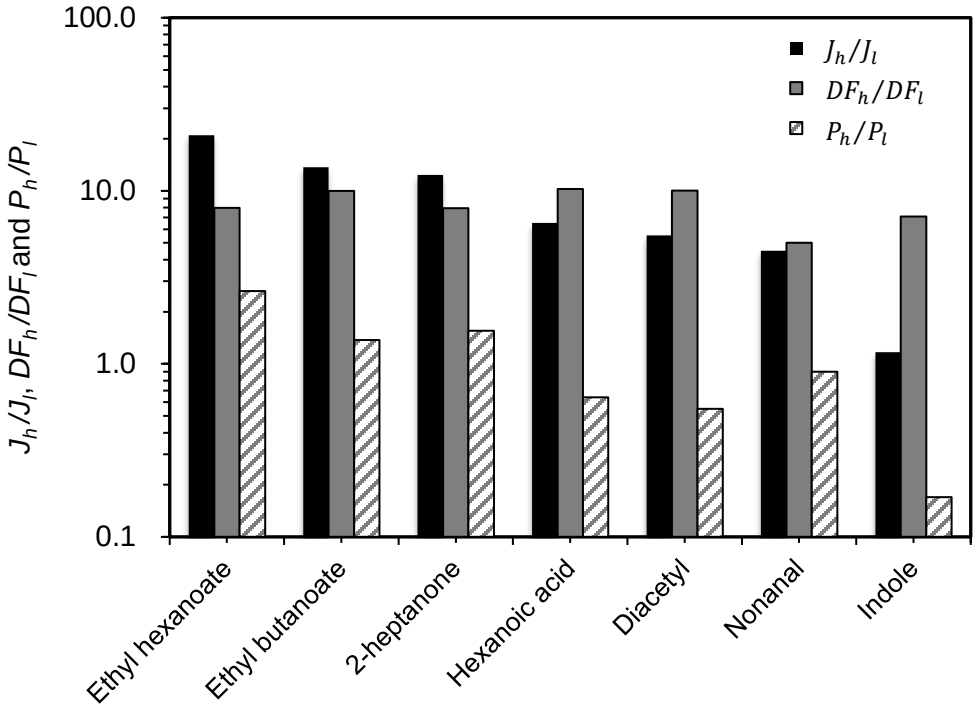

Figure 3.4 Ratios of J_h/J_l, DF_h/DF_l and P_h/P_l for the permeation of aroma compounds, where J is aroma flux, DF is driving force for permeation, P is permeability to aroma, subscripts $_h$ and $_l$ represent a relatively high feed concentration (50 ppm for nonanal, 500 ppm for the other aromas) and the lowest feed concentration used in this study (10 ppm for nonanal, 50 ppm for the other aromas).Temperature 36 ºC. Permeate pressure 400 Pa.

For water permeation, as shown in Figure 3.5, water was basically independent of feed aroma concentration within the feed concentration range studied, except for the 2-heptanone + water feed mixture, where an increase in water flux was observed. This seems to indicate negligible membrane swelling by the aroma compounds. Similar observations with alcohol/water, aldehyde/water and ester/water separations at low feed concentrations have been reported by other researchers (Garcia et al., 2009; Martinez et al., 2013; Niemistö et al., 2013). While for the pervaporative separation of 2-heptanone/water, with an increase in the feed aroma concentration from 50 to 2500 ppm, the corresponding water fluxes increased from 190 to 240 g/m^2h. Figure 3.6 shows the water permeability as a function of aroma concentration in the feed. The variation in water permeability was very consistent with the variation in the water flux. This is reasonable because all the model feeds are dilute aqueous solutions, a change in feed aroma concentration did not affect the driving force for water permeation considerably. In addition, when 2-heptanone concentration in feed increased, the increase in water permeability further confirms that 2-heptanone tended to swell the PEBA membrane, thereby enlarging the free volume of the polymer matrix and promoting the permeation of water molecules through the membrane.

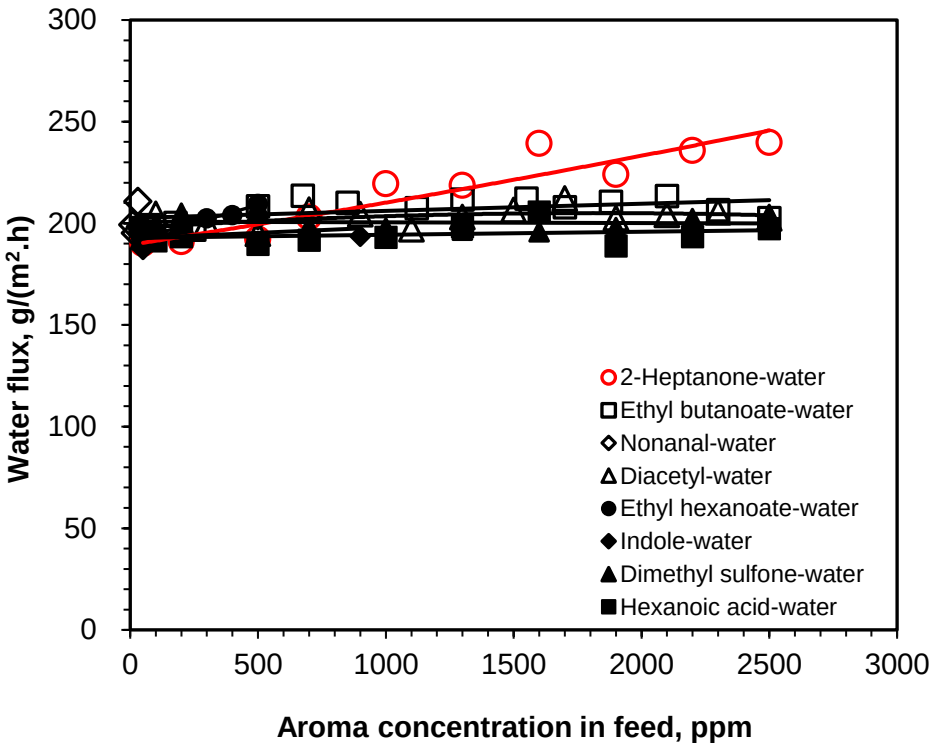

Figure 3.5 Effects of feed aroma concentration on water flux. Temperature: 36 °C. Permeate pressure: 400 Pa.

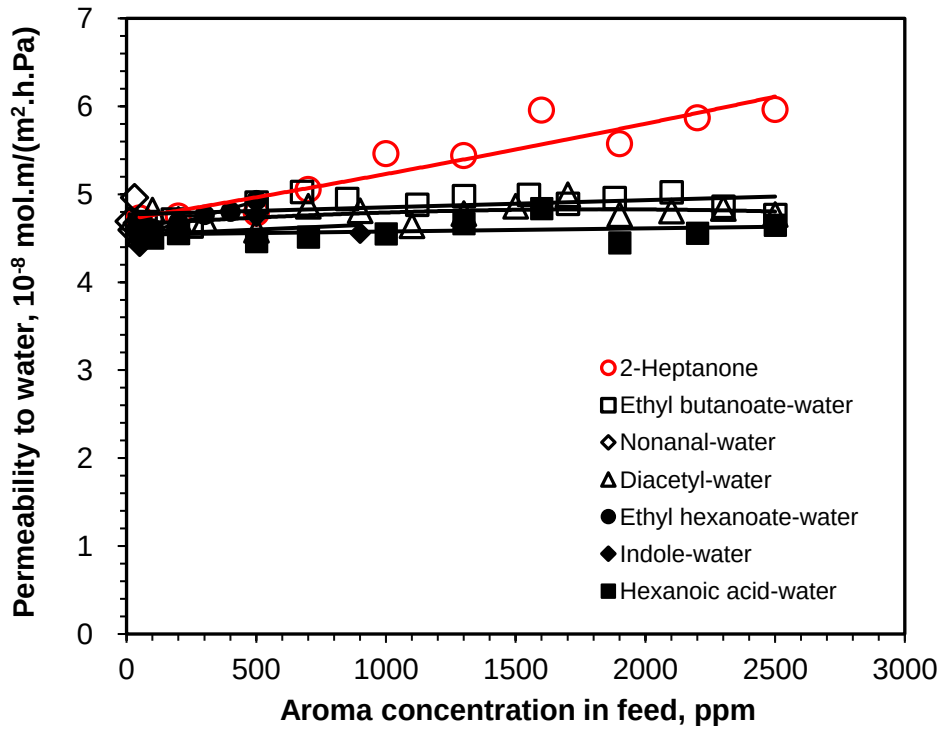

Figure 3.6 Effects of feed aroma concentration on membrane permeability to water. Temperature: 36 °C. Permeate pressure: 400 Pa.

Figure 3.7 shows the enrichment factors for the eight aromas at different feed concentrations. It is clear that 2-heptanone, ethyl butanoate, ethyl hexanoate and nonanal were better enriched than the other four aromas, which is consistent with the sequence of the aroma fluxes. In addition, the enrichment factors of 2-heptanone, ethyl butanoate and ethyl hexanoate increased with an increase in the feed aroma concentration. The increasing trend for nonanal enrichment was not obvious because of the narrow feed concentration range (10-50 ppm) studied. At low feed concentrations ($\leq$ 180 ppm), ethyl butanoate has the highest enrichment factor (153-173) among the eight aromas. At a feed concentration higher than 200 ppm, the enrichment factor of ethyl hexanoate exceeded that of ethyl butanoate. On the other hand, diacetyl, hexanoic acid, dimethyl sulfone and indole had relatively low enrichment factors, and their enrichment factors declined with an increase in their concentrations in the feed. The pervaporative recovery of indole was the worst as compared to the recovery of the other aromas using the PEBA 2533 membrane. In a feed concentration range of 50-900 ppm, indole enrichment factor varied between 0.33 and 7.34. An enrichment factor of less than 1 means the aroma was not enriched in the permeate at all because the permeate concentration was lower than the feed aroma concentration. Overall, the variations in the enrichment factor became less drastic at higher aroma concentrations in the feed, generally above 1000 ppm.

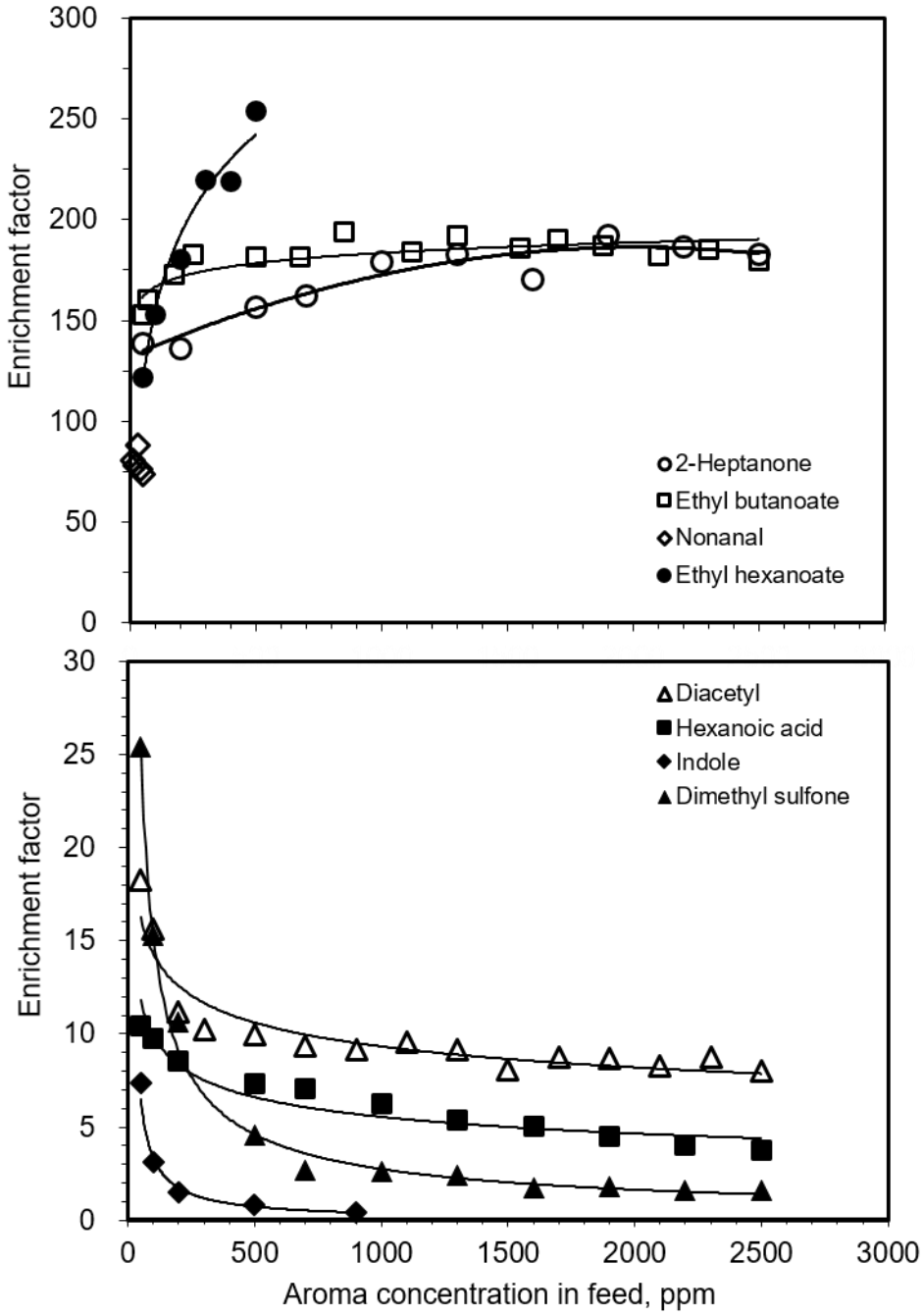

Figure 3.7 Effect of aroma concentration in feed on enrichment factor for recovery of aromas from binary feed solutions. Temperature: 36 °C. Permeate pressure: 400 Pa.

3.3.2 Effect of operating temperature

The effects of temperature on permeation flux, membrane permeability and enrichment factor for all the eight aroma compounds were investigated in this part of study. Single aroma-water pervaporation experiments were carried out at a fixed permeate pressure of 400 Pa and different feed aroma concentrations based on their solubility limits in water (50, 500, 1000, 2500 ppm for the permeation of diacetyl-water, ethyl butanoate-water, 2-hepatnone-water, hexanoic-water and dimethyl sulfone-water; 50, 100, 300, 500 ppm for the permeation of ethyl hexanoate-water; 50, 100, 200, 900 ppm for the permeation of indole-water; and 10, 30, 50 ppm for the permeation of nonanal-water). The operating temperature was varied from 25 to 65 °C, which was sufficiently below the boiling points of all the aromas. Relatively low temperatures are preferred to reduce energy cost and to protect the natural aroma properties of the aroma compounds.

As mentioned in Chapter 2, the temperature dependencies of permeation flux and permeability normally follow an Arrhenius-type equation, i.e.

$$J_i = J_{io}\exp(-\frac{E_{Ji}}{RT}) \tag{3.1}$$

$$P_i = P_{io}\exp(-\frac{E_{Pi}}{RT}) \tag{3.2}$$

where J_i is the permeation flux, J_{io} and P_{io} are pre-exponential factors, E_{Ji} is the apparent activation energy of permeation and T is the absolute temperature, P_i is the membrane permeability, E_{Pi} is the activation energy corresponding to permeability. The effects of temperature on the permeation fluxes of water and the eight aroma compounds were plotted, as shown in Figure 3.8 and Figure 3.9. Both the water flux and the aroma flux increased significantly with an increase in temperature. This is mainly because of the increased partial

vapor pressures of water and aroma on the feed side, resulting in higher driving forces for the permeation of water and aroma. It can be seen in Figure 3.8, in the permeation of aromas-water, water flux increased exponentially from around 100 to 1000 g/(m^2.h) as temperature increased from 25 to 65 ºC.

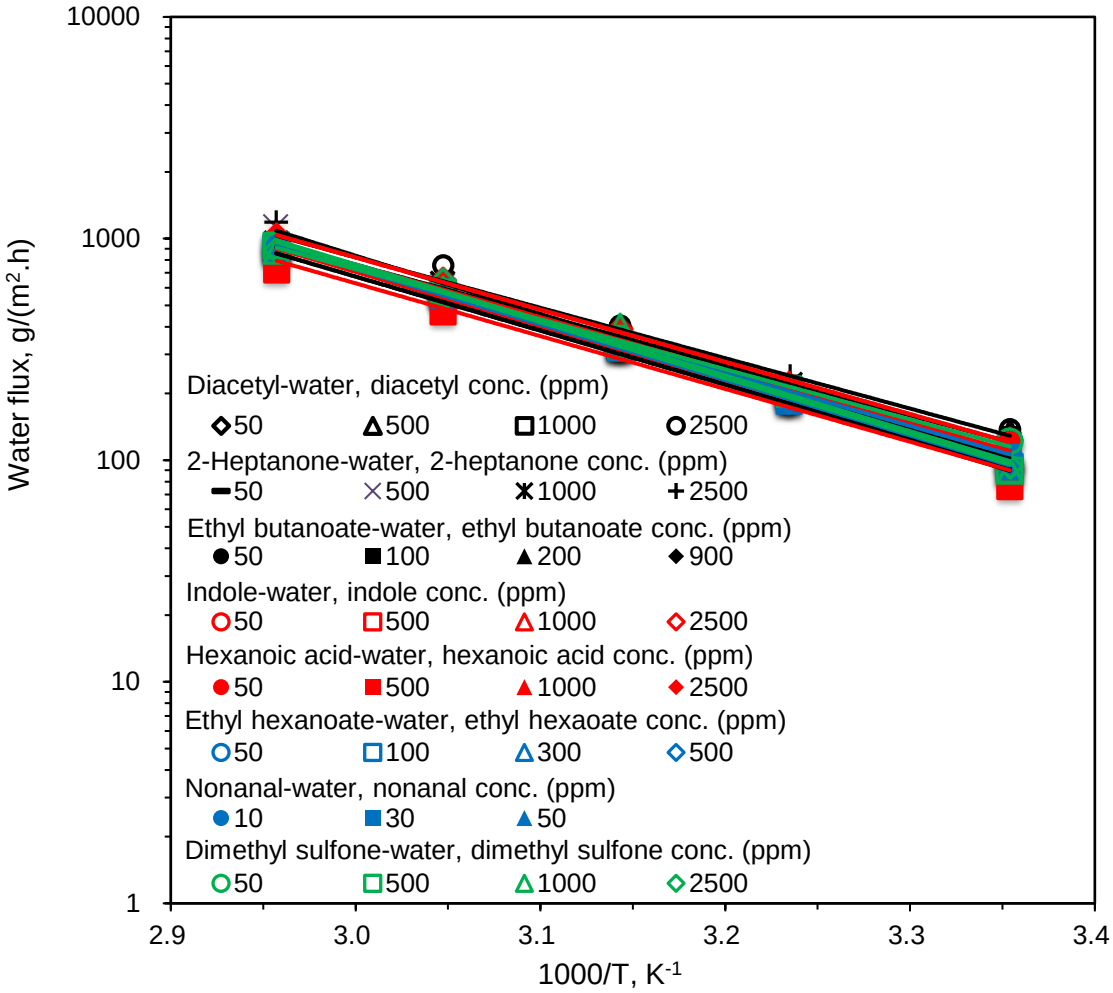

Figure 3.8 Effect of temperature on water flux during the permeation of aromas-water at different feed aroma concentrations and a permeate pressure of 400 Pa.

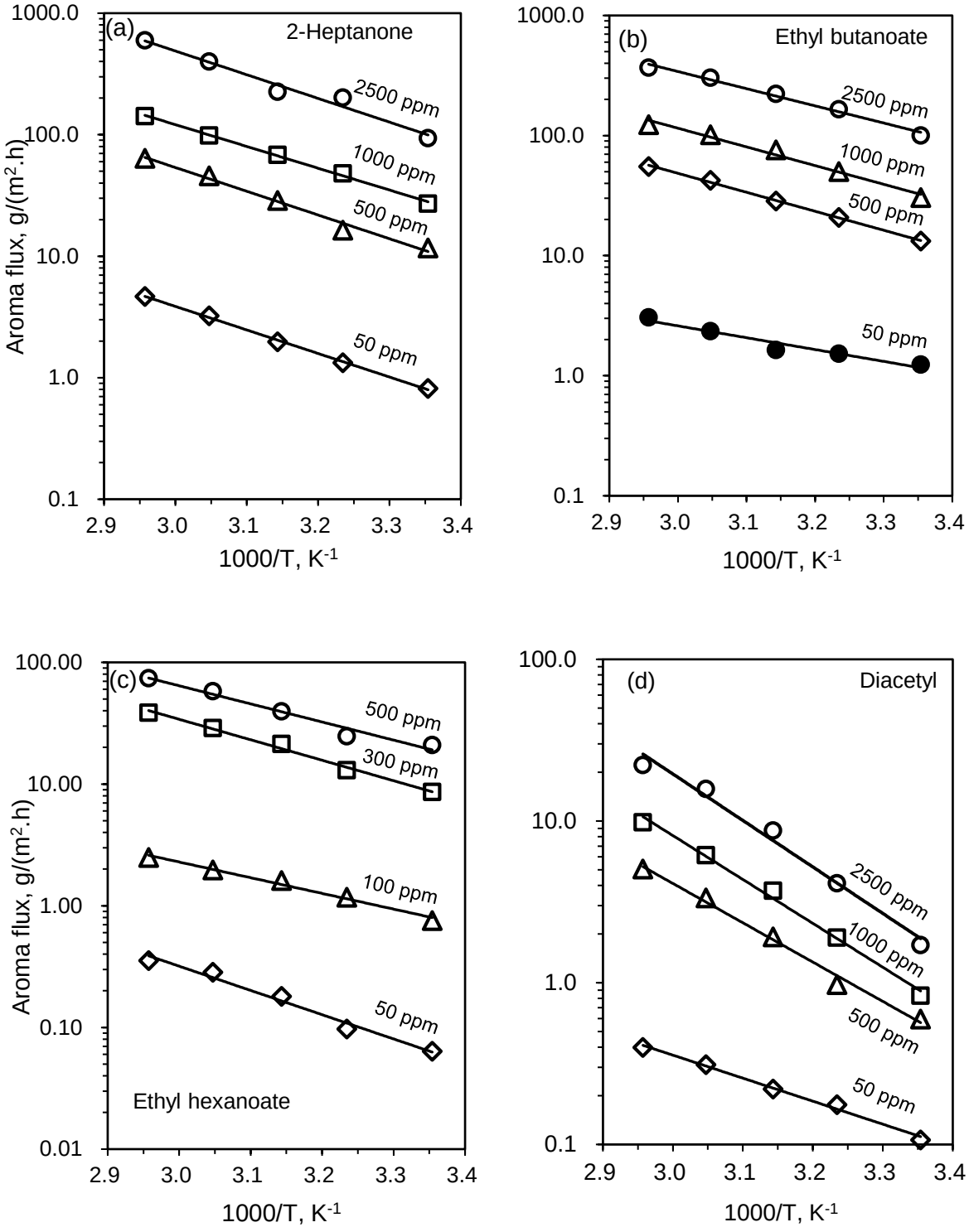
(a)
2-Heptanone
2500 ppm
1000 ppm
500 ppm
50 ppm
Aroma flux, g/(m².h)
1000/T, K-1
(b)
Ethyl butanoate
2500 ppm
1000 ppm
500 ppm
50 ppm
1000/T, K-1
(c)
500 ppm
300 ppm
100 ppm
50 ppm
Ethyl hexanoate
Aroma flux, g/(m².h)
1000/T, K-1
(d)
Diacetyl
2500 ppm
1000 ppm
500 ppm
50 ppm
1000/T, K-1

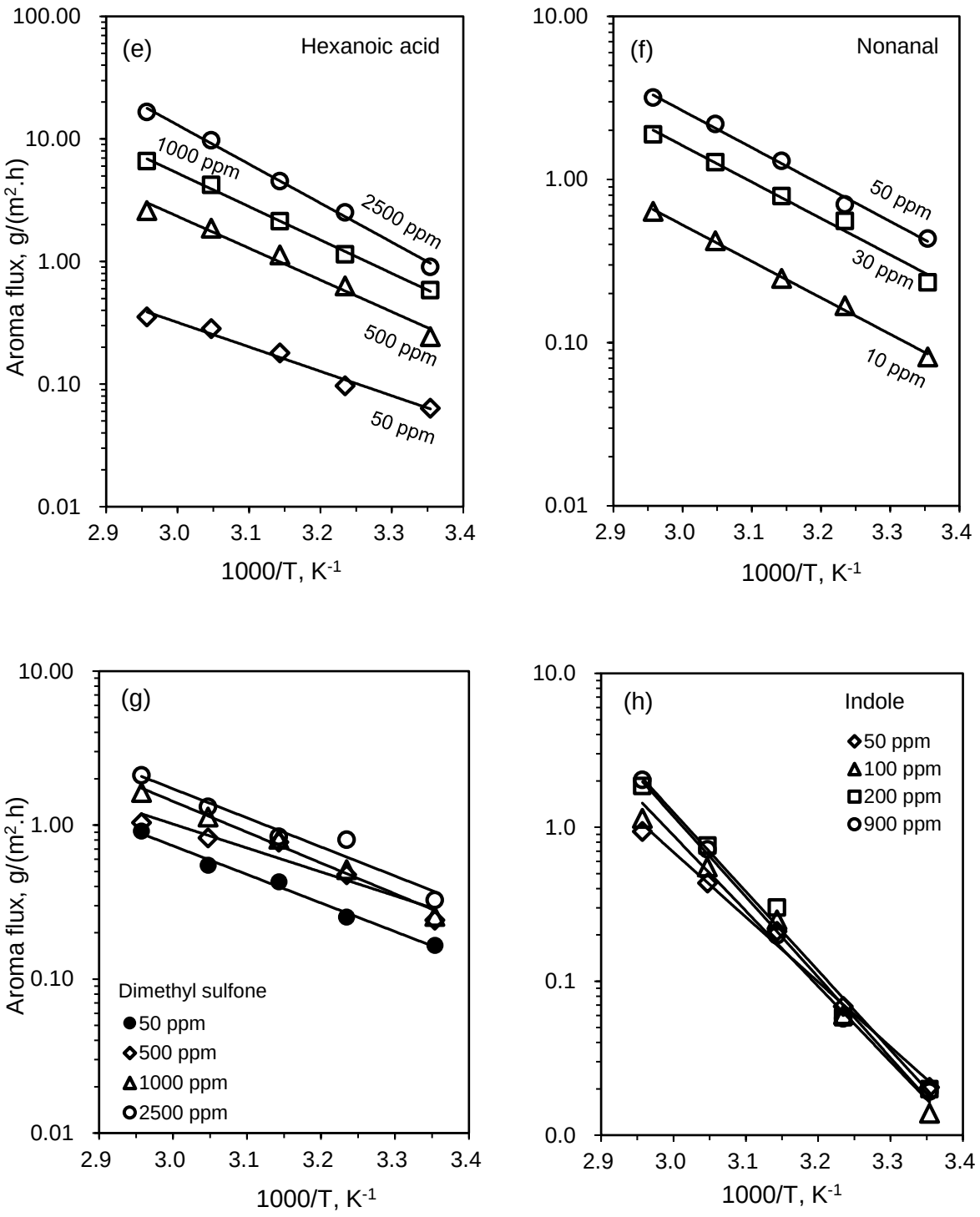

Figure 3.9 Effect of temperature on the permeation flux of, (a) 2-heptanone, (b) ethyl butanoate, (d) diacetyl, (c) ethyl hexanoate, (e) hexanoic acid, (f) nonanal, (g) dimethyl sulfone and (h) indole at different feed aroma concentrations and a permeate pressure of 400 Pa.

The apparent activation energy (E_{Ji}) for aroma compounds and water permeation at various feed concentrations were calculated from the slope of the plots (Figure 3.9), E_{Ji} describes the overall effect of temperature on permeation flux, and it has accounted for temperature effects on membrane permeability and permeation driving force. A high activation energy indicates the permeation flux is sensitive towards a temperature change. The E_{Ji} for aroma and water permeation at different aroma concentrations are listed in Table 3.4. At a low feed concentration of 50 ppm, the calculated apparent activation energy for the permeation of aromas (E_{Ja}) follows the order of indole > nonanal > hexanoic acid > 2-heptanone > dimethyl sulfone > ethyl hexanoate > diacetyl > ethyl butanoate. As the feed aroma concentration increased, the E_{Ja} values of indole, hexanoic acid and diacetyl increased significantly. As discussed in Section 3.3.1, when the concentration of these aroma compounds present in feed increased, more water-diacetyl, water-hexanoic acid and water-indole clusters may be formed, which resulted in a greater energy barrier for the permeation of the aroma. For the other four aromas, the E_{Ja} values showed little changes as aroma concentration in feed varied. The apparent activation energy for water permeation (E_{Jw}) was relatively constant for the different aroma-water systems at different feed aroma concentrations, and all the E_{Jw} values for water permeation were in the range of 42.3-50.3 kJ/mol.

Table 3.4 Apparent activation energy for the permeation of aromas (E_{Ja}) and water (E_{Jw}) based on permeation flux, activation energy based on the permeability coefficients of aromas (E_{Pa}) and water (E_{Pw}), and the B_i values characterizing the temperature dependency of permeation driving force for aromas (B_a) and water (B_w) at different feed aroma concentrations (C_a).

	C_a, ppm	E_{Ja}	E_{Pa}	B_a	E_{Jw}	E_{Pw}	B_w
Diacetyl-water	50	27.3	-16.4	43.6	45.2	1.6	43.6
	500	46.6	3.1	43.4	43.3	-0.3	43.6
	1000	52.0	8.6	43.4	42.4	-1.2	43.6
	2500	55.0	11.6	43.4	43.5	-0.1	43.6
Ethyl butanoate-water	50	27.0	-8.3	35.3	43.3	-0.3	43.6
	500	30.3	-5.1	35.4	42.3	-1.3	43.6
	1000	29.8	-5.6	35.4	45.0	0.4	44.6
	2500	27.4	-8.0	35.4	48.1	2.6	45.5
2-Heptanone-water	50	37.1	-8.5	43.9	46.7	3.2	43.5
	500	37.4	-8.5	43.9	47.8	4.3	43.5
	1000	34.3	-6.6	44.0	44.9	1.3	43.6
	2500	37.4	-6.9	44.3	50.3	6.8	43.5
Hexanoic acid-water	50	40.5	-31.1	71.6	46.8	3.3	43.6
	500	49.4	-17.3	66.7	45.6	2.0	43.6
	1000	53.2	-11.9	65.1	45.4	1.9	43.6
	2500	62.5	-1.2	63.7	45.1	1.5	43.6
Ethyl hexanoate-water	50	31.0	-12.5	43.5	47.9	4.3	43.5
	100	32.6	-10.9	43.5	48.1	4.5	43.5
	300	32.2	-11.4	43.6	47.5	4.0	43.6
	500	28.4	-15.1	43.6	47.0	3.4	43.5
Nonanal-water	10	42.7	-3.8	46.5	47.2	3.6	43.6
	30	43.3	-3.1	46.4	45.6	2.0	43.6
	50	41.4	-5.0	46.4	46.2	2.6	43.6
Indole -water	50	80.7	21.6	57.6	47.0	3.4	43.6
	100	93.8	35.9	57.6	48.7	5.1	43.6
	200	98.5	40.9	57.7	46.5	2.9	43.6
	900	100.2	42.6	57.6	47.3	3.8	43.5
Dimethyl sulfone-water [a]	50	35.5	-	-	43.3	-	-
	500	33.0	-	-	48.3	-	-
	1000	38.3	-	-	48.0	-	-
	2500	36.1	-	-	47.9	-	-

[a] The E_{Pa}, E_{Pw}, B_a and B_w for the dimethyl sulfone-water system were not available due to the lack of the data of activity coefficient of dimethyl sulfone in its dilute aqueous solution.

According to Feng and Huang (1996), it is the activation energy E_{Pi} (which characterizes the temperature effect on the intrinsic permeability of the membrane), rather than the apparent activation energy (E_{Ji}), that truly represents the activation energy for permeation in the membrane. E_{Pi} can be estimated by subtracting the heat of evaporation (ΔH_{Vi}) of the permeant from E_{Ji} when the activity coefficients of the permeating species are not significantly affected by temperature change or when the activity coefficients are not readily available. In this study, however, the activity coefficients of the aroma compounds change considerably with temperature because of the dilute solutions involved, as shown in Appendix A. Therefore, we directly calculated E_{Pi} from the slope of permeability (P_i) vs. 1000/T based on Equation 3.2. The effects of temperature on permeation driving force (DF_i) for the aromas and water molecules can also be approximated by an Arrhenius-type equation:

$$DF_i = DF_{io}\exp(-\frac{B_i}{RT}) \tag{3.3}$$

where DF_{io} is a pre-exponential factor, $B_i$value characterizes the temperature dependence of the permeation driving force. Therefore,

$$E_{Ji} = E_{Pi} + B_i \tag{3.4}$$

The calculated E_{Pi} and B_i $\left(= E_{Ji} - E_{Pi}\right)$ values for aroma compounds and water at different feed concentrations are listed in Table 3.4 as well.

It can be seen from Table 3.4 that at a low feed aroma concentration of 50 ppm, the E_{Pa} values for the aroma compounds are in the order of indole > nonanal > ethyl butanoate > 2-heptanone > ethyl hexanoate > diacetyl > hexanoic acid. The E_{Pw} values for water permeation were not affected significantly by the aromas present in feed. In general, the B_a and $B_w$values were significantly higher than the corresponding E_{Pa} and E_{Pw} values, which indicates that the increases in permeation

fluxes of aroma and water as a result of increased temperature are mainly attributed to the increased driving force for permeation.

As shown by the data presented in Table 3.4, among the aroma compounds (except for dimethyl sulfone, for which the aroma permeability cannot be evaluated due to the lack of activity coefficient at given concentrations and temperatures), only diacetyl (at 500-2500 ppm) and indole showed an increased permeability with temperature (positive E_{Pi} values), while the permeabilities of the other five aromas decreased with temperature (i.e., negative E_{Pi} values). By definition, E_{Pi} is equal to the activation energy of diffusion (E_{Di}) plus the enthalpy change of dissolution of the permeant in the membrane (ΔH_i) (Feng and Huang, 1996). E_{Di} is generally positive, because an increase in temperature generally enlarges the free volume in the polymer matrix and increases the diffusivity of a permeant (Kulkarni et al., 2003; Peng et al., 2003). However, ΔH_i is usually negative because of the exothermic sorption process (K. Liu et al., 2005), and the solubility generally decreases with an increase in temperature. It is the joint contributions of the two factors to the permeation process that determine whether the E_{Pi} is positive or negative. The negative values of E_{Pi} for ethyl butanoate, ethyl hexanoate, 2-heptanone, hexanoic acid, nonanal and diacetyl (at 50 ppm) appear to suggest that temperature has a greater impact on the sorption of these aroma compounds than on diffusion. On the contrary, the positive E_{Pi} values for diacetyl (500-2500 ppm), indole and water appear to show that the diffusion aspect was affected more significantly than sorption for these compounds.

The impact of temperature on enrichment factor depends on the apparent activation energy of the two components to be separated. As shown in Figure 3.10, ethyl butanoate, ethyl hexanoate, 2-heptanone, dimethyl sulfone and nonanal had lower enrichment factors at higher temperatures over all the concentration ranges studied here. This is because the apparent activation energies of

these aromas were lower than that of water (Table 3.4). In other words, the permeation of aroma was facilitated less significantly than water permeation when the feed temperature increased. In contrast, the enrichment factor of indole increased with temperature, in accord with its higher E_{Ja} than water (E_{Jw}). At a feed aroma concentration of 50 ppm, the enrichment factors of diacetyl and hexanoic acid increased with increasing temperature, but the opposite trend was observed when the feed concentration was significantly high. These trends are also consistent with the variation of E_{Ja} for diacetyl and hexanoic acid at different feed concentrations.

In general, PEBA 2533 showed a good performance for dairy aroma enrichment. PEBA 2533 compared favorably with other commonly used membranes, as shown in Table 3.5. One can see that, under similar operating conditions, PEBA 2533 performed better than PDMS, POMS, EVA and EPDM in terms of aroma flux, and it provided more balanced aroma enrichment for both oil- and water-based aroma components.

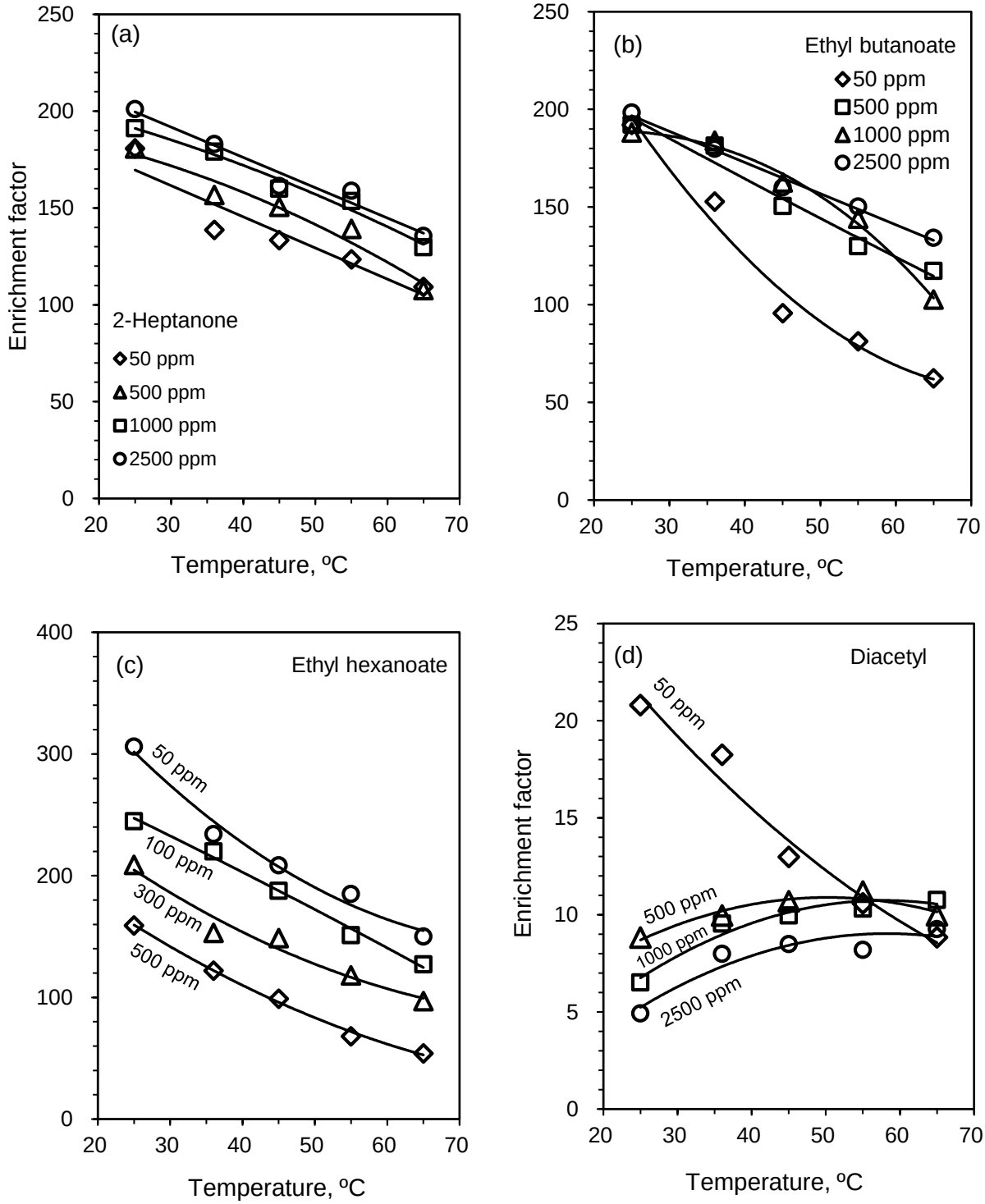
(a)
2-Heptanone
50 ppm
500 ppm
1000 ppm
2500 ppm
Enrichment factor
Temperature, ºC
(b)
Ethyl butanoate
50 ppm
500 ppm
1000 ppm
2500 ppm
Temperature, ºC
(c)
Ethyl hexanoate
50 ppm
100 ppm
300 ppm
500 ppm
Temperature, ºC
(d)
Diacetyl
50 ppm
500 ppm
1000 ppm
2500 ppm
Enrichment factor
Temperature, ºC

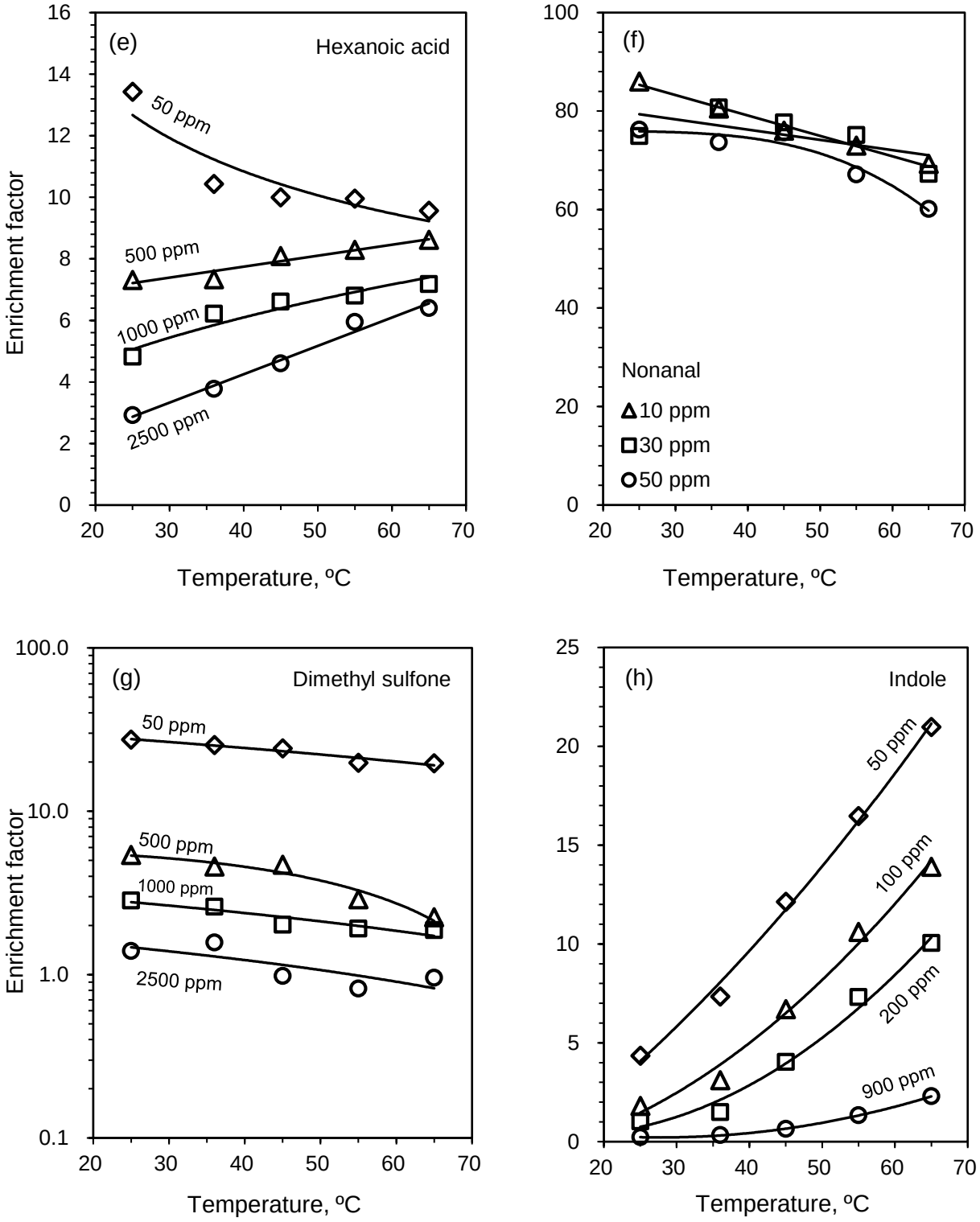

Figure 3.10 Effect of temperature on the enrichment factor of (a) diacetyl, (b) 2-heptanone, (c) ethyl butanoate, (d) ethyl hexanoate, (e) hexanoic acid, (f) nonanal, (g) dimethyl sulfone and (h) indole at different feed aroma concentrations. Permeate pressure: 400 Pa.

Table 3.5 Separation performances of membranes on recovery of aromas from their aqueous solutions.

Aroma	Membrane	T,ºC	X_{aroma}, ppm	J_{aroma}, g/(m^2.h)	β	Ref.
Ethyl butanoate	PDMS	35	100	-	158	(Djebbar, et al., 1998)
	POMS	35	300	0.01	118	(Sampranpiboon, et al., 2000)
	EVA	25	100	2	655	(Pereira, et al., 2005)
	EPDM	30	100	0.41	50	(Huang, et al., 2002)
	PEBA 2533	36	100	2.44	160	This study
Ethyl hexanoate	PDMS	25	100	-	213	(Pereira, et al., 2005)
	POMS	35	300	0.02	244	(Sampranpiboon, et al., 2000)
	PEBA 2533	36	100	3.04	154	This study
2-Heptanone	PDMS	30	100	0.03	18	(Overington, et al., 2008)
	POMS	30	100	0.04	23	(Overington, et al., 2008)
	PEBA 2533	36	100	2.65	138	This study
Diacetyl	PDMS	35	100	0.08	15	(Baudot and Marin, 1996)
	PEBA 2533	36	100	0.32	16	This study
Hexanoic acid	PDMS	30	100	0.09	2	(Overington, et al., 2008)
	POMS	30	100	0.09	2	(Overington, et al., 2008)
	PEBA 2533	36	100	0.2	10	This study

3.3.3 Recovery of aroma compounds from their multicomponent feed solutions

The pervaporation of multicomponent (multiple aroma compounds + water) feed solutions was carried out to determine whether there was a coupling effect among the permeating components. For this purpose, the pervaporation behavior was compared to the pervaporation performance of the binary feed solutions (i.e. a single aroma compound + water). The influence of feed concentration and temperature on the coupling effect was studied as well. Three multicomponent feed solutions with different aroma compositions (Table 3.6) were selected based on the aroma solubility in water. The operating temperature was in the range of 25-65 °C.

Table 3.6 Multicomponent feed solutions with different aroma compositions used in experiments

Concentration in feed (ppm)	Ethyl hexanoate	Ethyl butanoate	2-Heptanone	Diacetyl	Nonanal	Hexanoic acid	Indole	Dimethyl sulfone	Total aroma
Solution 1	50	50	50	50	10	50	50	50	360
Solution 2	100	500	500	500	15	500	100	500	2715
Solution 3	300	1000	1000	1000	30	1000	200	1000	5530

3.3.3.1 Coupling effect among permeating components

Pervaporation experiments with multicomponent feed solution 1 (nonanal, 10ppm; the other aroma compounds, 50 ppm each) were carried out at 36 °C. For convenience of comparison, the aroma flux for multi-component permeation was compared with the aroma flux for binary aroma-water feed solution at the same aroma concentration.

Figure 3.11 compares the fluxes of each aroma compound in binary and multicomponent feed solutions. It can be noted that the permeation fluxes of ethyl hexanoate, ethyl butanoate, 2-heptanone and nonanal in the multicomponent system were not significantly lower than their respective fluxes in their binary systems at the same concentrations. While the fluxes of the other four aromas, which were much less permeable, were decreased significantly by the presence of

other aroma compounds in the feed. This indicates that coupling effects among the aroma compounds exist in current system, and the slow-permeating components tended to be more sensitive than fast-permeating component to the coupling interactions among the permeating species.

The coupling effect may result from two aspects: a decreased aroma solubility or a decreased aroma diffusivity in the membrane. It may be perceived that the membrane had fixed adsorptive sites to organics, and thus adding other aroma compounds in feed could lead to competitive sorption of the aroma compounds in PEBA membrane, resulting in lower solubility of each aroma compound. Water permeation flux (195.5 $g/m^2.h$) was not significantly affected by the presence of multiple aromas in feed. It can thus be assumed that membrane structure and the free volume inside membrane did not change when multiple aromas were present. Therefore, after adding other aroma compounds to the feed, the competitive diffusion among aroma compounds inside the membrane could occur, leading to a lower diffusivity of each aroma compound (Berendsen et al., 2006). The enrichment factors of aroma compounds in the multicomponent feed solution were lower than those in their binary feeds, as presented in Figure 3.12.

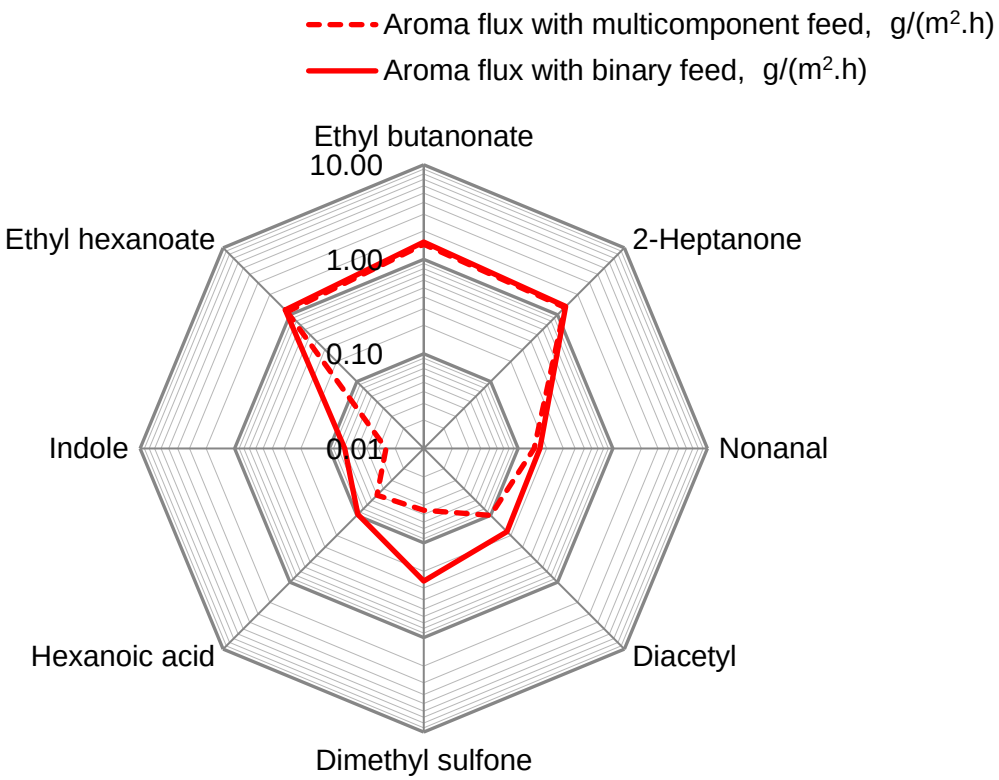

Figure 3.11 A comparison of aroma fluxes for binary (a single aroma + water) and multicomponent (multiple aromas + water) feed solutions. The multicomponent feed solution had a composition of 10 ppm nonanal and 50 ppm for the other seven aroma compounds. The individual aroma concentration in binary feed solutions was the same as that in the multicomponent feed solutions. Temperature: 36 °C. Permeate pressure: 400 Pa.

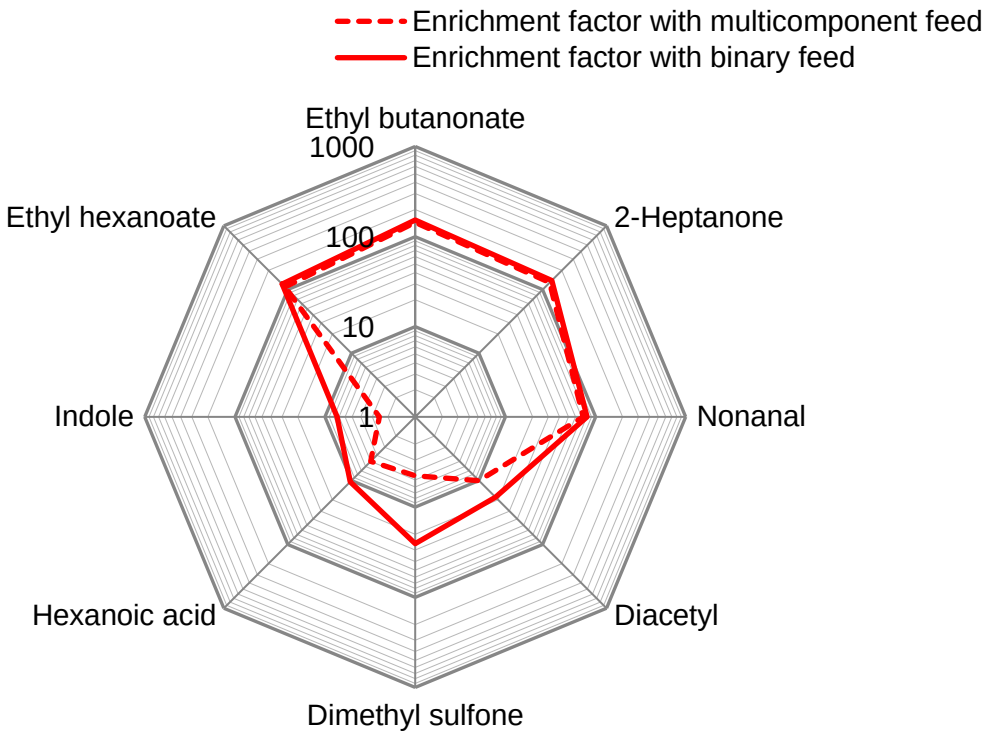

Figure 3.12 A comparison of aroma enrichment for binary (a single aroma + water) and multicomponent (multiple aromas + water) feed solutions. The multicomponent feed solution had a composition of 10 ppm nonanal and 50 ppm for the other seven aroma compounds. The individual aroma concentration in binary feed solutions was the same as that in the multicomponent feed solutions. Temperature: 36 °C. Permeate pressure: 400 Pa.

To quantify the coupling effect, Raisi et al. (2011) used the ratio of the flux of an aroma compound in the multicomponent mixture to its flux in the binary solution as a measure of the coupling. This ratio can be called as "coupling factor":

$$C_i = \frac{J_{im}}{J_{ib}} \tag{4.1}$$

where C_i is the coupling factor for component i, J_{im} is the permeation flux of aroma i in a multicomponent system, J_{ib} is the permeation flux of aroma i in its binary (aroma + water) feed solution.

A coupling factor of 1 indicates that there is no coupling between the compound of interest and other components in the multicomponent feed. A coupling factor higher than 1 indicates that

the permeation of a compound is enhanced by the presence of other components in the feed; a coupling factor lower than 1 indicates that the permeation of the compound is retarded by other compounds in the feed solution. Thus, the deviation of a coupling factor of an aroma compound from 1 represents the significance of the coupling effect. The coupling factors for all the eight aroma compounds with feed solution 1 are presented in Figure 3.13. Comparing to the other aromas, the flux of dimethyl sulfone was reduced most significantly due to the coupling effect (C_i = 0.18), followed by indole (C_i = 0.37), hexanoic acid (C_i = 0.52) and diacetyl (C_i = 0.57). The coupling factors of ethyl hexanoate, ethyl butanoate, 2-heptanone and nonanal were in the range of 0.87-0.94, indicating that there was only a small decrease in their fluxes as a result of the coupling effects among the aroma permeant in the multicomponent system.

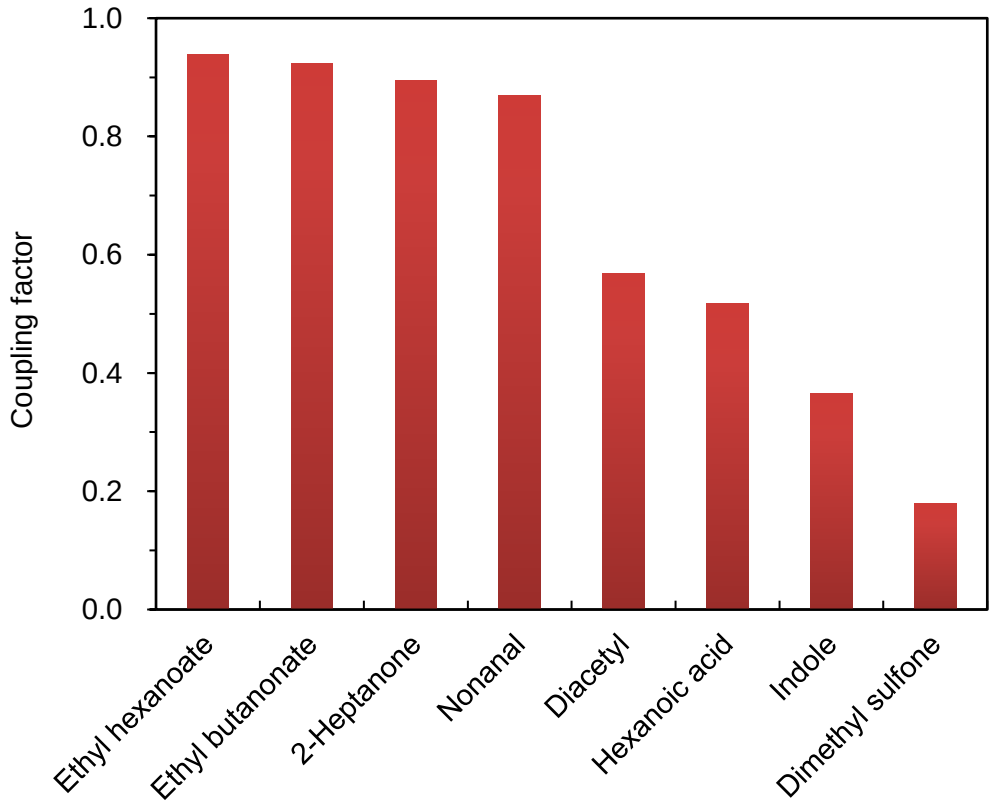

Figure 3.13 Coupling factors of aroma compounds. Feed composition: Solution 1 (composition shown in Table 3.6). Temperature 36 °C. Permeate pressure 400 Pa.

3.3.3.2 Influence of feed aroma concentration and temperature on coupling effect

As the concentration of each aroma compound increases, on one hand, the competition among aromas in terms of sorption into the membrane and diffusion through the membrane could be more intense, which could further reduce the coupling factors of the aroma components in the feed solution. On the other hand, the membrane was likely more swollen when more aroma compounds were sorbed into the membrane, which could lead to an enhancement in the coupling factors of the aroma compounds. Therefore, it was of interest to study the permeation behavior of aroma compounds when their concentrations were increased. The effects of temperature were also studied so as to determining how the coupling effects were influenced by the operating temperature.

The influences of feed aroma concentration and temperature on the coupling effects are shown in Figure 3.14. It can be seen that the coupling factors for all aroma compounds were smaller than 1, and with an increase in the aroma concentration in the feed solution, their coupling factors decreased significantly. This indicates that the competition among aroma compounds during the sorption and diffusion processes became more dramatic at higher aroma concentrations. Lipnizki and Hausmanns (2004) also found that the coupling factor depended on the feed concentration, and an increase in the concentrations of other aroma compounds in the feed increased the coupling effect on the permeation of 1-propanol. One should note that if the concentration of any component in the feed changes, the coupling factors of aromas are expected to change.

In general, the temperature dependence of the coupling factor was not significant for the permeation of ethyl hexanoate, ethyl butanoate, 2-heptanone, nonanal, dimethyl sulfone and indole. However, as the temperature increased from 25 to 65 °C, the coupling factors for diacetyl and hexanoic acid increased considerably. At a higher temperature, the diffusivity of the permeants

increased, but the solubility of the permeants decreased. The increase in coupling factors for diacetyl and hexanoic acid may be attributed to the joint effects of enhanced diffusivity and reduced solubility at different degrees.

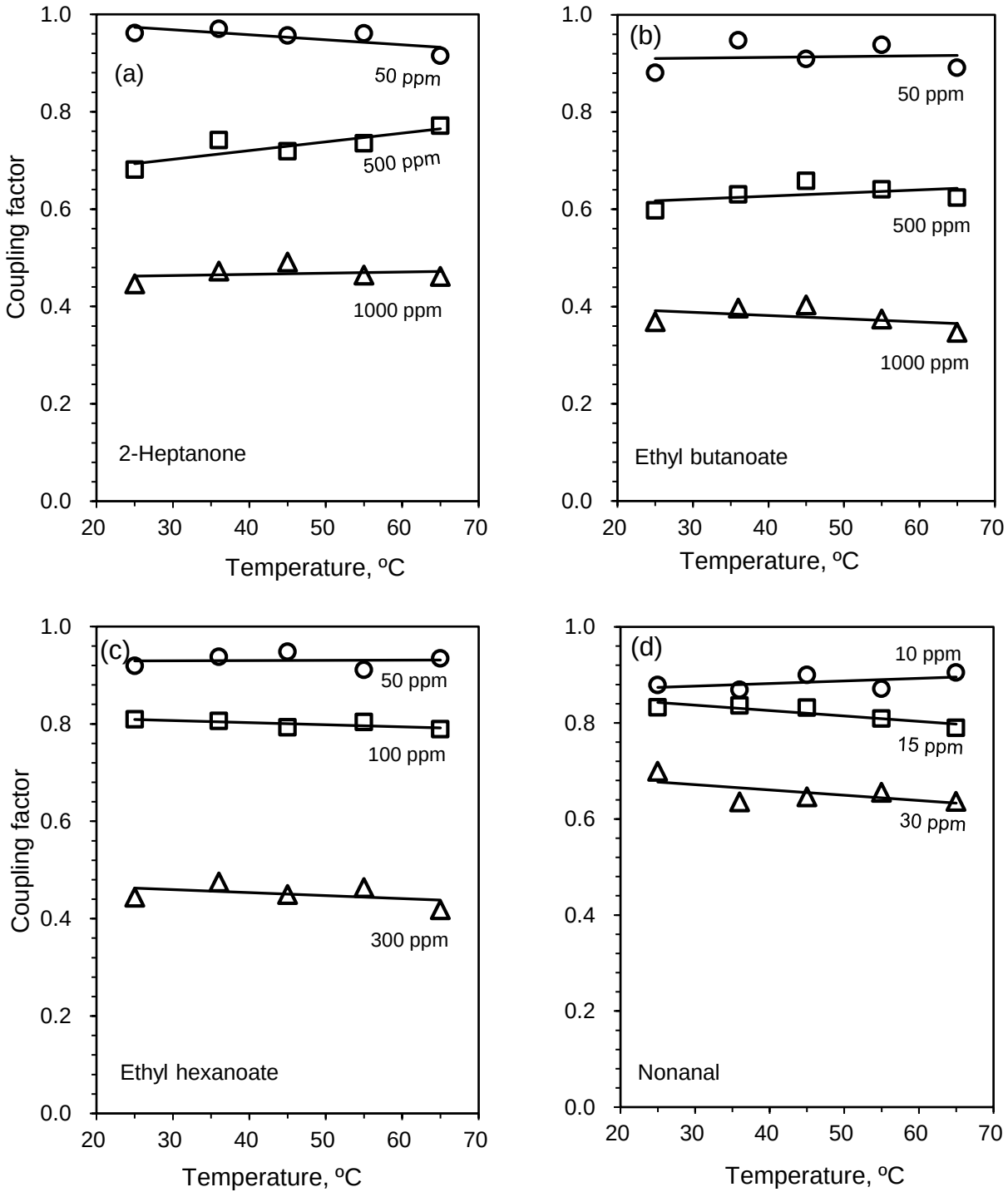

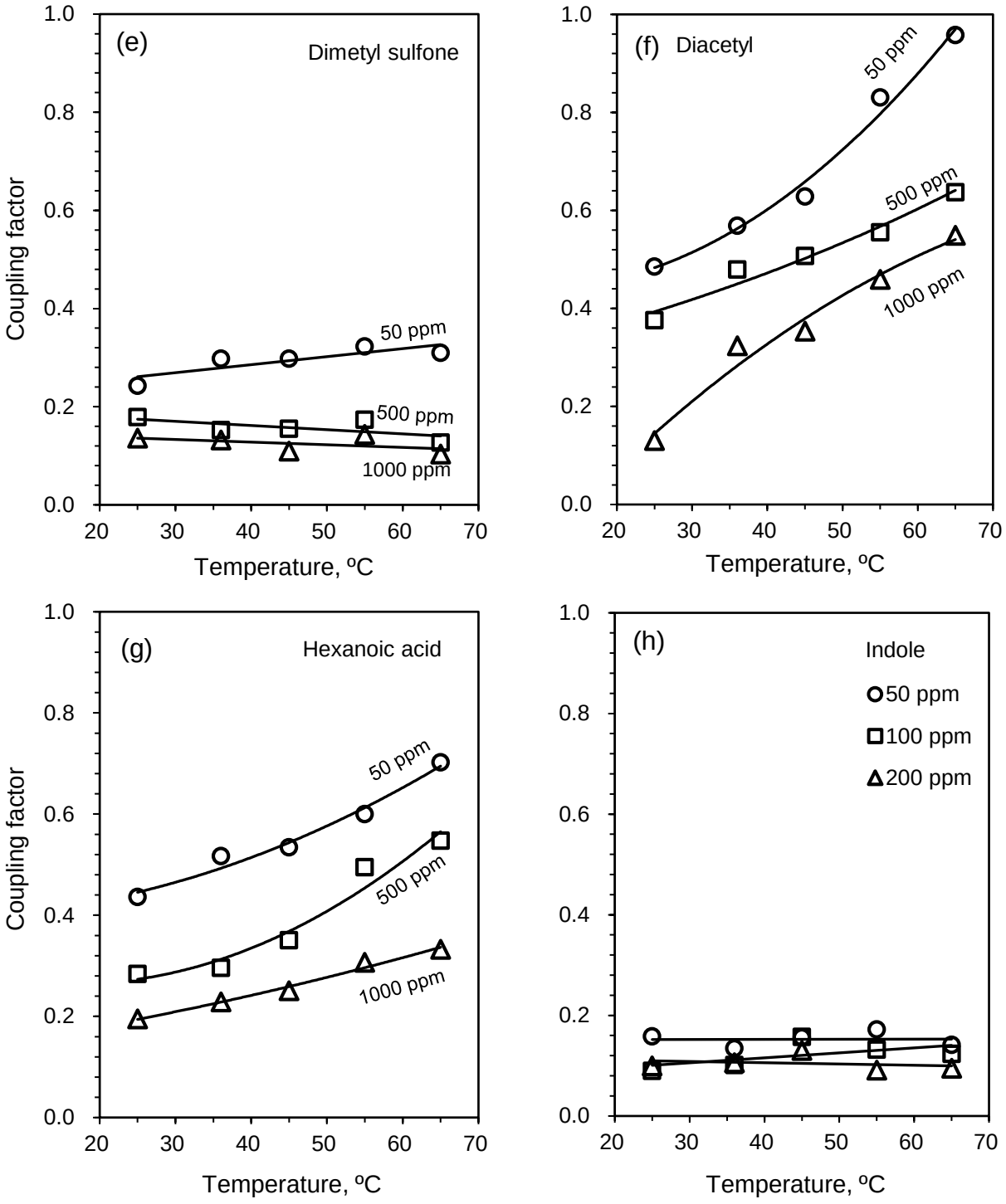

Figure 3.14 Effect of feed concentration and temperature on coupling factors for (a) 2-heptanone, (b) ethyl butanoate, (c) ethyl hexanoate, (d) nonanal, (e) dimethyl sulfone, (f) diacetyl, (g) hexanoic acid and (h) indole at a permeate pressure of 400 Pa.

3.4 Conclusions

In this part of the study, eight model aroma compounds were recovered from their binary and multicomponent feed solutions by pervaporation using PEBA 2533 membranes. The following conclusions can be drawn:

(1) PEBA 2533 was selective for the recovery of the aroma compounds studied here from their aqueous solutions. Volatile aroma compounds tended to have high permeation fluxes.

(2) With an increase in feed aroma concentration, aroma fluxes increased and the membrane permselectivity to the aroma compounds changed as well. The increase in aroma fluxes was mainly attributed to the increased driving force for permeation. The water flux was not significantly affected by the feed concentration, except for the 2-heptanone-water system, for which water flux increased with the aroma concentration in the feed.

(3) Increasing temperature increased both the aroma and water permeation fluxes significantly, and the temperature dependence could be described by the Arrhenius-type correlations.

(4) At low aroma concentrations (i.e., 50 ppm), the apparent activation energy for the permeation of aromas (E_{Ja}) was in the order of indole > nonanal > hexanoic acid > 2-heptanone > dimethyl sulfone > ethyl hexanoate > diacetyl > ethyl butanoate. As feed aroma concentration increased, the E_{Ja} values for indole, hexanoic acid and diacetyl increased significantly. The apparent activation energy for water permeation (E_{Jw}) was relatively constant for the different aroma-water systems at various feed concentrations, and all the E_{Jw} values for water permeation were in the range of 42.3-50.3 kJ/mol.

(5) There were coupling effects on the permeation of the aroma compounds in multiple aroma systems. In general, the permeation of an individual aroma compound decreased by the presence of other aroma compounds present in the feed.

(6) The coupling effect on the permeation of the aroma compounds depended on the aroma concentration in the feed and operating temperature. An increase in the feed aroma concentration generally increased the coupling effect among the aroma components. The coupling effects for the permeation of the aroma components were not significantly affected by temperature, except for the permeation of diacetyl and hexanoic acid, which experienced an increase in their coupling factors when the temperature was increased from 25 to 65 °C.

Chapter 4

Recovery of Dairy Aroma Compounds from Binary Aroma-Water Solutions by Pervaporation: Batch Operation

4.1 Introduction

In addition to continuous operation, batch operation of pervaporation was conducted in this study. For industrial application, a batch operation is sometimes preferred if the feed concentration of aroma compounds is relatively low (ppm levels) or the amount of feed solution is small. Generally, in lab scale, the batch process may run for several hours, and the permeate stream is continuously collected while the retentate stream is recycled back to the feed tank for further separation. As pervaporation proceeds, the feed aroma concentration decreases, while the aroma compounds recovered will be accumulated.

In this study, batch pervaporation experiments for five aroma compounds (ethyl butanoate, ethyl hexanoate, 2-heptanone, hexanoic acid and diacetyl) were conducted. The other three aroma compounds (nonanal, dimethyl sulfone and indole) were not selected in this part of study, because the solubility of nonanal in water is too low (< 0.1 g/Kg) and the permeation fluxes of dimethyl sulfone and indole were too small, which make them not perfect aroma candidates for modeling the batch pervaporation process. Three parameters (feed aroma concentration, overall aroma concentration in the accumulated permeate, and aroma recovery rate) were analyzed. Experimental results were fitted to the model proposed by Feng and Huang (1992) (see section 4.2).

As mentioned in previous chapters, organophilic membranes usually exhibit a high selectivity for aroma compounds from their aqueous solutions. In case of recovery of certain

aroma compounds, the permeate concentration attained can exceed their solubility limit in water, and thus the permeate stream will be spontaneously separated into two phases: an organic phase and an aqueous phase. Therefore, a calculation of the mass of aroma compound in the organic phase as a function of operating time was also attempted.

4.2 Modelling of batch pervaporation

In this study, we used the Feng and Huang model (1992) (equations 5.1-5.4) to simulate batch pervaporation:

$$t = \frac{F_0}{A}\int_X^{X_0} \frac{Y exp\left(-\int_X^{X_0} \frac{dX}{Y-X}\right)}{J(Y-X)} dX \tag{5.1}$$

$$Y_m = \frac{X_0 - X exp\left(-\int_X^{X_0} \frac{dX}{Y-X}\right)}{1 - exp\left(-\int_X^{X_0} \frac{dX}{Y-X}\right)} \tag{5.2}$$

$$M = F_0\left(1 - exp\left(-\int_X^{X_0} \frac{dX}{Y-X}\right)\right) \tag{5.3}$$

$$R_r = \frac{MY_m}{F_0X_0} = 1 - \frac{X}{X_0} exp\left(-\int_X^{X_0} \frac{dX}{Y-X}\right) \tag{5.4}$$

where t is the operating time; X_0 and F_0 are the initial aroma mass concentration in feed and the initial feed mass amount, respectively; A is the membrane area; X and Y are the instantaneous aroma mass concentration in the feed and in the permeate at a given time, respectively; J is the instantaneous aroma mass flux at a given time; Y_m and M are respectively

the overall aroma concentration and the total mass of the accumulated permeate at that time; R_r is the recovery rate of the aroma component at that time.

To use this model, the relationships $J - X$ and $Y - X$ are required, which can be obtained from steady state pervaporation with binary feed solutions at given concentrations (Chapter 3). They are listed in Table 4.1. From this information, the quantities *F*, *Y*, *J* and β (enrichment factor) as a function of batch processing time can be calculated. In this study *X*, Y_m and *R* are of particular interest as they represent the concentration of aroma in the aroma-enriched permeate product and the aroma recovery.

Table 4.1 Fitting equations used in the simulation of batch pervaporation

Aroma compounds	Equations of *J* (g/(m^2.h))	Equations of *Y* (ppm)	Range of *X* (ppm)
Diacetyl	$J = -10^{-7}X^2 + 0.002X$	$Y = -7 \times 10^{-4}X^2 + 9.9208X$	$50 < X < 2500$
Hexanoic acid	$J = 0.0036X^{0.8306}$	$Y = 22.342X^{0.7902}$	$50 < X < 2500$
Ethyl butanoate	$J = 1 \times 10^{-5}X^2 + 0.037X$	$Y = -0.0048X^2 + 194.08X$	$50 < X < 2500$
2-Heptanone	$J = 2 \times 10^{-5}X^2 + 0.021X$	$Y = 0.0078X^2 + 167.26X$	$50 < X < 2500$
Ethyl hexanoate	$J = 8 \times 10^{-5}X^2 + 0.022X$	$Y = 0.2292X^2 + 137.45X$	$50 < X < 320$

The mass of aroma (Q_a) in the organic phase of the accumulated permeate, if phase separation occurs, as a function of operating time was developed as well. Let S_a (g aroma/ g water) be the organic (aroma compound here) solubility in water at room temperature, and S_w (g water/g aroma) be the water solubility in the aroma at room temperature. When phase separation occurs, let Q_w be the mass of water in organic phase, and M_a be the mass of aroma compound in aqueous phase. The Q_w and M_a can be described as

$$Q_w = M_a S_w \tag{5.5}$$

$$M_a = (M - Q_a - Q_w)\frac{S_a}{1 + S_a} \tag{5.6}$$

On the basis of mass balance, the total mass of aroma compound in accumulated permeate product can be described as

$$MY_m = Q_a + M_a \tag{5.7}$$

Substituting Equations 5.5 and 5.6 into Equation 5.7, we obtain

$$Q_a = \frac{MY_m(1 + S_a) - MS_a}{1 - S_a S_w} \tag{5.8}$$

Then substituting Equations 5.2 and 5.3 into Equation 5.8, the accumulated mass of the organic phase in the permeate Q_a as a function of *X* and *Y* can be calculated

$$Q_a = \frac{F_0\left((X_0 + X_0S_a - S_a) - (X + XS_a - S_a)exp\left(-\int_X^{X_0}\frac{dX}{Y - X}\right)\right)}{1 - S_a S_w} \tag{5.10}$$

It should be noticed that this equation can be used only when the overall aroma concentration in the accumulated permeate (Y_m) is higher than $\frac{S_a}{1+S_a}$. When Y_m is lower than $\frac{S_a}{1+S_a}$, no phase separation will take place.

4.3 Experiments

4.3.1 Feed solutions

Binary aqueous feed solutions consisting of one of the dairy aroma compounds (i.e., ethyl butanoate, ethyl hexanoate, 2-heptanone, diacetyl, and hexanoic acid) were used as feed solutions in the batch pervaporation experiments. Based on the solubilities of the aroma compounds in water, the initial aroma concentrations were selected to be 2500 ppm for ethyl butanoate, 2-heptanone, diacetyl and hexanoic acid and 320 ppm for ethyl hexanoate. The volume of the initial feed solutions was 500 mL throughout the experiments. The solubilities of aroma compounds in water (S_a) and the solubility of water in aroma compounds (S_w) are listed in Table 4.2; the solubility of water in aroma compounds (S_w) were obtained using Aspen plus V8.0 UNIFAC equation.

Table 4.2 Aroma solubility in water and water solubility in aroma compounds at 25 °C.

Aromas	S_w [a] (g water/g aroma)	S_a (g aroma/g water)	Reference
Diacetyl	2.70×10^{-2}	2.50×10^{-1}	Yalkowsky et al. 2010
Hexanoic acid	1.00×10^{-1}	1.08×10^{-2}	Yalkowsky et al. 2010
Ethyl butanoate	1.30×10^{-2}	5.75×10^{-3}	Pereira et al. 2005
2-Heptanone	2.57×10^{-2}	4.30×10^{-3}	Kirk and Othmer 1981
Ethyl hexanoate	5.09×10^{-3}	4.60×10^{-4}	Pereira et al. 2005

Binary feed solutions were used instead of multicomponent feed solutions in the batch study considering the significant coupling effect among aroma compounds. The coupling effect will make it hard to model batch pervaporation because detailed information of aroma permeabilities during the entire course of batch pervaporation is unavailable at present.

4.3.2 Pervaporation procedures

The membranes used in this chapter were the same with those in Chapter 3. The operating conditions were the same as those in Chapter 3 (i.e., feed flow rate 1.14 L/min, feed temperature 36 °C and permeate pressure 400 Pa). Each batch operation was run for 9 hours. Two cold traps were installed in parallel to collect the permeate samples continuously. The permeate samples were collected in the cold trap on an hourly basis, and the aroma concentration in the permeate sample was used to approximate the instantaneous permeate concentration during the batch process. The variations in feed concentration during batch pervaporation was also monitored every half an hour. The aroma concentration in accumulated permeate and the aroma recovery rate were obtained from the mass and concentration of the permeate samples.

4.4 Results and discussion

4.4.1 Model validation and evaluation of aroma-water separation by batch pervaporation

The experimental results and model predictions for aroma recovery from aqueous solutions are plotted in Figures 4.1-4.4. The experimental data (symbols) agree with model calculations (lines) well. This indicates that the mathematical model and the fitting equations listed in Table 4.1 are adequate for batch pervaporation to extract aroma compounds from water.

Figure 4.1 shows how the concentration of aroma compound on the feed side decreased with batch time. The concentrations of ethyl butanoate, 2-heptanone and ethyl hexanoate declined quickly in the early period and the decrease became slower as pervaporation

proceeded. The decrease in the concentration of diacetyl and hexanoic acid in feed was much slower than ethyl butanoate, 2-heptanone and ethyl hexanoate. The rate of depletion in aroma compounds in the feed was in the order of 2-heptanone > ethyl butanoate > ethyl hexanoate > diacetyl > hexanoic acid. These results further illustrate that ester and ketone compounds normally have higher fluxes than acids.

The recovery rates of the aroma compounds as a function of operating time are plotted in Figure 4.2. The recovery rate is defined as the ratio of the total mass of aroma compound in the accumulated permeate to its initial mass in the feed. The increases in the recovery rates of ethyl butanoate, ethyl hexanoate and 2-heptanone were much faster than those of hexanoic acid and diacetyl. For a batch time of 10 hours, a high recovery rate of 78-88% was achieved for 2-heptanone, ethyl butanoate and ethyl hexanoate, while only 8-15% hexanoic acid and diacetyl were recovered in the permeate for the same period of time.

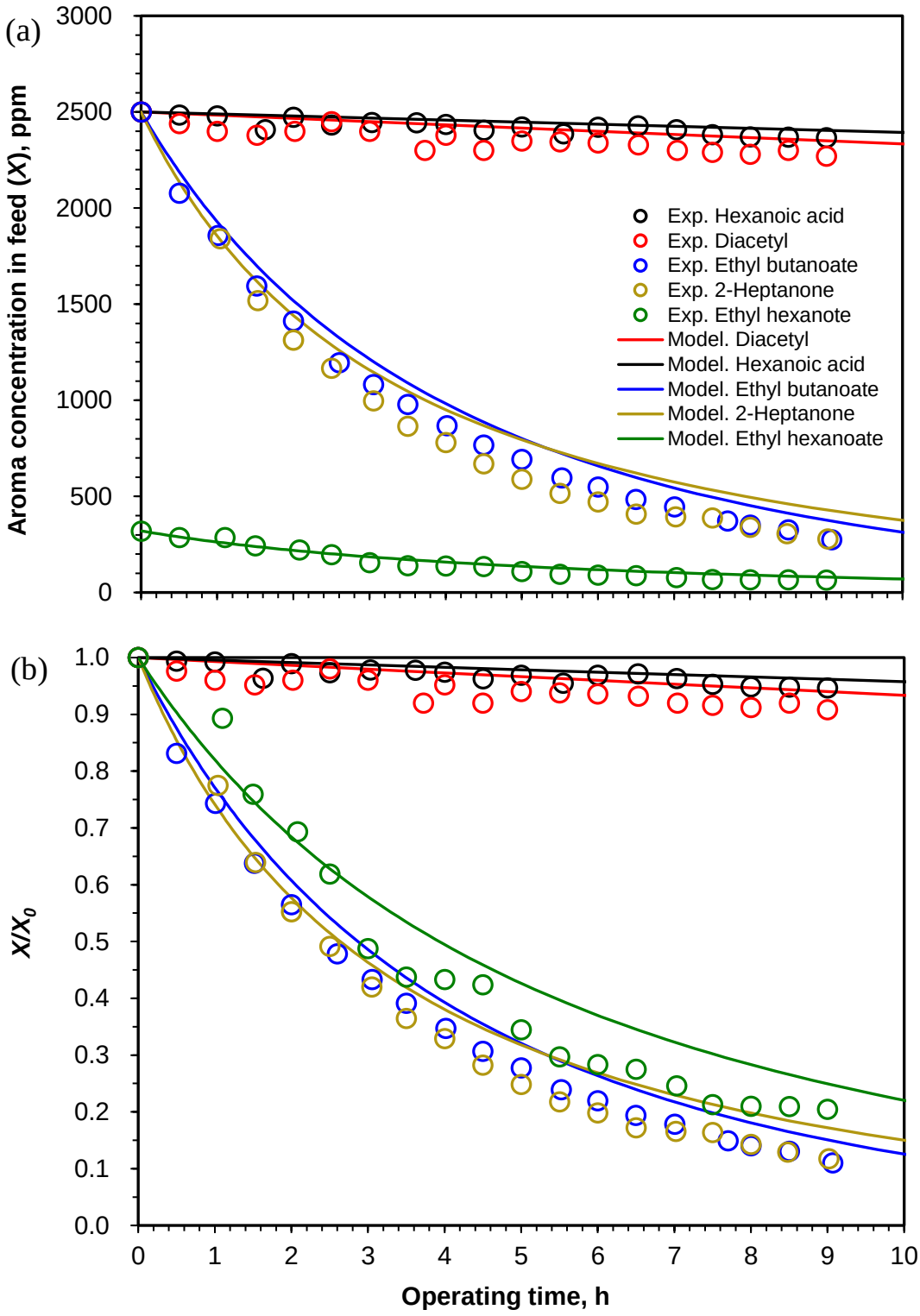

Figure 4.1 (a) Depletion of aroma concentration in feed (X) and (b) ratio of X/X_0 (X_0 is the initial aroma concentration in feed) as pervaporation proceeds with time. Symbols represent experimental data; solid lines represent model calculations.

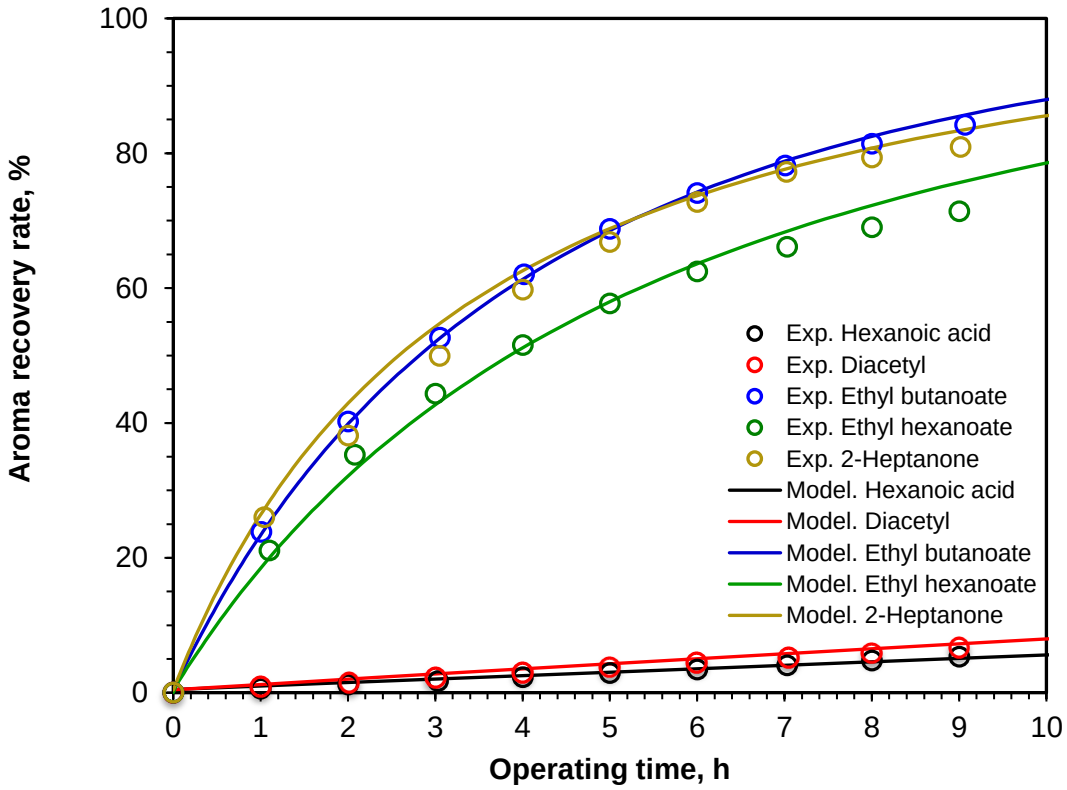

Figure 4.2 Enhancement of aroma recovery rate as pervaporation proceeds with time. Symbols represent experimental data; solid lines represent model calculations.

When batch pervaporation proceeded with time, the overall aroma concentration in the accumulated permeate decreased, as shown in Figure 4.3. This is because as permeation continued, the feed aroma concentration decreased and the aroma flux decreased accordingly, while the water flux did not change significantly. It is worth to notice that although the permeation flux of 2-heptanone was higher than that of ethyl butanoate, the overall concentration of 2-heptanone in the accumulated permeate was lower than that of ethyl butanoate for the first several hours. This is because water permeation fluxes were different from the two feed solutions. The water flux for pervaporation of 2-heptanone-water mixture was higher than that for the pervaporation of ethyl butanoate-water mixture when the feed

aroma concentration decreased from 2500 to 1000 ppm (based on the permeation flux data of binary solutions at different concentrations). A higher water flux will dilute the overall concentration of aroma compounds in the accumulated permeate. One also needs to notice that when the overall aroma concentration of the accumulated permeate reaches its solubility limit, phase separation will occur, which means an organic phase with a high aroma concentration can be obtained.

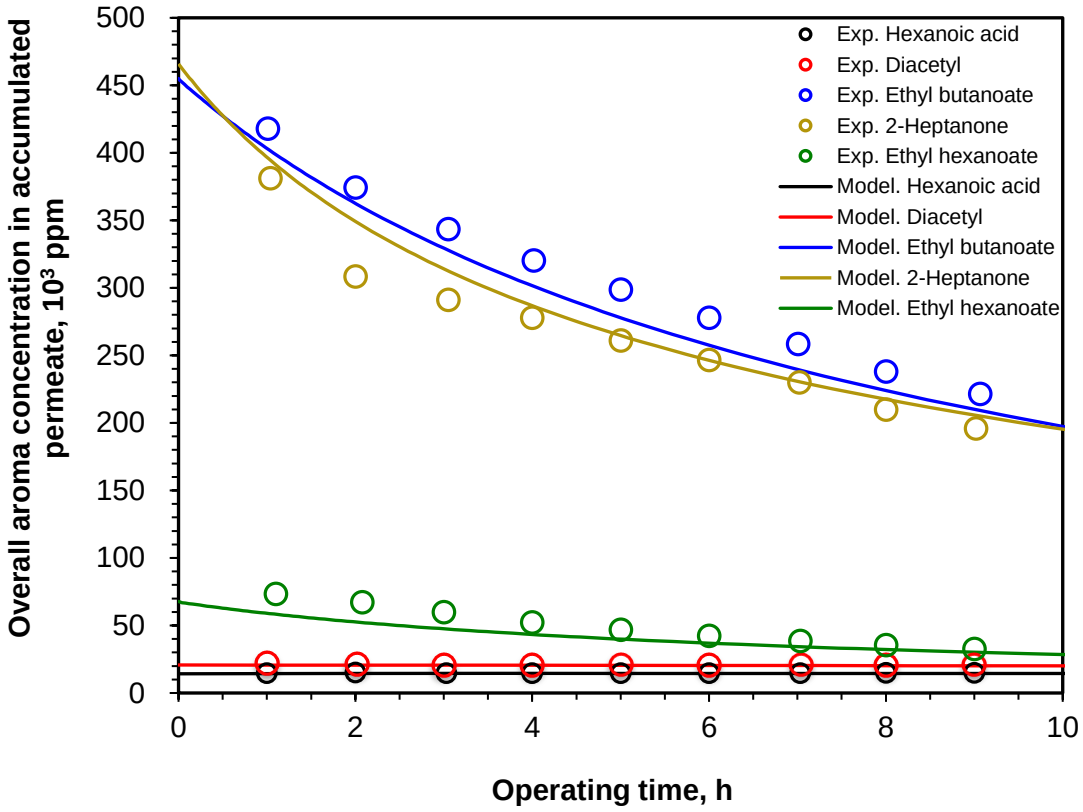

Figure 4.3 Overall aroma concentration in the accumulated permeate as a function of batch time. Symbols represent experimental data; solid lines represent model calculations.

Among the five aroma compounds investigated for the batch pervaporation, ethyl butanoate, ethyl hexanoate, and 2-heptanone underwent phase separation of their permeates. Figure 4.4 shows the calculated mass of aroma compounds in the organic phase of the

accumulated permeate as a function of time. At first, the mass of aroma in the organic phase increased with time until it reached a maximum value. This corresponds to the moment at which the instantaneous permeate concentration reached the solubility limit of aroma in water. The operating time at this moment is considered as the optimum operating time, and afterwards, the mass of aroma in the organic phase will begin to decrease with time. The organic phase will then gradually disappear when the overall aroma concentration in the accumulated permeate was lower than aroma solubility limit in water.

This phenomenon can be explained based on the phase equilibrium. In the early period of permeation, the overall aroma concentration in the accumulated permeate was above the aroma solubility in water, and so as the permeation proceeded, the mass of aroma in the organic phase of permeate kept increasing. However, both the aroma concentration in instantaneous permeate and the overall aroma concentration in accumulated permeate decreased with operating time, and the aroma concentration in instantaneous permeate decreased more quickly. When the aroma concentration in instantaneous permeate became lower than the aroma solubility limit, the newly collected permeate would add to the aqueous phase of the accumulated permeate. Thereafter, aroma in the organic phase would gradually enter the aqueous phase to reach new phase equilibrium and the mass of the aroma compound in the organic phase would decrease. If there is sufficient water collected in the accumulated permeate, the organic phase would not exist, leading only to an aqueous phase of the permeate.

The optimum operating time can be calculated by equating the instantaneous permeate concentration (Y) to the aroma solubility limit in water (S_a). Table 4.3 shows the optimum operating time corresponding to the maximum aroma mass in the organic phase of accumulated

permeate. Therefore, it is suggested that for practical industrial batch operations, the organic phase should be removed from the permeate before the optimum operating time was reached.

Table 4.3 Maximum mass of aroma compounds in the organic mass and optimum operating time.

Parameters	Diacetyl	Hexanoic acid	Ethyl butanoate	2-heptanone	Ethyl hexanoate
Maximum mass of aroma in the organic phase of permeate (g)	-	-	1.16	1.18	0.15
Optimum time (h)	-	-	20.0	27.1	32.1

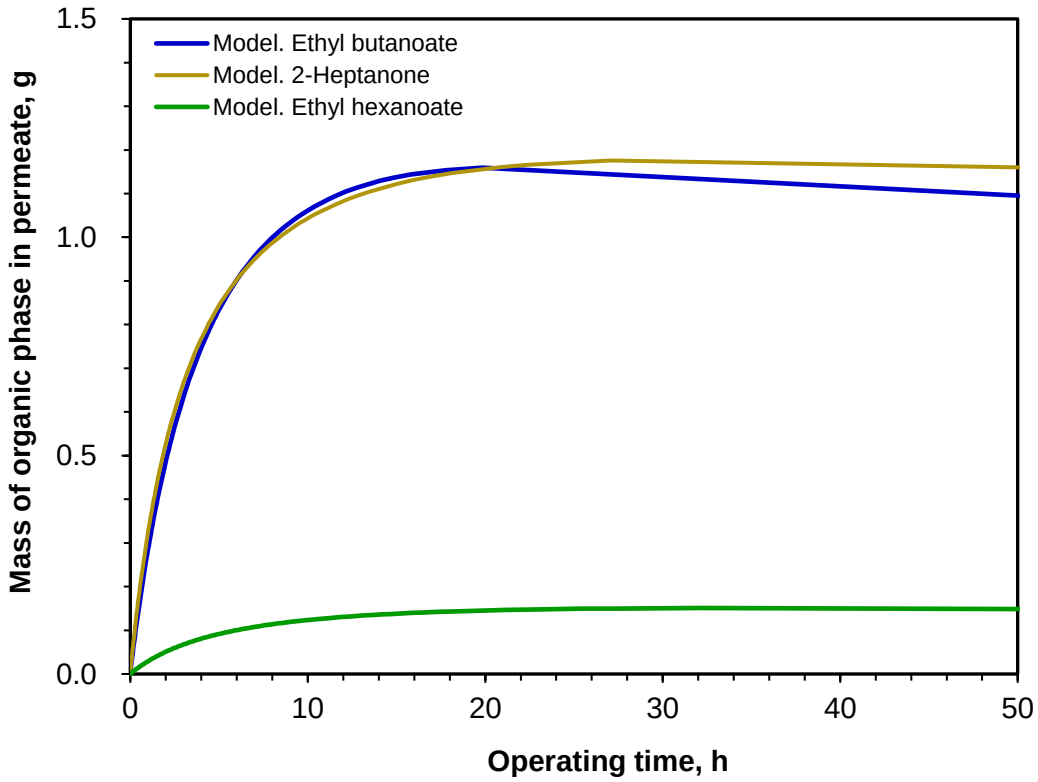

Figure 4.4 Mass of aroma compound in the organic phase of the accumulated permeate as a function of time.

4.4.2 Effect of F_0/A on batch pervaporation

For aroma compounds (such as diacetyl and hexanoic acid) that had a low permeation flux, a very long operating time was required to attain a satisfactory recovery rate, which is not favorable in industry. To improve the batch pervaporation efficiency, the effect of the quantity of feed solution to be processed per unit membrane area (F_0/A) on aroma recovery trough batch pervaporation was investigated. Variations in F_0 and/or A would be reflected in the F_0/A ratio. Among the five aroma compounds studied in this chapter, diacetyl had the second lowest recovery rate within a given period of time (the recovery rate of hexanoic acid was the lowest), and its recovery from dairy products is of more interest than hexanoic acid based on Figure 2.2. Therefore, diacetyl was selected as a representative aroma compound in this part of the study.

Figure 4.5 shows the calculated concentration of diacetyl in the feed tank and its recovery rate as the batch pervaporation proceeded at various (F_0/A) values. Clearly, the operating time needed for a good aroma recovery depends on the ratio of (F_0/A). A low (F_0/A) ratio means a large membrane area and/or a small initial amount of feed solution. It is reasonable to use a (F_0/A) ratio that is sufficiently low so that a good aroma recovery can be accomplished within a reasonable period of operating time. The calculation results showed that it took only 18 hours to recover almost all the diacetyl from feed when F_0/A was10 kg/m^2. However, when the F_0/A ratio was increased to 50 or 226 kg/m^2, 88 hours or even longer time was needed to reach an almost 100% recovery of diacetyl.

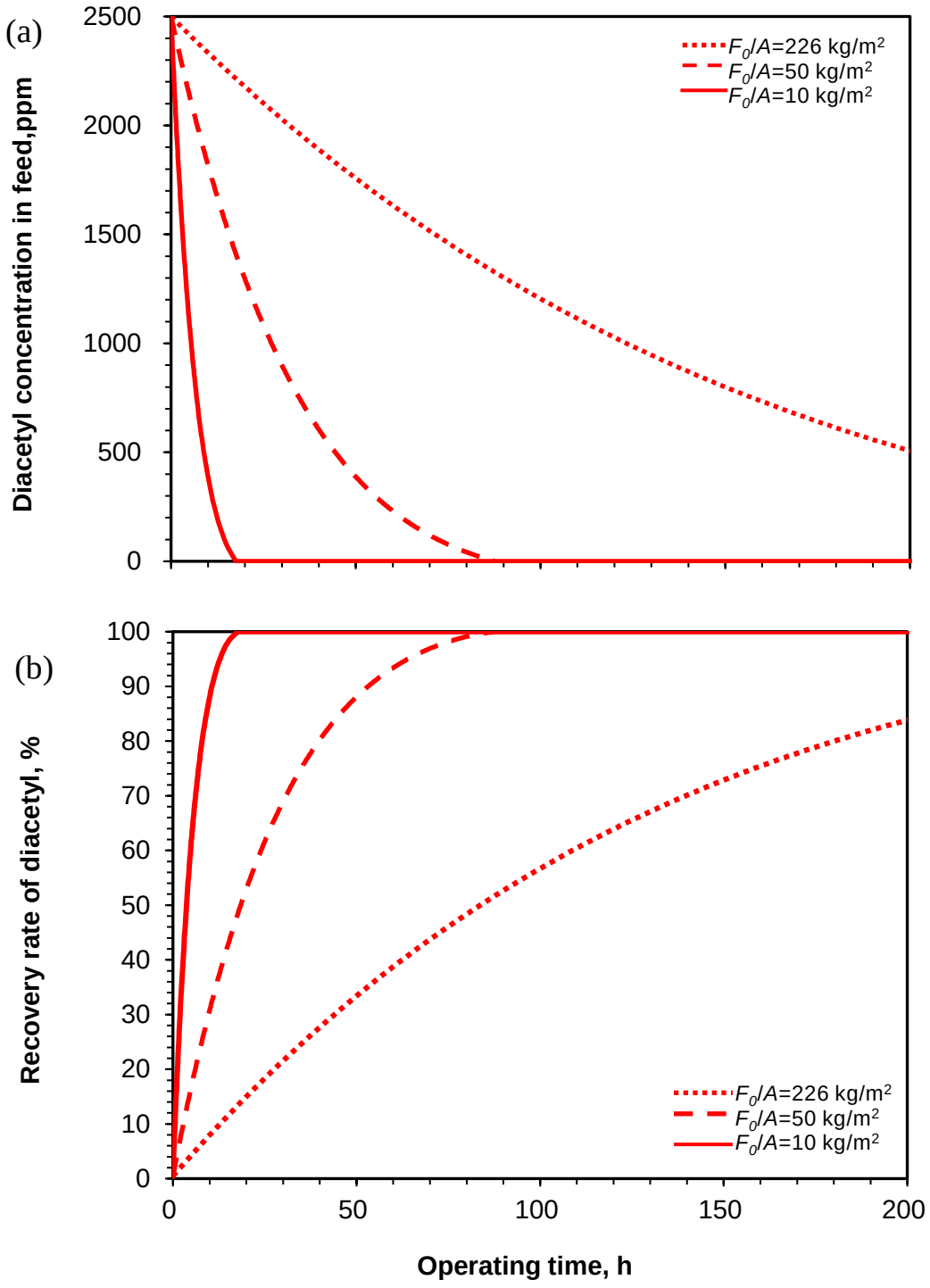

Figure 4.5 (a) Diacetyl concentration in feed and (b) its recovery rate as a function of operating time at different F_0/A ratios.

4.5 Conclusions

Based on the batch pervaporation study, the following conclusions can be drawn:

(1) Depending on the aroma solubility limit in water, the permeate accumulated would be phase separated if the overall aroma concentration in permeate reached its solubility limit.

(2) In order to get maximum aroma concentration in the permeate product, the organic phase in the permeate, if phase separation occurred, must be removed from the permeate when the instantaneous aroma concentration in the permeate leaving the membrane began to become lower than the aroma solubility limit in water.

(3) The recovery of aroma compound from its aqueous feed solutions was influenced by F_0/A for a given period of batch operating time.

Chapter 5

Effect of Non-volatile Components on Pervaporative Recovery of Aromas

5.1 Introduction

The pervaporation results with model feed solutions are expected to differ from the results with real dairy mixtures. Sugars (mainly lactose), proteins (caseins and whey proteins), fat and salts are the main non-volatile components of dairy products. Their concentrations in milk are quite low as compared to water, which represents more than 80% of the total weight (Baudot and Matin, 1996). In pervaporation, no significant sorption and diffusion of these non-volatile components in a dense membrane are expected, and they are unlikely pass the membranes (Aroujalian et al., 2006; Baudot and Marin, 1997; Baudot and Matin, 1996) due to their high molecular weights (fats, proteins, sugars), electric charges (proteins and salts), or low volatilities. However, the non-volatiles may alter the thermodynamic behavior of aroma compounds in the feed as a result of interactions with aromas (Baudot and Marin, 1997; Baudot and Matin, 1996; Dotremont et al., 1994; Martinez et al., 2011). For instance, lactose contains many hydroxyl groups and thus may be able to bind certain aroma compounds through hydrogen bonding (Overington et al., 2011). Proteins (e.g., caseins and whey) can interact with aroma compounds by two types of binding: reversible (physicochemical) binding (including hydrogen bonds, hydrophobic interactions, and ionic bonds) and irreversible (chemical) binding via covalent linkages (Kühn et al., 2006a). Fats can dissolve some aroma compounds and thus influence their partial pressure (Schirle-Keller et al., 1994). The effects of salts in dairy products on pervaporative recovery of aroma compounds should be a balance between

the “salting out” effect and the negative effect of the increased viscosity (Martinez et al., 2013). Therefore, during pervaporation, the interactions between aroma compounds and lactose, milk fat, milk protein or salts that are present in the dairy solutions may influence the recovery of the aroma compounds.

In spite of many studies on the interactions between these non-volatile compounds and aroma compounds, very limited work on how the interactions affect pervaporation has been published. Therefore, the purpose of this part of the study was to investigate the effects of the non-volatile components on the pervaporative recovery of dairy aromas.

5.2 Experimental

5.2.1 Feed solutions

Ternary feed solutions containing a single aroma compound, a non-volatile component and water were used in the pervaporation experiments. The aroma compounds used were the same as those described in Chapters 3 and 4. They were reagent grade and were purchased from Sigma-Aldrich Corporation. The concentration of each aroma compound in the feed solutions was 50 ppm, and the additional non-volatile dairy ingredients were as follows:

(1) Lactose (from NOW Foods Inc., 99.9% purity). Lactose concentrations used in this study were in the range of 0-5 wt.%. This range was selected because dairy products normally have a lactose level in range of 3-5 wt.%. Raw cow milk contains 4-5 wt.% lactose (Tsenkova et al., 2000).

(2) The concentration of whey protein isolate (from Bulk Burn Food Limited) was in the range of 0-3.5 wt.%. The concentration range was selected according to the protein

contents in milk, cream, cheese and yogurt. Milk and yogurt contain 3.2-3.5 wt.% protein (USDA National nutrient database, 2015).

(3) 35 wt.% table cream (produced by Neilson Dairy). It contains 33.3 wt.% milk fat. Various cream/water ratios were applied to prepare the mixture containing 0 wt.% to 3.5 wt.% fat. This range of fat concentration covers the fat content in raw cow milk (around 3.5 wt.%) (Tsenkova et al., 2000) and some other dairy products (e.g., whole milk, skimmed milk, yogurt).

(4) Sodium chloride (NaCl) (from Sigma-Aldrich Corporation). NaCl concentrations were in the range of 0-2 wt.%. Most dairy products (e.g., milk, butter and cheese) contain 0.05-2 wt.% NaCl (USDA National nutrient database, 2015).

The feed solutions containing lactose, protein and fat were placed at 4 ^{o}C for 24 h to reach equilibrium between aromas and these non-volatile components and then the mixture was heated to 36 ^{o}C for pervaporation studies.

5.2.2 Membrane and pervaporation procedures

The PEBA membrane and the pervaporation setup used in this chapter were the same with those in Chapters 3 and 4. The membrane thickness was 25 μm. The membrane was mounted onto the permeation cell with an effective membrane area of 22.05 cm^2. The feed solution was continuously circulated at a flow rate of 1.14 L/min through the membrane cell and back into the 1000 mL feed tank, using a circulation pump. The permeate pressure was maintained at 400 Pa by applying a vacuum pump on the permeate side. The temperature of the feed solution was controlled at 36 °C using a heating mantle and a Dyna-Sense® Thermoregulator Control

System, and a thermometer. The permeate sample was condensed in a cold trap immersed in liquid nitrogen (around -196 °C).

After each pervaporation run, the permeate sample was collected and weighed using an analytical balance. The permeate sample, which was highly enriched in aroma, was diluted with deionized water and then analyzed with a Shimadzu TOC-500 total organic carbon analyzer. The detection limit of TOC is 1 ppm. The standard deviation in the TOC measurements was ± 3%. Triplicate pervaporation runs were carried out with each of the feed mixtures. Following each run, the feed side of the pervaporation unit (including the membrane cell) was rinsed with water for 1 hour. If the feed solution contained protein and fat, the feed side connecting tubes (membrane cell was bypassed) were cleaned first with detergent for an hour and then rinsed with water for another hour; the membrane cell was cleaned separately with deionized water for an hour.

The pervaporation performance was characterized in term of flux and enrichment factor. The pervaporation data reported was the average of three measurements, and the average experimental error was estimated to be 10%.

5.3 Results and discussion

5.3.1 Effect of lactose on pervaporative recovery of aromas

To study the effect of lactose on aroma recovery using pervaporation. The experiments were carried out under the following conditions: lactose feed concentration in the range of 0–5 wt.%, a feed temperature of 36 ℃ and a permeate pressure of 400 Pa.

Figure 5.1-5.3 show the influences of lactose on water flux, aroma flux and aroma enrichment factors. Water flux did not differ significantly with the addition of 0-5 wt.% lactose

into feed, which suggests that a small portion of lactose in the feed did not alter water activity considerably in the feed solution. Therefore, the enrichment factors of aromas, shown in Figure 5.3, changed with increasing lactose concentration in a similar pattern to the aroma fluxes (Figure 5.2). It can be seen that the addition of lactose to the feed mixture resulted in decreases in the enrichment of these aromas, except for diacetyl, when compared with their enrichments from lactose-free feed solutions (i.e., lactose content 0%). These trends generally agree with the results of Overington et al. (2011a), who observed that 6 wt.% lactose in feed negatively affected the enrichment of 2-heptanone, ethyl butanoate, ethyl hexanoate and hexanoic acid using a polydimethylsiloxane membrane. Other researchers also found that sugars could have a negative effect on the pervaporative permeation of alcohols. For example, Aoujalian et al. (2006) found that glucose and xylose caused a reduction in the total permeation flux in pervaporation of a 2% ethanol/water solution using a polydimethylsiloxane membrane on a PVDF support, and that glucose also lowered the ethanol selectivity. Ikegami et al. (1999) also reported that the presence of glucose, lactose, myoinositol and xylitol all lowered the fluxes of both ethanol and water through a silicate pervaporation membrane prepared on a microporous stainless steel support. Interestingly, the flux of diacetyl was not significantly affected by the addition of lactose (Figure 5.3), and similar results were also observed by Rajagopalan et al. (1994), who used a polydimethylsiloxane-polycarbonate copolymer membrane.

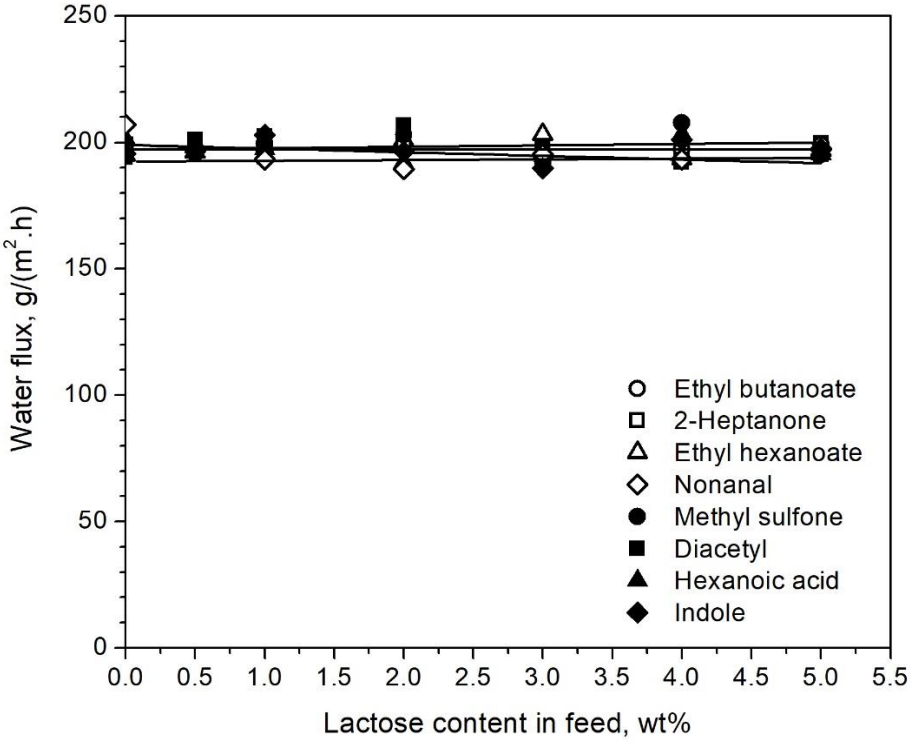

Figure 5.1 Effect of lactose on water flux. Feed aroma concentration 50 ppm, temperature 36 ℃, and permeate pressure 400 Pa.

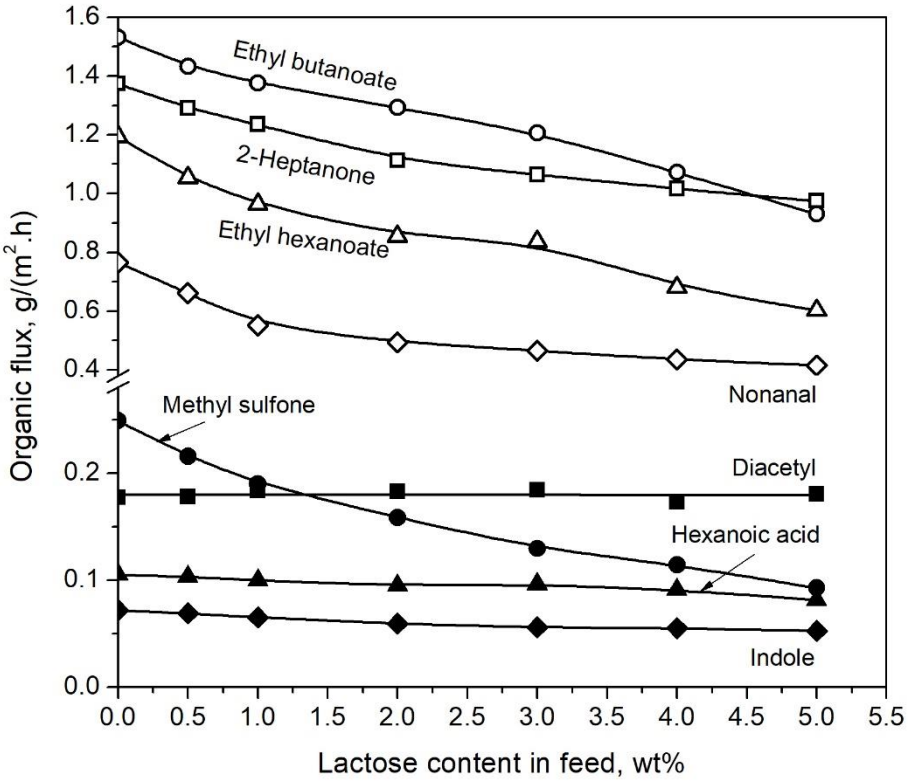

Figure 5.2 Effects of lactose on the permeation fluxes of aroma compounds. Aroma concentration 50 ppm, temperature 36 ℃, and permeate pressure 400 Pa.

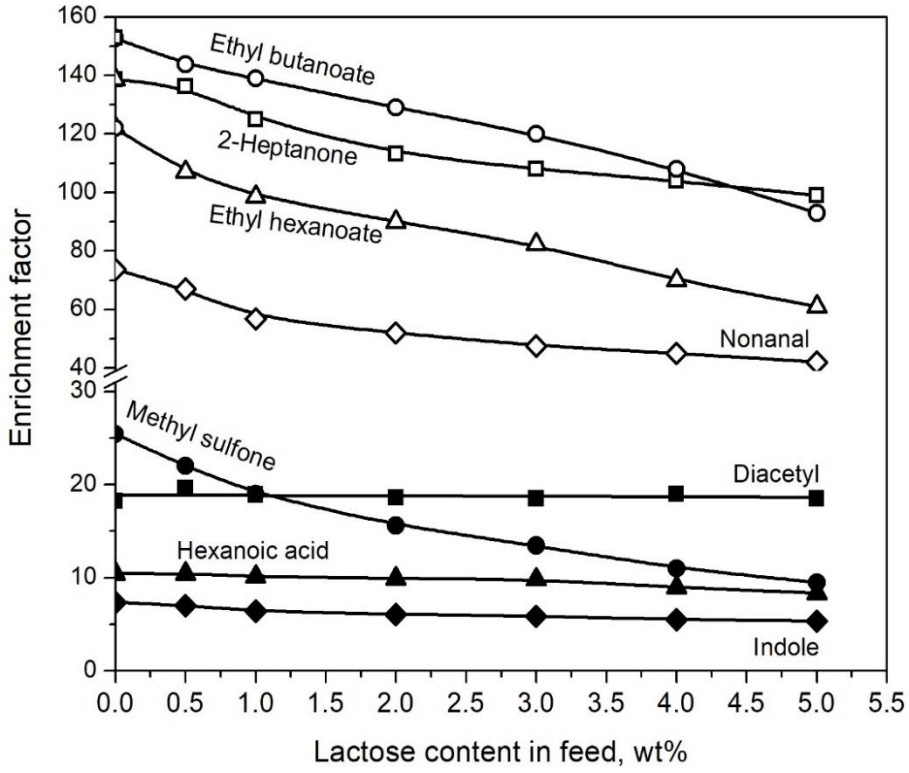

Figure 5.3 Effects of lactose on aroma enrichment. Aroma concentration 50 ppm, temperature 36 ℃, and permeate pressure 400 Pa.

The membrane permeability to aromas and water was not expected to be affected significantly by the addition of lactose, because lactose can hardly permeate through the membrane due to its large molecular size and low volatility (Baudot and Marin, 1997; Baudot and Matin, 1996; Lipnizki and Hausmanns, 2004). The reduction in the aroma enrichment or flux should be mainly attributed to the lowered partial pressure (headspace) of the aroma component by the addition of lactose in the feed. A 50-80% reduction in the content of some aroma compounds in the headspace has been reported after lactose or sucrose (an isomer of lactose) was added to the aroma-water solutions (see Table 5.1). On the other hand, the increasing viscosity after lactose was added in the feed also explains the reduction in aroma transport through the membrane. For the aroma compounds to be recovered at the downstream side of the membrane by pervaporation, they must first transport from the bulk feed solution

to the surface of the membrane before they can permeate through the membrane. Thus, the aroma transport will be affected by the increased feed viscosity. Adding lactose in the feed increases the solution viscosity, and thus slows the migration of aroma compounds to the membrane surface because of increased liquid phase mass transfer resistance.

Table 5.1 Percent reduction of aroma content in the headspace over feed after adding lactose or sucrose in aroma-water solutions.

Aroma (conc. in feed)	% reduction of aroma content in headspace	Content of sugars added	Reference
Ethyl hexanoate (100 ppm)	78	6 wt.% lactose	(Overington et al., 2011)
2-heptanone (101 ppm)	63	6 wt.% lactose	(Overington et al., 2011)
(75 ppm)	50	60 wt.% sucrose	(Nawar, 1971)
Hexanoic acid (9.8 ppm)	No change	6 wt.% lactose	(Overington et al., 2011)
Ethyl butanoate (111 ppm)	70	6 wt.% lactose	(Overington et al., 2011)

The mechanism that accounts for the depression of aroma in the headspace after adding lactose to the feed is not very clear (Matheis, 1998; Overington et al., 2011; Reineccius, 2006). One possible reason is hydrogen bonding between lactose and certain aromas (Overington et al., 2011). Indeed, polar alcohols (such as ethanol) have strong tendency to interact with sugars via hydrogen bonding, and this may it explain the reduction in alcohol flux by addition of sugars during pervaporation. However, the binding theory has difficulty to explain why lactose or sucrose has neutral or positive effects on some polar aromas (like diacetyl, acetone (Nawar, 1971) and polar acetates (Kieckbusch and King, 1979)) which also have the potential to form $O-H\cdots O$ bond with sugars, whereas the pervaporation flux or partial pressure of nonpolar aromas (e.g., ethyl butanoate, ethyl hexanoate and 2-heptanone) was negatively affected by sugar.

To further look into the possible reasons of aroma retention by lactose, the percentage reductions in aroma flux when lactose content was increased from 0 to 5 wt.% were calculated:

dimethyl sulfone (63% decrease) > ethyl hexanoate (50% decrease) > nonanal (43% decrease) > ethyl butanoate (39% decrease) > 2-heptanone (29% decrease) > indole (23% decrease) > hexanoic acid (20% decrease) > diacetyl (no change).

It is interesting to note that this is similar to the order of the aroma hydrophobicity (which may be represented by log *P* (octanol/water partition coefficient) (Table 5.2) or the order of the polarity of the aromas (which can be estimated according to aromas solubility in water in Table 5.2). It seems that less polar aromas are retained by sugar more significantly, and they tend to have lower flux in pervaporation.

Table 5.2 Log *P* (octanol/water partition coefficient) and solubility of aroma compounds.

Aroma	log *P* [a]	Solubility, g aroma/Kg water
Nonanal	3.171	0.096 [b]
Ethyl hexanoate	2.759	0.46 [c]
Ethyl butanoate	1.705	5.75 [c]
2-heptanone	1.822	4.3 [d]
Indole	2.060	1.9 [b]
Hexanoic acid	1.807	10.82 [b]
Diacetyl	-1.976	250 [b]
Dimethyl sulfone	-3.586	Miscible [b]

[a] (Howard and Meylan, 1997)

[b] (Yalkowsky et al., 2010)

[c] (Pereira et al., 2005)

[d] (Kirk and Othmer, 1981)

[e] Calculated using Aspen Plus, system parameters are: binary aroma-water system, aroma concentration 50 ppm, temperature 36 °C.

The results of studies on the release of aroma compounds from their dilute solutions containing sugars can support this postulate. The contents of nonpolar and hydrophobic aroma compounds, 2-heptanone, 2-heptanal (Nawar, 1971), butylbenzene (Massaldi and King, 1973), R-ionone, and naphthalene (De Roos and Wolswinkel, 1994) in their headspace, decreased considerably with added sucrose. In contrast, the contents of the polar compounds diacetyl

(Land and Reynolds, 1981), maltol and vanillin (Roberts et al., 1996) in their headspace were not significantly affected by the addition of glucose or sucrose to their aqueous solution. Polar compounds acetic acid and butanoic acid (Overington et al., 2011) were reported to have an 30-50% increase in their headspace mole fraction when 6 wt.% lactose was present in feed. Seuvre et al. (2006) studied the retention of six aromas (in a large hydrophobicity range) in sugar-water mixtures, ethyl hexanoate and trans-2-hexenal, which were the most hydrophobic aromas in the group, had the highest retention in the sugar-water mixture, while a lower retention was observed for the more polar compounds (e.g., 2-pentanone, cis-3-hexenol and diacetyl), and no variation in ethyl acetate retention was observed.

A plausible explanation of the above results is that the equatorial hydroxyl groups (see Figure 5.4) in lactose is possible to form hydrogen bonding with water, which could result in hydrophobic regions (Franks, 1983). Pairwise interactions of sucrose have been computed to be favorable and could form a hydrophobic region (Kozak et al., 1968). As a structural isomer of sucrose, the lactose-lactose interaction may also create hydrophobic regions, which are favorable to hydrophobic or nonpolar aroma compounds.

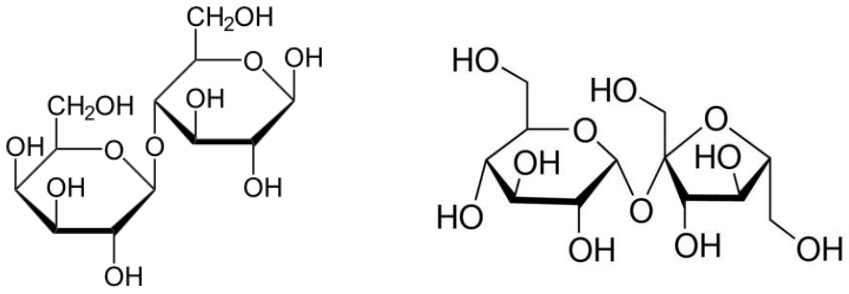

Lactose Sucrose

Figure 5.4 The structure of lactose and sucrose.

Dimethyl sulfone is an exception compared to the other aromas studied here. It is the most polar or hydrophilic aroma in this study, but experienced the greatest (63%) reduction in its flux when the aqueous aroma solutions contained 5 wt.% lactose. Very little work on sugar-dimethyl sulfone interaction is available. However, the depression of dimethyl sulfone flux may be partly explained by the nature of the sulfur-oxygen bonding in dimethyl sulfone (Clark et al., 2008). Through natural bond order analysis, Clark et al. (2008) found that the sulfur-oxygen linkages are not double bonds, as widely perceived, but rather they are coordinate covalent single $S^{+}\rightarrow O^{-}$ bonds, in which both shared electrons come from the sulfur. The oxygen in dimethyl sulfone shows highly negative electrostatic potentials, indicating its strong tendency of hydrogen bonding with hydroxyl groups in lactose. Therefore, a reasonable hypothesis can be made: the effects of lactose on aroma flux in pervaporation is related to the hydrophobicity or polarity of the aroma compounds. For highly polar aroma compounds (e.g., dimethyl sulfone and ethanol), the hydrogen bonds between lactose and the aroma may account for the retention of aroma compounds by lactose; For less polar or nonpolar aroma compounds, the lactose-water or lactose-lactose interactions may dominate over the lactose-aroma interaction, the possible hydrophobic regions in matrix would favor hydrophobic aromas, resulting in a large reduction in aroma flux.

5.3.2 Effect of whey protein on pervaporative recovery of aromas

Whey protein, a collection of globular proteins isolated from whey, is typically a mixture of β-lactoglobulin (β-lg) (~65%), α-lactalbumin (α-la) (~25%), bovine serum albumin (BSA) (~8%), and immunoglobulins (Haug et al., 2007). Similar to NaCl and lactose, whey protein did not show evident effect on water permeation during pervaporation (Figure 5.5), but the permeation fluxes and thus the enrichment factors of all aroma compounds are lowered by the

presence of whey protein, as shown in Figure 5.6 and Figure 5.7. These results are in agreement with those of Overington et al. (2011), who reported that the presence of 6 wt.% milk protein isolates in the feed solution reduced the enrichment factors of esters (ethyl butanoate and ethyl hexanoate), a ketone (2-heptanone) and acid (hexanoic acid) in pervaporation using a PDMS membrane. However, Aroujalian et al. (2003) reported a different effect of protein on aroma recovery; they found the pervaporation separation of ethanol from a 2 w% aqueous solution was not affected by the presence of 10g/L soy protein isolates in the feed.

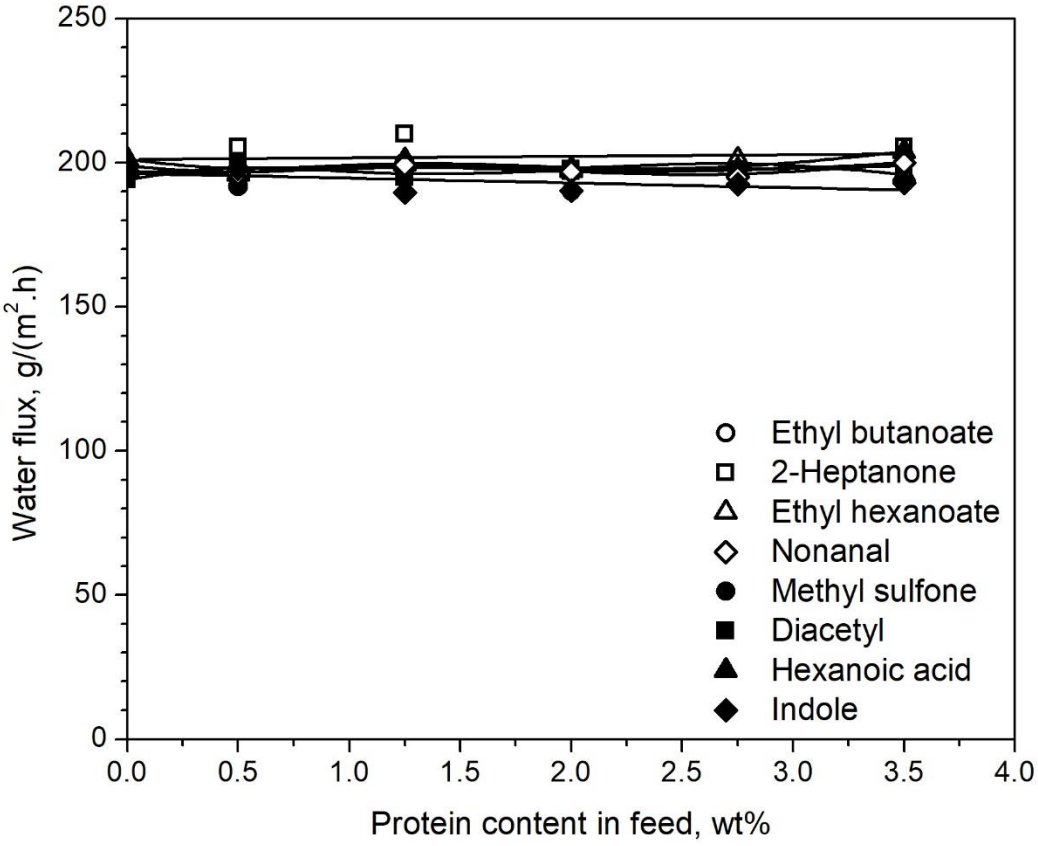

Figure 5.5 Effect of protein on water permeation flux. Aroma concentration 50 ppm, temperature 36 ℃, and permeate pressure 400 Pa.

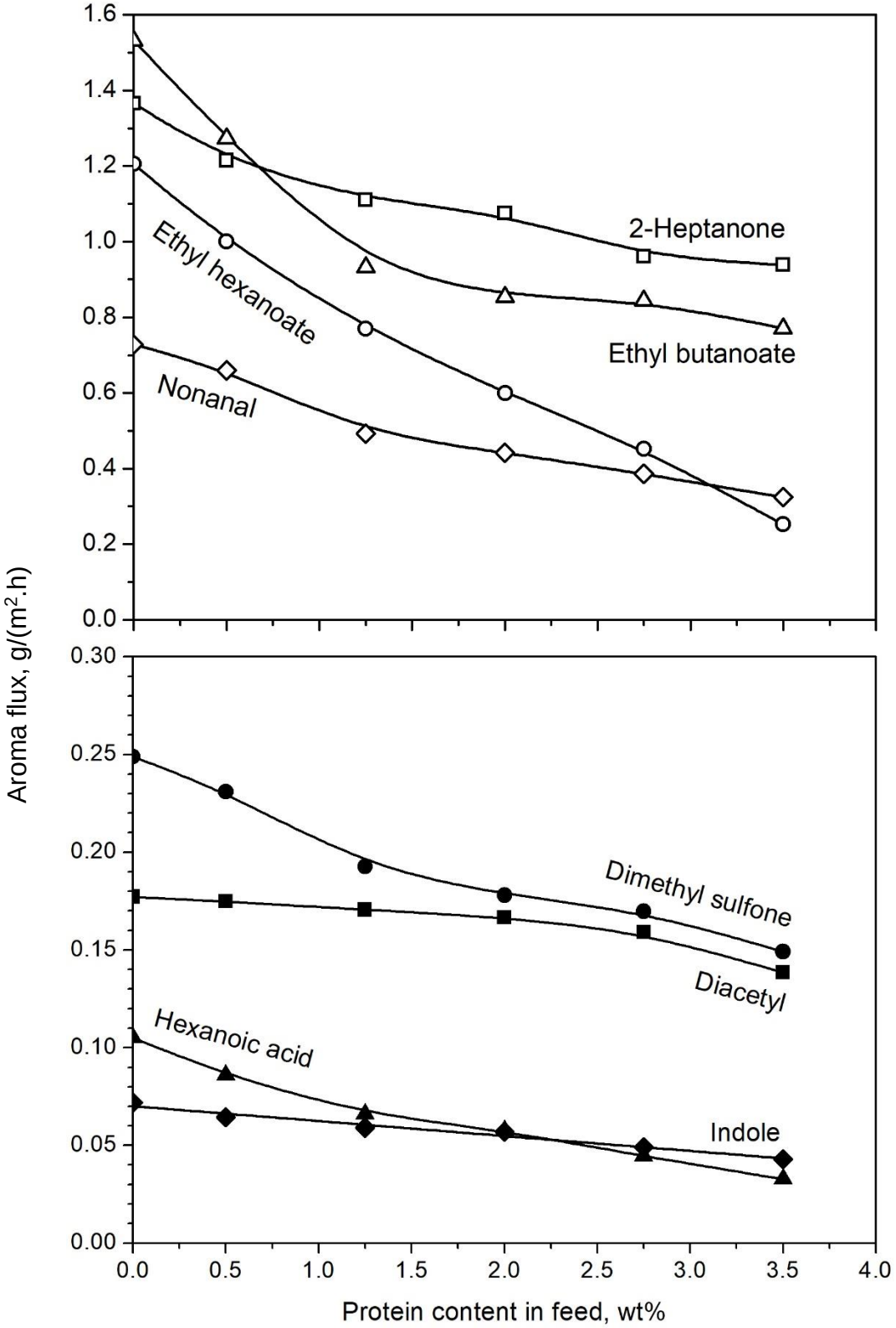

Figure 5.6 Effect of protein on the aroma permeation flux. Aroma concentration 50 ppm, temperature 36 °C, and permeate pressure 400 Pa.

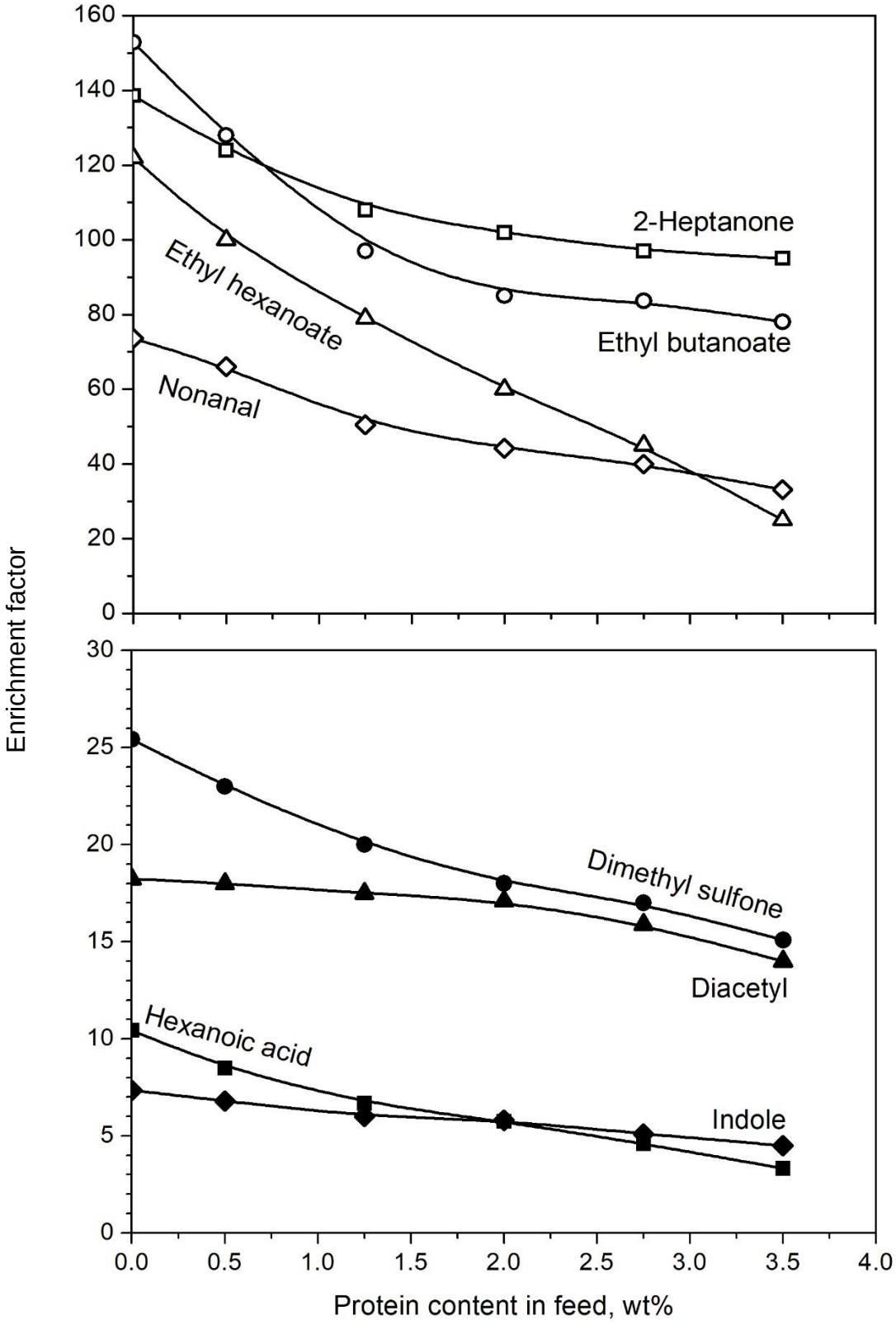

Figure 5.7 Effect of protein on aroma enrichment. Aroma concentration 50 ppm, temperature 36 ℃, and permeate pressure 400 Pa.

The reduction in aroma recovery was believed to result from two aspects: (1) The increased viscosity of the feed after whey protein was added, which increased the mass transfer resistance in the liquid phase. (2) Interactions between proteins and aroma compounds, as a result of hydrophobic, reversible binding (Kühn et al., 2006b; Landy et al., 1995; Reiners et al., 2000). The binding of aromas by protein can decrease the partial vapor pressures of the aromas above the feed solution, thereby lowering the permeation fluxes of the aromas through the membrane. Table 5.3 shows the extent of aroma bound with milk proteins reported in literature.

Table 5.3 Binding constants of aromas with whey proteins.

	Binding percentage of aromas by milk protein tested by headspace analysis, %	Binding constant, g/L
Nonanal	68 [c]	-
Ethyl hexanoate	83 [a] 49 [b]	863 [b]
2-heptanone	58 [a] 20 [b]	270 [d]
Hexanoic acid	No change [a]	-
Ethyl butanoate	73 [a] 72 [b]	-
Diacetyl	25 [f]	-

[a] 4 wt.% milk protein isolate was added in aroma-water solution at room temperature. The concentrations of ethyl hexanoate, ethyl butanoate, 2-heptanone and hexanoic acid were 100 ppm, 101 ppm, 9.8 ppm and 111 ppm (Overington et al., 2011) .

[b] The protein used was 3 wt.% β-lg, the feed pH was 3 (Charls et al., 1996).

[c] 0.5 wt.% milk protein isolate was added in nonanal-water solution at room temperature. The nonanal concentrations was 1 ppm (Kühn et al., 2008).

[d] Feed solution contained 0.6 wt.% bovine serum albumin (BSA) (Damodaran and Kinsella, 1980)

[f] 0.5 wt.% BSA was added in diacetyl-water solution at room temperature. The diacetyl concentrations was 1 ppm (Guichard and Langourieux, 2000).

In our study, it was shown that the eight aroma compounds responded differently in terms of their permeation fluxes and enrichment factors to the presence of whey protein in feed. When whey protein content increased from 0 to 3.5 wt.%, the significance of decreases in aroma fluxes is in the following order:

ethyl hexanoate (80% decrease) > hexanoic acid (68% decrease) > nonanal (55% decrease) > ethyl butanoate (49% decrease) > dimethyl sulfone (41% decrease) > indole (39% decrease) > 2-heptanone (31% decrease) > diacetyl (23% decrease).

It is evident that except for hexanoic acid and dimethyl sulfone, the reduction in the permeation fluxes of aroma compounds generally followed the decreasing order of their hydrophobicities (represented by activity coefficient and log *P* shown in Table 5.2): nonanal > ethyl hexanoate > ethyl butanoate > 2-heptanone > indole > diacetyl. This suggests that a relation between the affinity of whey protein to binding aromas and the hydrophobicity of the aroma compounds was an important factor to consider in aroma recovery by pervaporation.

This consideration is supported by the results of Guichard and Langourieux (2000), and Reiners et al. (2000). They found a good linear correlation between the hydrophobicity (log *P*) of aromas and the logarithm of aroma binding constants with β-lg basing on a group of aromas consisting of a series of esters, ketones, aldehydes and lactones, but not including some terpene alcohols and phenolic compounds. As mentioned before, β-lg is the main constituent of whey protein, followed by α-la and then BSA. Therefore, the binding between β-lg and aromas plays an important role in the overall aroma binding on whey protein. β-lg has been determined to consist of 2 β-sheets, formed from 9 strands converging at 1 end to form a hydrophobic pocket (Monaco et al., 1987; Papiz et al., 1986). The hydrophobic pocket is considered to be the most probable binding site for aroma compounds (Dufour and Haertle, 1990; Guichard, 2002). Therefore, β-lg favors interactions with hydrophobic aroma compounds. α-la has been reported to have weaker affinity to aromas than β-lg (Kühn et al., 2006a). α-la can bind aldehydes and methyl ketones to various extents (Franzen and Kinsella 1974). Jasinski and Kilara (1985) also reported a weak binding of 2-nonanone and nonanal to α-la. BSA only takes

8% of whey protein mass, but has been determined to have a higher flavor binding capacity than β-lg (Kühn et al., 2006a). A static headspace analysis showed that BSA at a concentration as low as 0.5 wt.% could cause a 25% reduction in the vapor pressure of diacetyl over its aqueous solution (Land and Reynolds, 1981), indicating a very strong binding affinity of BSA to diacetyl. Beyeler and Solms (1974) found the binding constants between BSA and aromas decreased in the sequence of aldehydes > ketones > alcohols. King and Solms (1979) confirmed that hydrophobic interactions were the dominant interactions between BSA and benzyl alcohol.

The permeation flux of hexanoic acid was reduced by the addition of whey protein. However, in the study of Overington et al. (2011), saturated fatty acids with short chain length, including hexanoic acid, were found not to bind with milk protein at all. A headspace analysis showed that the mole fraction of hexanoic acid did not change even with the presence and absence of 4 wt.% milk protein isolate in the feed solution. Among the fatty acids with a carbon number of 2-10, only octanoic acid ($C_8H_{16}O_2$) was found to weakly bond to milk protein. Similar results were also reported by Frapin et al. (1993), who found β-lg could only bind with long-chain fatty acids (the binding strength increased with the increasing of the chain length), but not with such short-chain fatty acids as caprylic and capric acids. If the reduction in the headspace of hexanoic acid is not due to its hydrophobic binding with whey protein, a possible reason could be the pH variation after the protein addition. The pH values of aqueous hexanoic acid solutions with different amount of whey protein were determined using a VWR-SB70P pH meter and are shown in Table 5.4.The pH value of the feed solution containing 50 ppm hexanoic acid was 3.67, and it increased to 5.66 when the feed contained 3.5 wt.% whey protein. At a higher feed pH, a larger amount of hexanoic acid would be in dissociated form in the feed

solution, resulting in a decline in its pervaporation flux (Overington et al., 2011). There was a large reduction of 41% in dimethyl sulfone permeation flux, which was not expected considering its high polarity. The reason for this was still not clear, and further work on their interaction was needed.

Table 5.4 pH values of aqueous hexanoic acid solutions with different amount of whey protein or milk fat.

	With 50 ppm hexanoic acid in feed	Without hexanoic acid in feed
No protein or fat	3.67	-
2.0 wt.% protein	5.53	5.62
3.5 wt.% protein	5.66	5.71
2.0 wt.% fat	6.48	6.93
3.5 wt.% fat	6.56	6.95

5.3.3 Effect of milk fat on pervaporative recovery of aromas

Milk fat also affected the permeation fluxes and enrichment factors of the aroma compounds negatively. This is especially the case for hydrophobic aromas, as shown in Figure 5.8 and 5.9. These results were in agreement with the work of Baudot and Matin (1996) who predicted that fat would deduce a decline in the pervaporative recovery of hydrophobic aromas. In addition, similar to lactose and whey protein, within the concentration ranges of non-volatile compounds studied here, milk fat did not have a significant influence on water permeation (see Figure 5.10).

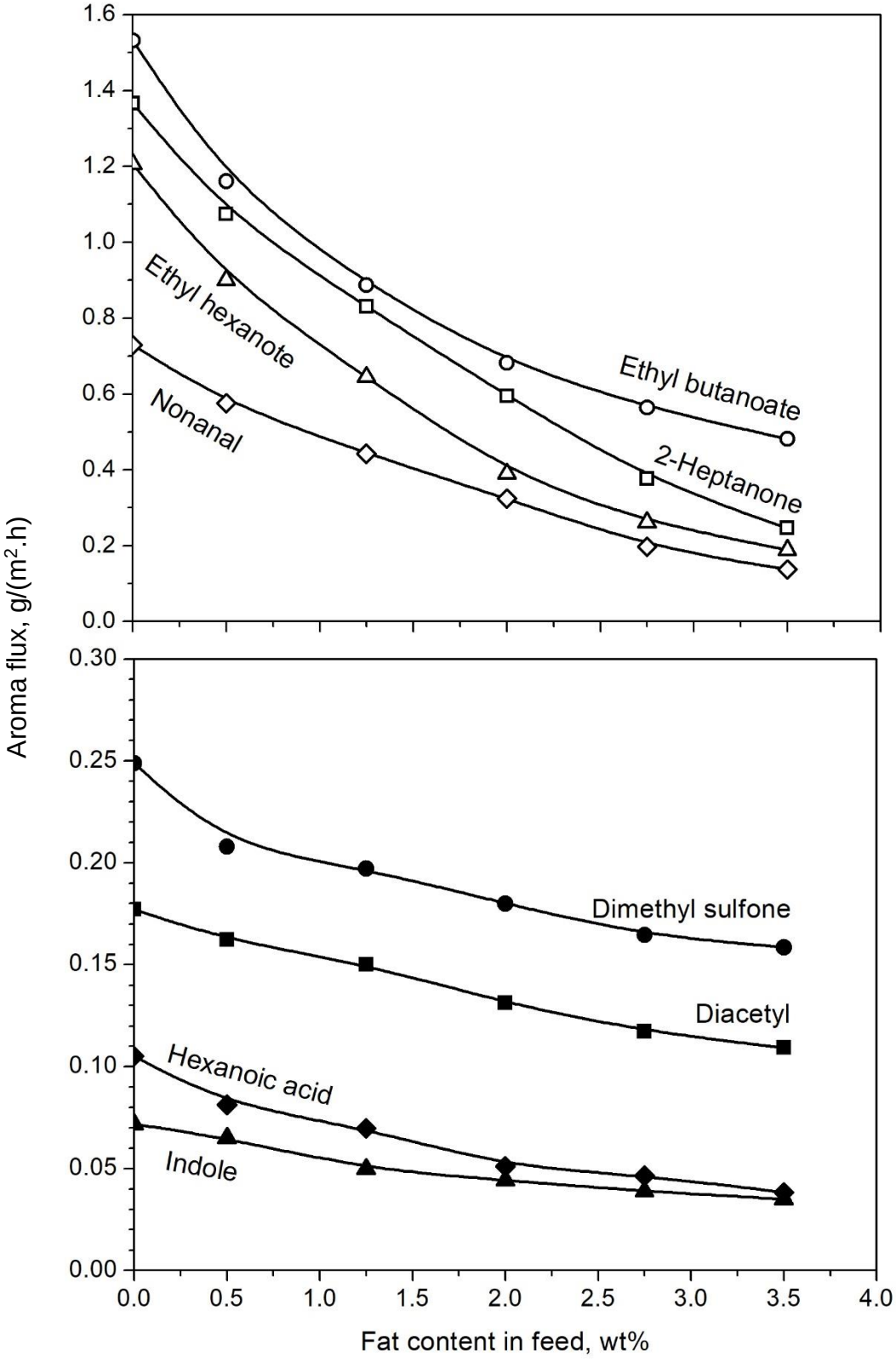

Figure 5.8 Effect of milk fat on aroma permeation flux. Aroma concentration 50 ppm, temperature 36 ℃, and permeate pressure 400 Pa.

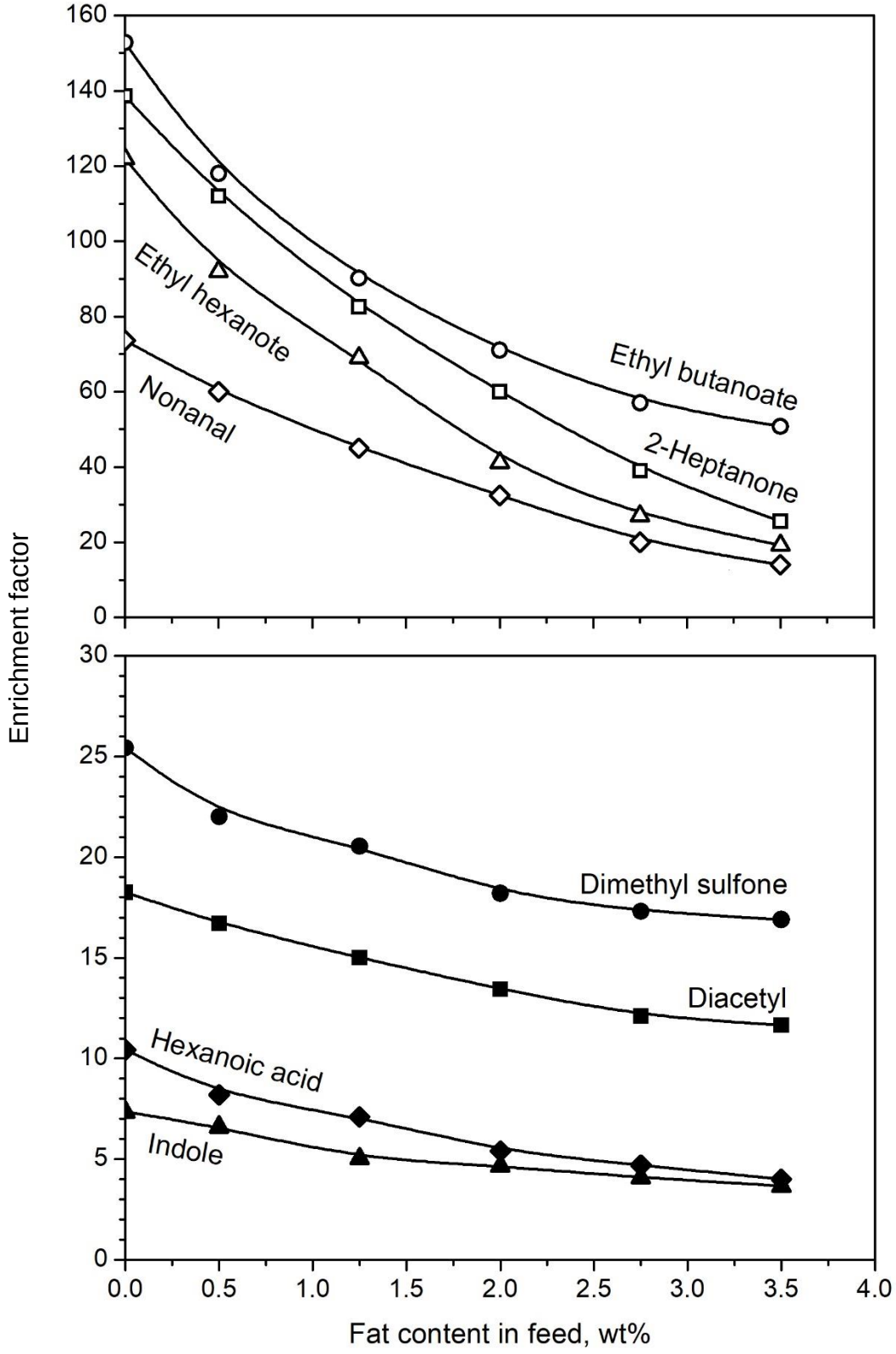

Figure 5.9 Effect of milk fat on aroma enrichment. Aroma concentration 50 ppm, temperature 36 ℃, and permeate pressure 400 Pa.

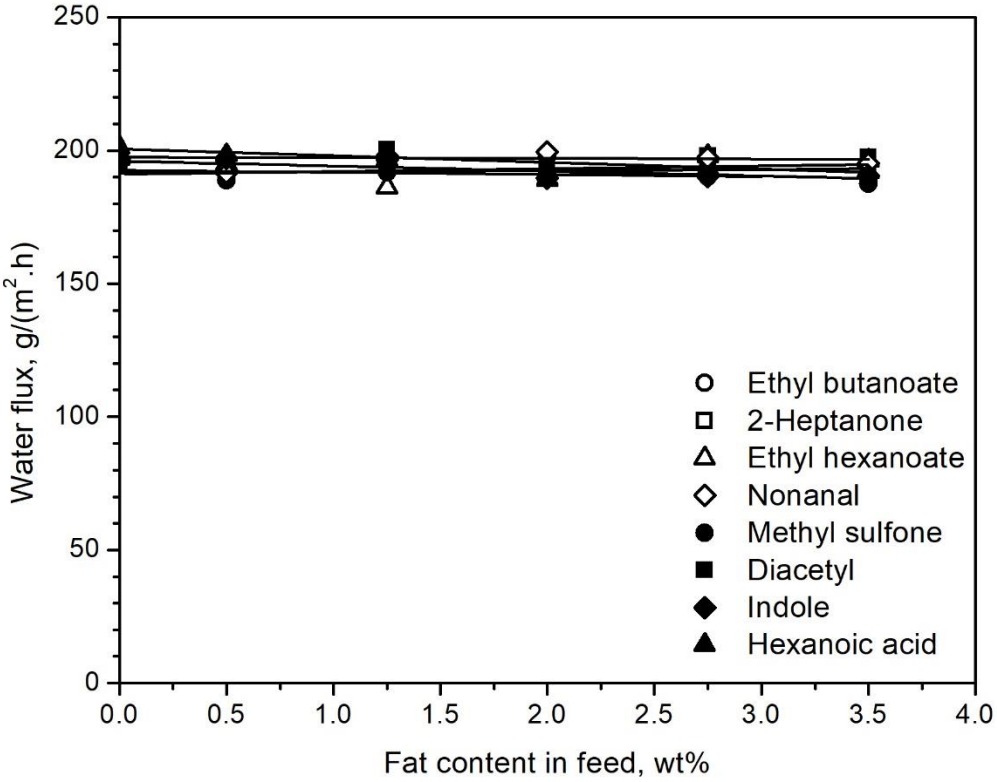

Figure 5.10 Effect of milk fat on water permeation flux. Aroma concentration 50 ppm, temperature 36 ℃, and permeate pressure 400 Pa.

Compared to the effect of lactose and whey protein, milk fat seems influence the pervaporation permeation of the aroma compounds more negatively than lactose and whey protein. As the concentration of milk fat in the feed increased from 0 to 3.5 wt.%, the reductions in aroma fluxes were in the following order:

ethyl hexanoate (84% decrease) > 2-heptanone (82% decrease) > nonanal (81% decrease)> ethyl butanoate (67% decrease) > hexanoic acid (62% decrease) > indole (50% decrease) > diacetyl (36% decrease) > dimethyl sulfone (33% decrease).

The sequence of the aroma flux reduction was generally in the decreasing order of the aroma hydrophobicity (Table 5.2). It appears that the hydrophobic interactions between aromas and fat were the leading cause for the aroma flux decline. Indeed, in the feed systems containing

fats, aroma compounds were distributed between the water and fat phases. It is reported that for many aroma compounds, the more hydrophobic the compound is, the larger portion of the compound will dissolve in the fat phase (Miettinen et al., 2003; Relkin et al., 2004; Le Thanh et al., 1998). Aromas tend to have a much lower volatility in the fat phase than in aqueous phase (Landy et al., 1996), and thus the aromas dissolved in the fat phase will have a lower permeation rate due to the reduced driving force for permeation. This is supported by the decreased aroma content in headspace over the feed solution after fat was added (Table 5.5).

Table 5.5 Percent reduction in the aroma content in headspace over feed after adding fat in feed solution.

Nonanal	90 [b]
Ethyl hexanoate	90 [a]
2-heptanone	69 [a] 70 [b]
Hexanoic acid	No change [a]
Ethyl butanoate	70 [a]
Diacetyl	19 [b] 20 [c]

[a] 5 wt.% milk fat was added in aroma-water solution. The concentrations of ethyl hexanoate, ethyl butanoate, 2-heptanone and hexanoic acid were 100 ppm, 101 ppm, 9.8 ppm and 111 ppm (Overington et al., 2011).

[b] 5 wt.% vegetable fat was added in aroma-propylene glycol solution. The concentration of nonanal and diacetyl was 5000 ppm (Schirle-Keller et al., 1994).

[c] 5 wt.% vegetable fat was added in aroma-water solution. Diacetyl concentration was 40 ppm (Miettinen et al., 2003).

As shown in Table 5.5, the partial vapor pressure of hexanoic acid was not affected by the presence of milk fat. Thus, similar to the effects of whey protein, the decreased recovery of hexanoic acid in pervaporation may be attributed to the change of the feed pH after fat addition (Table 5.4). 3.5 wt.% fat in the feed increased the pH of the feed mixture from 3.67 to 6.56, which favored the dissociation of hexanoic acid and lowered the permeation rate of hexanoic acid through the membrane.

5.3.4 Effects of NaCl on pervaporative recovery of aromas

NaCl is naturally present in or added into many dairy products, (i.e., milk, cheese and yogurt). Its concentration in dairy products ranges 0.3-2 wt.% (USDA National nutrient database, 2015). Therefore, in the present study, a NaCl concentration ranged of 0-2 wt.% was chosen to investigate the effects of NaCl on the pervaporative recovery of aromas. As shown in Figure 5.11 , water flux was not affected at all by the addition of as much as 2 wt.% NaCl to the feed, indicating that such a salt content did not affect water activity significantly. However, the aroma fluxes and enrichment factors experienced different changes when the NaCl content increased. As shown in Figure 5.12 and Figure 5.13, with an increase in NaCl concentration from 0 to 2 wt.%, the fluxes and enrichment of the more permeable aroma compounds (ethyl butanoate, ethyl hexanoate, 2-heptanone and nonanal) increased considerably, while the fluxes of the less permeable aroma compounds (indole, dimethyl sulfone, diacetyl and hexanoic acid) increased less significantly or did not change.

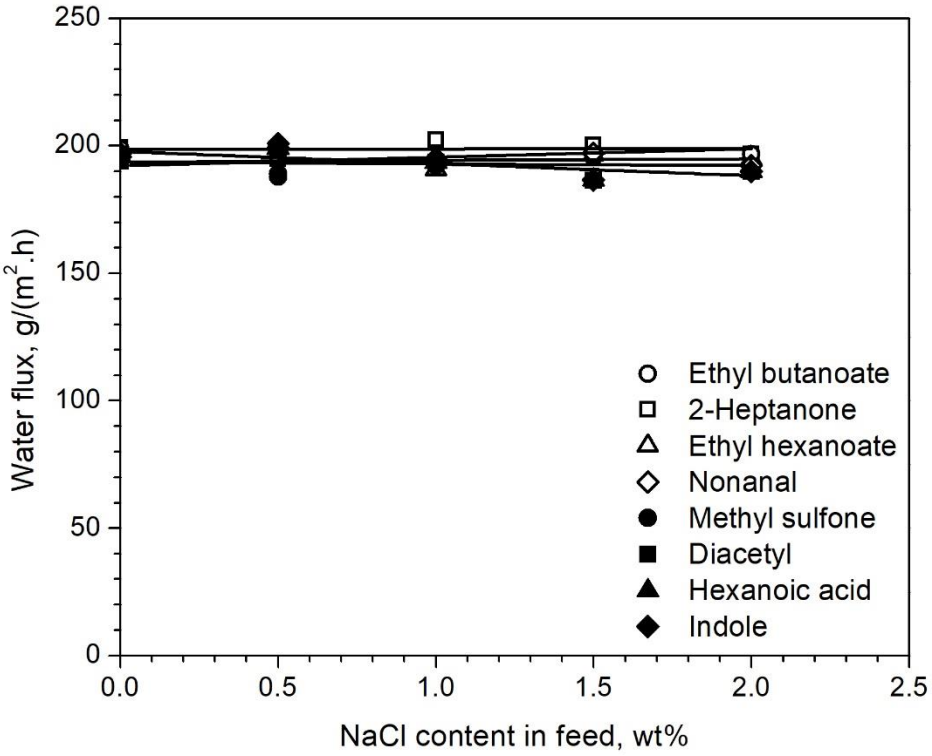

Figure 5.11 Effect of NaCl on water permeation flux. Aroma concentration 50 ppm, temperature 36 ℃, and permeate pressure 400 Pa.

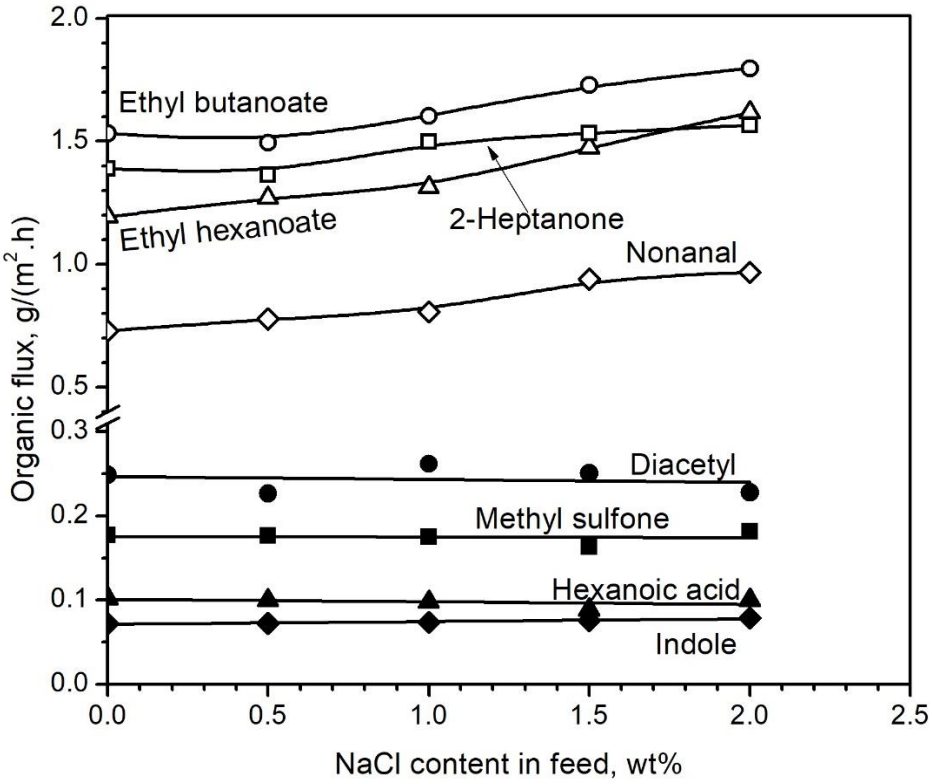

Figure 5.12 Effect of NaCl on aroma permeation flux. Aroma concentration 50 ppm, temperature 36 ℃, and permeate pressure 400 Pa.

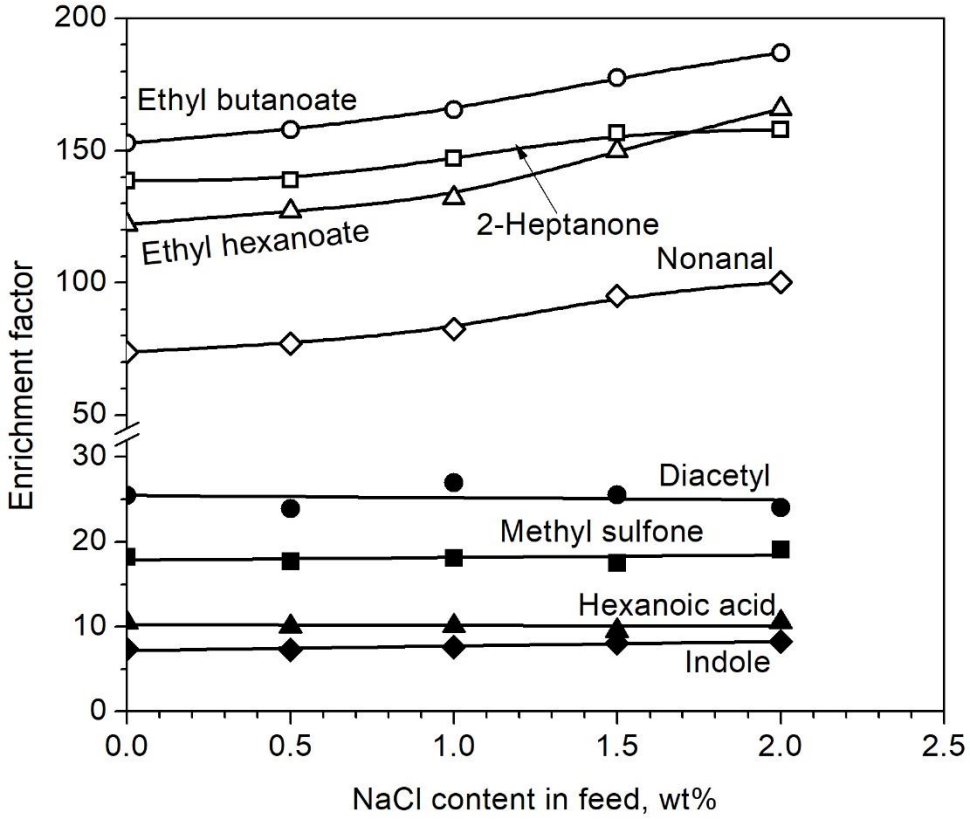

Figure 5.13 Effect of NaCl on aroma enrichment. Aroma concentration 50 ppm, temperature 36 ℃, and permeate pressure 400 Pa.

The presence of NaCl has two opposite effects on aroma permeation. On the one hand, the existence of salt can lead to a salting-out effect on certain aroma compounds, i.e. the solubility of the aroma compounds in water is reduced, and their activity coefficients and their permeation driving force are enhanced (García et al., 2009; Martinez et al., 2013) . On the other hand, the presence of salt increases the density and viscosity of the feed solution, lowering the aroma diffusion rate in the feed solution. In general, an overall positive effect of salt on the membrane selectivity in pervaporation was observed. For example, Martinez et al. (2013) reported that the enrichment factors of six aroma compounds (a ester, two alcohols, two aldehydes and a diketone) in a PDMS membrane were increased by 20-25% when the concentration of NaCl was increased from 0 to 3.4 wt.%. They also confirmed that the increase

in aroma selectivity was attributed to the increased activity coefficient of aromas by the presence of salt in the feed. However, some other studies showed an opposite effect of salt on the enrichment of aromas. For instance, Dotremont *et al*. (1994) reported that the addition of salts (KCl, NaCl, Na_3PO_4, $FeCl_3$, $CaCl_2$) at concentrations of 0.5-2.5 mol/L decreased the permeation flux of trichloroethylene, while the water flux for the pervaporation of DCM/NaCl/water using a silicone membrane was not affected. And in some studies the salt was shown to have no impact on aroma permeation and enrichment. For pervaporation extraction of volatile organic compounds from water, Nguyen and Nobe (1987) and García et al. (2009) noticed that there was no significant change in the flux and selectivity of dichloromethane in the pervaporation of dichloromethane/NaCl/water using either silicone membranes or hydrophobic CMX-GF-010-D membrane.

In the present study, in spite of the increased feed viscosity, as illustrated in Table 5.6 (which was determined by a GILMONT viscosity meter), the recovery of ethyl butanoate, ethyl hexanoate, 2-heptanone, nonanal and indole was all enhanced by the presence of NaCl in feed, which suggests that for these aromas, the salting-out effect was dominant. When salt-out effect is counterbalanced by the increased feed viscosity, the aroma permeation will be unaffected. This seems to be the case for diacetyl, dimethyl sulfone, and hexanoic acid. The increase in aroma flux due to the addition of salt is in the following order:

nonanal (36%) = ethyl hexanoate (36%) > ethyl butanoate (22%) > 2-heptanone (14%) > indole (12%) > hexanoic acid, diacetyl and dimethyl sulfone (no change).

It may be noticed the permeation flux of more hydrophobic aroma was enhanced by NaCl more significantly.

Table 5.6 Viscosity of feed solutions containing 50 ppm of ethyl butanoate and different concentrations of NaCl at 36 ºC.

NaCl concentration in feed, wt.%	Viscosity, 10^4 Pa.s
0.0	7.085
1.0	7.139
1.5	7.175
2.0	7.207
3.0	7.295

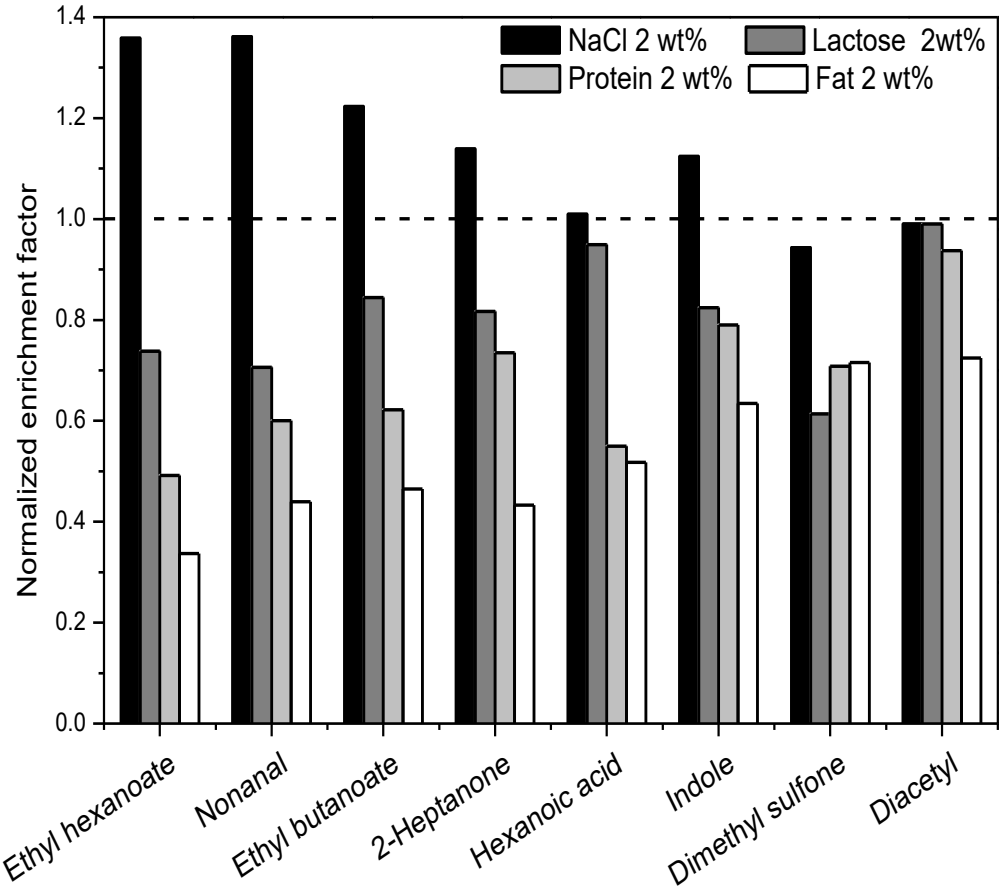

Figure 5.14 Comparison of the effects of four non-volatile components of dairy on recovery of aromas at an aroma concentration of 50 ppm, a temperature of 36 ℃, a permeate pressure of 400 Pa and a non-volatile component content of 2 wt.%.

The effects of the four non-volatile dairy ingredients on the recovery of the aroma compounds by pervaporation was compared and presented in Figure 5.14. The normalized enrichment factor is defined here as the enrichment factor of the aromas in the presence of 2

wt.% non-volatile component divided by the enrichment factor of the aroma in the absence of non-volatile component. A normalized enrichment factor of 1 means the non-volatile component has no effect on aroma enrichment. It is evident that, in general, the addition of NaCl to the feed tended to enhance aroma recovery. However, the presence of lactose, whey protein and milk fat all affected the pervaporative permeation of aromas negatively. Among the four non-volatile components, fat showed the largest negative effect on aroma recovery, followed by whey protein and lactose. This was due to the fact that milk fat interacted with many aroma compounds more strongly than protein and lactose. From a practical application point of view, to reach a high recovery of the aromas, the fat, protein and lactose in the dairy product can be removed if possible prior to pervaporation. Addition of NaCl into the dairy product is also favorable to improve the enrichment of aromas.

5.3.5 Effect of operating time on pervaporation

The membrane-fouling was also studied by measuring the permeation flux and enrichment factor using ethyl butanoate-water mixture over a 24-hour period. Permeate samples were collected every hour and sent back to the feed to keep the feed concentration constant. Permeate concentration was measured every hour for the first three hours, and then every three hours afterward. As shown in Figure 5.15 and Figure 5.16, there was no noticeable decline for the permeation flux and the aroma enrichment factor over a period of 24 h with and without the non-volatile components in the feed. These results indicate that under the operating conditions applied, concentration polarization or membrane fouling on the membrane surface was insignificant. This was presumably due to the nonporous nature of the membrane and the high flow rate of the feed solution, which rendered the boundary layer effect negligible.

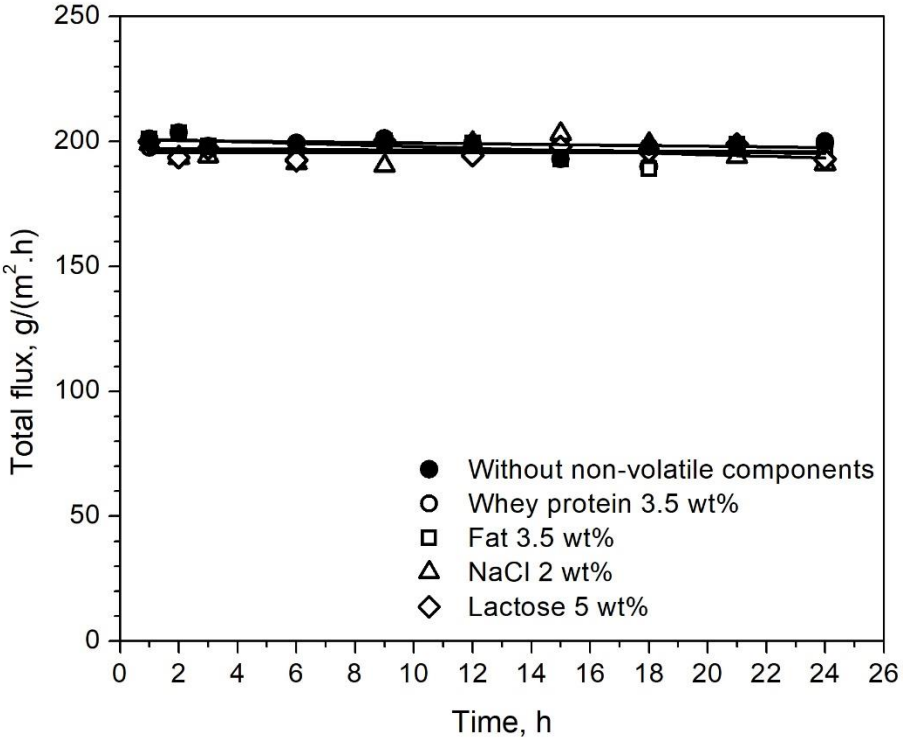

Figure 5.15 Total flux over a period of 24 h with and without the presence of lactose, whey protein, fat or NaCl. Feed solution: ethyl butanoate-water, ethyl butanoate concentration 50 ppm, temperature 36 ℃, permeate pressure 400 Pa.

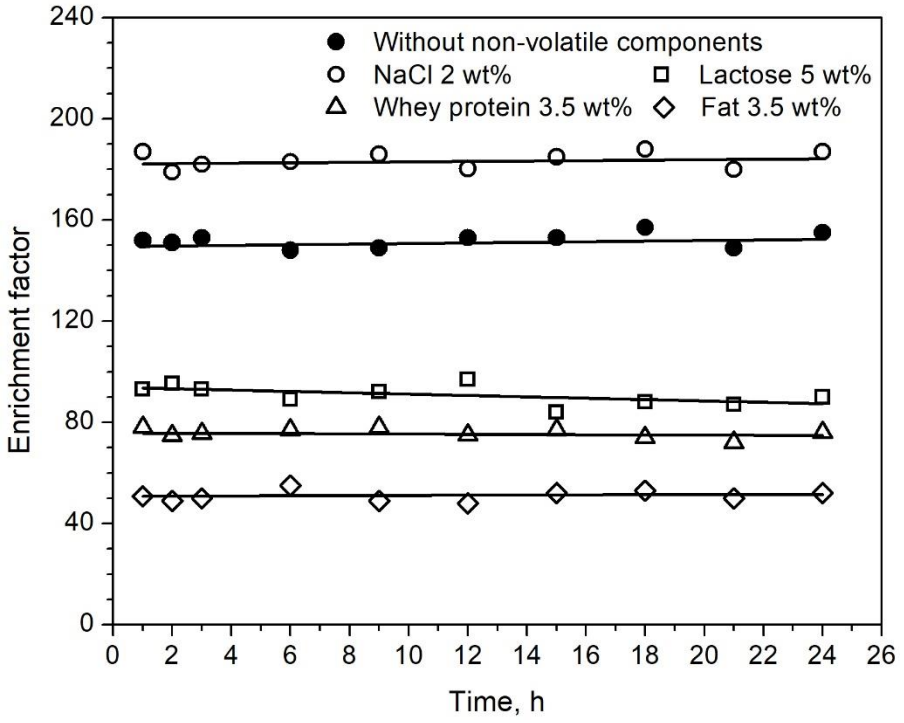

Figure 5.16 Enrichment factor of ethyl butanoate over a period of 24 h with and without the presence of lactose, whey protein, fat or NaCl. Feed solution: ethyl butanoate-water, ethyl butanoate concentration 50 ppm, temperature 36 ℃, permeate pressure 400 Pa.

5.4 Conclusions

The effect of non-volatile dairy ingredients on the pervaporative recovery of aroma compounds were investigated, and the following conclusions can be drawn:

(1) The presence of the non-volatile dairy components (e.g. NaCl, lactose, whey protein and milk fat) did not affect the permeation of water.

(2) The presence of NaCl enhanced the permeation of more hydrophobic aroma compounds (i.e. nonanal, ethyl hexanoate, ethyl butanoate, 2-heptanone and indole) from their aqueous solutions, while the permeation of less hydrophobic or hydrophilic aromas (i.e., hexanoic acid, diacetyl and dimethyl sulfone) was not affected.

(3) In general, the permeation of aroma compounds was affected negatively by the presence of lactose, whey protein or milk fat in the feed solution. The reductions in the aroma flux by these non-volatile compounds were consistent with the hydrophobicity of the aroma compounds, and there appeared to be considerable hydrophobic interaction, between these non-volatile compounds and the aromas compounds.

(4) Dimethyl sulfone, the most polar compound among the eight aromas studied here, was influenced most negatively by the presence of lactose. This was believed to arise from the hydrogen bonding of dimethyl sulfone by lactose.

(5) No concentration polarization or membrane fouling was observed when lactose (5 wt.%), whey protein (3.5 wt.%), fat (3.5 wt.%) and NaCl (2 wt.%) were present in the feed solution. This suggests that in pervaporative extraction of aroma compounds from dairy solutions, membrane contamination and cleaning are not a concern.

Chapter 6

Concentration of Dairy Solutions by Pervaporation, Ultrafiltration, Nanofiltration and Reverse osmosis

6.1 Introduction

In the processing of dairy products, one of the important processing units is the concentration of milk or other semi-finished dairy products. The concentration of dairy products is a necessary operation unit in manufacturing certain dairy products. The main objectives of concentration are: to produce milk powder or protein (or other nutritional components) enriched products, or to reduce the weight and volume during packaging and transportation, to improve the stability and handling of the product, or to reduce water activity to prolong the shelf life of dairy products. Evaporation, freeze concentration and membrane concentration (especially reverse osmosis) are three major methods for concentration of dairy products, while evaporation is widely used for the removal of water in the dairy industry. However, there are technical issues of high energy consumption, possible thermal degradation of nutritious components (such as proteins and vitamins) and aroma compounds, and flux decline due to membrane fouling in the case of reverse osmosis. Pervaporation may be an alternative to these methods considering its low energy consumption, mild operating conditions and insignificant fouling problems. The aim of this chapter was to evaluate whether pervaporation has the potential to concentrate dairy solutions, and how the pervaporation performance was affected by operating conditions. For this purpose, the dairy solutions were concentrated by using pervaporation, ultrafiltration, nanofiltration and reverse osmosis, and their separation performance was evaluated and compared.

6.2 Experimental

6.2.1 Materials

6.2.1.1 Feed mixtures

Model milk solutions were prepared by mixing whole milk powder with water, with and without whey protein/lactose/35 wt.% cream/NaCl. The whole milk powder and whey protein were purchased from Bulk Barn Foods Limited. The nutrition facts in the whole milk powder are listed in Table 6.1 (These data were provided by Bulk Barn Foods Limited). Lactose (from Now Foods Inc.), the 35 wt.% cream (containing 35 wt.% milk fat, from Neilson Dairy) and sodium chloride (NaCl) (from Sigma-Aldrich Corporation) were added to the solution as needed.

Table 6.1 The nutrition facts in whole milk powder

Nutrition facts	Amount per 100 g milk powder, g
Fat	27
Protein	27
Lactose	40
Sodium	0.37

6.2.1.2 Dead-end filtration systems (UF, NF, RO and PV)

The dehydration experiments were conducted using laboratory-scale dead-end test setups, which are shown in Figure 6.1. In the dead-end pervaporation experiments (Figure 6.1 (a)), PEBA 1074 membrane was mounted to the stainless steel membrane cell with an effective membrane area of 14.85 cm^2. The feed volume was 200 mL and the feed solution was stirred using a magnetic stirrer at 1000 rpm, which corresponded to a *Re* number of 64 (Wu et al.). A vacuum pump was applied at the downstream side of the membrane to maintain a permeate

pressure of 400 Pa. The permeate sample was condensed and collected in a cold trap immersed in liquid nitrogen (around -196 °C).

In UF, NF and RO processes, the 200 mL dead-end membrane cell was pressurized with nitrogen. The maximum pressure that the system could withstand was 1.5 MPa. The pressure gauge and regulator (by ProStar) were used to control and adjust the feed pressure. The feed solution was stirred at 1000 rpm. The permeate was collected in a sample vial and weighed using a digital balance. In Sections 6.3.1-6.3.3 and 6.3.5, the feed concentration was kept constant by sending back the permeate to the feed continuously, while in Section 6.3.4 and 6.3.6 the operations were batch-wise and the permeate collected was not sent back to the feed. in Section 6.3.4 and 6.3.6. The cleaning of the fouled UF, NF and RO membranes was performed following a procedure recommended by the membrane manufacturers. At the end of each run, the upstream side of the system was flushed sequentially with water-NaOH solution-water at room temperature and at a pressure of 0.8 MPa. All experiments were carried out in duplicates, and the experimental errors were estimated to be 10%, an example of experimental error bars is shown in Appendix E.

.

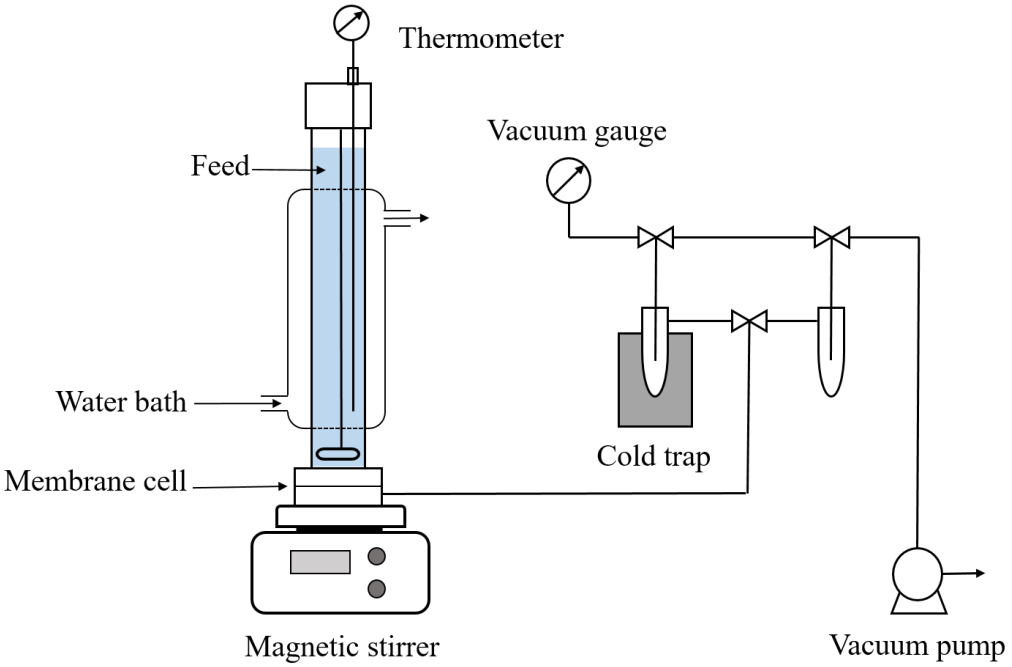

(a)

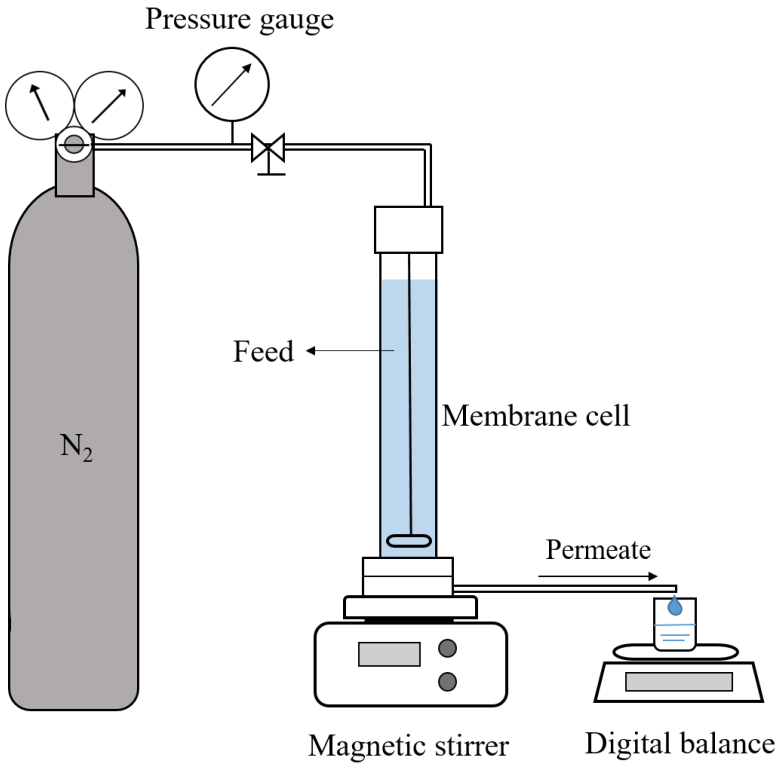

(b)

Figure 6.1 The experimental setup for (a) PV and (b) UF, NF, and RO processes.

6.2.1.3 Membranes

Table 6.2 lists the specifications of the membranes used in this research. PEBA 1074 dense membranes were prepared in the lab. At first, 18 wt.% homogeneous PEBA solution was prepared by dissolving Pebax® 1074 pellets (supplied by Arkema Inc.) in 1-methyl-2-pyrrolidinone (NMP) (99%) (supplied by Sigama) with vigorous stirring at 105 °C for 12 h. The polymer solution was kept in 105 °C for another 12 h to degas any bubbles trapped during the agitation. The degassed solution was then cast on a pre-heated glass plate (80 °C) using a glass rod with wires at both ends to control the membrane thickness. After solvent evaporation 80 °C for 24 h, the membrane was immersed in deionized water, and the membrane detached itself from the glass plate. The membrane was then dried in the oven at 50 °C for 5 hours and stored in a desiccator at room temperature. The thickness of the membrane was 35 μm, which was the average of the thicknesses measured at 6 different spots using a micrometer. The UF, NF and RO membranes were commercially composite membranes. Prior to testing, these membranes were immersed in deionized water for 24 h to remove any surface preserving agents and then stored in deionized water with water replaced frequently to prevent microbial growth. For SR3D and HRX membranes, they were rinsed with NaOH solution (0.0001 mol/L) for 30 mins and then with deionized water for 30 mins, as recommended by the manufacturers installation instructions. Before filtration experiment started, all membranes were pre-conditioned with pressurized pure water on the feed side at given operating pressures until a stable water flux was produced.

Table 6.2 Characteristics of membranes or membrane material (polymer) provided by suppliers.

Membrane Processes	Pervaporation	Ultrafiltration	Nanofiltration	Nanofiltration	Reverse osmosis	Reverse osmosis
Membrane	PEBA 1074	UF1	SR3D [a]	NF8	HRX [a]	RO6
Manufacturer	Made in lab	Development Center of Water Treatment Technology, China	KOCH Membrane Systems	Nanostone Water	KOCH Membrane Systems	Nanostone Water
Membrane material	PEBA 1074 [b]	Polysulfone	polyamide	Polyamide	polyamide	Polyamide

[a] These two membranes were especially designed for dairy products separations.

[b] This copolymer was comprised of 55 wt.% polyethylene oxide and 45 wt.% polyamide.

6.2.2 Methods

6.2.2.1 Measurement of contact angle

The hydrophilicity of the membranes was characterized by the contact angle of water on the membrane surface at room temperature. The contact angle measurements were carried out with a contact angle meter (Cam-plus Micro, Tantec Inc.) using the sessile drop (about 3 µl) method. Ten measurements were conducted at different locations on the membrane surface, and the reported data were the average values of the ten measurement.

6.2.2.2 Measurement of total solid content in permeate

The concentration of total solid in the permeate could not be determined simply by HPLC or TOC because of the complex compositions of permeate sample involved that contained minerals, organic acids, ash components, sugars and proteins. In order to take all the components into account in the calculation of percentage retention of the membranes, each permeate sample was weighed and then dried in an oven at 80 ^{o}C for 15 h to allow all of the water to evaporate. The remaining solids were weighed, and the mass concentration of the permeate sample was determined from the mass of dried solids and the initial mass of the permeate sample.

6.2.2.3 Characterization of PV, UF, NF and RO membranes performance

(1) Total flux and retention

$$J = \frac{V}{At} \tag{6.1}$$

$$R = \left(1 - \frac{C_p}{C_f}\right) \times 100\% \tag{6.2}$$

where J is the total flux of permeation, V is the permeate volume collected over operating time t, A is membrane area, R is the solute retention, C_p and C_f are the total solid concentrations in permeate and in feed, respectively.

(2) Total resistance and individual mass transfer resistances in PV, UF, NF and RO processes

The permeation flux can be described in the following phenomenological equations for different membrane processes:

Pervaporation:

$$J = \frac{\Delta P}{R_{tot}} = \frac{\Delta P}{R_m + R_{cp} + R_f} = \frac{a_w P^{sat} - P^p y}{R_m + R_{cp} + R_f} \quad (6.3)$$

Ultrafiltration:

$$J = \frac{\Delta P}{\mu R'_{tot}} = \frac{\Delta P}{\mu(R'_m + R'_{cp} + R'_f)} \quad (6.4)$$

Nanofiltration and reverse osmosis:

$$J = \frac{\Delta P - \Delta \pi}{R_{tot}} = \frac{\Delta P - \Delta \pi}{R_m + R_{cp} + R_f} \quad (6.5)$$

where J is instantaneous flux. ΔP is pressure differential across the membrane. For pervaporation, ΔP will be the partial vapor pressure difference (i.e., $\Delta P = a_w P^{sat} - P^p y$, where a_w is water activity, P^{sat} is saturated vapor pressure of water, which is 2635 Pa at 22 °, P^p is the pressure on the permeate side, which was 400 Pa, and y (≈ 1) is water mole fraction in permeate). R_{tot} (or R'_{tot}) is the total resistance to permeation, R_m (or R'_m), R_{cp} (or R'_{cp}) and R_f (or R'_f) represent the resistances from the membrane, concentration polarization boundary layer and membrane fouling, respectively. μ is the viscosity of the UF permeate. The a_w values of different dairy solutions were obtained from literature, as presented in Table 6.3:

Table 6.3 The water activity (a_w) values of dairy solutions with different solid contents.

Solid content of dairy solution, wt.%	Aw	Reference
4	0.99	(Bylund, 2015)
12	0.99	(Bylund, 2015)
20	0.99	(Bylund, 2015)
30	0.99	(Bylund, 2015)
40	0.95	(Ruegg, 1985)

For ultrafiltration and reverse osmosis, $\Delta\pi$ is the osmotic pressure difference between the feed solution and the permeate. In principle, at a transmembrane pressure equal to $\Delta\pi$, the permeation flux will be zero, based on Equation 6.5. Therefore, the $\Delta\pi$ in the NF and RO processes using SR3D and HRX membranes with a 12 wt% feed solution was estimated by plotting the J_o vs. TMP (Figure 6.2), where J_o is the initial permeation flux at the beginning of the NF and RO processes, and TMP is the transmembrane pressure. Note that for RO process, the solid content in permeate stream was essentially zero, and thus $\Delta\pi$ was equal to the osmotic pressure of the feed. For NF, only small salts (mainly NaCl, KCl and $CaHPO_4$) will permeate through the membrane, and when the feed solid content changed from 4 to 16 wt%, there were only a slight variation in rejections of milk solids in NF (within 3%) (see Section 6.3.2), therefore, the osmotic pressure of the NF permeate was considered to be constant when the feed solid contents ranged from 4 to 16 wt%. Thus in the NF and RO processes, the $\Delta\pi$ values at different feed dairy solutions were approximated to be proportional to the solid content of the feed solution. The estimated $\Delta\pi$ values are presented in Table 6.4.

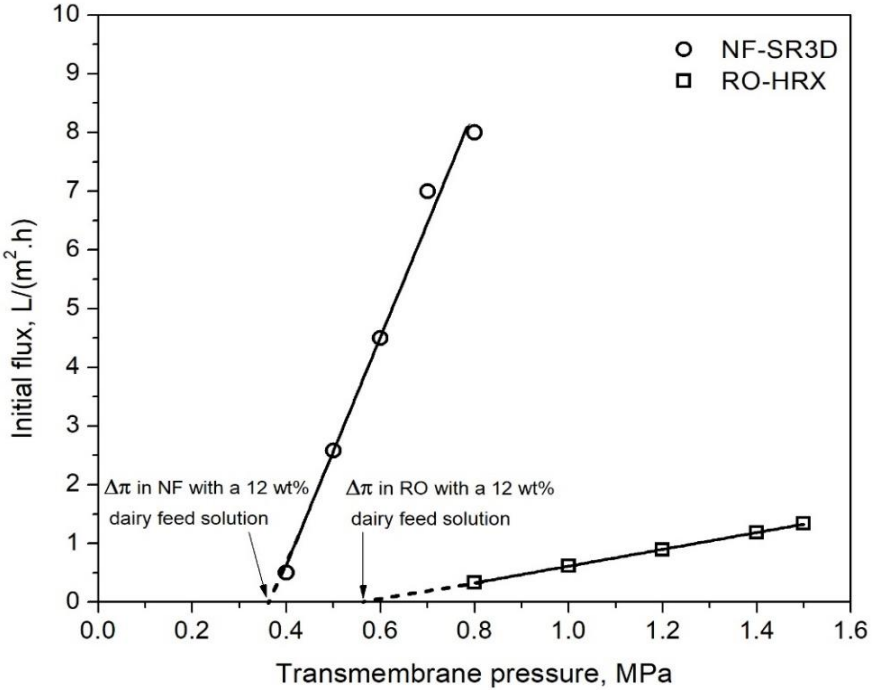

Figure 6.2 The initial permeation flux at the beginning of NF and RO continuous operations as a function of transmembrane pressure, using 12 wt% dairy solution at 22 ˚C.

Table 6.4 The osmotic pressure difference ($\Delta\pi$) across the NF and RO membranes at different feed solid contents, MPa

	Feed solid content		
	4 wt%	12 wt%	16 wt%
NF-SR3D	0.122	0.367	0.489
RO-HRX	0.190	0.571	0.761

To better compare the resistance to permeation in the different membrane processes, the units of the mass transfer resistance need to be unified. Therefore, the ultrafiltration flux equation (Equation 6.4) was expressed as:

$$J = \frac{\Delta P}{R_{tot}} = \frac{\Delta P}{R_m + R_{cp} + R_f} \tag{6.6}$$

where $R_{tot} = \mu R'_{tot}$, $R_m = \mu R'_m$, $R_{cp} = \mu R'_{cp}$, $R_f = \mu R'_f$.

6.3 Results and discussion

6.3.1 Pure water permeation through UF, NF, RO and PV membranes

To compare the permeance of different membrane processes and membranes for water permeation, the pure water flux through UF, NF, RO and PV membranes were determined at room temperature. For pressure-driven UF, NF and RO processes, water fluxes at different transmembrane pressures (TMP) were measured, and the water permeance was obtained from the slop of the Flux Vs. TMP plot (Figure 6.3). For the PV process, the pure water flux of the PEBA 1074 membrane at room temperature was determined to be 2.45 L/(m^2.h), which corresponded to a water permeance of 1096.20 L/(m^2.h.MPa).

Table 6.5 shows the water contact angle, water permeance and membrane resistances to water permeation to water permeation for the membrane tested; here the membrane resistance to water permeation was considered to be the reciprocal of pure water permeance). PEBA 1074 membrane for pervaporation showed the highest water permeance among all the membranes studied, followed by the UF and NF membranes. The RO membrane showed the lowest water permeance, as expected. The membrane resistances to water permeation of these membranes followed the opposite sequence.

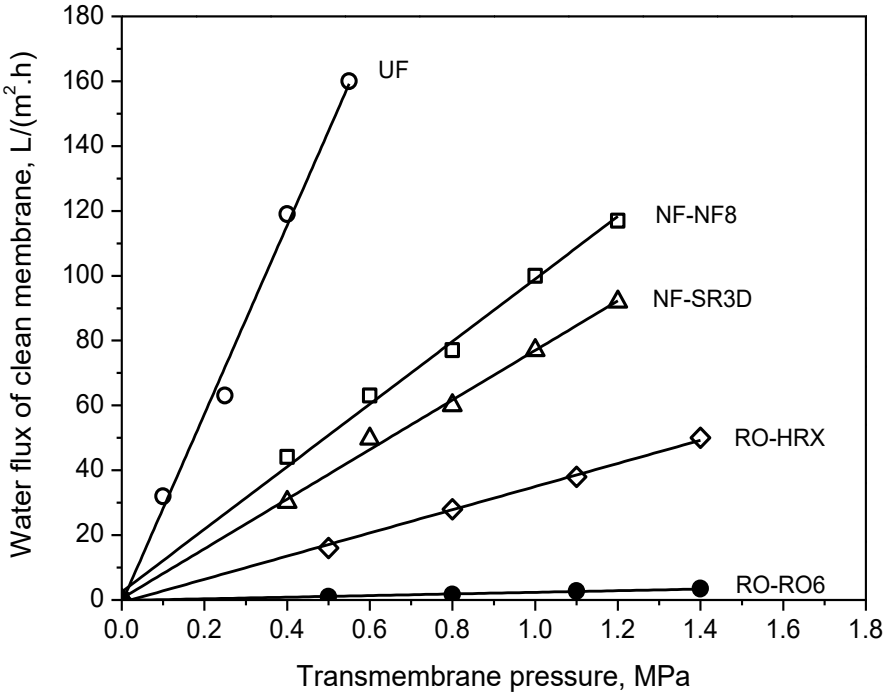

Figure 6.3 Pure water fluxes of clean membranes in UF, NF, RO operations under different transmembrane pressures at 22 ˚C.

Table 6.5 Contact angle, MWCO, water permeance and membrane resistance of all detected membranes.

Membrane	Contact angle of water (°)	MWCO[a] (Da)	Pure water permeance using clean membranes at 22 ˚C (L/(m^2.h.MPa))	R_m, (10^9 Pa.s/m)
Pervaporation				
PEBA 1074	67	Dense	1,096.20 [b]	3.28 [b]
Ultrafiltration				
UF1	53	100,000	288.88	12.46
Nanofiltration				
SR3D	59	200	77.03	46.73
NF8	37	200-300	99.29	36.26
Reverse osmosis				
HRX	41	< 200	35.03	102.78
RO6	33	< 200	2.37	1,518.09

a. MWCO data was taken from the membrane manufactures.

b. The typical values are calculated based on the PV pure water flux (2.45 L/m^2.h) and the corresponding pressure difference across PEBA 1074 membrane (2235 Pa) at 22 ˚C.

The hydrophilicity/hydrophobicity of the membrane surface, which was determined by the chemical characteristics of the membrane material, affected the water permeance of a membrane. The contact angle of water on the membranes provided a quantitative measure of the membrane hydrophobicity/hydrophilicity. Hydrophilic membrane surface is not very vulnerable to fouling by a dairy solution. The tightness of membrane structure was another parameter that determined membrane water permeability. The membrane "pore size" can be described by molecular weight cut-off (MWCO), which is defined as the lowest molecular weight (in Daltons) at which greater than 90% of a solute with a known molecular weight is retained by the membrane. The pervaporation membrane had a dense structure, and the concept of MWCO was not relevant.

The contact angle values (Table 6.5) suggest that all the membranes tested were hydrophilic, but the PEBA 1074 is the least hydrophilic membrane. This means PEBA 1074 membrane had a low water solubility compared to the other membranes. Nonetheless, water transport in the PV membrane was by the solution-diffusion mechanism, and the diffusion of water molecules in the PEBA 1074 membrane was significantly fast, resulting in a high water permeance in this membrane.

In the cases of UF, NF and RO processes, it is the membrane pore size that mainly determined water permeance and thus membrane resistance to water permeation. UF1 membrane has a high MWCO of 100,000 Da, which displayed a high water permeance of 288.88 L/(m^2.h.MPa), while the MWCO of RO membranes was less than 200 Da, therefore they had a lower water permeance than the UF and NF membranes due to the tighter structure of the RO membranes.

6.3.2 Comparisons of UF, NF, RO and PV performance for concentrating dairy solutions

The performance of the UF, NF, RO and PV membranes for concentrating dairy solutions was evaluated by conducting the continuous filtration experiments under different feed solid contents and TMP. The dead-end membrane cell used for all experiment was the same, with an equal membrane area irrespective of the membrane types and operating conditions. The permeate was continuously sent back to the feed solutions to keep the feed concentration constant. In the case of NF and RO membranes, NF-SR3D and RO-HRX manufactured by KOCH Membrane Systems were selected to treat the dairy solutions because of their higher steady-state permeation fluxes (2.7 $L/m^2.h$ and 0.12 $L/m^2.h$ for a feed solid content of 12 wt.% at 0.8 MPa) than NF8 and RO6 (0.1 $L/m^2.h$ and 0.01 $L/m^2.h$ for a feed solid content of 12 wt.% at 0.8 MPa). Figure 6.4 (a-c) shows the total fluxes during the concentration of the milk solutions using UF1, NF-SR3D and RO-HRX membranes at a fixed TMP of 0.8 MPa and different feed solid contents; Figure 6.4 (d) shows the water flux for pervaporative dehydration of the milk solutions at a permeate pressure of 400 Pa. Figure 6.7 shows the percentage retention of total solids at the 10^{th} hour of the filtration at different feed solid contents using the four membrane processes.

As expected, at a given TMP for a given feed solid content, UF1 had a higher permeation flux than NF-SR3D and RO-HRX because of the loose structure of UF membranes. PV transport was not driven by the TMP, rather it was determined by the partial vapor pressure difference across the membrane, which was normally much smaller than the TMP used in pressure-driven processes. This resulted in a low permeation flux comparing to UF1 and NF-SR3D. Interestingly, PV exhibited a higher permeation flux than RO, in spite of its dense membrane structure. In PV, there was a phase change from liquid to vapor as permeant passed

the membrane. The membrane resistance for water transport in PV was low (as discussed in 6.3.1). In addition, unlike UF, NF and RO, the high osmotic pressure of the feed had no impact on water permeation in PV process. These two reasons lead to a higher flux using PV-PEBA1074 than using RO-HRX.

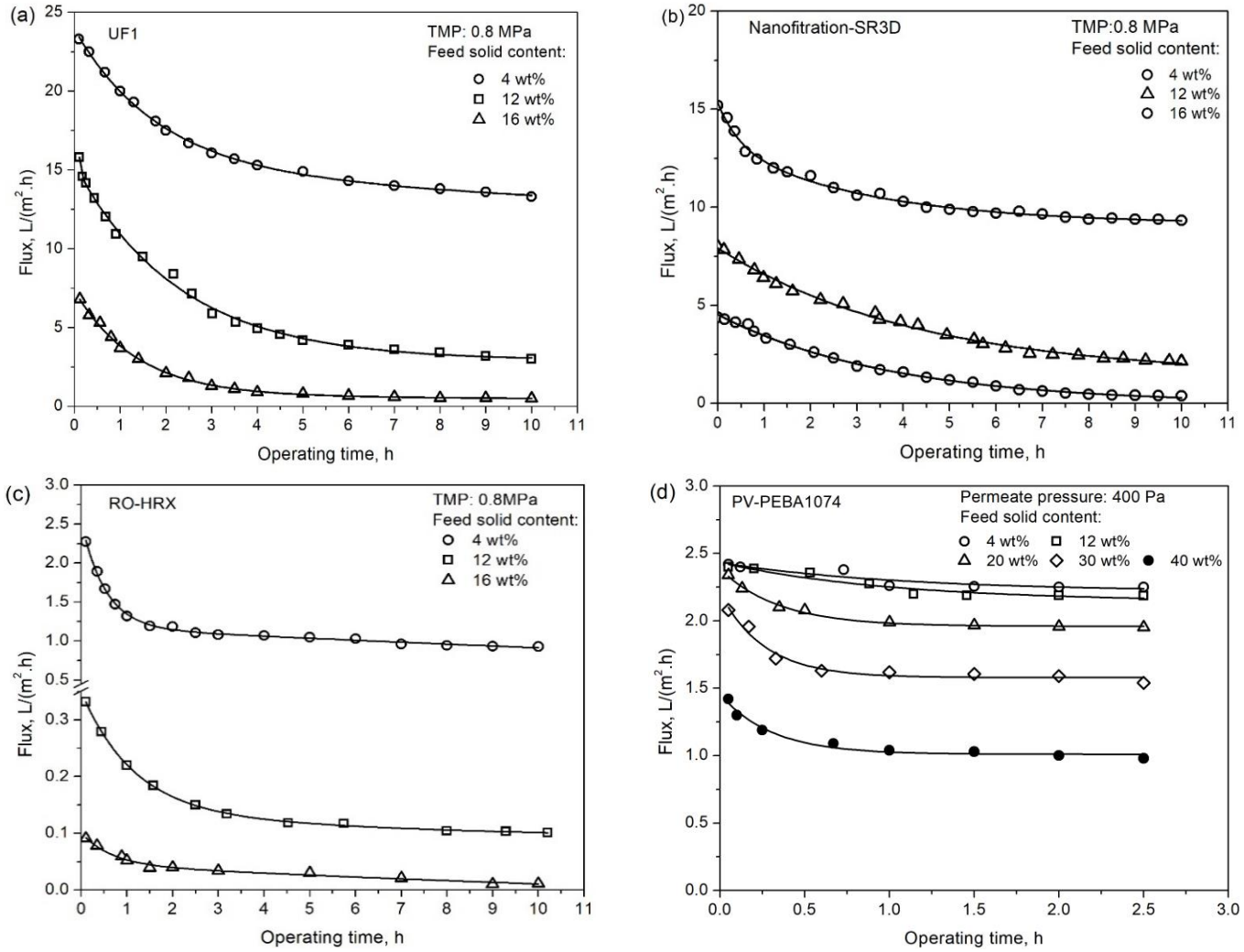

Figure 6.4 Total flux during concentration of dairy solutions using (a) UF1, (b) NF-SR3D, (c) RO-HRX and (d) PV-PEBA 1074 membranes at different feed solid contents. TMP for UF, NF and RO 0.8 MPa; the permeate pressure for PV 400 Pa. Temperature for all experiments 22 ˚C.

It is also interesting to note that as the feed solid content increased, the steady-state permeation flux in all the membrane processes decreased, but water flux in the PV membrane was not as sensitive to feed solid content change as the other membrane processes. As shown in Figure 6.4 (a-c), at a TMP of 0.8 MPa, when the feed solid content increased from 4 to 16 wt.%, the UF, NF, and RO steady-state fluxes decreased from 15 to 1 L/m^2.h, 10 to 0.5 L/m^2.h and 1 to 0.02 L/m^2.h, respectively. At a higher feed solid content, the feed osmotic pressure increases, thereby decreasing the flux. Based on these experimental data, it is believed that it will be difficult to use UF1, NF-SR3D and RO-HRX membranes to concentrate a dairy solution above16 wt.%. On the other hand, UF and NF membranes appeared to be superior to PV membrane when the milk solid content was below 16 wt.%, while the PV membrane had a higher flux when the solid content in the solution was over 16 wt.%. At a solid content as high as 40 wt.%, a permeation flux of 1 L/m^2.h could still be obtained by the PV membrane. Based on work reported in literature, the highest milk solid content in the feed than can be treated with RO is around 25 wt.% (Pouliot, 2008). Clearly, this suggests that pervaporation is more applicable than other membrane processes in concentrating dairy solutions of high solid contents.

In addition, a flux decline with time was observed in UF, NF, RO and PV processes, and then stable flux was reached. The flux decline was more dramatic at higher feed solid contents for all the four membranes, as shown in Figure 6.4 (a-d). The percent flux decline (FD) was calculated as follows:

$$FD\ (\%) = (1 - \frac{J_d}{J_w}) \times 100\% \qquad (6.3)$$

where J_d is the permeation flux of dairy solution at a given time during the filtration, J_o is the initial permeation flux of the dairy solution at the beginning of the filtration. Figure 6.5 shows

the ratio of J_d/J_o during continuous UF, NF, NF and PV operations at different feed solid contents with a TMP of 0.8 MPa, and different TMPs with a feed solid content of 12 wt.%. UF1, NF-SR3D and RO-HRX membranes experienced extremely severe flux declines with time for all the dairy solutions. At 0.8 MPa, when the feed solid content was 16 wt.%, almost 90% flux decline occurred in the UF, NF and RO processes, indicating the difficulty of using these three membranes to concentrate dairy solutions at a high solid content, primarily due to severe membrane fouling. Comparing to the other three membranes, PV-PEBA 1074 membrane had the lowest flux decline: when the permeation flux was stabilized, a 7-17% flux decline was observed at 4-20 wt.% feed solid contents, and a 26-31% flux decline occurred as the feed solid content increased from 20 wt.% to 40 wt.%.

The flux decline was well expected, because during filtration, there was an accumulation of retained colloidal particles at the membrane surface, giving rise to a concentration gradient of particles perpendicular to the membrane surface, known as concentration polarization (CP) (Rice et al., 2008; Rinaldoni et al., 2009). This concentration gradient served as the driving force for diffusion of the particles back to the bulk feed, which at steady state, was in balance with the bulk movement of particles to the membrane surface. This layer of concentrated particles generates a resistance to water permeation, as a physical barrier or increased osmotic pressure which reduces the effective transmembrane pressure. Besides concentration polarization, membrane fouling is another reason for the flux reduction. Membrane fouling can occur in two forms: reversible and irreversible membrane fouling. A gel layer formed on the UF1, NF-SR3D and RO-HRX membranes after filtration. Figure 6.6 (a) is an example of the gel layer on the surface of NF-SR3D after 10 hours of filtration of 12 wt.% milk solution. It was considered as reversible membrane fouling because it can be removed by water rinsing,

as can be seen in Figure 6.6 (b). However, gel layer on PEBA 1074 membrane surface was not observed after 2.5 h of pervaporation. This is easy to understand since the water flux in the PV process is relatively low, which renders concentration polarization less significant. This explains the low flux reduction using PV-PEBA 1074. Irreversible membrane fouling was only found on UF1 membrane. After filtrating dairy solutions and membrane cleaning, the pure water flux through the UF1 membrane did not reach the pure water flux of the virgin membrane, indicating that irreversible membrane fouling occurred. The details will be discussed in Section 6.3.4. The low flux decline percentage of PV-PEBA 1074 suggests its potential in concentrating dairy solutions, especially at high solid contents.

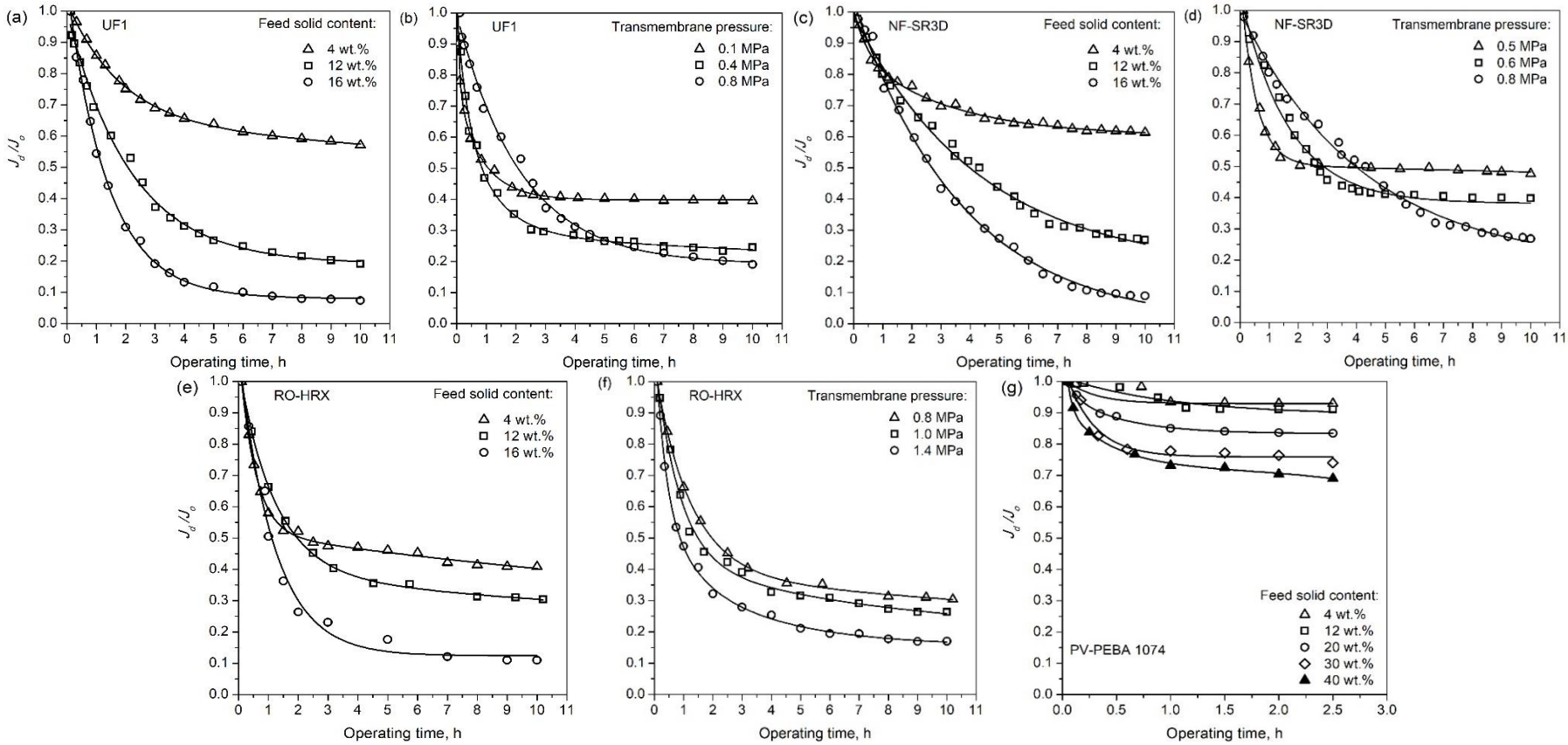

Figure 6.5 The ratio of J_d/J_o during the continuous UF, NF, NF and PV operations at different feed solid contents (TMP 0.8 MPa) or different TMPs (feed solid content 12 wt.%). Temperature 22 ˚C.

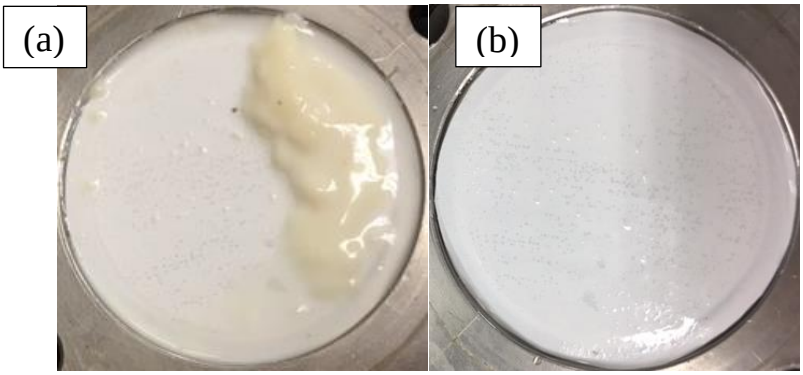

Figure 6.6 (a) The gel layer on the surface of NF-SR3D after 10 hours filtration of 12 wt.% milk solution; (b) the surface of the NF-SR3D membrane after water rinse.

In addition to permeation flux, the ability to retain the solute compounds in milk was also an important metric for comparison. As shown in Figure 6.7, UF1 had the lowest retention to milk solids, although it had a higher flux than the other membranes. The retention of milk components by UF1 decreased when the feed solid content was increased, and only 58% retention was achieved at a feed solid content of 16 wt.% at 0.8 MPa, which means a significant amount of the milk components also passed the membrane. NF-SR3D and RO-HRX had a retention of 95-98% and ≥99% at a solid content in the range of 4-16 wt.%. PV-PEBA 1074 exhibited the best retention performance (almost 100% solid retention) among these membranes. As expected, excellent solute retention was highly correlated to the non-porous structure of the PEBA 1074 membrane. Therefore, UF and NF are suitable to treat dairy solutions with a low solid content in order to get a high permeation flux with reasonable solute retention, while PV is superior to UF, NF and RO when treating a dairy solution of high solid content.

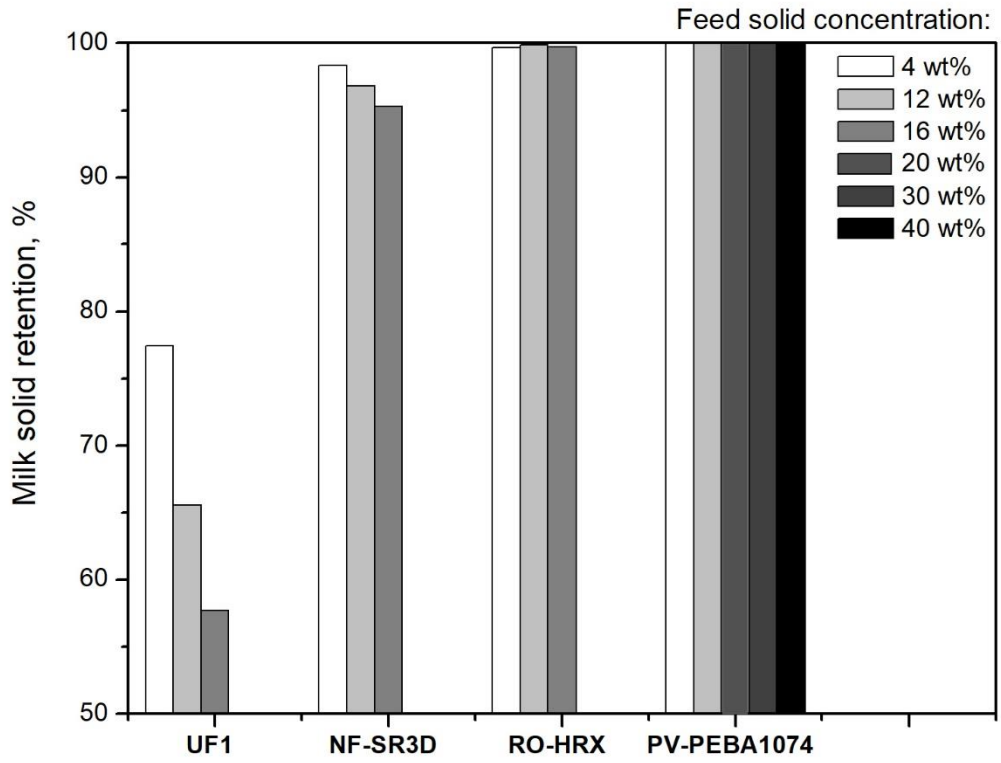

Figure 6.7 Retention of total solid (%) at the 10th hour of the filtration using UF1, NF-SR3D, RO-HRX and PV-PEBA 1074 membranes at different feed solid contents. TMP for UF, NF and RO processes was 0.8 MPa. Permeate pressure for PV was 400 Pa. Temperature for all experiments was 22 ˚C.

Transmembrane pressure provides the driving force for pressure driven UF, NF and RO separation, and it plays an important role in membrane performance. Figure 6.8 shows the effects of TMP on the permeation flux of a milk solution at a solid content of 12 wt.% using UF1, NF-SR3D and RO-HRX. The effect of feed pressure on PV was not studied here because the feed pressure had little impact on permeation flux, and a low permeate pressure was always preferred in PV (the permeate pressure was 400 Pa throughout the studies). A higher TMP tended to produce a higher permeation flux, and the flux decline was also more significant for UF, NF, and RO, as seen in Figure 6.5. This indicates that a high TMP was likely to render the concentration polarization or membrane fouling more significantly.

As far as the milk solid retention was concerned, there was no significant change with RO-HRX membrane, and a milk solid retention of greater than 99% was obtained over a wide range of TMP tested (i.e. 0.8-1.4 MPa), as shown in Figure 6.9. However, the TMP was found to affect the retention of the NF-SR3D membrane, and a higher TMP favored the membrane retention. On the contrary, the milk solid retention of UF1 membrane decreased with an increases in TMP. In general, there are two competing factors dictating the separation behavior. On the one hand, with an increase in TMP, the water flux increases while the milk solid flux is sterically hindered, leading to a higher solid retention. This is the so called “dilute effect”. On the other hand, more solute molecules transport from the bulk solution toward the membrane surface as the flux increases, which enhances the concentration polarization and subsequently reduces the solute retention (Seidel et al., 2001). It seems that the latter effect played a more significant role in ultrafiltration process with UF1 membrane while the dilute effect was dominant in nanofiltration with SR3D membrane.

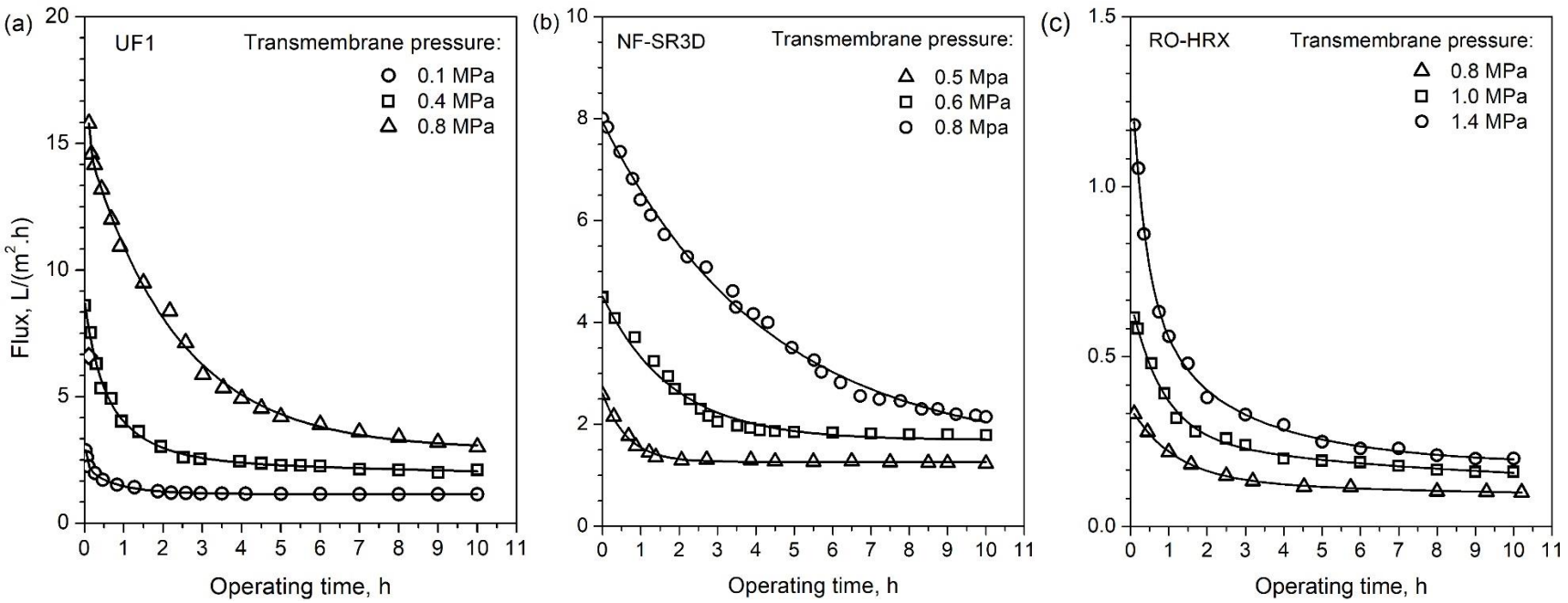

Figure 6.8 Permeation flux for concentration of dairy solutions using UF1, NF-SR3D and RO-HRX membranes at different TMP. Feed solid content 12 wt.%. Temperature 22 ˚C

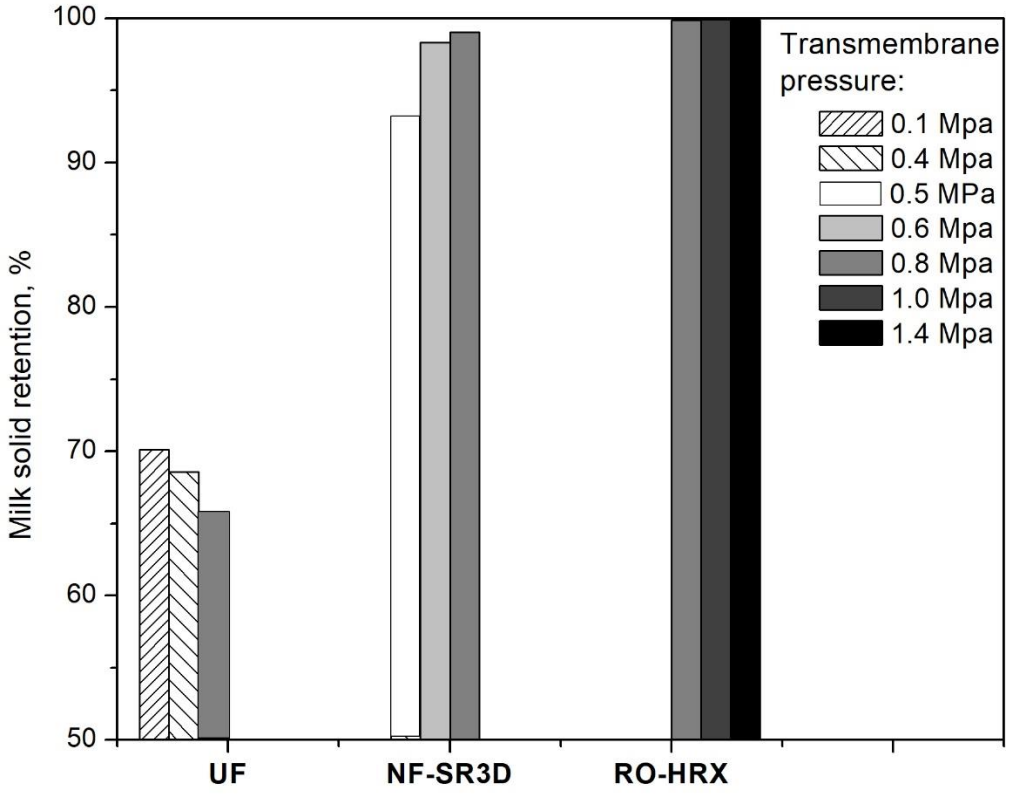

Figure 6.9 Retention of milk solid (%) using UF1, NF-SR3D and RO-HRX 1074 membranes at different TMP. Feed solid content 12 wt.%. Temperature 22 ˚C.

6.3.3 Fouling behavior of the UF, NF, RO and PV membranes and the effect of feed solid content and transmembrane pressure on membrane fouling

It is known that flux decline can be caused by such factors as concentration polarization and membrane fouling (gel layer formation and blocking of the pores). This will result in additional resistances on the feed side for molecules to transport across the membrane. In this study, the resistance of the concentration polarization layer (R_{cp}), membrane resistance (R_m) and membrane fouling resistance (R_f), and their contribution to total resistance were evaluated to explain the flux decline in the continuous filtration operations described in Section 6.3.2.

The effects of TMP and feed concentration on the flux decline during the continuous operations were also analyzed.

In continuous UF, NF, RO and PV filtrations, the total resistance (R_{tot}) at a given operating condition was calculated using Equation 6.3, 6.5 or 6.6. The water activities (a_w) in dairy solutions with different solid contents were presented in Table 6.3, and the osmotic pressure differences ($\Delta\pi$) between the feed dairy solutions and the permeates in NF and RO processes were shown in Table 6.4. The membrane resistance (R_m) was experimentally determined from the steady-state pure water permeation flux of a clean virgin membrane, in which case the R_{cp} and R_f were equal to 0. The concentration polarization layer was assumed to form quickly at the early stage of the filtration, and therefore, the resistance from the concentration polarization boundary layer (R_{cp}) was determined from the initial permeation flux at the beginning of the filtration of the dairy solutions. At this time point the membrane fouling was assumed to have not started yet ($R_f \approx 0$). The resistance from membrane fouling (R_f) was obtained by subtracting R_{cp} and R_f from R_{tot}.

Figure 6.10 shows the individual resistance components as a function of operating time for the various feed dairy solutions at 0.8 MPa with UF1 membrane. The resistances R_{cp} and R_m were constant, and R_f increased as permeation proceeded with time, resulting in an increase in R_{tot}. R_f began to increase soon after the experiment started, indicating the formation of the gel layer on the membrane surface or membrane pore blocking happened at the very early stage of the filtration. In addition, a higher feed solid content caused a higher R_{cp}. For instance, when the solid content in the dairy solution increased from 4 to 16 wt.%, the R_{cp} was increased from 112×10^9 to 412×10^9 Pa.s/m. The increased concentration polarization resulted in more severe membrane fouling, and therefore the R_f increased as well, from

93×10^9 to 5337×10^9 Pa.s/m at the end of filtration. Therefore, the UF separation experienced increased total resistance (R_{tot}) to permeation, resulting in flux decline as the feed solid content increased. Therefore, the UF separation experienced increased total resistance (R_{tot}) to permeation, resulting in flux decline as the feed solid content increased.

TMP also had a siginificant effect on the permeation resistances. As seen in Figure 6.11, for the UF1 membrane, both R_{cp} and R_f increased with TMP. It is understandable because as TMP increased, a higher flux was obtained, thereby resulting in more solute molecules deposited on the upstream surface of membrane, leading to a higher degree of concentration polariztion and membrane fouling. For example, at a TMP of 0.1 MPa, R_{cp} and R_f were 113 and 191×10^9 Pa.s/m respectively at the end of filtration of the 12 wt.% dairy solution, whereas when TMP was increased to 0.8 MPa, R_{cp} and R_f reached 170×10^9 and 775×10^9 Pa.s/m, respectively. The increased R_{cp} and R_f resulted in an increase in R_{tot}, and thus a higher flux decline occurred at a higher TMP. One may also notice that at a low TMP of 0.1 MPa, R_f and R_{tot} first increased then leveled off, while at a high TMP of 0.8 MPa, within the first 10 h of operation R_f and R_{tot} kept increasing. This is because at higher TMPs, water flux was higher, which made concentration polarization and fouling more severe. It appears that at a TMP of 0.8 MPa, the fouling layer continued to develop, and did not reach a steady state after 10 h of continuous operation.

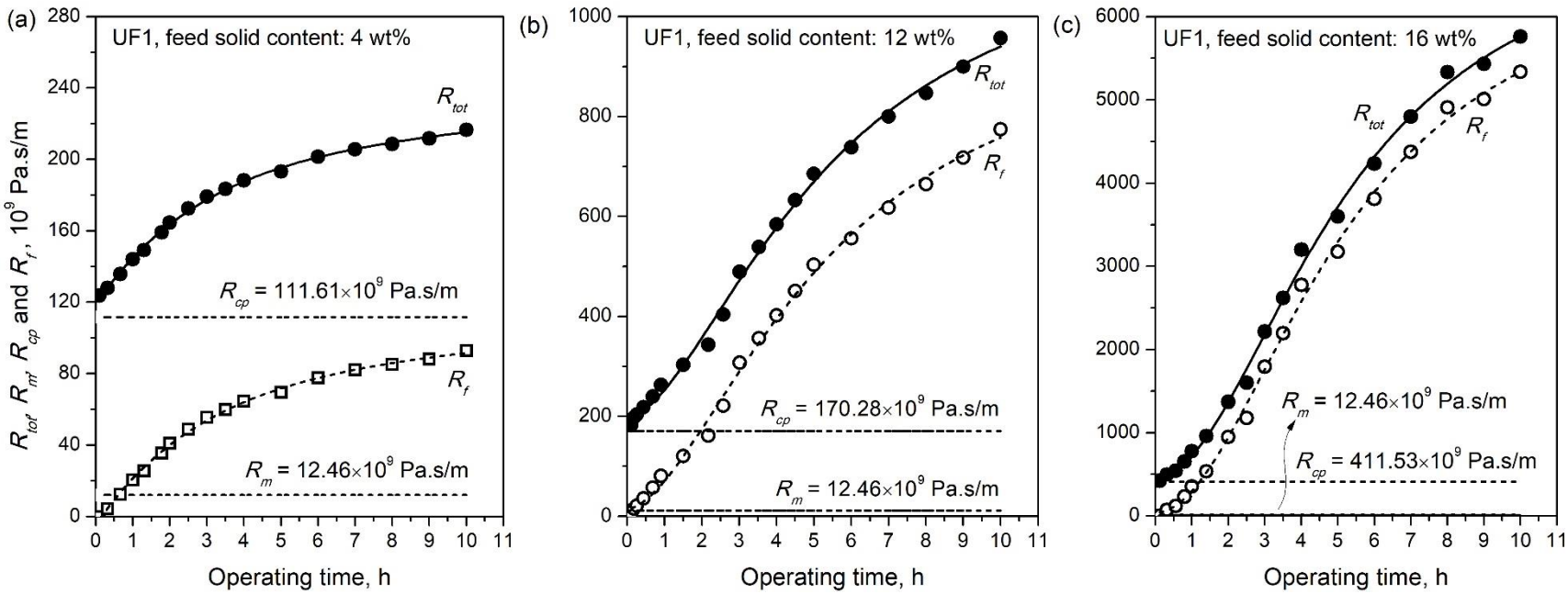

Figure 6.10 Individual resistance as a function of time during concentration of milk solutions using UF1 membrane at different feed solid contents. Temperature: 22 °C. Transmembrane pressure: 0.8 MPa.

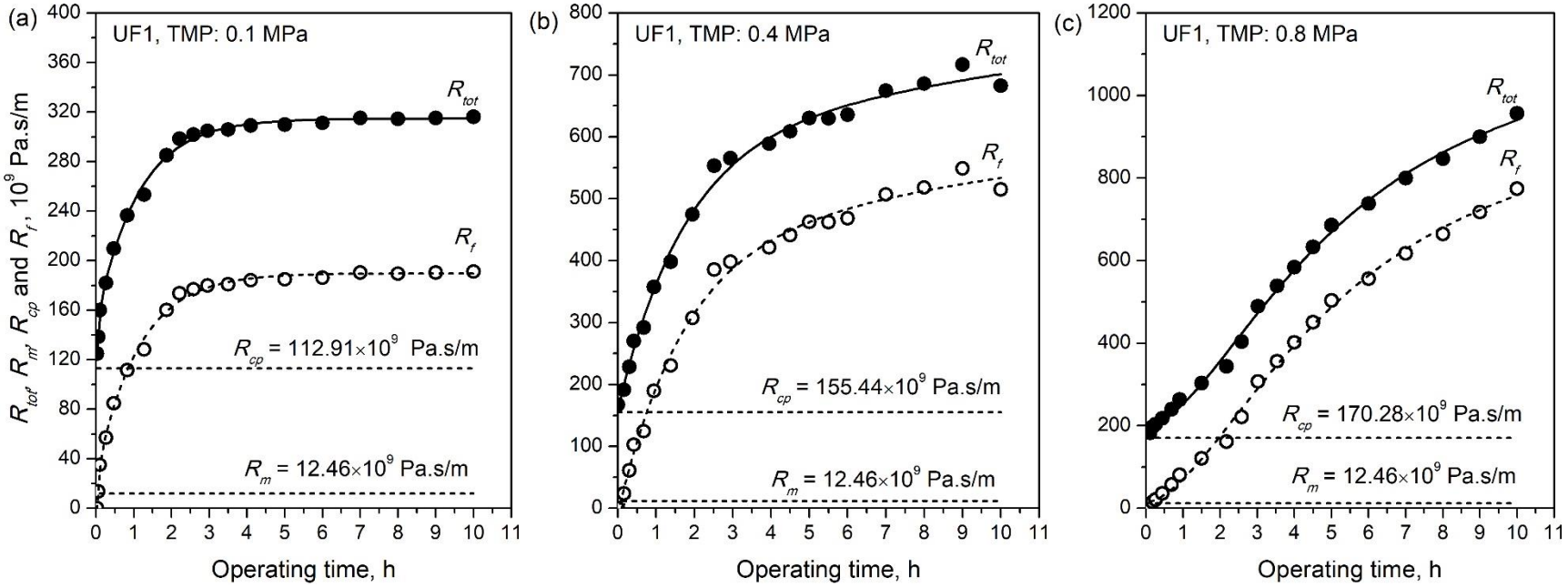

Figure 6.11 Individual resistance as a function of time during concentration of milk solutions using UF1 membrane at different TMP. Temperature: 22 °C. Feed solid content: 12 wt.%.

Both R_{cp} and R_f were increased at a higher feed solid content and a higher TMP. However, generally the membrane fouling was dominant over concentration polarization, based on the percentage contribution of R_{cp}, R_f and R_m to R_{tot} (see Table 6.6). The ratio of an individual resistance component (R_i) to the overall resistance (R_{tot}) as a function of operating time was presented in Figure B.1 and B.5. Increasingly, the feed solid content and TMP also increased the percentage contribution of R_f to the overall permeation resistance, while R_{cp} became less important. For instance, at 0.8 MPa, as the feed solid content changed from 4 to 16 wt.%, the ratio R_f/R_{tot} 0.43 to 0.93, while R_{cp}/R_{tot} decreased from 0.52 to 0.71. At a given feed solid content of 12 wt.%, increasing TMP from 0.1 to 0.8 MPa increased R_f/R_{tot} from 0.61 to 0.81, while decreased R_{cp}/R_{tot} from 0.36 to 0.18. In addition, it should also be noted that the membrane resistance R_m of UF1 only contributed 0.2-5.5% to the total resistance in all the experiments. These results indicate that membrane fouling was the main reason for the permeation flux decline.

Table 6.6 The individual resistances at the end of filtration, and the contributions of the individual resistances to the total resistance. Temperature: 22 °C.

Membrane	Dairy solution solid content, wt.%	TMP, MPa	Resistance, 10^9 Pa.s/m				Resistance contribution percentage, %		
			R_{tot}	$R_{cp}{}^{a}$	R_f	$R_m{}^{b}$	R_{cp}/R_{tot}	R_f/R_{tot}	R_m/R_{tot}
UF1	4	0.8	217	112	93	12	51.5	42.9	5.5
	12	0.1	316	113	191		35.7	60.5	3.8
		0.4	682	155	515		22.8	75.5	1.8
		0.8	957	170	775		17.8	80.9	1.3
	16	0.8	5760	412	5336		7.1	92.6	0.2
NF-SR3D	4	0.8	261	113	101	47	43.4	38.6	18.0
	12	0.5	389	189	204		35.6	52.3	12.1
		0.6	467	139	282		29.7	60.2	10.0
		0.8	725	148	530		20.4	73.1	6.5
	16	0.8	2868	208	2613		7.2	91.1	1.6
RO-HRX	4	0.8	2362	861	1398	103	36.5	59.2	4.3
	12	0.8	8162	2380	5679		29.2	69.6	1.3
		1.0	9533	2408	7022		25.3	73.7	1.1
		1.4	14848	2422	12323		16.3	83.0	0.7
	16	0.8	9280	1427	7750		15.4	83.5	1.1
PV-PEBA1074	4		3.58	0.04	0.25	3.28	1.3	7.0	91.7
	12		3.68	0.07	0.33		2.0	8.9	89.1
	20		4.12	0.16	0.68		3.8	16.5	79.6
	30		5.22	0.59	1.36		11.3	26.0	62.8
	40		8.21	2.39	2.54		29.1	31.0	40.0

[a] Calculated from the initial permeation flux of the continuous filtration.
[b] Calculated from pure water permeance of the clean membrane.

Figure 6.12-6.16 show the resistance components for dairy solution concentration at various solid contents and operating pressures with NF-SR3D, RO-HRX and PV-PEBA 1074 membranes. Similar to the UF1 membrane, increasing feed solid content and TMP increased R_{cp}, R_f, R_m and R_{tot} for all the NF, RO and PV processes. However, when the RO-HRX membrane was used, the individual resistances during permeation were the largest among all the four filtration processes. For example, at a feed solid content of 12 wt.% and a TMP of 0.8 MPa, the R_f and R_{cp} values at the end of the membrane processes were: RO-HRX (R_f = 5679×10^9 Pa.s/m, R_{cp} = 2380×10^9 Pa.s/m) > UF1 (R_f = 775×10^9 Pa.s/m, R_{cp} = 170×10^9 Pa.s/m) > NF-SR3D (R_f = 538×10^9 Pa.s/m, R_{cp} =148×10^9 Pa.s/m). The R_f and R_{cp} for PV using PEBA 1074 membrane were the lowest comparing to the other membranes, which explains the flux decline during the PV process was the least significant.

In terms of resistance contribution, Table 6.6, similarly to UF1 membrane, the contribution of R_f to overall resistance was dominant over the contributions of R_{cp} and R_m for NF-SR3D and RO-HRX membranes. At 12 wt.% feed solid content and 0.8 MPa, the R_f/R_{tot} was 0.73 for NF-SR3D and 0.70 for RO-HRX, indicating that there was significant membrane fouling in these membrane process. However, it was interesting to notice that with PV using PEBA 1074 membrane, even though the ratios of R_f/R_{tot} and R_{cp}/R_{tot} increased as feed concentration increased, R_m was still greater than R_f and R_{cp} to R_{tot} for all the dairy solutions tested. These results suggest that in pervaporation, the concentration polarization and membrane fouling were less significant. Even at a high concentration of dairy solution with 40 wt.% solid, the R_f/R_{tot} and R_{cp}/R_{tot} ratios were 0.29 and 0.30, respectively. These values explained why the PV-PEBA 1074 experienced a relatively low flux decline with time. The analysis of the individual permeation resistances in the four membrane processes,

pervaporation with PEBA 1074 membrane was shown to be advantages for concentrating dairy solutions, especially at a solid content as high as 20-40 wt.%, from a membrane fouling standpoint.

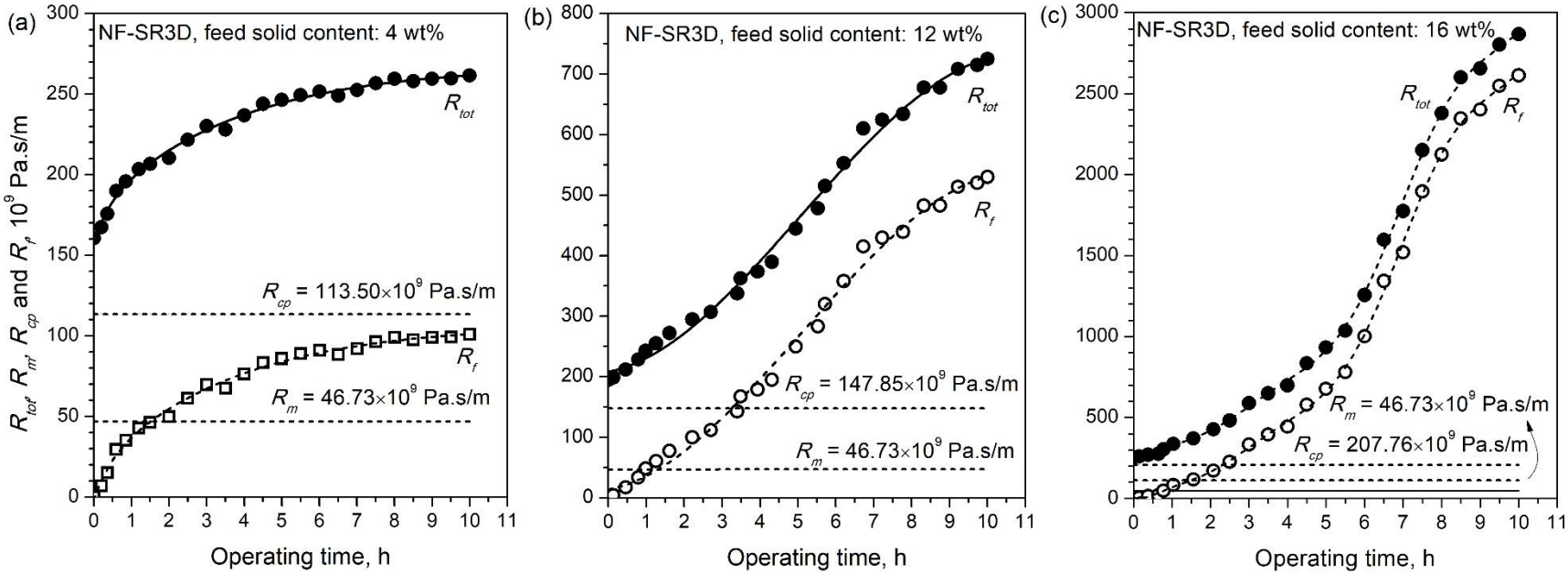

Figure 6.12 Individual resistance as a function of time during concentration of milk solutions using NF-SR3D membrane at different feed solid contents. Temperature: 22 °C. Transmembrane pressure: 0.8 MPa.

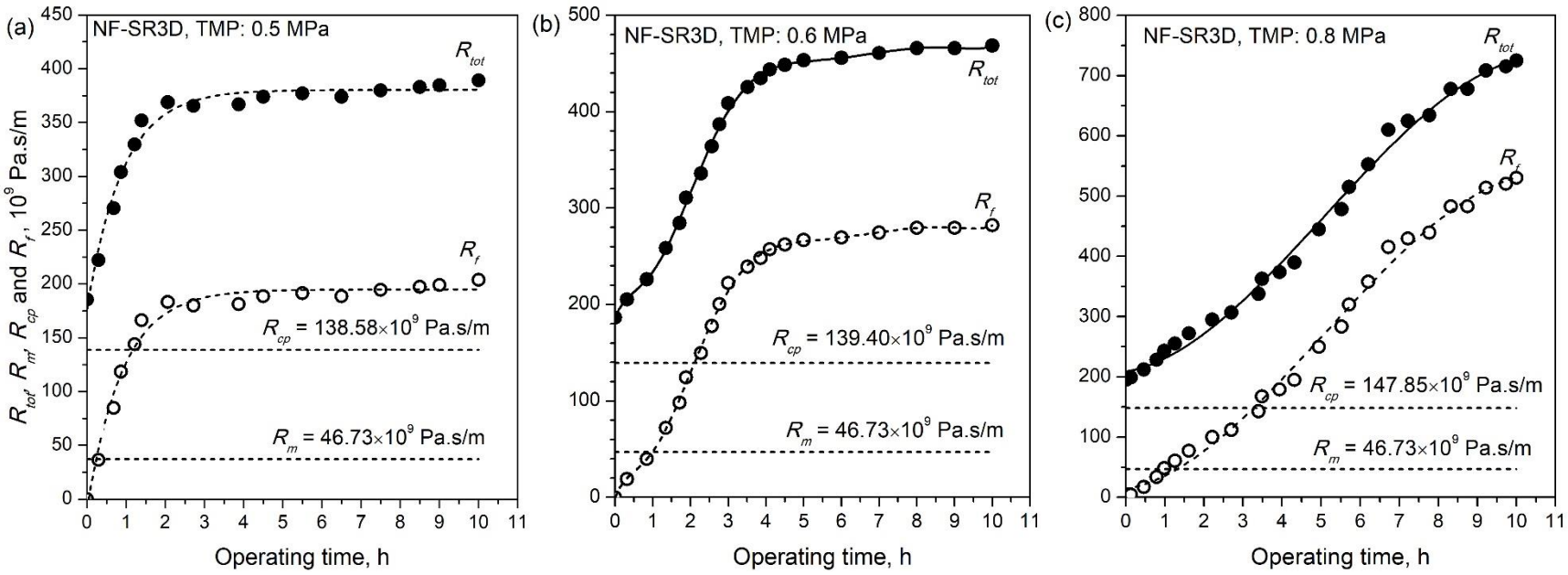

Figure 6.13 Individual resistance as a function of time during concentration of milk solutions using NF-SR3D membrane at different TMPs. Temperature: 22 °C. Feed solid content: 12 wt.%.

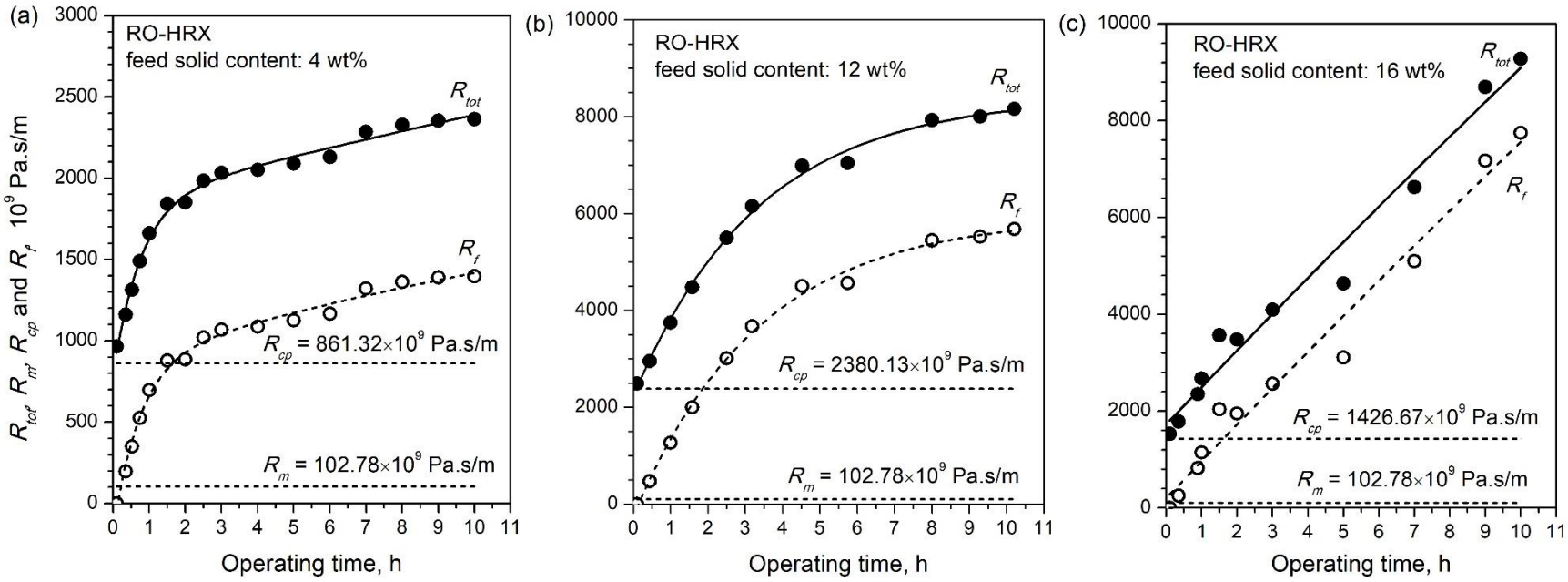

Figure 6.14 Individual resistance as a function of time during concentration of milk solutions using RO-HRX membrane at different feed solid contents. Temperature: 22 °C. Transmembrane pressure: 0.8 MPa.

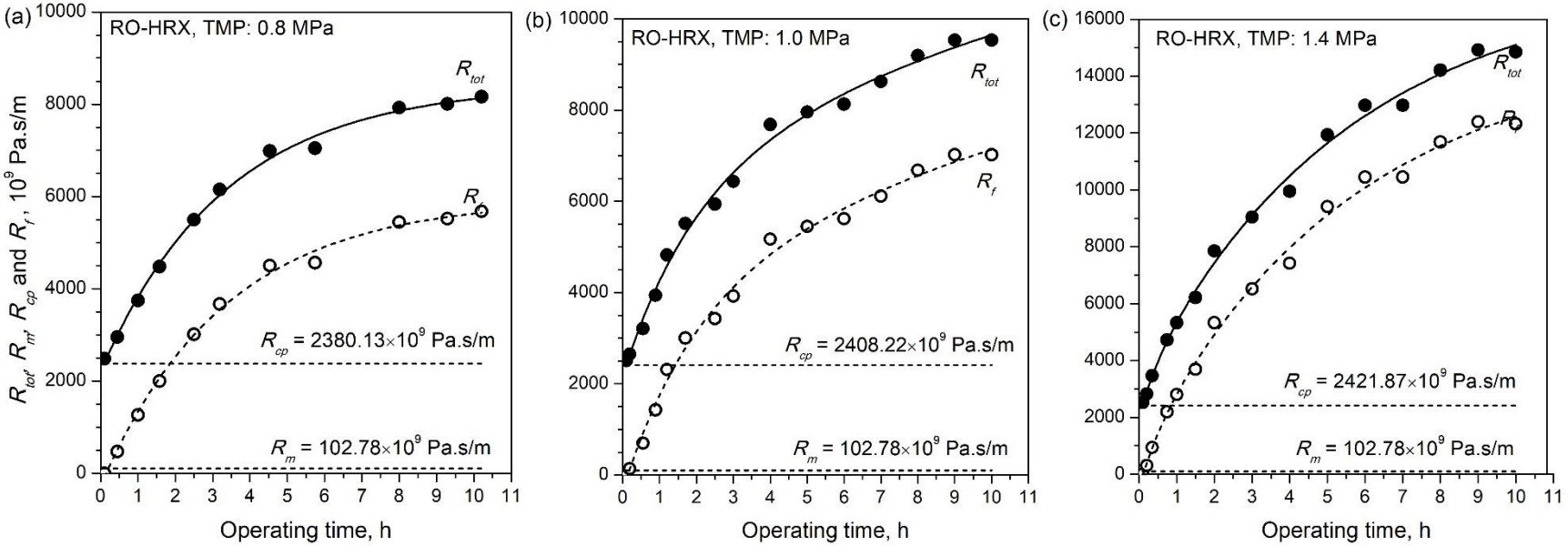

Figure 6.15 Individual resistance as a function of time during concentration of milk solutions using RO-HRX membrane at different TMPs. Temperature: 22 °C. Feed solid content: 12 wt.%.

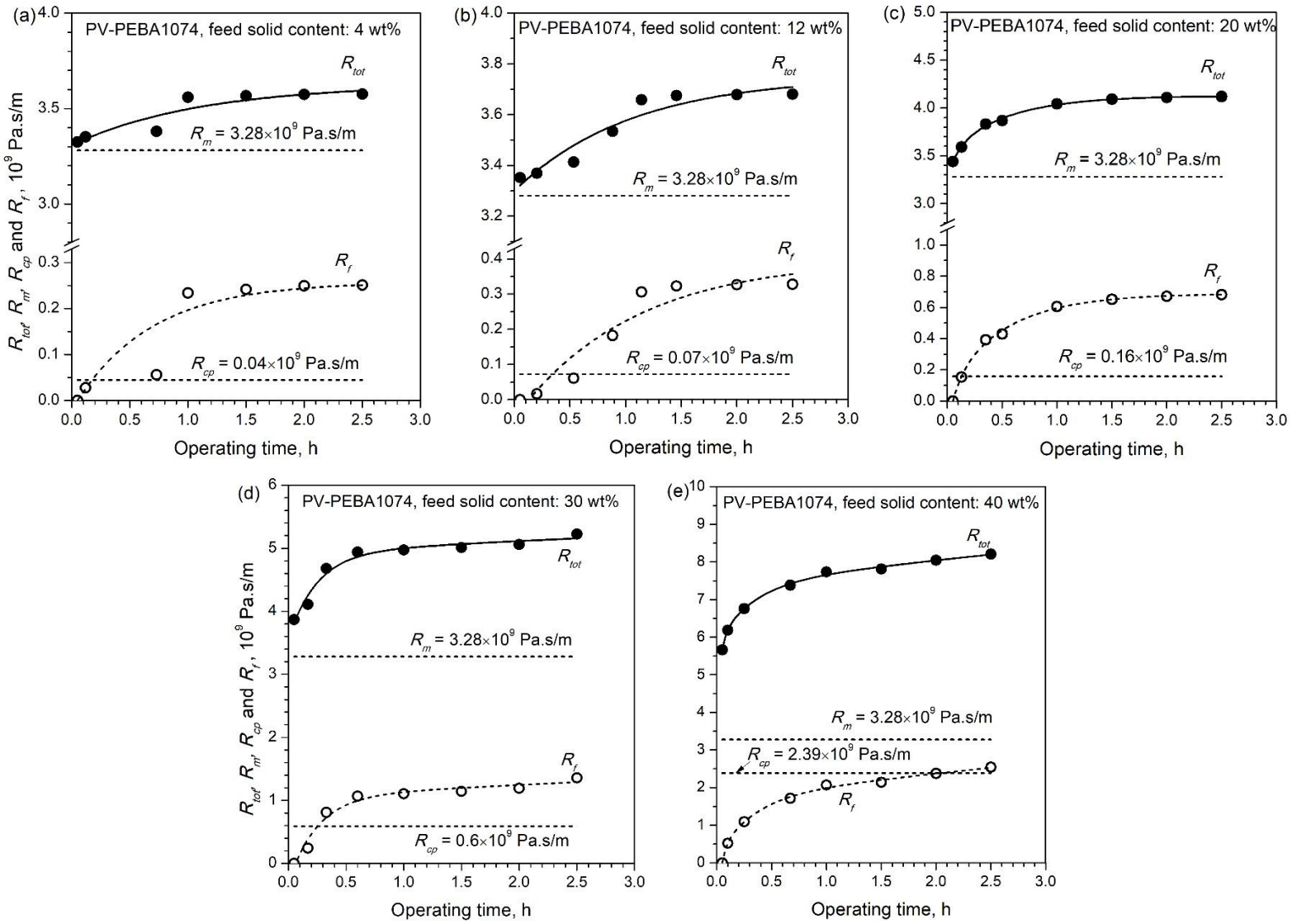

Figure 6.16 Individual resistance as a function of time during concentration of milk solutions using PV-PEBA 1074 membrane at different feed solid contents. Temperature: 22 °C. Permeate pressure: 400 Pa.

6.3.4 Membrane cleaning and flux recovery

Membrane fouling, which results in flux declines over time, is one of the limiting factors for membrane application in dairy industry. As discussed in Section 6.3.3, all the membranes studied here showed a flux decline as a result of concentration polarization and membrane fouling. Periodic cleaning of the membrane with clean water and other suitable cleaning agents is often used to reduce membrane fouling. To further study and compare the fouling vulnerability and stability of these membranes, 5 cycles of batch experiments with periodic membrane cleanings were conducted. The feed solutions for all experiments were the same: 200 mL 12 wt.% milk solution (12 wt.% whole milk powder + 88 wt.% water), the milk solid and water compositions are close to those in raw cow milk. The TMP for UF, NF and RO processes was 0.8 MPa, the permeate pressure of PV process was 400 Pa. Each operating cycle was composed of 10 h of concentration of feed solution with an initial solid content of 12 wt.%, and 3 h of membrane cleaning. Figure 6.17-6.20 show the flux decline over time during filtration and flux recovery by membrane cleaning as well as the milk solid retention over the 5 cycles by UF1, NF-SR3D, RO-HRX and PV-PEBA 1074 membranes. The membrane surface and cross-sections were examined under a FEI Quanta FEG 250 scanning electron microscopy (SEM) to clarify membrane fouling, as shown in Figure 6.21 and Appendix C.

Among the four membrane processes, UF1 membrane was the only one that experienced significant irreversible flux decline. As shown in Figure 6.17, after the first cycle of UF filtration and water cleaning the pure water flux declined from 231 to 115 $L/m^2.h$, representing a flux loss of 50.2%. To further clean the membrane, 0.0001 M and 0.1 M NaOH solutions were applied for membrane washing for 1 h, respectively. The pure water flux of UF1 was recovered to 142 $L/m^2.h$ after cleaning with 0.0001 M NaOH solution and 200 $L/m^2.h$ when

0.1 M NaOH solution was used to clean the membrane. Since NaOH is caustic alkaline that decomposes fat and proteins, it is frequently used as a removing the cleaning agent in the industry. Here 0.1 M NaOH solution was proved to be more effective on removing the foulant (mainly milk proteins and calcium phosphate (Van Boxtel et al., 1991)) on the membrane surface and/or inside membrane pores. Therefore, for the rest four recycles, the membrane cleaning protocol was 1.5 h water wash/1 h 0.1 M NaOH solution wash/0.5 h water wash. However, it appeared the foulants precipitated on the membrane surface were not completely swiped away since the first cleaning step, and the residuals accumulated on the membrane surface after each cleaning cycle would result in a further drop in the permeation flux in subsequent filtration cycles. After 4 filtration-cleaning cycles, the permeation flux was only 45% of the initial permeation flux with the virgin membrane.

The degree of concentration by filtration is usually expressed as the volume concentration ratio (VCR), defined as the quotient of initial feed volume (V_O) and concentrated retentate volume (V_R) (Cheryan, 1986):

$$VCR = \frac{V_O}{V_R} \tag{6.8}$$

In RO or PV processes, the solid concentration of permeate (C_P) is normally very low (≈ 0) due to the dense structure of RO and PV membranes, therefore,

$$V_O C_O = V_R C_R + V_P C_P \approx V_R C_R \tag{6.9}$$

So,

$$\frac{C_R}{C_O} = \frac{V_O}{V_R} = VCR \tag{6.10}$$

which means that in RO or PV operations VCR also represents how many times the dairy solution can be concentrated. In these five UF-membrane cleaning cycles, the VCR value

decreased from 1.69 for the first cycle to 1.12 for the fifth cycle. The pure water permeability through the membrane declined by 21.7% after 5 cycles of filtration/cleaning.

Figure 6.21 (a) and (b) are the SEM images of the surfaces of the virgin UF1 membrane and the UF1 membrane after cleaning. It clearly shows that some foulants, presumably to be whey protein and casein, are still left on the surface of UF1 membrane after water/0.1 M NaOH/water washing. Figure 6.21 (c) and (d) show the cross-section of the UF1 membrane before use and after washing. No significant pore blocking by macromolecules inside the finger pores was observed. These results suggest that the irreversible fouling on the UF1 membrane by dairy solution was mainly due to the binding between the membrane (polysulfone based) and milk proteins on the membrane surface. This was consistent with the work of Brink & Romijn (1990) that the major cause of irreversible protein fouling on polysulfone membrane was whey protein adsorption on the membrane surface, instead of pore-blocking.

It should also be mentioned that the flux reduction was not fully recovered after membrane cleaning with the cleaning protocol used in the study, therefore, more effective cleaning methods for the flux recovery are needed. Nonetheless, Figure 6.17 also shows that a full recovery and even a higher value in the milk solid retention was achieved with the membrane cleaning protocol used. This is probably because the foulants assembled on the membrane surface, acted as an extra resistance to milk solid permeation through the membrane.

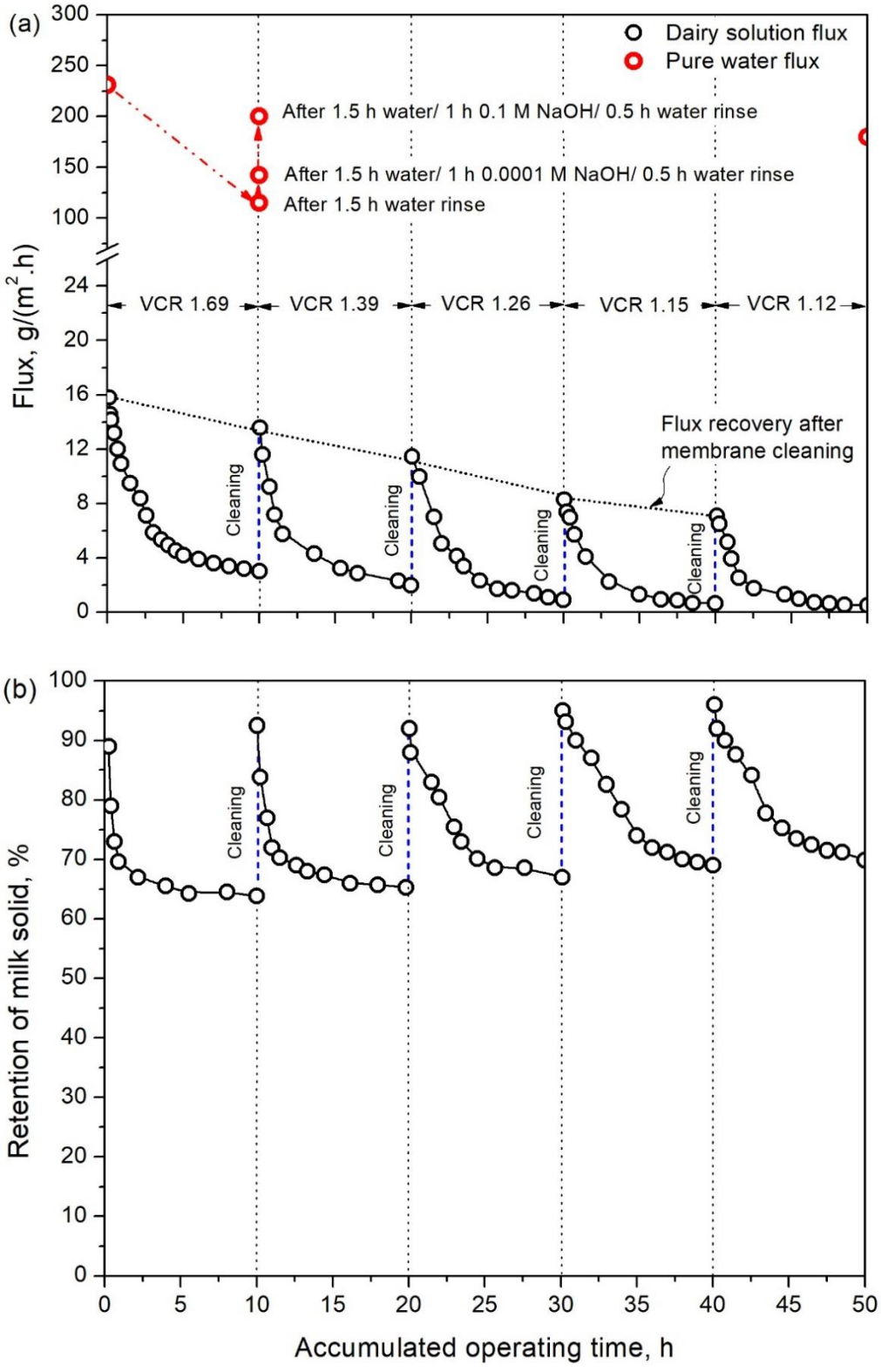

Figure 6.17 Decline and recovery of (a) permeation flux and (b) retention of milk solid over 5 cycles of batch operation and cleaning using UF1. Feed solid content: 12 wt.%, temperature:

22 °C, TMP: 0.8 MPa. Membrane cleaning protocol: 1.5 h water/1 h 0.1 M NaOH/ 0.5 h water rinse.

The NF-SR3D membrane was easier to clean than the UF1 membrane, as shown by the results in Figure 6.18. However, water washing alone could not fully remove the foulants from the membrane. After the first 10 h of NF operation, the membrane was washed by water, and 83.3% of the pure water flux was restored. A 0.0001 M NaOH solution was then used for further membrane cleaning for 0.5 h, leading to a 90.8% recovery in pure water flux. To further clean the membrane, the washing time with NaOH solution was extended to 1 h, then the pure water flux was fully recovered. This washing protocol (water wash for 1.5 h + 0.0001 M NaOH solution wash for 1 h + water wash for 0.5 h) was then used for the rest subsequent filtration-cleaning cycles. It is shown that after each cycle, both the dairy solution permeation flux and the solid retention was fully restored. The SEM images in Figure C.1 show that the membrane surface was almost as clean as the fresh membrane. However, it should be mentioned that, right after each NaOH solution wash, the permeation flux was slightly higher than the cleaned membrane in previous cycles. This is probably caused by a slight degradation of the polyamide by NaOH. In addition, after each water/NaOH/water wash, the permeation flux due to membrane fouling dropped more quickly. This suggests that though NaOH solution was effective for cleaning the SR3D membrane, the cleaned membrane became tends to make the membrane more vulnerable to protein fouling.

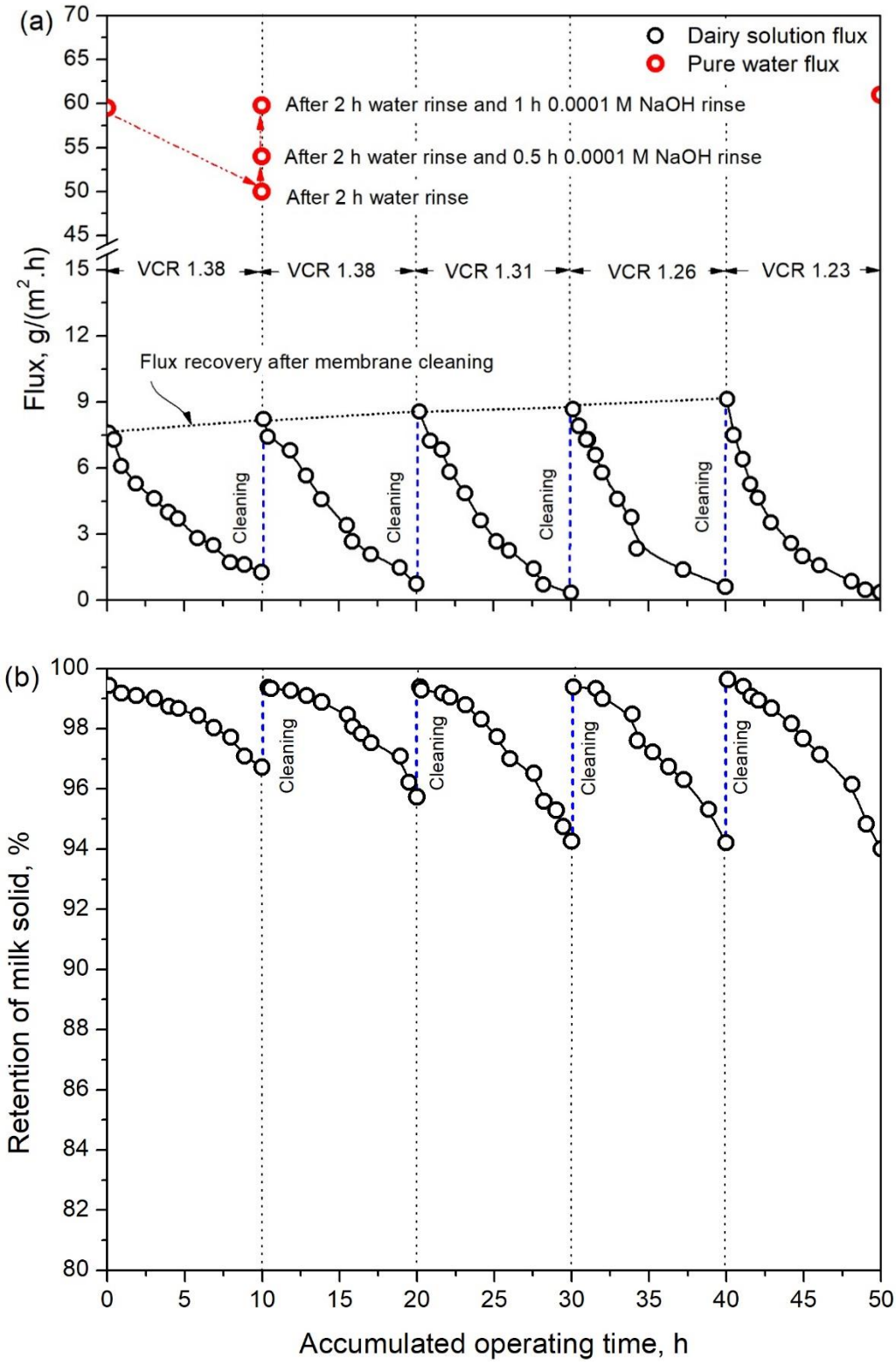

Figure 6.18 Decline and recovery of (a) permeation flux and (b) retention of milk solid for milk concentration using NF-SR3D. Feed solid content: 12 wt.%, temperature: 22 °C, TMP: 0.8 Pa. Membrane cleaning protocol: 1.5 h water/1 h 0.0001 M NaOH/ 0.5 h water rinse.

Water rinse alone could not fully clean the RO-HRX membrane either. As shown in Figure 6.19, after the first cycle, 71.4% of the initial pure water flux was restored by rising with water for 1.5 h. By using 1.5 h water/ 1 h 0.0001 M NaOH/ 0.5 h water cleaning steps, the pure water flux could be fully recovered. On the other hand, after continuous filtration for 10 h in each filtration cycle, the dairy solution flux decreased by 64%, the solid retention decreased slightly (ca. 1%). The water/0.0001 M NaOH/water cleaning protocol successfully recovered the dairy solution flux. The VCR in all filtration cycles was 1.01 during the entire course of the filtration experiments.

Among the four membranes tested, PEBA 1074 membrane used in pervaporation was the only one that required no chemical cleaning. The PEBA 1074 membrane was advantageous over the other three membranes. As shown in Figure 6.20, the PEBA 1074 membrane exhibited a low dairy solution flux decline (26.5%), and the solid retention remained very high (> 99.9%). In addition, the dairy solution flux was fully restored by water wash alone. After five pervaporation-water rinse cycles, the pure water flux was essentially the same as that of a fresh membrane. Membrane cleaning with NaOH solution was thus not needed. The PEBA 1074 membrane is hydrophilic and non-porous, which accounts for its good anti-fouling property. Meanwhile, pervaporation requires relatively low TMP (< 0.1 MPa). As discussed in the previous section, the gel layer attached on membrane surface is normally more significant at higher feed pressures. Therefore, the low pressure applied to the permeation side in the pervaporation, instead of applying a high pressure on the feed side as in other membrane processes, that helped reduce gel layer formation on the PEBA membrane surface, which could be removed by water flush alone.

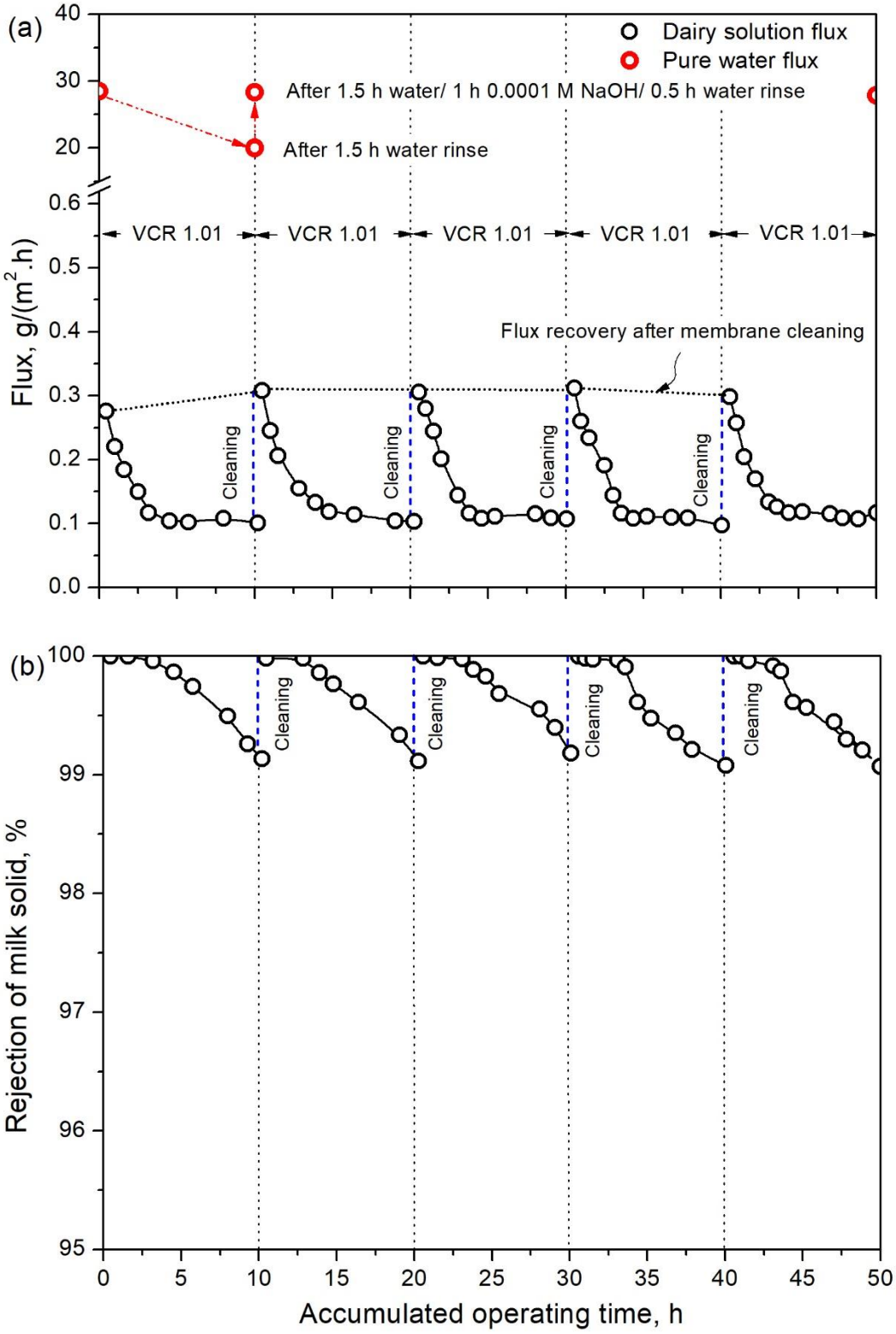

Figure 6.19 Decline and recovery of (a) permeation flux and (b) retention of milk solid for milk concentration using RO-HRX. Feed solid content: 12 wt.%, temperature: 22 °C, TMP: 0.8 Pa. Membrane cleaning protocol: 1.5 h water/1 h 0.0001 M NaOH/ 0.5 h water rinse.

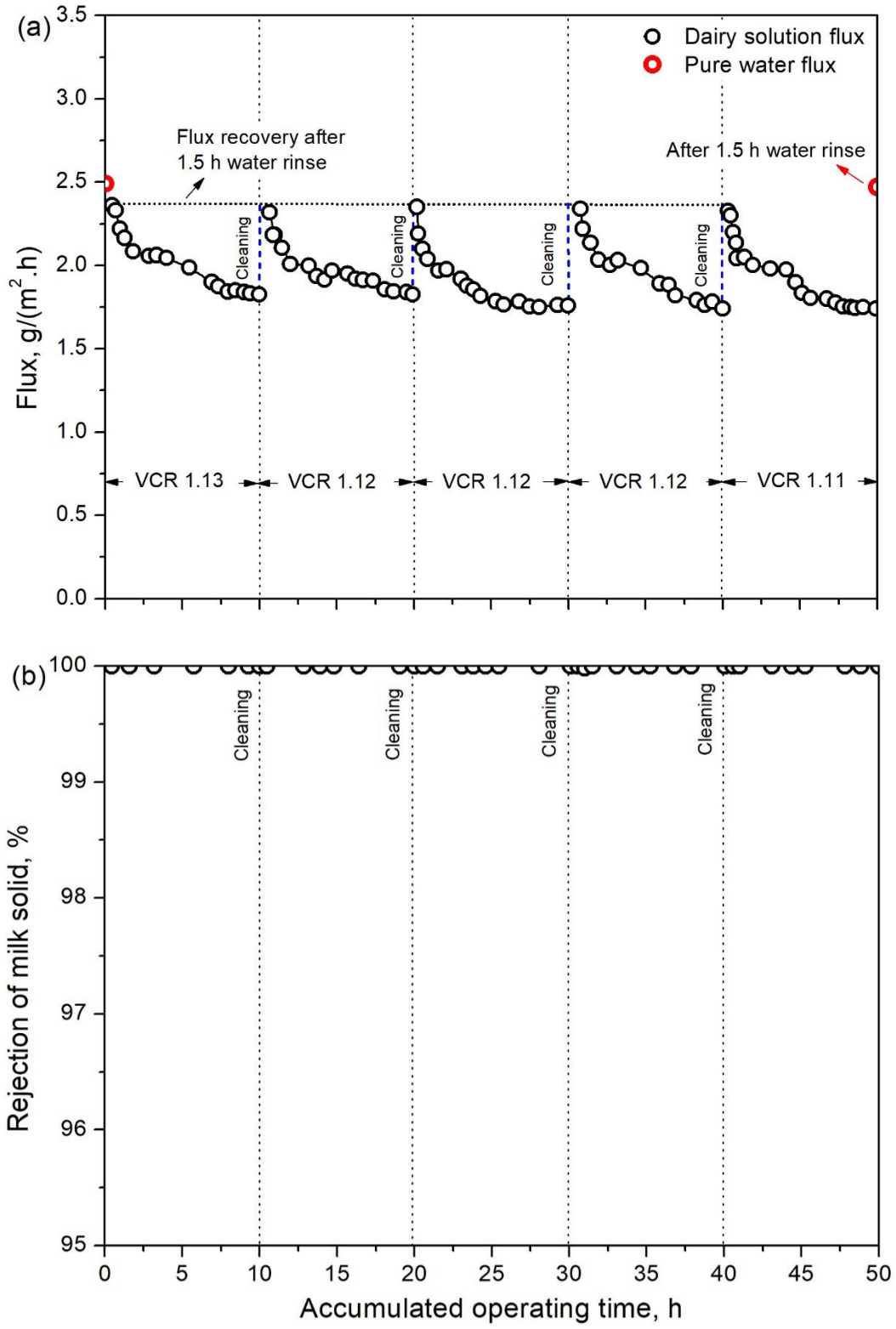

Figure 6.20 Flux decline and recovery for pervaporative using PEBA membrane. Feed solid content: 12 wt.%, temperature: 22 °C. Permeate pressure: 400 Pa. Membrane cleaning protocol: 1.5 h water rinse.

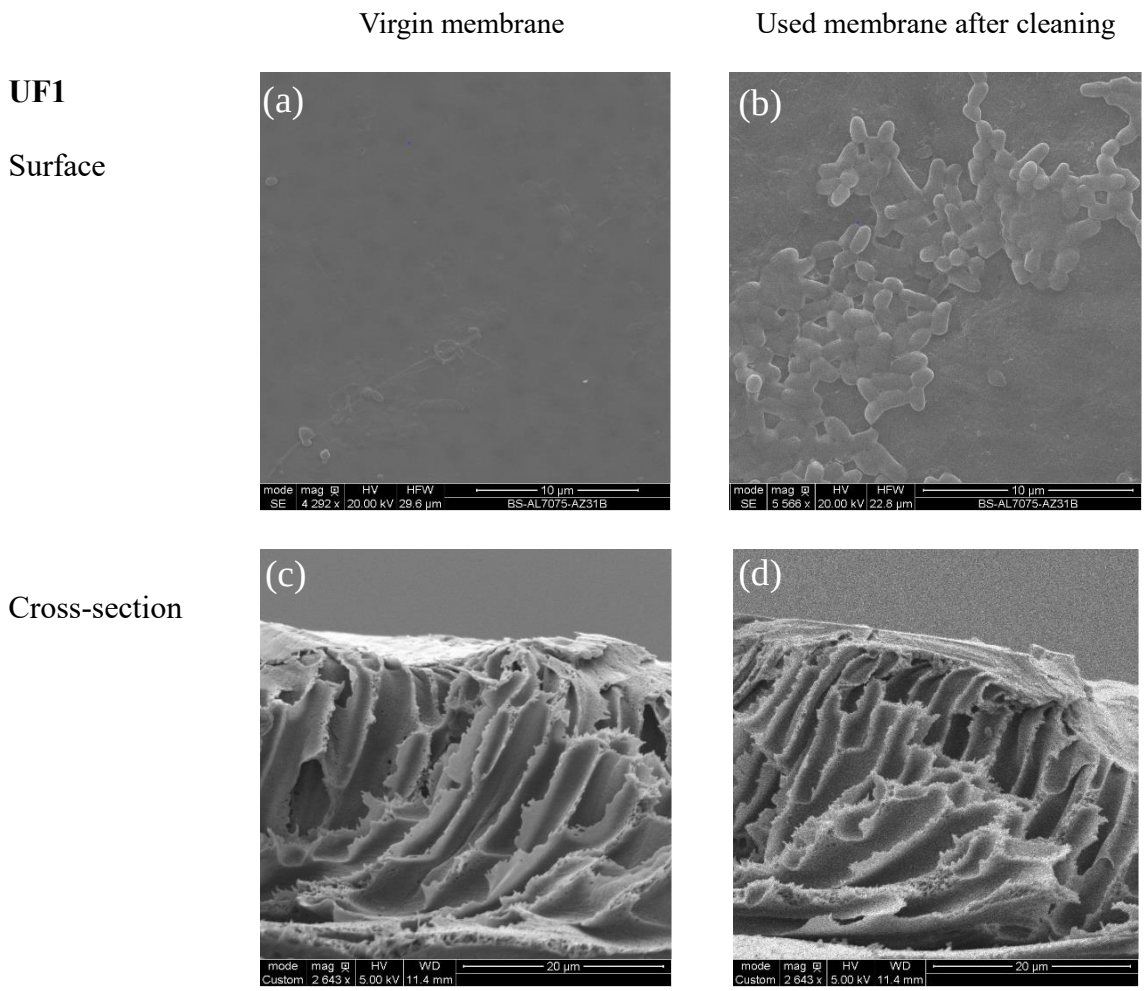

Figure 6.21 SEM images of virgin UF1 membrane and used UF1 membranes after cleaning

6.3.5 Effects of temperature and milk solid components on pervaporative concentration of dairy solution

Pervaporation had shown to be a potential method of concentrating dairy solutions, especially solutions with high solid contents. The operating temperature and the composition of the feed solution were expected to affect the pervaporative dehydration performance. Higher temperatures would increase the driving force for permeation, but the flux decline could become more significant due to foulant accumulation on the membrane surface (Kaya et al.,

2009). Adding additional non-volatile components, (e.g., salts, protein, lactose or fat) into dairy solutions would alter water activity in the dairy solution and change the pervaporation flux. Therefore, the influences of temperature and non-volatile components on concentrating dairy solutions using PEBA 1074 membrane were studied through experiments at various operating temperatures using milk solutions of different solid components.

Figure 6.22 illustrates the effects of temperature on steady-state flux of pervaporation at different milk solid contents using the PEBA 1074 membrane. The highest solid content studied here was 50 wt.%. As temperature increased from 22 to 42 °C, the pure water flux increased from 2.45 to 4.13 L/(m^2.h), and the permeation flux of the dairy solutions at 50 wt.% solid content increased from 0.38 to 1.01 L/(m^2.h). At higher temperatures, the partial pressures of water on the feed side increases, which facilitate the transport of water through the membrane.

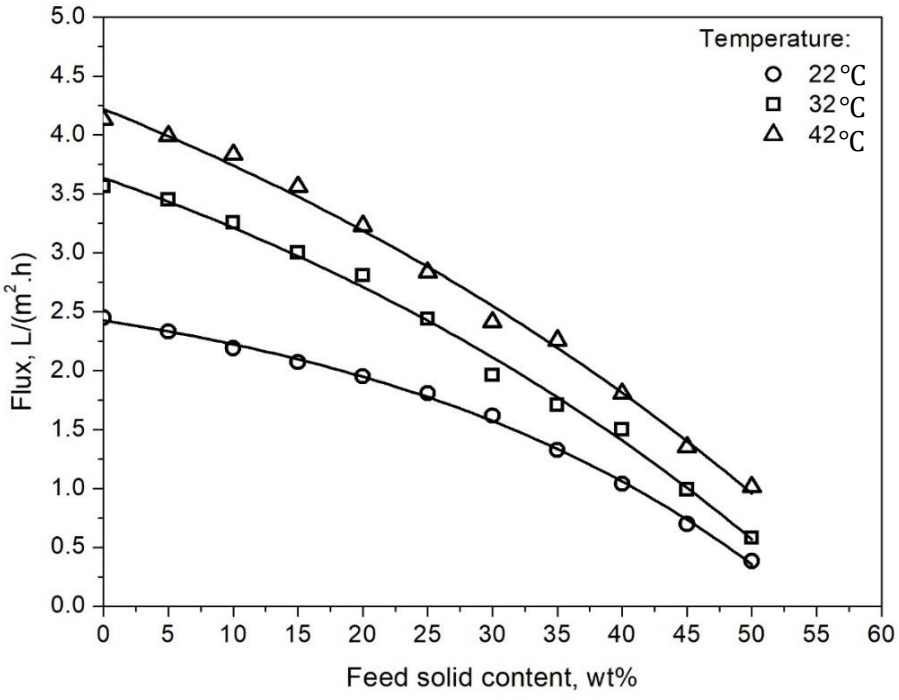

Figure 6.22 Effects of temperature on concentration of milk solution by pervaporation using PEBA 1074 membrane. Membrane thickness 30 µm. Permeate side pressure: 400 Pa.

To study how additional non-volatile dairy components (e.g., NaCl, lactose, whey protein and milk fat) affected the membrane performance for concentrating dairy solutions, each non-volatile component was mixed with milk powder in ratios of 0:1, 0.1:1, 0.3:1and 0.5:1. Then these mixtures were dissolved in water, making a series of dairy solutions with a milk powder content of 5-40 wt.% (or 5-30 wt% for fat-milk powder-water mixtures). These model solutions were used because along the process of concentrating real dairy products, the mass ratio of an added non-volatile component to the original milk solids is always constant, but the total content of the original milk solids and added component would increase gradually.

Figure 6.23 shows the effect of adding NaCl to dairy solutions on the permeation flux for dairy solutions with milk powder contents in the range of 0-40 wt.%. NaCl was added into these solutions with a NaCl/milk powder mass ratio ranging from 0-0.5. At a given milk powder content in the feed solution, when NaCl was added, the permeation flux of water decreased. For instance, the dairy solution containing 40 wt.% milk powder had a permeation flux of 1.04 L/(m^2.h); if NaCl was added to this solution in the amount that was equal to 50% of solid mass of the milk powder, the permeation flux dropped to 0.37 L/(m^2.h). This is understandable because when salt and milk powder contents were increased in the feed solution, the water content in feed would drop accordingly, thus lowering the water permeation driving force and resulting in a lower permeation flux. In addition, the addition of NaCl to the system reduced water activity, which further decreased the water permeation flux.

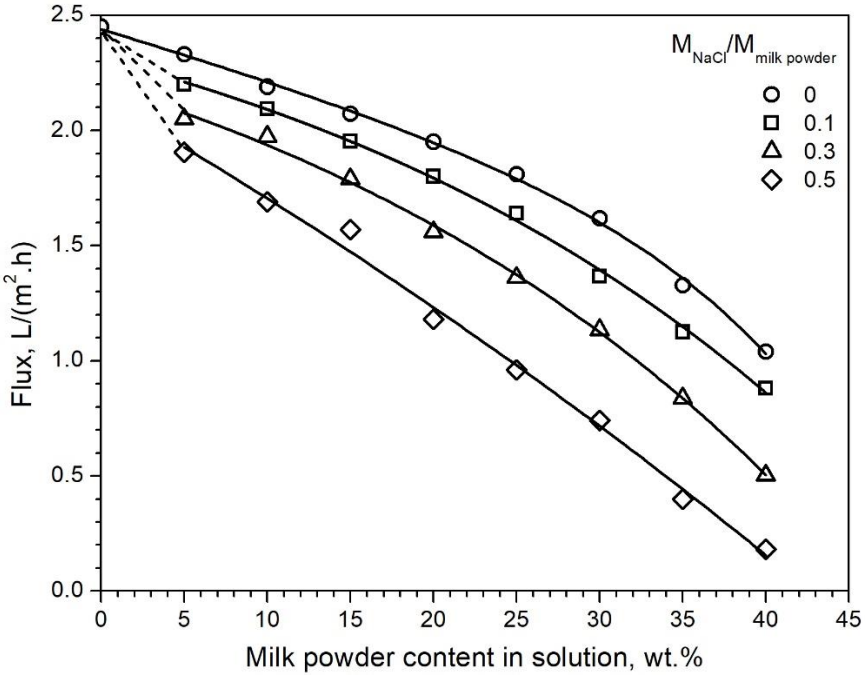

Figure 6.23 Effect of presence of NaCl to the dairy solution at different solid contents on permeation flux. Amount of NaCl added: $M_{NaCl}/M_{milk\ powder}$ = 0, 0.1, 0.3 and 0.5. Temperature: 22 °C, permeate side pressure 400 Pa.

Figure 6.24-6.26 show that the adding lactose, protein and fat to the dairy solutions also decreased the permeation flux in pervaporation. For example, for a dairy solution containing 30 wt% milk powder, the permeation flux will be decreased by 32.8%, 33.4% and 37.3% when 15 wt% lactose, protein or milk fat was added in the solution. There was a considerable decrease in water activity in the solution when lactose (Roos, 2009), protein or fat was added.

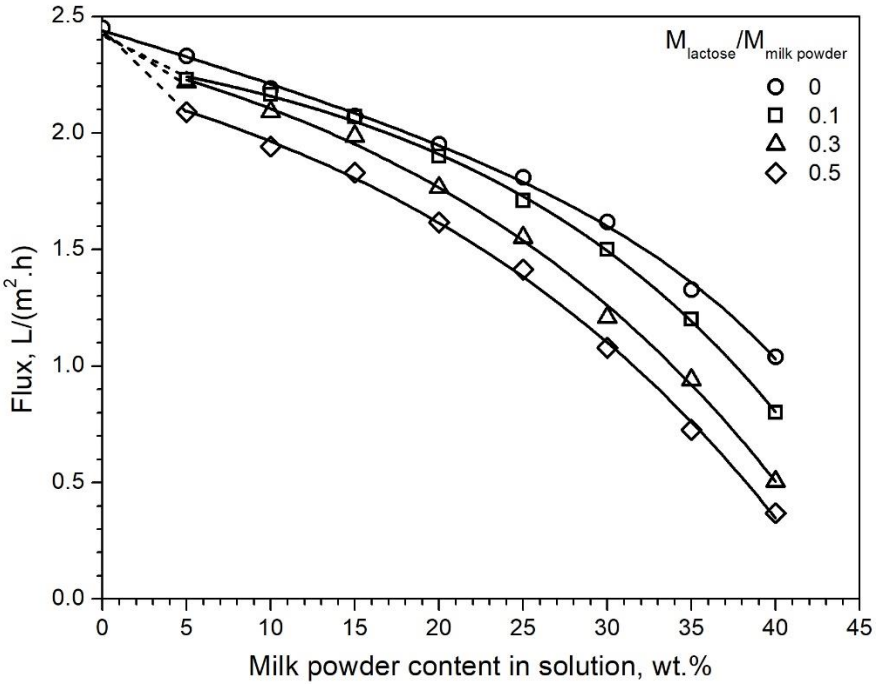

Figure 6.24 Effects of adding lactose to dairy solution at different solid contents on permeation flux, Amount of lactose added: $M_{lactose}/M_{milk\ powder}$ = 0, 0.1, 0.3 and 0.5. Temperature: 22 °C, permeate side pressure: 400 Pa.

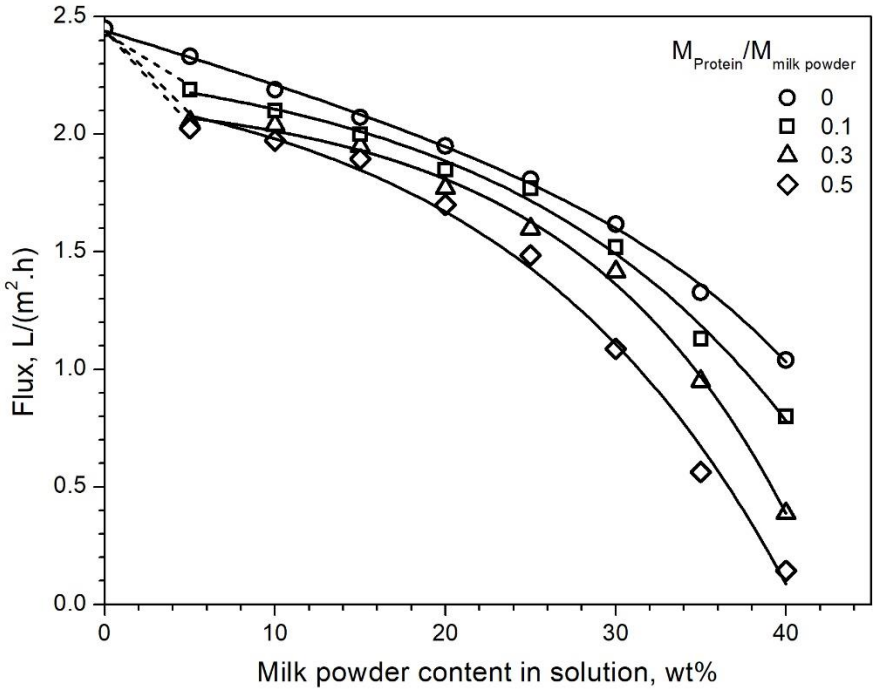

Figure 6.25 Effects of adding protein to dairy solution at different solid contents on permeation flux. $M_{protein}/M_{milk\ powder}$ = 0, 0.1, 0.3, and 0.5. Temperature: 22 °C, permeate side pressure: 400 Pa.

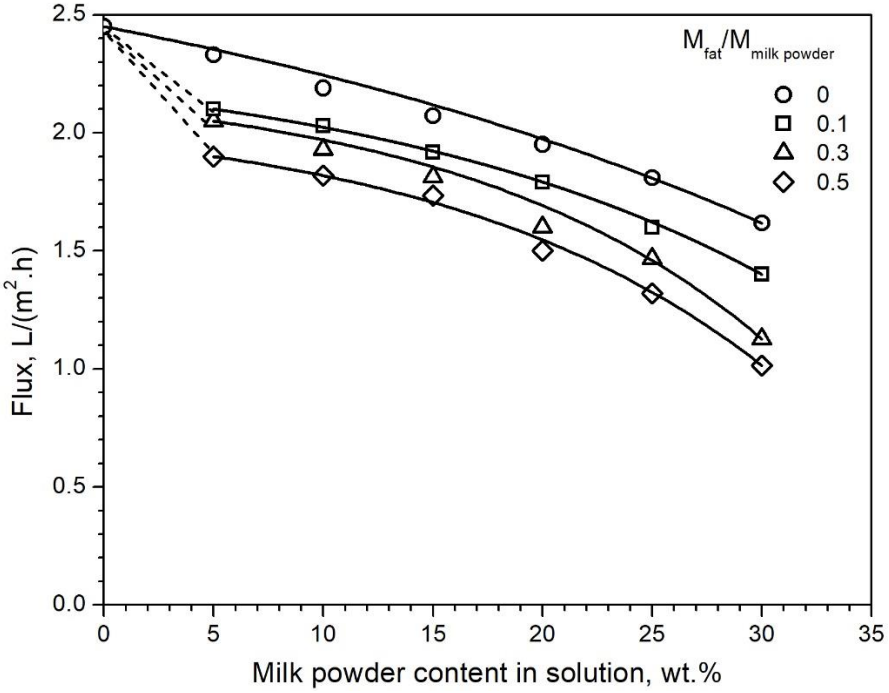

Figure 6.26 Effects of adding milk fat to dairy solution at different solid contents on permeation flux. $M_{fat}/M_{milk\ powder}$ = 0, 0.1, 0.3, and 0.5. Temperature: 22 °C, permeate side pressure: 400 Pa.

Adding non-volatile components to the dairy solution all negatively affected the water flux in concentrating the dairy solutions. The reductions in the permeation fluxes were different and it followed that NaCl > milk fat > whey protein ≈ lactose. This is more clearly illustrated in Figure 6.27, where initial milk powder content in the dairy solution was in the range of 5-30 wt% and the amount of NaCl, lactose, protein or milk fate added was 50% of the mass of milk powder in the solution. It appeared that the pervaporative concentration of dairy solutions worked well for processing dairy streams rich in protein or lactose (i.e., milk protein isolate or lactose powder) rather than those rich in NaCl or milk fat (i.e., cheddar cheese or cream).

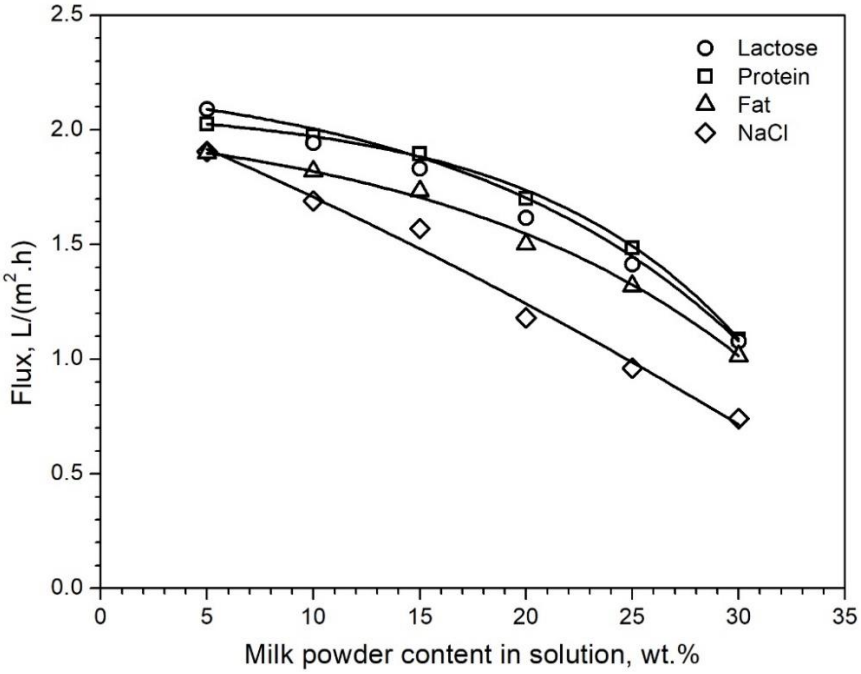

Figure 6.27 Comparison of the effects of non-volatile components added to the dairy solution at different solid contents on permeation flux. The amount of the non-volatile components was 50% of the milk powder contents in the solution. Temperature 22 °C, permeate side pressure 400 Pa.

6.3.6 Batch treatment of real whole milk using pervaporation

To further demonstrate the efficiency of pervaporation with the PEBA 1074 membrane for concentrating dairy solutions, a commercial dairy product (fine filtered 3.25% M.F. Natrel® whole milk) was used as feed, and pervaporation concentration was conducted for a period of 50 h at 22 °C and a permeate pressure of 400 Pa. The nutrition facts of the milk is present in Table 6.7. The initial solid content of the milk was tested as 11.47 wt%, and the pH value of the milk was 6.7, determined using a pH meter.

Table 6.7 The nutrition facts in Natrel® whole milk per 250 mL (obtained from the product package).

Nutrition facts	Amount, g	Weight percentage, wt.%
Fat	8	3.11
Carbohydrate	12	4.67
Proteins	9	3.50
Sodium	0.10	0.04
Potassium	0.39	0.15
Total	29.49	11.47

As shown in Figure 6.28, at the beginning of the pervaporation process, the initial permeation flux was 2.26 L/(m^2.h). As concentration continued with time, the permeation flux gradually decreased and eventually reached 0.15 L/(m^2.h) after 50 hours of operation. This is easy to understand because when the batch experiment was running, water was continuously removed by the membrane from the solution feed to permeate side , leading to an increased solid content in the feed (Figure 6.29). Naturally, water content in the feed decreased with time, resulting in a decreased water permeation flux. Another reasons for the flux decline was the concentration polarization and accumulated deposition on the membrane surface (as discussed before). The VCR (volume concentration ratio, here in PV operations VCR also represents how many times the dairy solution can be concentrated, as illustrated in Equations 6.8-6.10) increased with time as well. After 50 h, the solid content of the feed solution reached 37.8 wt%, and the corresponding VCR was 3.15. More than 3-fold concentration of milk solution was obtained at the end of experiment. Note that the time needed to reach a given VCR or the VCR value that can be obtained during a given time period is determined by the ratio of $\frac{V_O}{A}$, where V_O is the initial volume of the feed solution, and A is the membrane area. Therefore, applying a smaller initial feed volume and a larger membrane will produce a concentrate with higher solid content for a given period of time. Pervaporation with PEBA 1074 membrane was shown to be a promising process for dehydration and concentration of milk or other dairy solutions that can be operated under mild operating conditions.

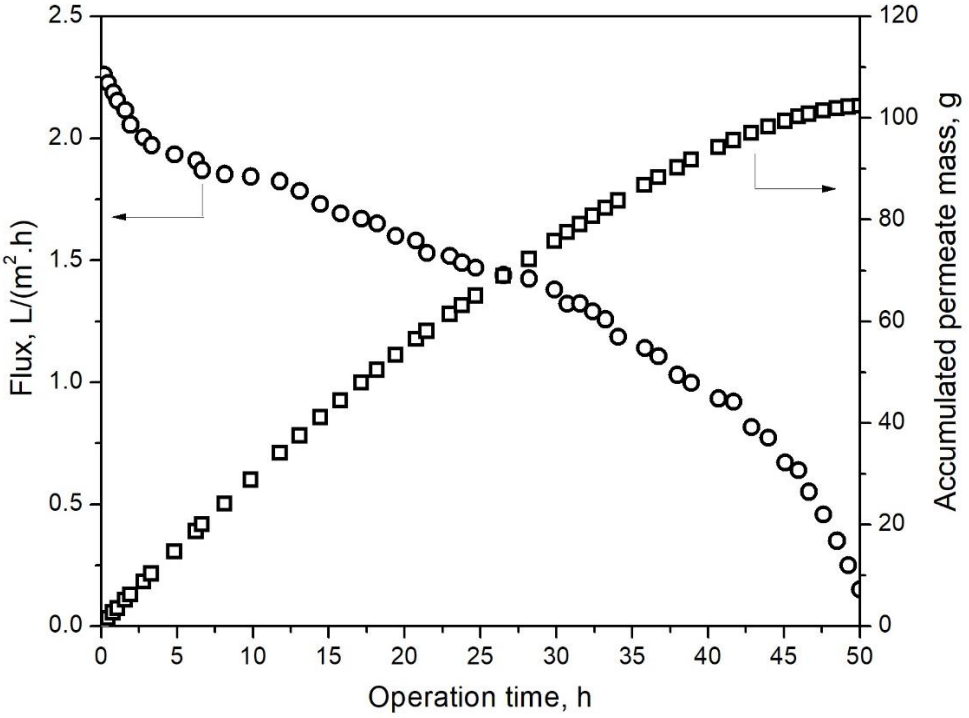

Figure 6.28 The permeation flux and accumulated permeate mass during the concentration of milk by batch pervaporative dehydration. Membrane material: PEBA 1074, membrane thickness 35 µm. Temperature: 22 °C. Permeate side pressure: 400 Pa.

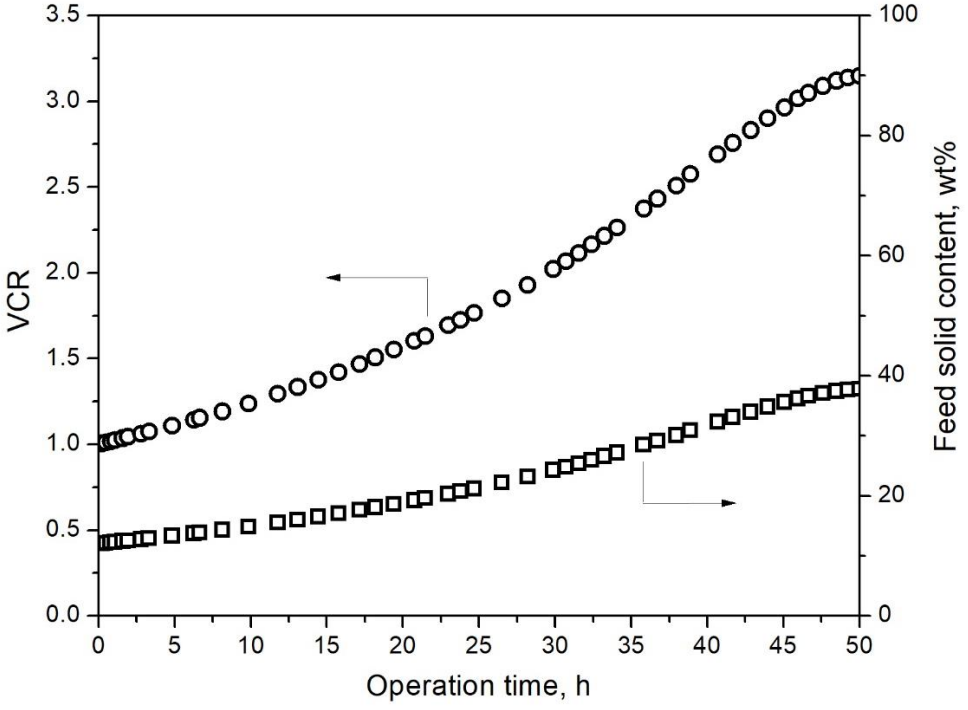

Figure 6.29 The VCR values and feed solid content during the concentration of milk by bath pervaporative dehydration. Membrane material: PEBA 1074, membrane thickness 35 µm. Temperature: 22 °C. Permeate side pressure: 400 Pa.

6.4 Conclusions

Water removed from dairy solutions by UF, NF, RO and PV using UF1, SR3D, HRX and PEBA 1074 membranes were investigated, respectively. The following conclusions can be obtained from this part of the study:

(1) The water permeance of the four membranes follows the order of PEBA 1074 > UF1 > SR3D > HRX. This suggests that PEBA 1074 membrane was promising for dehydration and concentration dairy solutions by pervaporation.

(2) The performance of the four membranes for concentration of dairy solutions were evaluated by studying the effects of operating conditions (e.g., feed solid contents and TMPs) on permeation flux and solid retention. In general, a high flux was observed with ultrafiltration, and PV exhibited almost 100% retention of all the dairy components on the feed side. In addition, flux decline due to concentration polarization and membrane fouling was observed to different extents in all the membrane processes. Among the four membranes, PEBA 1074 membrane showed the smallest flux decline. At a solid content above 16 wt% in dairy solution, the flux decline became too significant for UF, NF or RO to work, and they could not adequately treat dairy solutions at a high solid content. However, the flux decline in PV was much less significant, even at a feed solid content as high as 40 wt%. Thus, PV with PEBA 1074 membrane was suitable to treat high concentration dairy solutions.

(3) Flux decline was analyzed using the resistance-in-series model, and the resistance due to membrane (R_m), concentration polarization (R_{cp}) and membrane fouling (R_f) were evaluated. It was shown that for UF, NF and RO, the resistance due to membrane fouling and concentration polarization were greater than the resistance of membrane itself, which membrane resistance was dominant in PV. This explained the less significant flux decline in

PV compared to the other three filtration processes. In all cases, the resistance due to membrane fouling was more significant to flux decline than concentration polarization.

(4) Continuous filtration was conducted with periodic cleaning to test the fouling vulnerability and stability of the membranes. UF1 membrane was irreversibly fouled by milk macromolecules, and the fouled membrane could not be fully cleaned with 0.1 M NaOH solution. The flux declines for NF-SR3D and RO-HRX could be recovered by cleaning the membrane with 0.0001 M NaOH solution. PV-PEBA 1074 membrane was easiest to clean and no chemical agent was needed; a simple water rise would fully restore the permeation flux.

(5) Adding NaCl, protein, lactose or milk fat to dairy solutions would decrease the permeation. Pervaporation appeared to work well for concentrating protein or lactose-rich dairy solutions, whereas the performance was compromised when concentrating dairy streams that were rich in NaCl or fat (e.g., cheese or cream).

(6) Batch PV for concentration of whole milk was performed to demonstrate the efficiency of the PV process and PEBA 1074 membrane for water removal from the milk solutions. The milk was concentrated several times.

Chapter 7

General Conclusions, Contributions to Original Research, and Recommendations

7.1 General conclusions

7.1.1 Pervaporative recovery of dairy aroma compounds from aqueous solutions

(1) PEBA 2533 membrane was shown to be permselective to the eight model aroma compounds (ethyl hexanoate, ethyl butanoate, 2-heptanone, diacetyl, dimethyl sulfone, indole, nonanal, and hexanoic acid).

(2) With an increase in feed aroma concentration or temperature, aroma flux also increased. The temperature dependence of enrichment factor depended on the apparent activation energies of aroma compounds and water. The temperature effects on the permeation fluxes of water and aroma compounds followed an Arrhenius type of relations.

(3) There were coupling effects among the aroma compounds for aroma extraction from feed solutions containing multicomponent aromas. The coupling effects on the permeation of aroma components were generally more significant at higher aroma concentration. An increase in temperature had little impact on the coupling permeation of ethyl hexanoate, ethyl butanoate, 2-heptanone, nonanal, dimethyl sulfone and indole, but the coupling factors for permeation of diacetyl and hexanoic acid were significantly influenced.

7.1.2 Batch pervaporative recovery of aroma compounds from their binary feeds

(1) The Feng & Huang model was suitable to describe the batch operation of pervaporative enrichment of aroma compounds from dairy solutions.

(2) To get maximum aroma concentration in permeate product, the organic phase in the permeate needed to be removed at the moment when the instantaneous permeate concentration began to reach the aroma solubility limit in water.

(3) The recovery of aroma compound from aqueous solutions was influenced by F_0/A for a given period of batch operating time.

7.1.3 Presence of non-volatile dairy components on pervaporative extraction of aroma compounds from aqueous solutions using PEBA 2533 membrane

(1) The presence of non-volatile dairy components (e.g. NaCl, lactose, whey protein and milk fat) had little effect on the permeation of water.

(2) The addition of NaCl in dairy solutions could enhance the recovery of hydrophobic aroma compounds (i.e. nonanal, ethyl hexanoate, ethyl butanoate, 2-heptanone and indole) from their aqueous solutions, but had no effect on the recovery of less hydrophobic or hydrophilic aromas (such as hexanoic acid, diacetyl and dimethyl sulfone).

(3) The pervaporative recovery of aroma compounds was compromised by the presence of lactose, whey protein or milk fat in the dairy solutions. In general, the reductions in the aroma fluxes due to these non-volatile compounds were in accord with the hydrophobicity of the aroma compounds.

(4) No significant concentration polarization or membrane fouling occurred during pervaporation of aroma compounds at increased contents of lactose, whey protein, fat and NaCl;

the PEBA 2533 membranes showed good anti-fouling properties. This was espercially important for the recovery of aroma compounds from dairy solutions from a practical point of view.

7.1.4 Concentration of dairy solutions by ultrafiltration, nanofiltration, reverse osmosis membranes and pervaporation

(1) PV with PEBA 1074 membrane exhibited the highest total solid retention among the four membranes processes. Flux decline due to concentration polarization and membrane fouling was observed in all the membrane process, and the flux decrease was more drastic at higher feed solid contents or higher TMP. The flux decline in pervaporation with PEBA 1074 membrane was the least significant among the four membranes processes. Thus PV-PEBA 1074 was shown to be a good candidate for concentration of dairy solutions, especially at high solid contents.

(2) For all the four membrane processes, the resistance due to membrane fouling was a greater contributor to the flux decline than concentration polarization under the operating conditions studied. Membrane fouling was more significant at higher TMP and/or higher feed solid contents.

(3) Among the four membranes studied, PEBA 1074 membrane used for pervaporative concentration of dairy solutions was the easiest to clean. Only water and no chemical agent was required to clean the fouled membrane and the permeation flux could be recovered by simple rinsing with water.

(4) The addition of NaCl, whey protein, lactose or milk fat to the dairy solution would decrease the water flux for pervaporative dehydration of milk solution. The impacts of these

non-volatile dairy ingredients on water flux were in the order NaCl > milk fat > whey protein ≈ lactose.

(5) Using pervaporation with PEBA 1074 membrane, the whole milk was concentrated by 3.15 fold corresponding to a total solid content of 37.8 wt% in 50 h using F/A_o ratio 0.13 m^3/m^2.

7.2 Contributions to the original research

(1) Recovery of aroma compounds from their binary and multicomponent aqueous solutions was achieved by pervaporation using PEBA 2533 membrane. This membrane was proved to be effective on recovering not only hydrophobic aroma compounds but also hydrophilic ones, which were not easy with most commonly used PV membranes. In addition, the coupling effect among aroma species during molecular transportation in the membrane was proved to exist, even at low aroma concentrations in the feed. Therefore, it is not realistic to assume that there is no competition among the aroma permeants in modeling and simulation of the aroma recovery by PV, as many studies did. The effects of feed aroma concentration and temperature on pervaporation performance were clarified as well.

(2) The Feng and Huang model was selected to describe the batch operation of pervaporative enrichment of aroma compounds from aqueous solutions. This model was validated with experiments. The maximum amounts of highly enriched aroma compounds during the process was predicted, and the recovery of aroma compounds from their aqueous feed solutions at different F_0/A ratios was also simulated. The membrane area required and the amount feed solution to be processed were correlated to the batch operation time.

(3) Four non-volatile dairy components: NaCl, lactose, whey protein and milk fat were confirmed to affect the recovery of aroma compounds from feed solutions. The interactions

between the non-volatile components and aromas were analyzed based on the aroma flux. It was found that the enrichment of hydrophobic aromas was enhanced by addition of NaCl in the feed, while the opposite was often true for aroma enrichment when lactose, protein and fat were added to the feed. Additionally, the anti-fouling property of PEBA 2533 membrane was validated, and it was proved to be a promising membrane to recover aroma compounds from dairy solutions.

(4) To our knowledge, PV process had never been applied to concentrating dairy products. In this study, the potential of PV process with hydrophilic PEBA 1074 membrane for concentrating dairy solutions as a non-thermal dehydration process was evaluated. The performance of PEBA 1074 membrane for dairy concentration by pervaporation was compare to UF, NF and RO. The PEBA 1074 membrane was proved to have the highest water permeance, the least flux decline with time during the operation and the highest retention of milk solid. This membrane was also the easiest to clean among all the four membranes studied, and a simple water rinse was found to be adequate to clean the fouled membrane for a complete flux restoration.

7.3 Recommendations for the future work

(1) Most of the currently available research of pervaporative recovery of aroma components are based on model aroma-water solutions. A more complex feed system containing aroma compounds and non-volatile components were investigated in this study. Based on the results and findings in this research, the aroma recovery from real dairy solutions, such as whole milk or cream, may be conducted by pervaporation using PEBA 2533 membranes. This would provide a better reference for industrial application of PV for aroma recovery from dairy streams.

(2) For bath PV process of recovering aromas, the Feng and Huang model provided a good prediction of aroma recovery rate and the yield of enriched aromas. The model is suitable for dilute binary solutions, but may fail to predict the aroma recovery from solution with multicomponent aromas and non-volatile components. In addition, the present form of the model was based on the assumption of no competitive permeation among the permeants present in the feed. The results in this thesis showed that the coupling effect among different aroma compounds did exist in multicomponent feed systems, which would affect the permeation of certain aromas. Therefore, it will be of interest to modify the existing model or to develop a new model for enrichment of multiple aroma components from real dairy solutions by taking the competitions among aroma permeants into consideration.

(3) In this study, PV with PEBA 1074 membrane was demonstrated to be a promising non-thermal process for concentrating dairy solutions. From an application point of view, a mathematical model to describe flux decline with time during the course of dehydration is of great interest. Considering that PEBA 1074 membrane is nonporous and the fouling on the membrane surface is reversible, as shown in this study, only concentration polarization and the formation of a removable foulant layer deposited on membrane surface need to be considered in the model. This aspect should be explored.

(4) PEBA 2533 or PEBA 1074 polymers may be blended with some hydrophilic nanoparticles to improve the adsorptive performance of PEBA 2533 for some water-based aromas (such as acids and diacetyl) or the adsorption of water by PEBA 1074. However, it should be noted that the nanoparticle should be retained in the membrane to ensure no nanoparticles will leach from the membrane; otherwise there will be significant food safety problems.

Bibliography

Aider, M., D. Halleux, and A. Akbache. 2007. “Whey Cryoconcentration and Impact on Its Composition.” *Journal of Food Engineering* 82: 92–102.

Aroujalian, A., K. Belkacemi, S.J. Davids, G. Turcotte, and Y. Pouliot. 2006. “Effect of Residual Sugars in Fermentation Broth on Pervaporation Flux and Selectivity for Ethanol.” *Desalination* 193: 103–08.

Aroujalian, A., K. Belkacemi, S.J. Davids, G. Turcotte, and Y.Pouliot. 2003. “Effect of Protein on Flux and Selectivity in Pervaporation of Ethanol from a Dilute Solution.” *Separation Science and Technology* 38: 3239–47.

Aroujalian, A., and A. Raisi. 2007. “Recovery of Volatile Aroma Components from Orange Juice by Pervaporation.” *Journal of Membrane Science* 303: 154–61.

Bai, Y., J. Qian, Q. An, Z. Zhu, and P. Zhang. 2007. “Pervaporation Characteristics of Ethylene–vinyl Acetate Copolymer Membranes with Different Composition for Recovery of Ethyl Acetate from Aqueous Solution.” *Journal of Membrane Science* 305: 152–59.

Bai, Y., J. Qian, C. Zhang, L. Zhang, Q. An, and H. Chen. 2008. “Cross-Linked HTPB-Based Polyurethaneurea Membranes for Recovery of Ethyl Acetate from Aqueous Solution by Pervaporation.” *Journal of Membrane Science* 325: 932–39.

Baker, R.W. 2012. “Microfiltration.” In *Membrane Technology and Applications,* 3rd edition. California, USA: John Wiley & Sons.

Overington, A.R., M. Wong, J. Harrison. 1996. “The Recovery of Sulfur Aroma Compounds of Biological Origin by Pervaporation." In *Flavour Science: Recent Developments,* A. J.

Taylor and D. S. Mottram (eds.), Royal Society of Chemistry, Cambridge, UK.

Baudot, A., and M. Marin. 1997. “Pervaporation of Aroma Compounds: Comparison of Membrane Performances with Vapour-Liquid Equilibria and Engineering Aspects of Process Improvement.” *Food and Bioproducts Processing* 75: 117–42.

Baudot, A., and M. Marin. 1999. “Improved Recovery of an Ester Flavor Compound by Pervaporation Coupled with a Flash Condensation.” *Industrial & Engineering Chemistry Research* 38: 4458–69.

Baudot, A., and M. Matin. 1996. “Dairy Aroma Compounds Recovery by Pervaporation.” *Journal of Membrane Science* 120: 207–20.

Baudot, A., I. Souchon, and M. Marin. 1999. “Total Permeate Pressure Influence on the Selectivity of the Pervaporation of Aroma Compounds.” *Journal of Membrane Science* 158: 167–85.

Beaumelle, D., M. Marin, and H. Gibert. 1992. “Pervaporation of Aroma Compounds in Water-Ethanol Mixtures: Experimental Analysis of Mass Transfer.” *Journal of Food Engineering* 16 (4): 293–307.

Berendsen, W.R., P. Radmer, and M. Reuss. 2006. “Pervaporative Separation of Ethanol from an Alcohol-ester Quaternary Mixture.” *Journal of Membrane Science* 280: 684–92.

Best, D.E., and K.C. Vasavada. 1993. “Freeze Concentration of Dairy Products Phase 2. Final Report.” Elk Grove Village.

Beyeler, M., and J. Solms. 1974. “Interaction of Flavor Model Compounds with Soy Protein and Bovine Serumalbumin.” *LWT-Food Science and Technology* 7: 217–219.

Binning, R.C., R.J. Lee, J.F. Jennings, and E.C. Martin. 1961. “Separation of Liquid Mixtures

by Permeation.” *Industrial and Engineering Chemistry* 53. 45–50.

Bocquet, S., F.G. Viladomat, C.M. Nova, J. Sanchez, V. Athes, and I. Souchon. 2006. “Membrane-Based Solvent Extraction of Aroma Compounds: Choice of Configurations of Hollow Fiber Modules Based on Experiments and Simulation.” *Journal of Membrane Science* 281: 358–68.

Boddeker, K.W., I.L. Gatfield, J. Jahnig, and C. Schorm. 1997. “Pervaporation at the Vapor Pressure Limit: Vanillin.” *Journal of Membrane Science* 137: 155–58.

Borjesson, J., H.O.E. Karlsson, and G. Tragardh. 1996. “Pervaporation of a Model Apple Juice Aroma Solution : Comparison of Membrane Performance.” *Journal of Membrane Science* 119: 229–39.

Bowen, T.C., S. Li, R.D. Noble, and J.L. Falconer. 2003. “Driving Force for Pervaporation through Zeolite Membranes.” *Journal of Membrane Science* 225: 165–76.

Brink, L.E.S, and D.J. Romijn. 1990. “Reducing the Protein Fouling of Polysulfone Surfaces and Polysulfone Ultrafiltration Membranes: Optimization of the Type of Presorbed Layer.” *Desalination* 78: 209–33.

Brun, J. P., C. Larchet, G. Bulvestre, and B. Auclair. 1985. “Sorption and Pervaporation of Dilute Aqueous Solutions of Organic Compounds through Polymer Membranes.” *Journal of Membrane Science* 25: 55–100.

Bylund, G., ed.. 2015. *Dairy Processing Handbook*. Sweden: Tetra Pak Processing Systems.

Charls, M., B. Bernal, and E. Guichard. 1996. “Interaction of β-Lactoglobulin with Flavour Compounds.” In *Flavoer Science, Recent Developments: Proceedings of the 8th Weurman Symposium*, A. J. Taylor and D. S. Mottram (eds.), 433–36.

Chen, Z., Y. Li, D. Yin, and J. Wang. 2012. “Microstructural Optimization of Mordenite Membrane for Pervaporation Dehydration of Acetic Acid.” *Journal of Membrane Science*, 411–12, 182-92.

Cheng, H.. 2010. “Volatile Flavor Compounds in Yogurt: A Review.” *Critical Reviews in Food Science and Nutrition* 50: 938–50.

Cheryan, M.. 1986. *Ultrafiltration. Handbook.* USA: Technomic Publishing Co.

Cheryan, M.. 1998. *Ultrafiltration and Microfiltration Handbook*. Urbana, USA: Technomic Publishing Co.

Clark, T., J.S. Murray, P. Lane, and P. Politzer. 2008. “Why Are Dimethyl Sulfoxide and Dimethyl Sulfone Such Good Solvents?” *Journal of Molecular Modeling* 14: 689–97.

Cuartas-Uribe, B., M.I. Alcaina-Miranda, E. Soriano-Costa, J. A. Mendoza-Roca, M. I. Iborra-Clar, and J. Lora-García. 2009. “A Study of the Separation of Lactose from Whey Ultrafiltration Permeate Using Nanofiltration.” *Desalination* 241. 244–55.

Cussler, E.L. 1997. *Diffusion: Mass Transfer in Fluid Systems.* 2nd edition, UK: Cambridge University Press.

Damodaran, S., and J.E. Kinsella. 1980. “Flavor Protein Interactions. Binding of Carbonyls to Bovine Serum Albumin: Thermodynamic and Conformational Effects.” *Journal of Agricultural and Food Chemistry* 28: 571–78.

Daufin, G., J.P. Escudier, H. Carrère, S. Bérot, L. Fillaudeau, and M. Decloux. 2001. “Recent and Emerging Applications of Membrane Processes in the Food and Dairy Industry.” *Food and Bioproducts Processing* 79: 89–102.

De Roos, K.B.. 1997. “How Lipids Influence Food Flavor.” *Food Technology* 51: 60–62.

Djebbar, M.K., Q.T. Nguyen, R. Clement, and Y. Germain. 1998. “Pervaporation of Aqueous Ester Solutions through Hydrophobic Poly(ether-Block-Amide) Copolymer Membranes.” *Journal of Membrane Science* 146: 125–33.

Dong, Y., M. Wang, L. Chen, and M. Li. 2012. “Preparation, Characterization of P(VDF-HFP)/[bmim]BF4 Ionic Liquids Hybrid Membranes and Their Pervaporation Performance for Ethyl Acetate Recovery from Water.” *Desalination* 295: 53–60.

Dotremont, C., S. van den Ende, H. Vandommele, and C. Vandecasteele. 1994. “Concentration Polarization and Other Boundary Layer Effects in the Pervaporation of Chlorinated Hydrocarbons.” *Desalination* 95: 91–113.

Dotremont, C., B. Brabants, K. Geeroms, J. Mewis, and C. Vandecasteele. 1995. “Sorption and Diffusion of Chlorinated Hydrocarbons in Silicatlite-Filled PDMS Membranes.” *Journal of Membrane Science* 104: 109–17.

Dufour, E., and T. Haertle. 1990. “Binding Affinities of Beta-Ionone and Related Flavor Compounds to Beta-Lactoglobulin : Effects of Chemical Modifications.” *Journal of Agricultural and Food Chemistry* 38: 1691–95.

Farber, L.. 1935. “American Association for the Applications of Pervaporation.” *Science* 82: 158.

Feng, X., and R.Y.M. Huang.. 1996. “Estimation of Activation Energy for Permeation in Pervaporation Processes.” *Journal of Membrane Science* 118, 127–31.

Feng, X., and R.Y.M. Huang. 1992. “Separation of Isopropanol from Water by Pervaporation Using Silicone-Based Membranes.” *Journal of Membrane Science* 74: 171–81.

Feng, X., and R.Y.M. Huang. 1997. “Liquid Separation by Membrane Pervaporation: A

Review." *Industrial & Engineering Chemistry Research* 36: 1048–66.

Fischer, N., and S. Widder. 1997. "How Proteins Influence Food Flavor." *Food Technology* 51: 68–70.

Fleming, H.L.. 1990. "Membrane Pervaporation: Separation of Organic/aqueous Mixtures." *Separation Science and Technology* 25: 1239–55.

Fouda, A., J. Bai, S.Q. Zhang, O. Kutowy, and T. Matsuura. 1993. "Membrane Separation of Low Volatile Organic Compounds by Pervaporation and Vapor Permeation." *Desalination* 90: 209–33.

Fox, P.F., and P.L.H. McSweeney, eds. 2003. *Advanced Dairy Chemistry: Volume 1: Proteins*. 3rd editio. New York, USA: Kluwer Academic/Plenum Publishers.

Franks, F.. 1983. "Solute-Water Interactions: Do Polyhydroxy Compounds Alter the Properties of Water?" *Cryobiology* 20: 335–45.

Frapin, D., E. Dufour, and T. Haertle. 1993. "Probing the Fatty Acid Binding Site of Beta-Lactoglobulins." *Journal of Protein Chemistry* 12: 443–49.

Garcia, V., N. Diban, D. Gorri, R. Keiski, A. Urtiaga, and I. Ortiz. 2008. "Separation and Concentration of Bilberry Impact Aroma Compound from Dilute Model Solution by Pervaporation." *Journal of Chemical Technology and Biotechnology* 83: 973–82.

Garcia, V., E. Pongracz, E. Muurinen, and R.L. Keiski. 2009. "Recovery of N-Butanol from Salt Containing Solutions by Pervaporation." *Desalination* 241: 201–11.

García, V., E. Pongrácz, E. Muurinen, and R.L. Keiski. 2009. "Pervaporation of Dichloromethane from Multicomponent Aqueous Systems Containing N-Butanol and Sodium Chloride." *Journal of Membrane Science* 326: 92–102.

Godshall, M.A.. 1997. “How Carbohydrates Influence Food Flavor.” *Food Technology* 51: 63–67.

Gu, J., X. Zhang, Y. Bai, L. Yang, C. Zhang, and Y. Sun. 2013. “ZSM-5 Filled Polyether Block Amide Membranes for Separating EA from Aqueous Solution by Pervaporation.” *International Journal of Polymer Science* 2013: 1–10.

Guichard, E.. 2002. “Interactions between Flavor Compounds and Food Ingredients and Their Influence on Flavor Perception.” *Food Reviews International* 18: 49–70.

Guichard, E., and S. Langourieux. 2000. “Interactions between β-Lactoglobulin and Flavour Compounds.” *Food Chemistry* 71: 301–8.

Hansen, A.P., and D.C. Booker. 1996. “Flavor Interaction with Casein and Whey Protein.” In *Flavor-Food Interactions*, R. J. McGorrin and J. V. Leland (eds.). Washington, DC: American Chemical Society.

Hartel, R.W.. 1993. “Freeze Concentration of Skim Milk.” *Journal of Food Engineering* 20: 101–20.

Hatchwell, L.C.. 1996. “Implications of Fat on Flavor.” In *Flavor-Food Interactions*, R.J. McGorrin and J.V. Leland (eds.). Washington, DC: American Chemical Society.

Haug, A., A.T Høstmark, and O.M. Harstad. 2007. “Bovine Milk in Human Nutrition-a Review.” *Lipids in Health and Disease* 6: 25.

Heldman, R.D. 2003. *Encyclopedia of Agricultural, Food and Biological Engineering*. New York: Marcel Dekker Inc.

Te Hennepe, H.J.C., C.A. Smolders, D. Bargeman, and M.H.V. Mulder. 1991. “Exclusion and Tortuosity Effects for Alcohol/Water Separation by Zeolite-Filled PDMS Membranes.”

Separation Science and Technology 26: 585–96.

Henning, D.R., R.J. Baer, A.N. Hassan, and R. Dave. 2006. "Major Advances in Concentrated and Dry Milk Products, Cheese, and Milk Fat-Based Spreads." *Journal of Dairy Science* 89: 1179–88.

Howard, P.H., and W.M. Meylan. 1997. *Handbook of Physical Properties of Organic Chemicals.* Boca Raton, USA: CRC Press LLC.

Hu, K., J.M. Dickson, and S.E. Kentish. 2015. "Microfiltration for Casein and Serum Protein Separation." In *Membrane Processing for Dairy Ingredient Separation*, K. Hu and J.M. Dickson (eds.). Chichester, West Sussex, UK: John Wiley & Sons.

Huang, R.Y.M., G.Y. Moon, and R. Pal. 2002. "Ethylene Propylene Diene Monomer (EPDM) Membranes for the Pervaporation Separation of Aroma Compound from Water." *Industrial & Engineering Chemistry Research* 41: 531–37.

Huddleston, J.G., A.E. Visser, W.M. Reichert, H.D. Willauer, G.A. Broker, and R.D. Rogers. 2001. "Characterization and Comparison of Hydrophilic and Hydrophobic Room Temperature Ionic Liquids Incorporating the Imidazolium Cation." *Green Chemistry* 3: 156–64.

Ikegami, T., H. Yanagishita, D. Kitamoto, K. Haraya, T. Nakane, H. Matsuda, N. Koura, and T. Sano. 1999. "Highly Concentrated Aqueous Ethanol Solutions by Pervaporation Using Silicalite Membrane-Improvement of Ethanol Selectivity by Addition of Sugars to Ethanol Solution." *Biotechnology Letters* 21: 1037–41.

Isci, A., S. Sahin, and G. Sumnu. 2006. "Recovery of Strawberry Aroma Compounds by Pervaporation." *Journal of Food Engineering* 75: 36–42.

Fleshcer, J.R.. 1986. “PEBA Polyether Block Amide-A New Family of Engineering Thermoplastic Elastomers.” in *High Performance Polymers. Their Origin and Development*, R.B. Seymor, G.S. Kirshenbaum (eds.), Paris, France: Tech & Doc Lavoisier.

Ji, W.C., S.K. Sikdar, and S.T. Hwang. 1995. “Sorption, Diffusion and Permeation of 1,1,1-Trichloroethane through Adsorbent-Filled Polymeric Membranes.” *Journal of Membrane Science* 103: 243–55.

Jiang, J.-S., L.M. Vane, and S.K. Sikdar. 1997. “Recovery of VOCs from Surfactant Solutions by Pervaporation.” *Journal of Membrane Science* 136: 233–47.

Jiraratananon, R., P. Sampranpiboon, D. Uttapap, and R.Y.M. Huang. 2002. “Pervaporation Separation and Mass Transport of Ethylbutanoate Solution by Polyether Block Amide (PEBA) Membranes.” *Journal of Membrane Science* 210: 389–409.

Jullok, N., R. Martínez, C. Wouters, P. Luis, M.T. Sanz, and B. van der Bruggen. 2013. “A Biologically Inspired Hydrophobic Membrane for Application in Pervaporation.” *Langmuir : The ACS Journal of Surfaces and Colloids* 29: 1510–16.

Kanani, D.M., B.P. Nikhade, P. Balakrishnan, G. Singh, and V.G. Pangarkar. 2003. “Recovery of Valuable Tea Aroma Components by Pervaporation.” *Industrial & Engineering Chemistry Research* 42: 6924–32.

Karlsson, H.O.E., and G. Tragardh. 1997. “Aroma Recovery during Beverage Processing.” *Journal of Food Engineering* 34: 159–78.

Karlsson, H.O.E, and G.Tragardh. 1 993. “Pervaporation of Dilute Organic-Waters Mixtures. A Literature Review on Modelling Studies and Applications to Aroma Compound

Recovery.” *Journal of Membrane Science* 76: 121–46.

Kaya, Y., H. Barlas, and S. Arayici. 2009. “Nanofiltration of Cleaning-in-Place (CIP) Wastewater in a Detergent Plant: Effects of pH, Temperature and Transmembrane Pressure on Flux Behavior.” *Separation and Purification Technology* 65: 117–29.

Kedem, O.. 1989. “The Role of Coupling in Pervaporation.” *Journal of Membrane Science* 47: 277–84.

Kellam, S. 1998. “The Manufacture of Lactose.” In *Chemical Processes in New Zealand, Online Edition*, online edition. New Zealand: New Zealand Institute of Chemistry.

Kieckbusch, T.G., and C.J. King. 1979. “Partition Coefficients for Acetates in Food Systems.” *Journal of Agricultural and Food Chemistry* 27: 504–7.

King, B.M., and J. Solms. 1979. “Interaction of Flavour Compounds in Model Food Systems Using Benzyl Alcohol as an Example.” *Journal of Agricultural and Food Chemistry* 27: 1331–34.

Kirk, R.E., and D.F. Othmer, eds. 1981. *Kirk-Othmer Encyclopedia of Chemical Technology, Volumes 13*. 3rd edition. New York, USA: John Wiley and Sons.

Kozak, J.J., W.S. Knight, and W. Kauzmann. 1968. “Solute-Solute Interactions in Aqueous Solutions.” *The Journal of Chemical Physics* 48: 675.

Kühn, J., X. Q. Zhu, T. Considine, and H. Singh. 2007. “Binding of 2-Nonanone and Milk Proteins in Aqueous Model System.” *Journal of Agricultureal and Food Chemistry* 55: 3599–3604.

Kühn, J., T. Considine, and H. Singh. 2006. “Interactions of Milk Proteins and Volatile Flavor Compounds: Implications in the Development of Protein Foods.” *Journal of Food Science*

71: R72–82.

Kühn, J., T. Considine, and H. Singh. 2008. “Binding of Flavor Compounds and Whey Protein Isolate as Affected by Heat and High Pressure Treatments.” *Journal of Agricultural and Food Chemistry* 56: 10218–24.

Kujawa, J., S. Cerneaux, and W. Kujawski. 2015. “Removal of Hazardous Volatile Organic Compounds from Water by Vacuum Pervaporation with Hydrophobic Ceramic Membranes.” *Journal of Membrane Science* 474: 11–19.

Kulkarni, S.B., M.Y. Kariduraganavar, and T.M. Aminabhavi. 2003. “Sorption, Diffusion and Permeation of Esters, Aldehydes, Ketones and Aromatic Liquids into Tetrafluoroethylene/propylene at 30, 40 and 50 °C.” *Journal of Applied Polymer Science* 89: 3201–9.

Lamer, T., and A. Voilley. 1991. “Influence of Different Parameters on the Pervaporation of Aroma Compounds.” In *Proceedings of the 5th International Conference on Pervaporation Processes in the Chemical Industry*, R. Bakish (ed.), Englewood, NJ: Bakish Materials Corporation.

Lamer, T., M.S. Rohart, A. Voilley, and H. Baussart. 1994. “Influence of Sorption and Diffusion of Aroma Compounds in Silicone Rubber on Their Extraction by Pervaporation.” *Journal of Membrane Science* 90: 251–63.

Land, D. G., and J. Reynolds. 1981. “The Influence of Food Components on the Volatility of Diacetyl.” In *Flavour ’81*, P. Schreier (ed.), Berlin: Walter de Gruyter.

Landy, P., C. Druaux, and A. Voilley. 1995. “Retention of Aroma Compounds by Proteins in Aqueous Solution.” *Food Chemistry* 54: 387–92.

Landy, P., J.-L. Courthaudon, C. Dubois, and A. Voilley. 1996. “Effect of Interface in Model Food Emulsions on the Volatility of Aroma Compounds.” *Journal of Agricultural and Food Chemistry* 44: 526–30.

Le Thanh, M., I. Goubet, J.L. Le Quere, and A. Voilley. 1998. “Interactions between Volatiles and Lipids in Complex Systems.” *Journal of the American Oil Chemists’ Society* 75: 441–45.

Leland, J. V. 1997. “Flavor Interactions: The Greater Whole.” *Food Technology* 51: 75–80.

Li, C., X. Zhang, X. Hao, M. Wang, C. Ding, Z. Wang, Y. Wang, G. Guan, and A. Abudula. 2015. “Efficient Recovery of High-Purity Aniline from Aqueous Solutions Using Pervaporation-Fractional Condensation System.” *AIChE Journal* 61: 4445–55.

Lipnizki, F., and G. Tragardh. 2001. “Modelling of Pervaporation: Models To Analyze and Predict the Mass Transport in Pervaporation.” *Separation & Purification Reviews* 30: 49–125.

Lipnizki, F., and S. Hausmanns. 2004. “Hydrophobic Pervaporation of Binary and Ternary Solutions: Evaluation of Fluxes, Selectivities, and Coupling Effects.” *Separation Science and Technology* 39: 2235–59.

Liu, F., L.Liu, and X. Feng. 2005. “Separation of Acetone–butanol–ethanol (ABE) from Dilute Aqueous Solutions by Pervaporation.” *Separation and Purification Technology* 42: 273–82.

Liu, K., Z. Tong, L. Liu, and X. Feng. 2005. “Separation of Organic Compounds from Water by Pervaporation in the Production of N-Butyl Acetate via Esterification by Reactive Distillation.” *Journal of Membrane Science* 256: 193–201.

Mah, S.K., S.P. Chai, and T.Y. Wu. 2014. “Dehydration of Glycerin Solution Using Pervaporation: HybSi and Polydimethylsiloxane Membranes.” *Journal of Membrane Science* 450: 440–46.

Mandal, M.K., and P.K. Bhattacharya. 2006. “Poly(ether-Block-Amide) Membrane for Pervaporative Separation of Pyridine Present in Low Concentration in Aqueous Solution.” *Journal of Membrane Science* 286: 115–24.

Martinez, R., M.T. Sanz, and S. Beltran. 2011. “Concentration by Pervaporation of Representative Brown Crab Volatile Compounds from Dilute Model Solutions.” *Journal of Food Engineering* 105: 98–104.

Martinez, R., M.T. Sanz, and S. Beltran. 2013. “Concentration by Pervaporation of Brown Crab Volatile Compounds from Dilute Model Solutions: Evaluation of PDMS Membrane.” *Journal of Membrane Science* 428: 371–79.

Massaldi, H.A., and C.J. King. 1973. “Simple Technique to Determine Solubilities of Sparingly Soluble Organics. Solubility and Activity Coefficients of D-Limonene, Butylbenzene, and N-Hexyl Acetate in Water and Sucrose Solutions.” *Journal of Chemical & Engineering Data* 18: 393–97.

Matheis, G.. 1998. “Application: Introduction.” In *Flavouring*, E. Ziegler and H. Ziegler (eds.), Weinheim, Germany: Wiley-VCH.

McGorrin, R. J.. 2001. “Advance in Dairy Flavor Chemistry.” In *Food Flavor and Chemistry Advances of the New Millennium*, A.M. Spanier, F. Shahidi, T.H. Parliment, C. Mussinan, C.-T. Ho, and E. Tratras Contis (eds.), Cambridge, UK: The Royal Society of Chemistry.

Miettinen, S.M., L. Hyvönen, and H. Tuorila. 2003. “Timing of Intensity Perception of a Polar

vs Nonpolar Aroma Compound in the Presence of Added Vegetable Fat in Milk." *Journal of Agricultural and Food Chemistry* 51: 5437–43.

Mishima, S., and T. Nakagawa. 2002. "Pervaporation of Volatile Organic Compounds/water Mixtures through poly(1H,1H,9H-Hexadecafluorononyl Methacrylate)-Filled poly(1-Trimethylsilyl-1-Propyne) Membranes." *Journal of Applied Polymer Science* 83: 1054–60.

Mishima, S., and T. Nakagawa. 2000. "Sorption and Diffusion of Volatile Organic Compounds in Fluoroalkyl Methacrylate-Grafted PDMS Membrane." *Journal of Applied Polymer Science* 75: 773–83.

Mohammadi, T., T. Kikhavandi, and M. Moghbeli. 2008. "Synthesis and Characterization of Poly(ether-Block-Amide) Membranes for the Pervaporation of Organic/aqueous Mixtures." *Journal of Applied Polymer Science* 107: 1917–23.

Monaco, H.L., G. Zanotti, P. Spadon, M. Bolognesi, L. Sawyer, and E.E. Eliopoulos. 1987. "Crystal Structure of the Trigonal Form of Bovine Beta-Lactoglobulin and of Its Complex with Retinol at 2.5 Å Resolution." *Journal of Molecular Biology* 197: 695–706.

Mujiburohman, M., and X. Feng. 2007. "Permselectivity, Solubility and Diffusivity of Propyl Propionate/water Mixtures in Poly(ether Block Amide) Membranes." *Journal of Membrane Science* 300: 95–103.

Mulder, M.. 1996. *Basic Principles of Membrane Technology*. Boston, USA: Kluwer Academic Publishers.

Nawar, W.W.. 1971. "Some Variables Affecting Composition of Headspace Aroma." *Journal of Agricultural and Food Chemistry* 19: 1057–59.

Nguyen, Q.T., Z. Bendjama, R. Clement, and Z. Ping. 2000. “Poly (Dimethylsiloxane) Crosslinked in Different Conditions.” *Physical Chemistry Chemical Physics* 2: 395–400.

Nguyen, Q.T., and K. Nobe. 1987. “Extraction of Organic Contaminants in Aqueous Solutions by Pervaporation.” *Journal of Membrane Science* 30: 11–22.

Niemistö, J., W. Kujawski, and R.L. Keiski. 2013. “Pervaporation Performance of Composite Poly(dimethyl Siloxane) Membrane for Butanol Recovery from Model Solutions.” *Journal of Membrane Science* 434: 55–64.

Nursten, H.E. 1997. “The Flavour of Milk and Dairy Products : I . Milk of Different Kinds, Milk Powder, Butter and Cream.” *International Journal of Dairy Technology* 50: 48–56.

Olsson, J., G. Tragardh, and F. Lipnizki. 2002. “The Influence of Permeant and Membrane Properties on Mass Transfer in Pervaporation of Volatile Organic Compounds from Dilute Aqueous Solutions.” *Separation Science and Technology* 37: 1199–1223.

Olsson, J., G. Tragardh, and C. Tragardh. 2001. “Pervaporation of Volatile Organics from Water II . Influence of Permeate Pressure on Partial Fluxes” 186: 239–47.

Olsson, J., and G. Tragardh. 1999. “Influence of Temperature on Membrane Permeability during Pervaporative Aroma Recovery.” *Separation Science and Technology* 34: 1643–59.

Overington, A.R., M. Wong, and J. Harrison. 2011. “Effect of Feed pH and Non-Volatile Dairy Components on Flavour Concentration by Pervaporation.” *Journal of Food Engineering* 107: 60–70.

Overington, A.R., M. Wong, J. Harrison, and L.B. Ferreira. 2009. “Estimation of Mass Transfer Rates through Hydrophobic Pervaporation Membranes.” *Separation Science and*

Technology 44: 787–816.

Overington, A.R., M. Wong, J. Harrison, and L. Ferreira. 2008. “Concentration of Dairy Flavour Compounds Using Pervaporation.” *International Dairy Journal* 18: 835–48.

Panek, D., and K. Konieczny. 2007. “Preparation and Applying the Membranes with Carbon Black to Pervaporation of Toluene from the Diluted Aqueous Solutions.” *Separation and Purification Technology* 57: 507–12.

Papiz, M.Z., L. Sawyer, E.E. Eliopoulos, A.C. North, J.B. Findlay, R. Sivaprasadarao, T.A. Jones, M.E. Newcomer, and P.J. Kraulis. 1986. “The Structure of Beta-Lactoglobulin and Its Similarity to Plasma Retinol-Binding Protein.” *Nature* 324: 383–85.

Parliment, T.H., and R.J. McGorrin. 2000. “Critical Flavor Compounds in Dairy Products.” In *Flavor Chemistry: Industrial and Academic Research*, Washington, D.C.: American Chemical Society.

Peng, M., and S. Liu. 2003. “Recovery of Aroma Compounds from Dilute Model Blueberry Solution by Pervaporation.” *Journal of Food Science* 68: 2706–10.

Peng, M., and S. Liu. 2003. “Recovery of Aroma Compounds from Dilute Model Blueberry Solution by Pervaporation.” *Food Engineering and Physical Properties* 68: 2706–10.

Peng, M., L.M. Vane, and S.X. Liu. 2003. “Recent Advances in VOCs Removal from Water by Pervaporation.” *Journal of Hazardous Materials* B98: 69–90.

Pereira, C.C., J.R.M. Rufino, A.C. Habert, R. Nobrega, L.M.C. Cabral, and C.P. Borges. 2005. “Aroma Compounds Recovery of Tropical Fruit Juice by Pervaporation: Membrane Material Selection and Process Evaluation.” *Journal of Food Engineering* 66: 77–87.

Pereira, C.C., J.M. Rufinob, A.C. Habert, R. Nobrega, L.M.C. Cabral, and C.P. Borges. 2002.

"Membrane for Processing Tropical Fruit Juice." *Desalination* 148: 57–60.

Pereira, C.C., C.P. Ribeiro, R. Nobrega, and C.P. Borges. 2006. "Pervaporative Recovery of Volatile Aroma Compounds from Fruit Juices." *Journal of Membrane Science* 274: 1–23.

Pierre, F.X., I. Souchon, and M. Marin. 2001. "Recovery of Sulfur Aroma Compounds Using Membrane-Based Solvent Extraction." *Journal of Membrane Science* 187: 239–53.

Pouliot, Y.. 2008. "Membrane Processes in Dairy Technology-From a Simple Idea to Worldwide Panacea." *International Dairy Journal* 18: 735–40.

Raisi, A., and A. Aroujalian. 2011. "Aroma Compound Recovery by Hydrophobic Pervaporation: The Effect of Membrane Thickness and Coupling Phenomena." *Separation and Purification Technology* 82: 53–62.

Raisi, A., A. Aroujalian, and T. Kaghazchi. 2008. "Multicomponent Pervaporation Process for Volatile Aroma Compounds Recovery from Pomegranate Juice." *Journal of Membrane Science* 322: 339–48.

Rajagopalan, N., M. Cheryan, and T. Matsuura. 1994. "Recovery of Diacetyl by Pervaporation." *Biotechnology Techniques* 8: 869–72.

Rautenbach, R., and R. Albrecht. 1985. "The Separation Potential of Pervaporation. Part 2. Process Design and Economics." *Journal of Membrane Science* 25: 25–54.

Rautenbach, R., and F.P. Helmus. 1994. "Some Considerations on Mass-Transfer Resistances in Solution—diffusion-Type Membrane Processes." *Journal of Membrane Science* 87: 171–80.

Reineccius, G.. 2006. *Flavor Chemistry and Technology*. 2nd edition. Boca Raton, USA: Taylor and Francis.

Reiners, J., S. Nicklaus, and E. Guichard. 2000. “Interactions between β -Lactoglobulin and Flavour Compounds of Different Chemical Classes. Impact of the Protein on the Odour Perception of Vanillin and Eugenol.” *Le Lait* 80: 347–60.

Relkin, P., M. Fabre, and E. Guichard. 2004. “Effect of Fat Nature and Aroma Compound Hydrophobicity on Flavor Release from Complex Food Emulsions.” *Journal of Agricultural and Food Chemistry* 52: 6257–63.

Ribeiro Jr, C.P., P.L.C. Lage, and C.P. Borges. 2004. “A Combined Gas-Stripping Vapour Permeation Process for Aroma Recovery.” *Journal of Membrane Science* 238: 9–19.

Rice, G., S. Kentish, V. Vivekanand, A. O’Connor, G. Stevens, and A. Barber. 2008. “Membrane-Based Dairy Separation: A Comparison of Nanofiltration and Electrodialysis.” *Developments in Chemical Engineering and Mineral Processing* 13: 43–54.

Rinaldoni, A.N., C.C. Tarazaga, M.E. Campderrós, and A.P. Padilla. 2009. “Assessing Performance of Skim Milk Ultrafiltration by Using Technical Parameters.” *Journal of Food Engineering* 92: 226–32.

Roberts, D.D, J.S. Elmore, K.R Langley, and J. Bakker. 1996. “Effects of Sucrose, Guar Gum, and Carboxymethylcellulose on the Release of Volatile Flavor Compounds under Dynamic Conditions.” *Journal of Agricultural and Food Chemistry* 44: 1321–26.

Roos, Y.H. 2009. “Solid and Liquid States of Lactose.” In *Advanced Dairy Chemistry*, P.L.H. McSweeney and P.F. Fox (eds), New York, NY: Springer.

Rossi, S.C., A.B.P. Medeiros, T.A. Weschenfelder, A. de Paula Scheer, and C.R. Soccol. 2017. “Use of Pervaporation Process for the Recovery of Aroma Compounds Produced by P.

Fermentans in Sugarcane Molasses." *Bioprocess and Biosystems Engineering* 40: 959–67.

Routray, W., and H.N. Mishra. 2011. "Scientific and Technical Aspects of Yogurt Aroma and Taste: A Review." *Comprehensive Reviews in Food Science and Food Safety* 10: 208–20.

Ruegg, M. 1985. "Water in Dairy Products Related to Quality, with Special Reference to Cheese." In *Properties of Water in Foods*, D. Simatos and J.L Multon (eds). Springer Netherlands.

Sampranpiboon, P., R. Jiraratananon, D. Uttapap, X. Feng, and R.Y.M. Huang. 2000a. "Pervaporation Separation of Ethyl Butyrate and Isopropanol with Polyether Block Amide (PEBA) Membranes." *Journal of Membrane Science* 173: 53–59.

Sampranpiboon, P., R. Jiraratananon, D. Uttapap, X. Feng, and R.Y.M. Huang. 2000b. "Separation of Aroma Compounds from Aqueous Solutions by Pervaporation Using Polyoctylmethyl Siloxane (POMS) and Polydimethyl Siloxane (PDMS) Membranes." *Journal of Membrane Science* 174: 55–65.

Sánchez, J., E. Hernández, J.M. Auleda, and M. Raventós. 2011. "Review: Freeze Concentration Technology Applied to Dairy Products." *Food Science and Technology International* 17: 5–13.

Schafer, T., J. Vital, and J.G. Crespo. 2004. "Coupled Pervaporation/mass Spectrometry for Investigating Membrane Mass Transport Phenomena." *Journal of Membrane Science* 241: 197–205.

Schirle-Keller, J.P., G.A. Reineccius, and L.C. Hatchwell. 1994. "Flavor Interactions with Fat Replacers: Effect of Oil Level." *Journal of Food Science* 59: 813–15..

Schultz, W.G., and J.M. Randall. 1970. “Liquid Carbon Dioxide for Selective Aroma Extraction.” *Food Technology* 24:1282-6.

Seidel, A., J.J. Waypa, and M. Elimelech. 2001. “Role of Charge (Donnan) Exclusion in Removal of Arsenic from Water by a Negatively Charged Porous Nanofiltration Membrane.” *Environmental Engineering Science* 18: 105–13.

Semenova, S.I., H. Ohya, and K. Soontarapa. 1997. “Hydrophilic Membranes for Pervaporation: An Analytical Review.” *Desalination* 110: 251–86.

Seuvre, A.M., E. Philippe, S. Rochard, and A. Voilley. 2006. “Retention of Aroma Compounds in Food Matrices of Similar Rheological Behaviour and Different Compositions.” *Food Chemistry* 96: 104–14.

Shao, P., and R.Y.M. Huang. 2007. “Polymeric Membrane Pervaporation.” *Journal of Membrane Science* 287: 162–79.

She, M., and S.-T. Hwang. 2004. “Concentration of Dilute Flavor Compounds by Pervaporation: Permeate Pressure Effect and Boundary Layer Resistance Modeling.” *Journal of Membrane Science* 236: 193–202.

She, M., and S.-T. Hwang. 2006a. “Effects of Concentration, Temperature, and Coupling on Pervaporation of Dilute Flavor Organics.” *Journal of Membrane Science* 271: 16–28..

She, M., and S.-T. Hwang. 2006b. “Recovery of Key Components from Real Flavor Concentrates by Pervaporation.” *Journal of Membrane Science* 279: 86–93.

Sheldon, R.A., and F. van Rantwijk. 2008. “Ionic Liquids as Media for Enzymatic Transformations.” In *Organic Synthesis with Enzymes in Non-Aqueous Media*, G. Carrea and S. Riva (eds), 227–54. Weinheim: Wiley-VCH.

Shepherd, A., A.C. Habertb, and C.P. Borges. 2002. “Hollow Fibre Modules for Orange Juice Aroma Recovery Using Pervaporation.” *Desalination* 148: 111–14.

Shirazi, Y., A. Ghadimi, and T. Mohammadi. 2012. “Recovery of Alcohols from Water Using Polydimethylsiloxane-Silica Nanocomposite Membranes : Characterization and Pervaporation Performance.” *Journal of Applied Polymer Science* 124: 2871–82.

Slater, C.S.. 1997. “Recovery of Ethyl Acetate from Process Effluents Using Pervaporation Technology.” *Journal of Environmental Science and Health* A32: 1339–52.

Song, K.-H., and K.-R. Lee. 2005. “Pervaporation of Flavors with Hydrophobic Membrane.” *Korean Journal of Chemical Engineering* 22: 735–39.

Song, K.-H., K.-R. Lee, and J.-M. Rim. 2004. “Pervaporation of Esters with Hydrophobic Membrane.” *Korean Journal of Chemical Engineering* 21: 693–98.

Souchon, I., F.X. Pierre, V. Athes-Dutour, and M. Marin. 2002. “Pervaporation as a Deodorization Process Applied to Food Industry Effluents: Recovery and Valorisation of Aroma Compounds from Cauliflower Blanching Water.” *Desalination* 148: 79–85.

Swaisgood, H.E.. 1996. “Characteristics of Milk.” In *Food Chemistry,* New York, USA: Marcel Dekker.

Graham, T.. 1866. “On the Absorption and Dialytic Separation of Gases by Colloid Septa. Part I. Action of a Septum of Caoutchouc.” *Philosophical Transactions of the Royal Society* 156: 399–439.

Tanaka, S., Y. Chao, S. Araki, and Y. Miyake. 2010. “Pervaporation Characteristics of Pore-Filling PDMS/PMHS Membranes for Recovery of Ethylacetate from Aqueous Solution.” *Journal of Membrane Science* 348: 383–88.

Thujssen, H.A.C. 1970. “Concentration Process for Liquid Foods Containing Volatile Flavours and Aromas.” *Journal of Food Technology* 5: 211–29.

Tian, X., and X. Jiang. 2008. “Poly(vinylidene Fluoride-Co-Hexafluoropropene) (PVDF-HFP) Membranes for Ethyl Acetate Removal from Water.” *Journal of Hazardous Materials* 153: 128–35.

Toso, B., G. Procida, and B. Stefanon. 2002. “Determination of Volatile Compounds in Cows’ Milk Using Headspace GC-MS.” *The Journal of Dairy Research* 69: 569–77.

Tossavainen, O., and J. Sahlstein. 2003. Lactose-free milk product and processes for producing the same. US patent 8,449,938B2.

Trifunovic, O., and G. Tragardh. 2003. “The Influence of Permeant Properties on the Sorption Step in Hydrophobic Pervaporation.” *Journal of Membrane Science* 216: 207–16.

Trifunovic, O., and G. Tragardh. 2005. “The Influence of Support Layer on Mass Transport of Homologous Series of Alcohols and Esters through Composite Pervaporation Membranes.” *Journal of Membrane Science* 259: 122–34.

Trifunovic, O., and G. Tragardh. 2006. “Mass Transport of Aliphatic Alcohols and Esters through Hydrophobic Pervaporation Membranes.” *Separation and Purification Technology* 50: 51–61.

Tsenkova, R., S. Atanassova, K. Itoh, Y. Ozaki, and K. Toyoda. 2000. “Near Infrared Spectroscopy for Biomonitoring: Cow Milk Composition Measurement in a Spectral Region from 1,100 to 2,400 Nanometers.” *Journal of Animal Science* 78: 515–22.

Urbach, G. 1997. “The Flavour of Milk and Dairy Products: II. Cheese: Contribution of Volatile Compounds.” *International Journal of Dairy Technology* 50: 79–89.

United States Department of Agriculture 2015. *USDA National Nutrient Database* [database]. Retrieved from https://ndb.nal.usda.gov/ndb/.

van Boxtel, A.J.B., Z.E.H. Otten, and H.J.L.J. van der Linden. 1991. "Evaluation of Process Models for Fouling Control of Reverse Osmosis of Cheese Whey." *Journal of Membrane Science* 58 (1): 89–111.

van der Horst, H.C., J.M.K. Timmer, T. Robbertsen, and J. Leenders. 1995. "Use of Nanofiltration for Concentration and Demineralization in the Dairy Industry: Model for Mass Transport." *Journal of Membrane Science* 104: 205–18.

van Mil, P.J.J.M., and S. Bouman. 1990. "Freeze Concentration of Dairy Products." *Netherlands Milk and Dairy Journal* 44: 21–31.

Vankelecom, I.F.J., S. De Beukelaer, and J.B. Uytterhoeven. 1997. "Sorption and Pervaporation of Aroma Compounds Using Zeolite-Filled PDMS Membranes." *Journal of Physical Chemistry B* 101: 5186–90.

Voilley, A., G. Charbit, and F. Gobert. 1990. "Recovery and Separation of 1-Octen-3-ol from Aqueous Solutions by Pervaporation through Silicon Membrane." *Journal of Food Science* 55: 1399–1402.

Voilley, A., T. Lamer, T. Nguyen, and D. Simatos. 1989. "Extraction of Aroma Compounds by Pervaporation." In *Proceedings of the 4th International Conference on Pervaporation Processes in the Chemical Industry*, R. Bakish (ed.), Englewood, NJ: Bakish Materials Corporation.

Willemsen, J.H.A., B.H. Dijkink, and A. Togtema. 2004. "Organophilic Pervaporation for Aroma Isolation-industrial and Commercial Prospects." *Membrane Technology*, 2004: 5–

10.

Wu, D., J. Martin, J. Du, Y. Zhang, D. Lawless, and X. Feng. 2015. “Thin Film Composite Membranes Comprising of Interfacially-Polymerized Polyamide and Self-Polymerized Polydopamine for Dehydration of Ethylene Glycol by Pervaporation.” *Journal of Membrane Science* 493: 622–35.

Wu, D., Z. Tan, H. Yu, Q. Li, J. Thé, X. Feng. 2016. “Use of Nanofiltration to Reject Cobalqt (II) from Ammoniacal Solutions Involved in Absorption of SO_2/NO_x.” *Chemical Engineering Science* 145: 97–107.

Wu, Y., H. Tan, D. Li, and Y. Jin. 2012. “Pervaporation of Aqueous Solution of Acetaldehyde through ZSM-5 Filled PDMS Composite Membrane.” *Chinese Journal of Chemical Engineering* 20: 625–32.

Wu, Y., H. Tan, Da. Zhang, and T. Li. 2011. “Pervaporation of Acetaldehyde Aqueous Solution through Zeolite 3A-Polyurethane (PU) Composite Membrane.” *Separation Science and Technology* 46: 1908–14.

Yalkowsky, S.H., Y. He, and P. Jain. 2010. *Handbook of Aqueous Solubility Data*. Second edi. Boca Raton, USA: CRC Press LLC.

Yu, C., Y. Liu, G. Chen, X. Gu, and W. Xing. 2011. “Pretreatment of Isopropanol Solution from Pharmaceutical Industry and Pervaporation Dehydration by NaA Zeolite Membranes.” *Chinese Journal of Chemical Engineering* 19: 904–10.

Zhu, B., X. Tian, and Y. Xu. 2005. “Recovering Ethyl Acetate from Aqueous Solution Using P(VDF-Co-HFP) Membrane Based Pervaporation.” *Desalination* 184: 71–78.

Zou, Y., Y. Liu, Y. Muhammad, Z. Tong, and X. Feng. 2018. “Experimental and Modelling

Studies of Pervaporative Removal of Odorous Diacetyl and S-Methylthiobutanoate from Aqueous Solutions Using PEBA Membrane." *Separation and Purification Technology* 200: 1–10.

Appendix A

Activity coefficient and vapor pressure of aroma compound and water

Table A.1 lists the activity coefficients, saturated vapor pressure and partial vapor pressure of the aroma compounds and water under various operating conditions, these data were predicted by Aspen plus V8.0. Table A.2 shows the saturated vapor pressure of pure water. For these dilute solutions, the activity coefficient of water was 1.00, and thus the partial vapor pressure of water was essentially the same as the saturated vapor pressure of pure water.

Table A.1 Activity coefficients and vapor pressure of the aromas and water under various operating conditions.

Aroma compounds	Temperature (°C)	Aroma concentration in liquid (ppm)	Activity coefficient of aroma	Saturated vapor pressure of pure aroma (Pa)	Partial vapor pressure of aroma (Pa)
Ethyl butanoate	25	50	898	2231	16
	25	500	895	2231	155
	25	1000	893	2231	309
	36	50	867	3971	27
	36	75	867	3971	40
	36	175	866	3971	93
	36	250	866	3971	133
	36	500	864	3971	266
	36	675	864	3971	359
	36	850	863	3971	452

Table A.1 Activity coefficients and saturated vapor pressure of the aromas and water under various operating conditions (continued).

Aroma compounds	Temperature (°C)	Aroma concentration in liquid (ppm)	Activity coefficient of aroma	Saturated vapor pressure of pure aroma (Pa)	Partial vapor pressure of aroma (Pa)
Ethyl butanoate	36	1125	861	3971	598
	36	1300	860	3971	690
	36	1550	859	3971	822
	36	1700	858	3971	901
	36	1875	857	3971	993
	36	2100	856	3971	1111
	36	2300	855	3971	1215
	36	2500	854	3971	1320
	45	50	831	6153	40
	45	500	829	6153	396
	45	1000	826	6153	789
	55	50	782	9691	59
	55	500	780	9691	587
	55	1000	778	9691	1171
	65	50	727	14802	83
	65	500	725	14802	833
	65	1000	722	14802	1662
Ethyl hexanoate	25	50	9337	215	13
	25	100	9333	215	25
	25	300	9318	215	75
	36	50	8726	452	25
	36	90	8723	452	44
	36	100	8723	452	49

Table A.1 Activity coefficients and saturated vapor pressure of the aromas and water under various operating conditions (continued).

Aroma compounds	Temperature (°C)	Aroma concentration in liquid (ppm)	Activity coefficient of aroma	Saturated vapor pressure of pure aroma (Pa)	Partial vapor pressure of aroma (Pa)
	36	170	8717	452	84
	36	250	8712	452	123
	36	300	8708	452	148
	36	330	8706	452	162
	36	400	8701	452	197
	45	100	8111	793	80
	45	50	8115	792	40
	45	300	8098	793	241
	55	100	7356	1416	130
	55	50	7359	1416	65
	55	300	7343	1416	390
	65	100	6559	2427	199
	65	50	6562	2427	99
	65	300	6548	2428	596
2-Heptanone	25	50	743	522	3
	25	500	740	522	31
	25	1000	738	522	61
	36	50	735	1024	6
	36	200	734	1024	24
	36	400	733	1024	47
	36	500	732	1024	59
	36	700	731	1024	83
	36	1000	730	1024	118

Table A.1 Activity coefficients and saturated vapor pressure of the aromas and water under various operating conditions (continued).

Aroma compounds	Temperature (°C)	Aroma concentration in liquid (ppm)	Activity coefficient of aroma	Saturated vapor pressure of pure aroma (Pa)	Partial vapor pressure of aroma (Pa)
	36	1300	728	1024	153
	36	1600	727	1024	188
	36	1900	725	1024	223
	36	2200	723	1024	258
	36	2500	722	1024	292
	45	50	718	1705	10
	45	500	716	1705	96
	45	1000	713	1705	192
	55	50	690	2890	16
	55	500	688	2891	157
	55	1000	686	2891	313
	65	50	654	4723	24
	65	500	652	4724	243
	65	1000	649	4726	485
Nonanal	25	10	16450	60	1.25
	25	30	16447	60	3.75
	25	50	16444	60	6.25
	36	10	15273	133	2.58
	36	20	15272	133	5.15
	36	30	15271	133	7.73
	36	40	15269	133	10.3
	36	50	15268	133	12.9
	45	10	14073	244	4.35

Table A.1 Activity coefficients and saturated vapor pressure of the aromas and water under various operating conditions (continued).

Aroma compounds	Temperature (°C)	Aroma concentration in liquid (ppm)	Activity coefficient of aroma	Saturated vapor pressure of pure aroma (Pa)	Partial vapor pressure of aroma (Pa)
	45	30	14070	244	13
	45	50	14068	244	21.7
	55	10	12586	457	7.28
	55	30	12584	457	21.8
	55	50	12581	457	36.4
	65	10	11031	819	11.4
	65	30	11029	819	34.3
	65	50	11027	819	57.2
Diacetyl	25	50	7.12	7521	0.56
	25	500	7.12	7521	5.61
	25	1000	7.12	7521	11.2
	36	50	7.76	13033	1.06
	36	100	7.76	13033	2.12
	36	200	7.76	13033	4.23
	36	300	7.76	13033	6.35
	36	500	7.76	13033	10.6
	36	700	7.76	13033	14.8
	36	900	7.76	13033	19.1
	36	1100	7.75	13033	23.3
	36	1300	7.75	13033	27.5
	36	1500	7.75	13033	31.7
	36	1700	7.75	13033	36
	36	1900	7.75	13033	40.2

Table A.1 Activity coefficients and saturated vapor pressure of the aromas and water under various operating conditions (continued).

Aroma compounds	Temperature (°C)	Aroma concentration in liquid (ppm)	Activity coefficient of aroma	Saturated vapor pressure of pure aroma (Pa)	Partial vapor pressure of aroma (Pa)
	36	2100	7.75	13033	44.4
	36	2300	7.74	13033	48.7
	36	2500	7.74	13033	52.9
	45	50	8.28	19739	1.71
	45	500	8.28	19740	17.1
	45	1000	8.28	19740	34.2
	55	50	8.85	30298	2.81
	55	500	8.84	30298	28
	55	1000	8.84	30298	56.1
	65	50	9.38	45077	4.43
	65	500	9.38	45078	44.3
	65	1000	9.37	45079	88.5
Hexanoic acid	25	50	249	7	0.01
	25	500	248	7	0.13
	25	1000	248	7	0.26
	36	50	235	18	0.03
	36	100	235	18	0.07
	36	200	235	18	0.13
	36	500	234	18	0.33
	36	700	234	18	0.46
	36	1000	234	18	0.66
	36	1300	233	18	0.86
	36	1600	233	18	1.06

Table A.1 Activity coefficients and saturated vapor pressure of the aromas and water under various operating conditions (continued).

Aroma compounds	Temperature (°C)	Aroma concentration in liquid (ppm)	Activity coefficient of aroma	Saturated vapor pressure of pure aroma (Pa)	Partial vapor pressure of aroma (Pa)
	36	1900	233	18	1.25
	36	2200	232	18	1.45
	36	2500	232	18	1.65
	45	50	221	39	0.07
	45	500	221	39	0.66
	45	1000	220	39	1.32
	55	50	205	84	0.13
	55	500	204	84	1.34
	55	1000	204	84	2.67
	65	50	187	174	0.25
	65	500	186	174	2.52
	65	1000	186	174	5.03
Indole	25	50	551	4	0.016
	25	100	551	4	0.031
	25	200	550	4	0.063
	36	50	525	9	0.036
	36	100	525	9	0.073
	36	200	524	9	0.145
	36	500	523	9	0.362
	36	800	522	9	0.579
	45	50	501	18	0.069
	45	100	500	18	0.137
	45	200	500	18	0.275

Table A.1 Activity coefficients and saturated vapor pressure of the aromas and water under various operating conditions (continued).

Aroma compounds	Temperature (°C)	Aroma concentration in liquid (ppm)	Activity coefficient of aroma	Saturated vapor pressure of pure aroma (Pa)	Partial vapor pressure of aroma (Pa)
	55	50	472	37	0.133
	55	100	472	37	0.265
	55	200	471	37	0.53
	65	50	442	72	0.244
	65	100	442	72	0.487
	65	200	442	72	0.973

Table A.2 The statured vapor pressure of pure water at different temperatures.

Temperature (°C)	Saturated vapor pressure of pure water (Pa)
25	3170
36	5949
45	9596
55	15760
65	25030

Appendix B

The ratio of individual resistance/total resistance

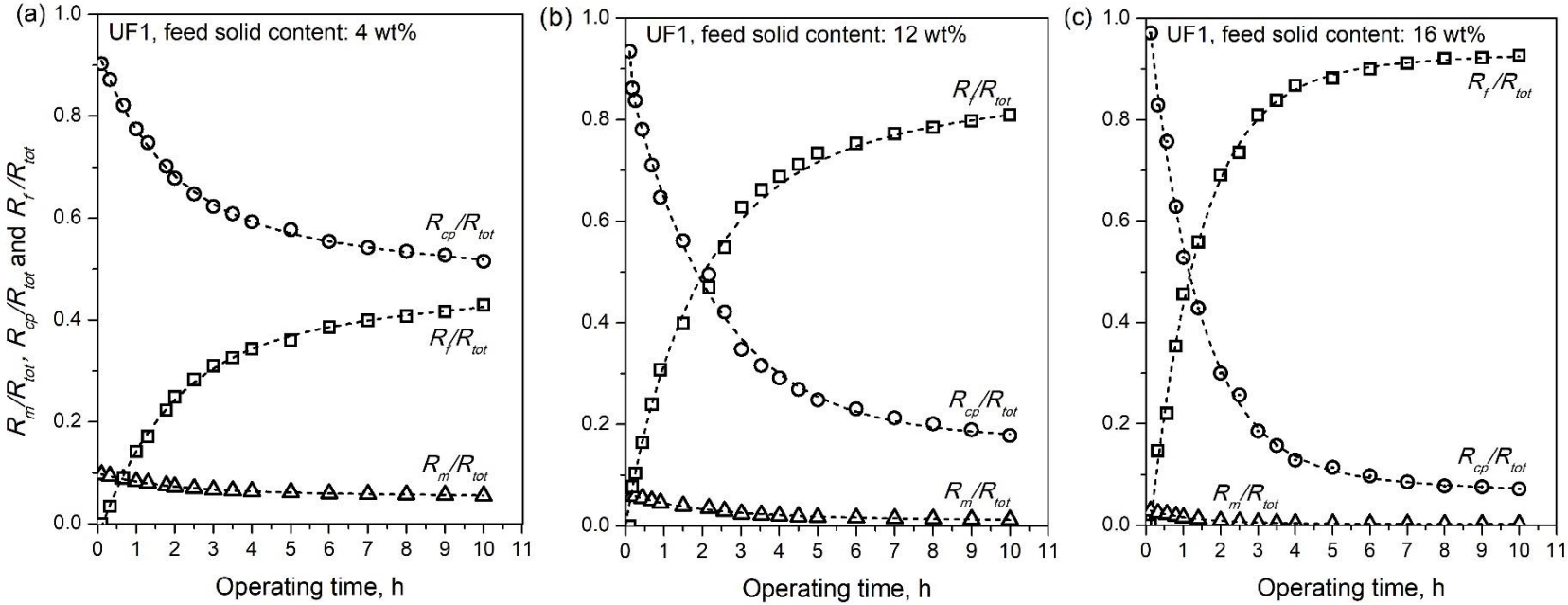

Figure B.1 Individual resistance/total resistance ratio as a function of time at a feed solid content of (a) 4 wt.%, (b) 12 wt.% and (c) 16 wt.% using UF1 membrane. Temperature: 22 °C. Transmembrane pressure: 0.8 MPa.

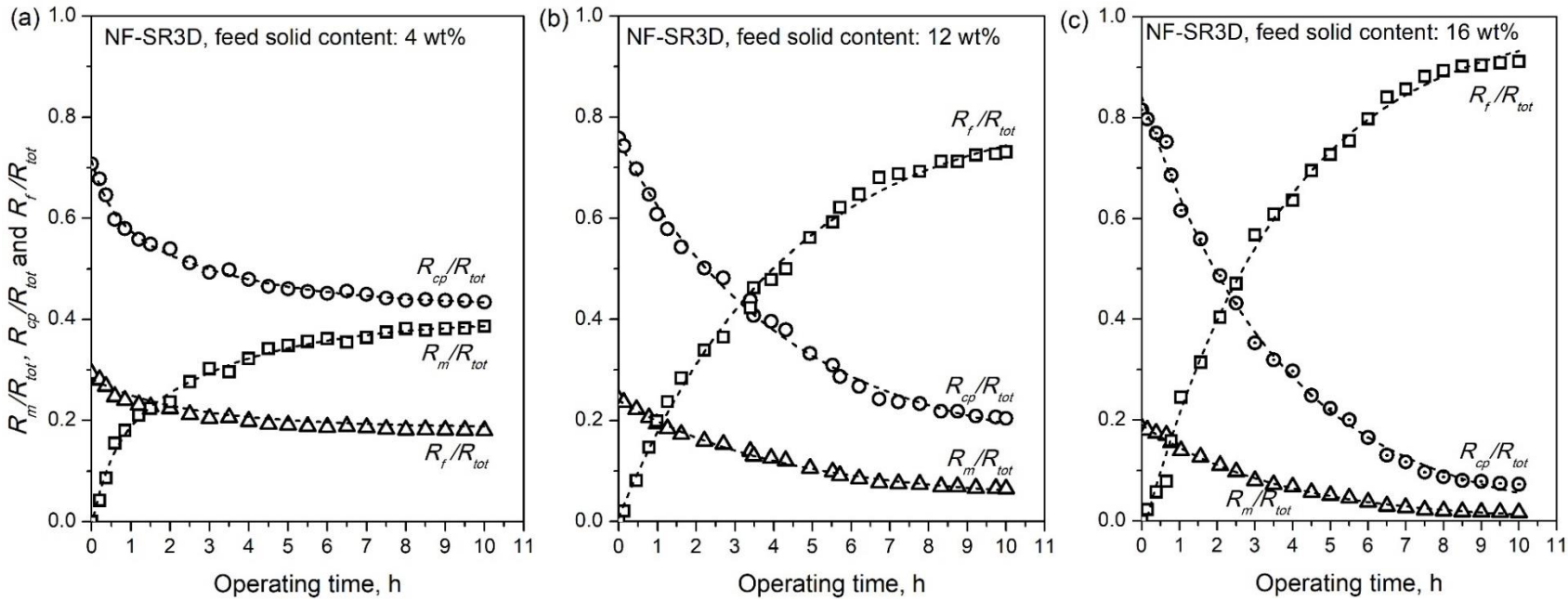

Figure B.2 Individual resistance/total resistance ratio as a function of time at a feed solid content of (a) 4 wt.%, (b) 12 wt.% and (c) 16 wt.% using NF-SR3D membrane. Temperature: 22 °C. Transmembrane pressure: 0.8 MPa.

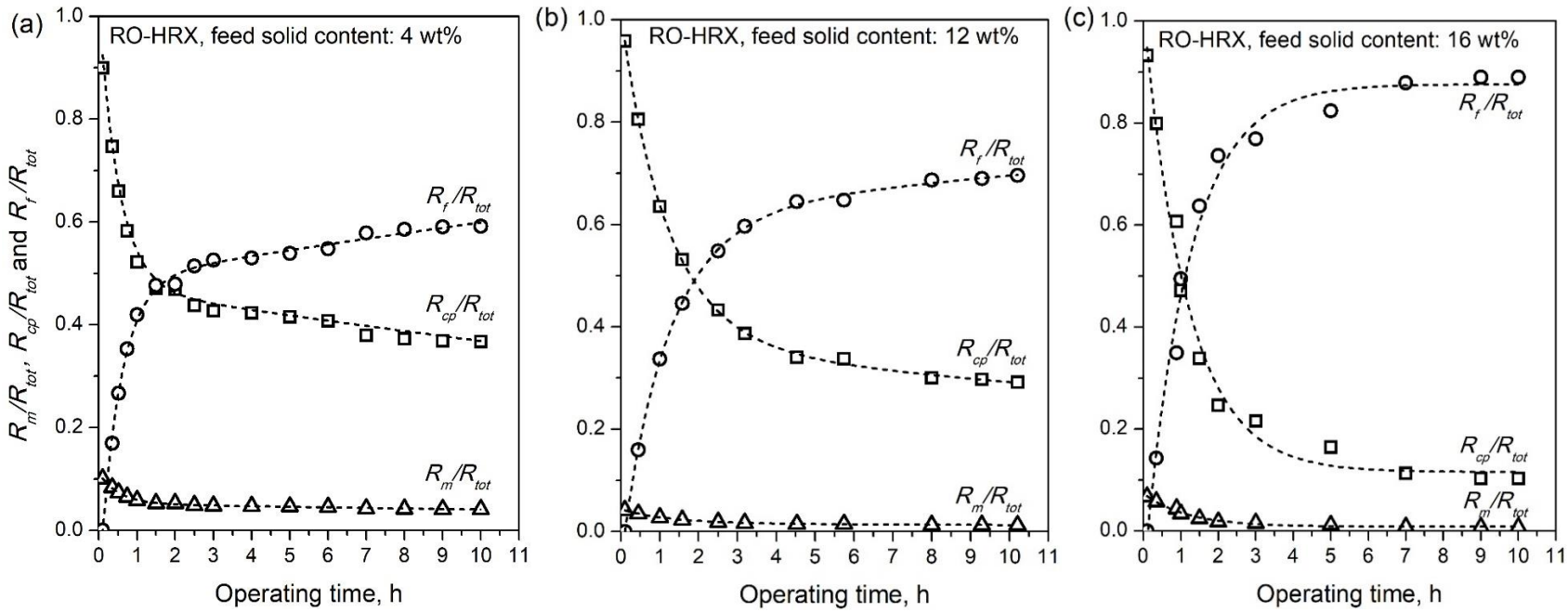

Figure B.3 Individual resistance/total resistance ratio as a function of time at a feed solid content of (a) 4 wt.%, (b) 12 wt.% and (c) 16 wt.% using RO-HRX membrane. Temperature: 22 °C. Transmembrane pressure: 0.8 MPa.

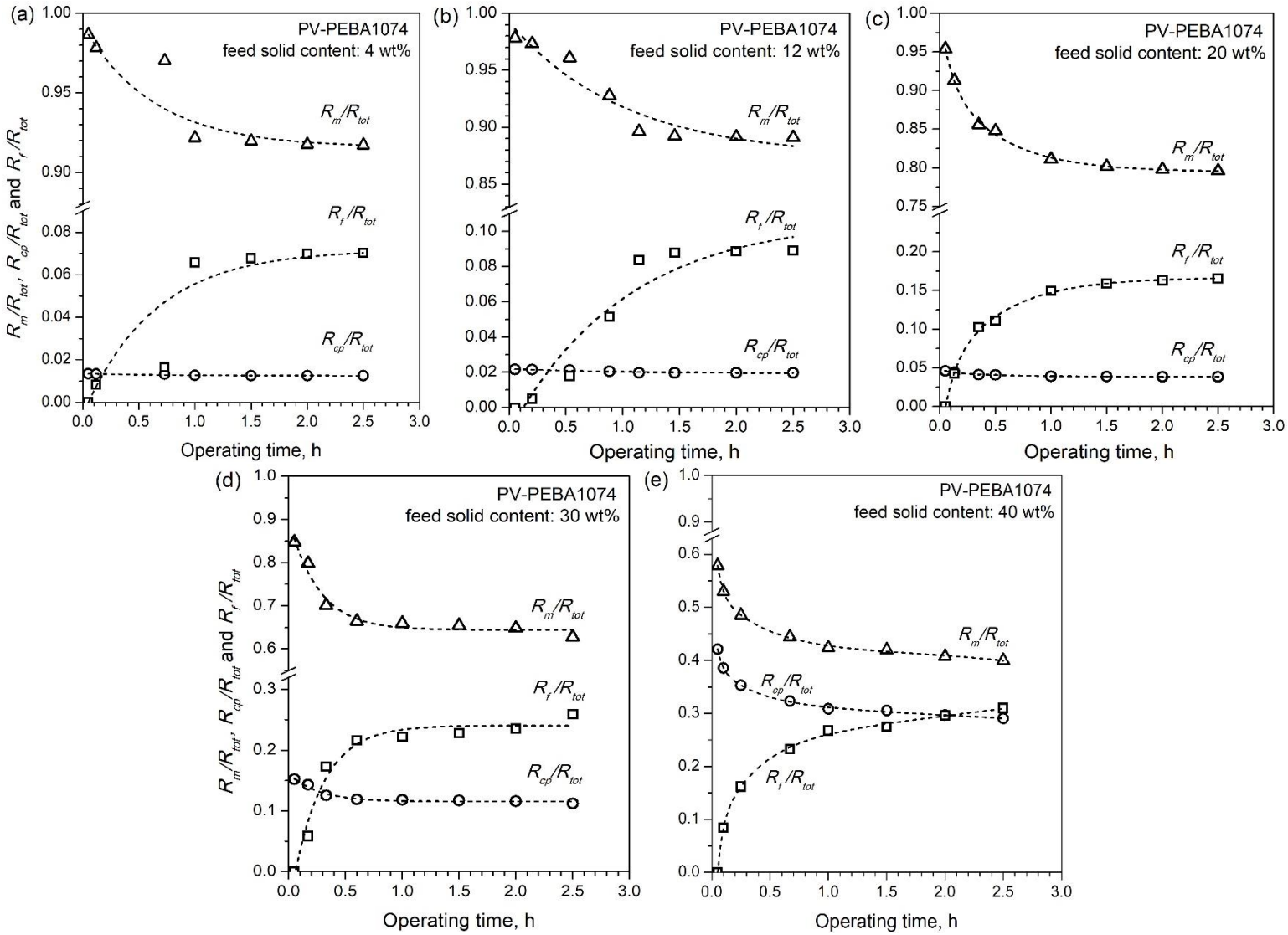

Figure B.4 Individual resistance/total resistance ratio as a function of time at a feed solid content of (a) 4 wt.%, (b) 12 wt.%, (c) 20 wt.%, (d) 30 wt.% and (e) 40 wt.% using PV-PEBA 1074 membrane. Temperature: 22 °C. Permeate pressure: 400 Pa.

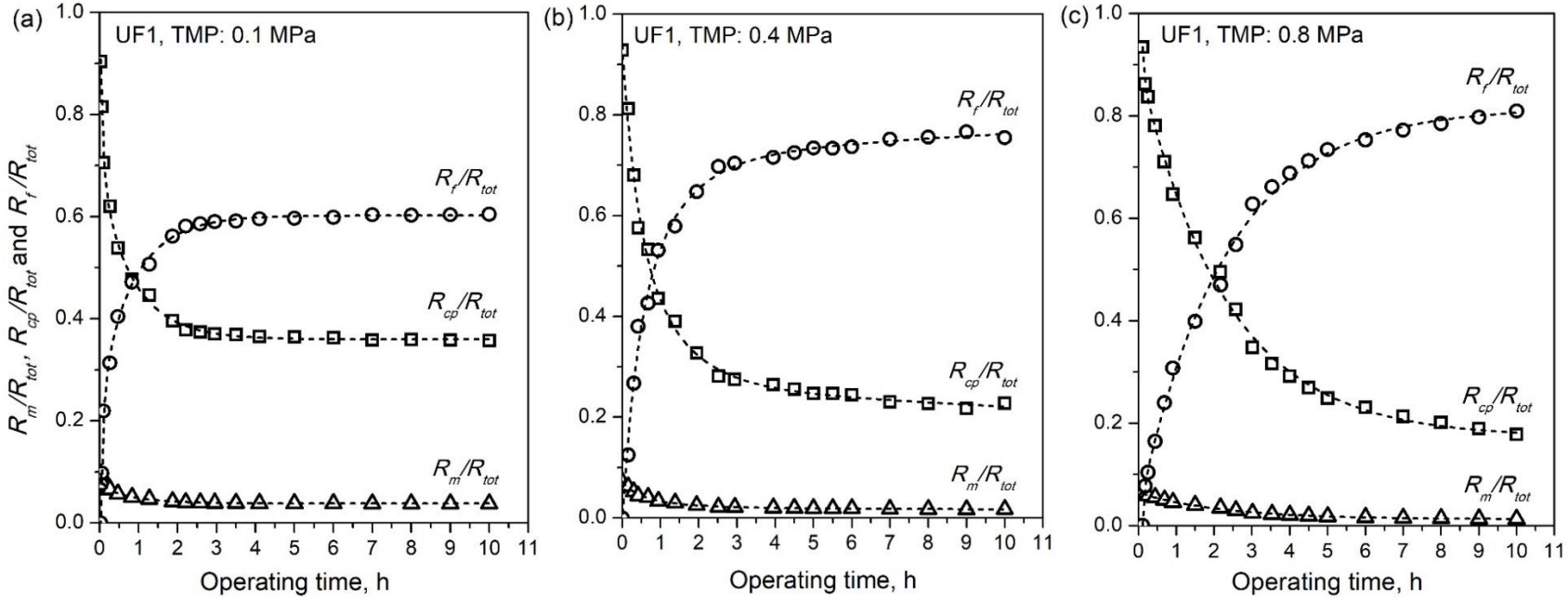

Figure B.5 Individual resistance/total resistance ratio as a function of time at a transmembrane pressure of (a) 0.1 MPa, (b) 0.4 MPa and (c) 0.8 MPa using UF1 membrane. Temperature: 22 °C. Feed solid content: 12 wt.%.

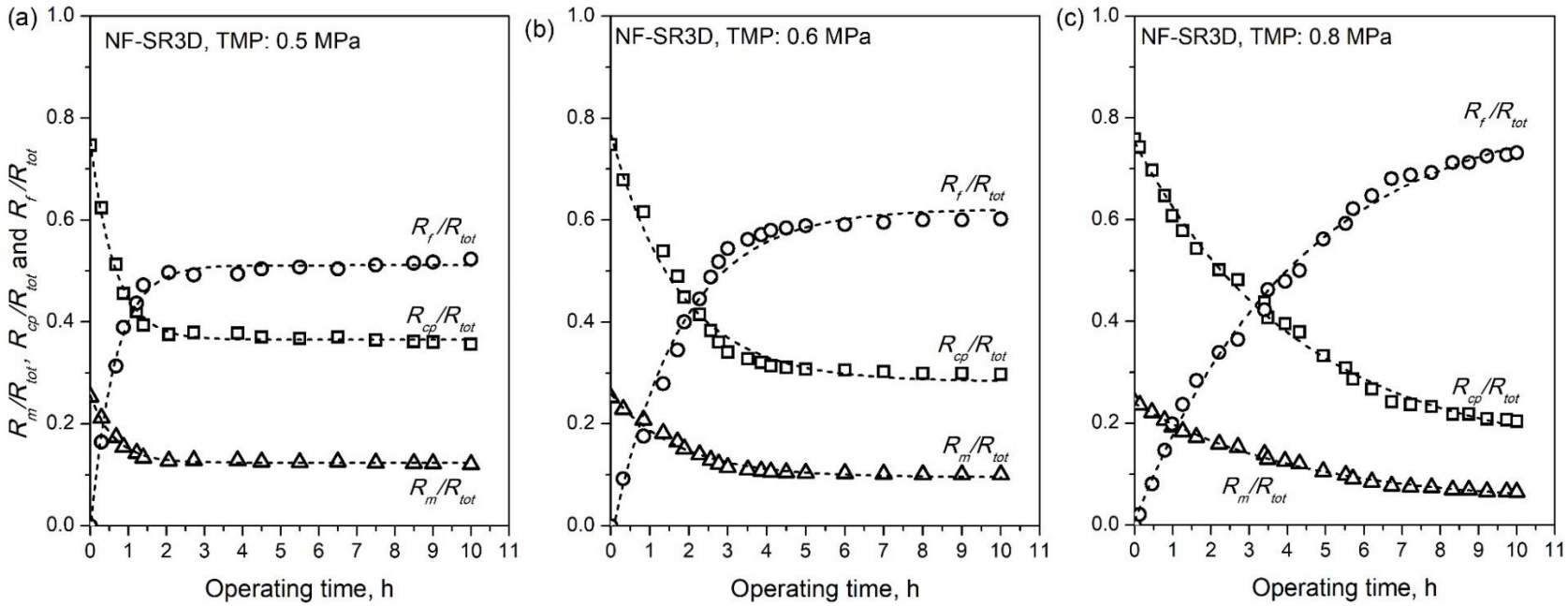

Figure B.6 Individual resistance/total resistance ratio as a function of time at a transmembrane pressure of (a) 0.5 MPa, (b) 0.6 MPa and (c) 0.8 MPa using NF-SR3D membrane. Temperature: 22 °C. Feed solid content: 12 wt.%.

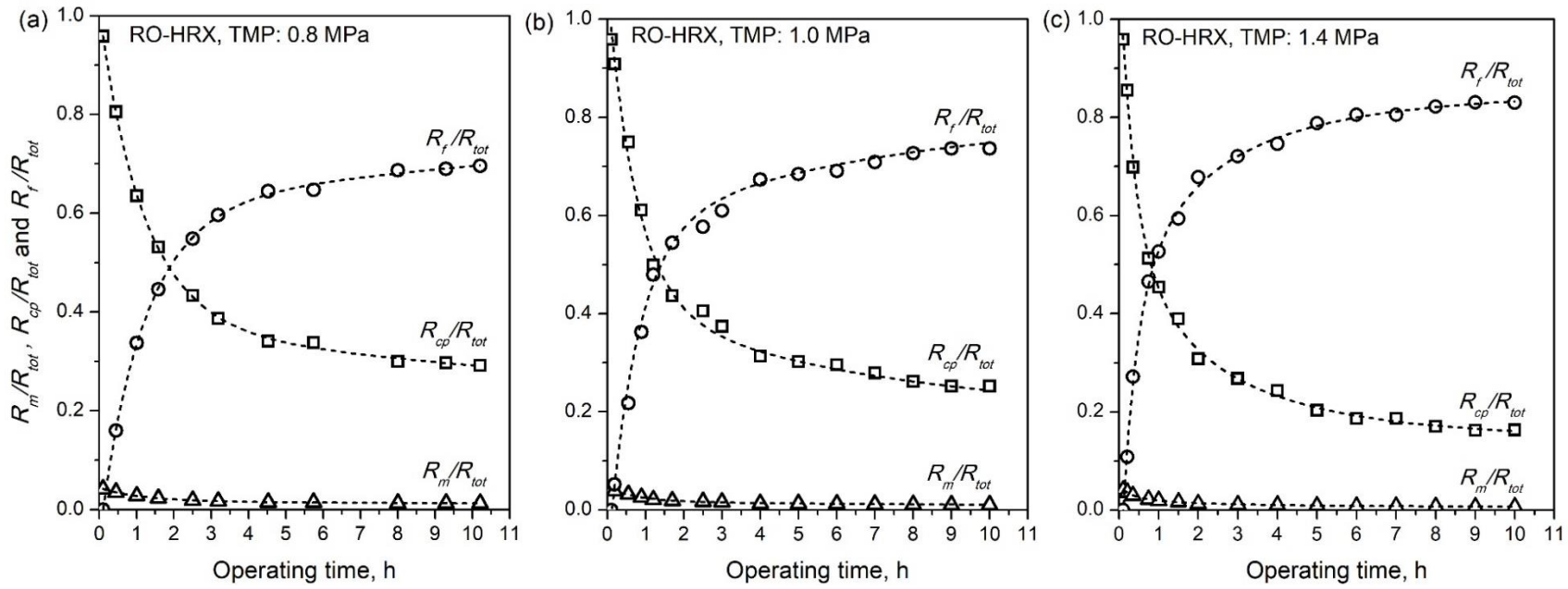

Figure B.7 Individual resistance/total resistance ratio as a function of time at a transmembrane pressure of (a) 0.8 MPa, (b) 1.0 MPa and (c) 1.4 MPa using RO-HRX membrane. Temperature: 22 °C. Feed solid content: 12 wt.%.

Appendix C

Surfaces of SR3D, HRX and PEBA 1074 membranes

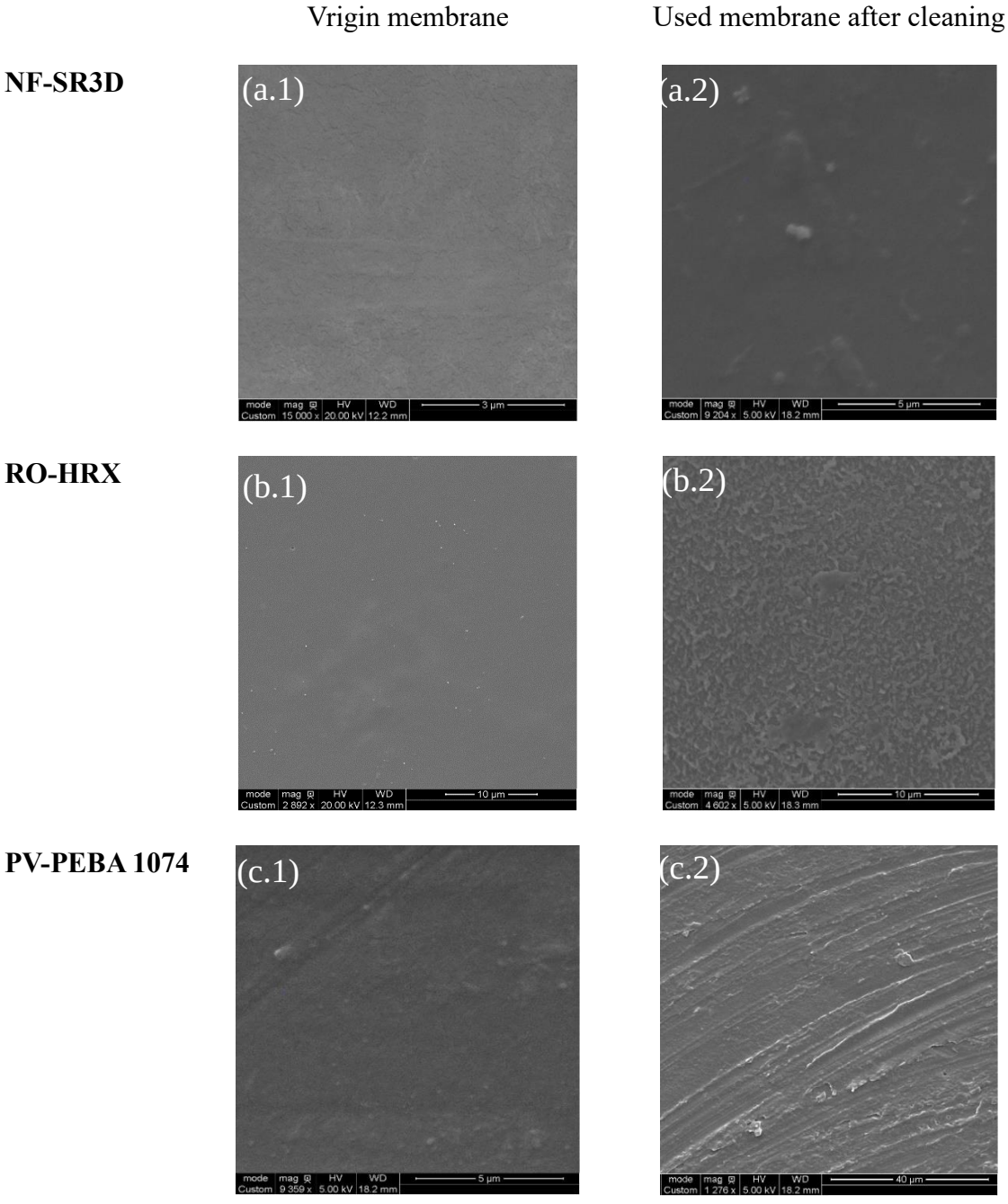

Figure C.1 SEM images of virgin membranes and used membranes after cleaning (a) SR3D membrane, (b) HRX membrane and (c) PEBA 1074. Note that the NF, RO and PV membranes had tight structure in the active membrane layer, and no visible pores could be observed under SEM.

Appendix D

Calibrations of aroma aqueous solutions by TOC

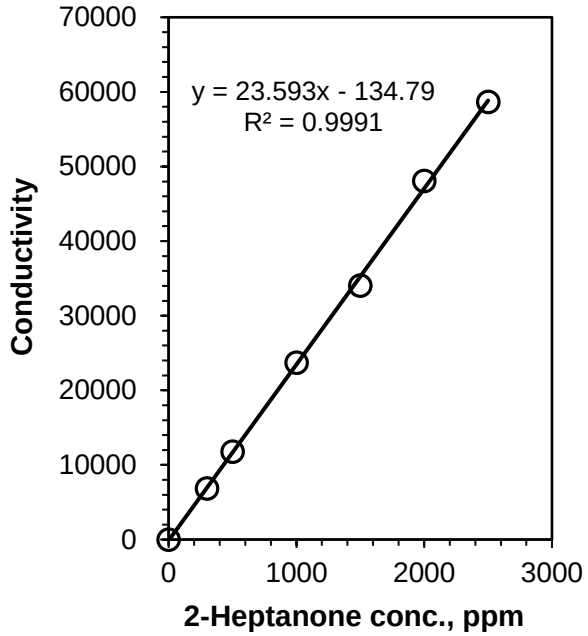

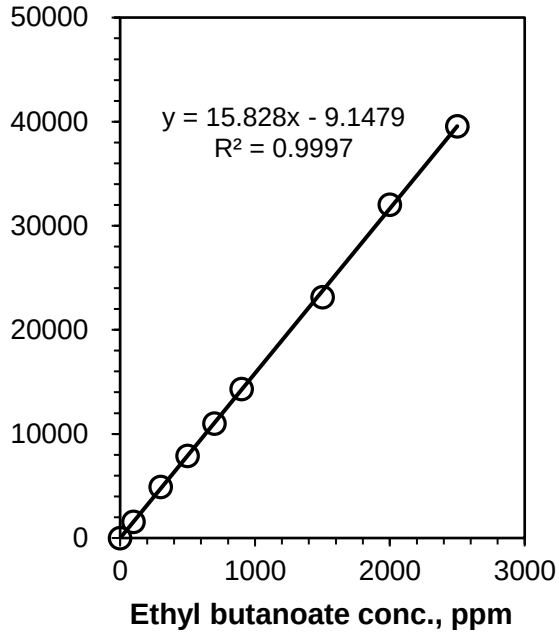

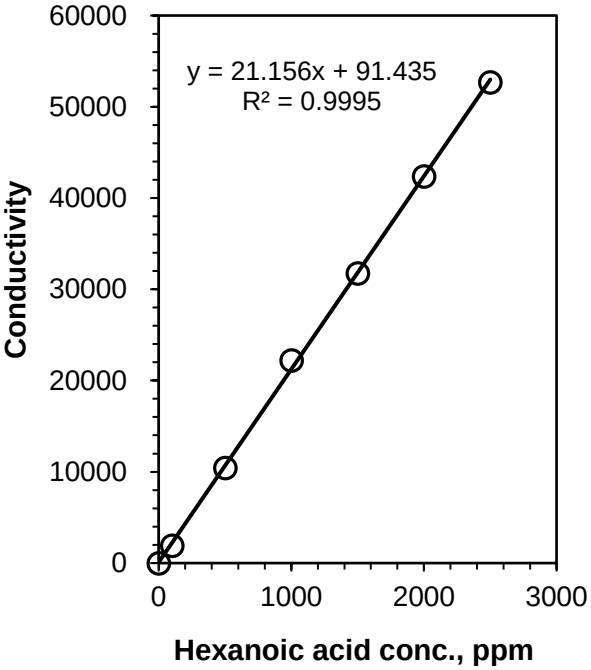

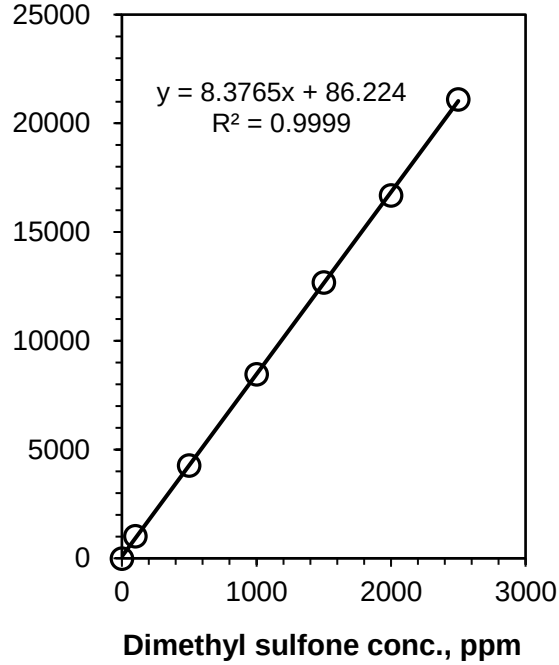

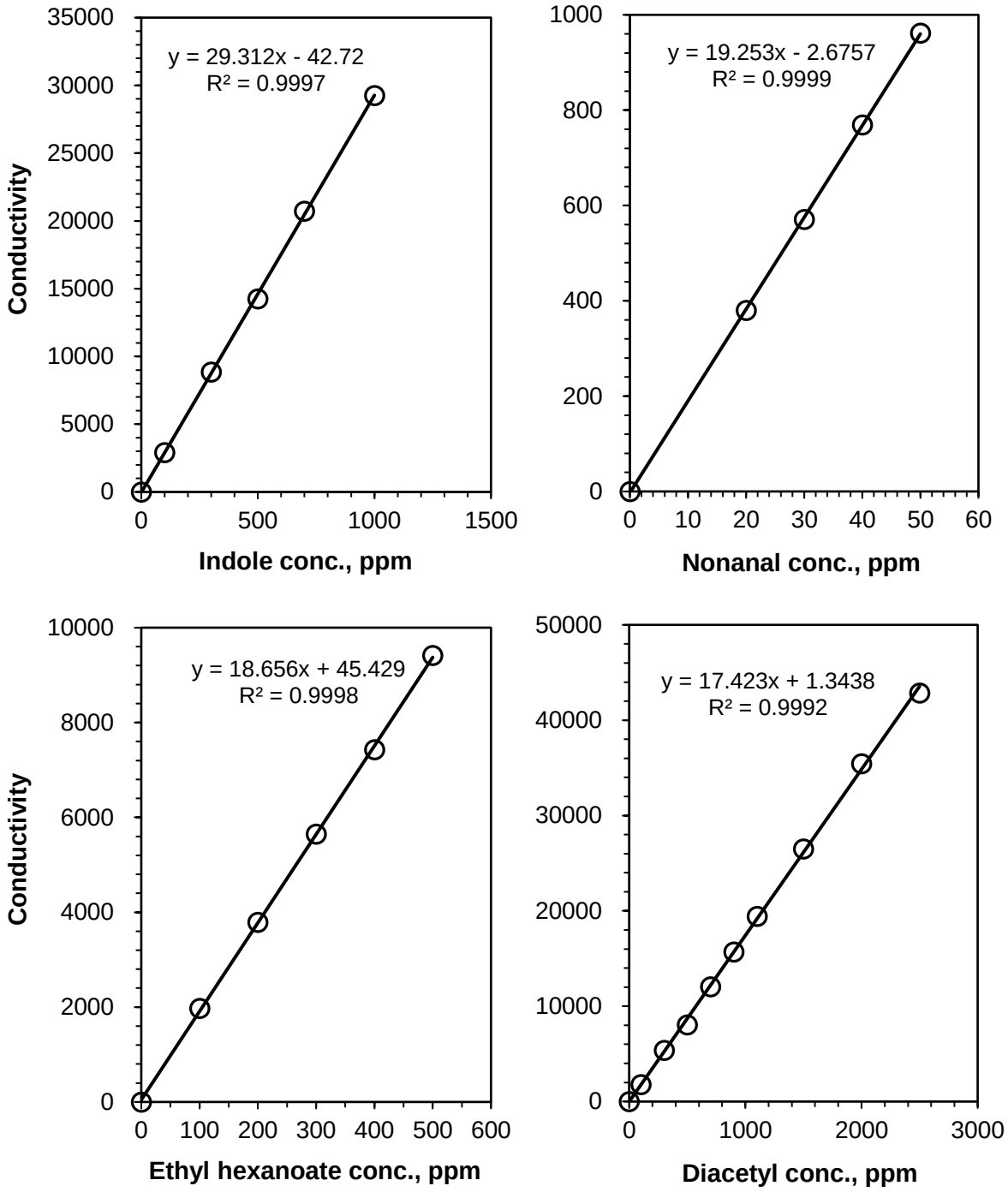

Figure D.1 Calibration of aroma standard aqueous solutions.

Appendix E

Example of calculation of experimental error

$$Experimental\ error = \frac{Standard\ deviation}{Average}$$

An example of errors in the experiments is shown in Figure E.1.

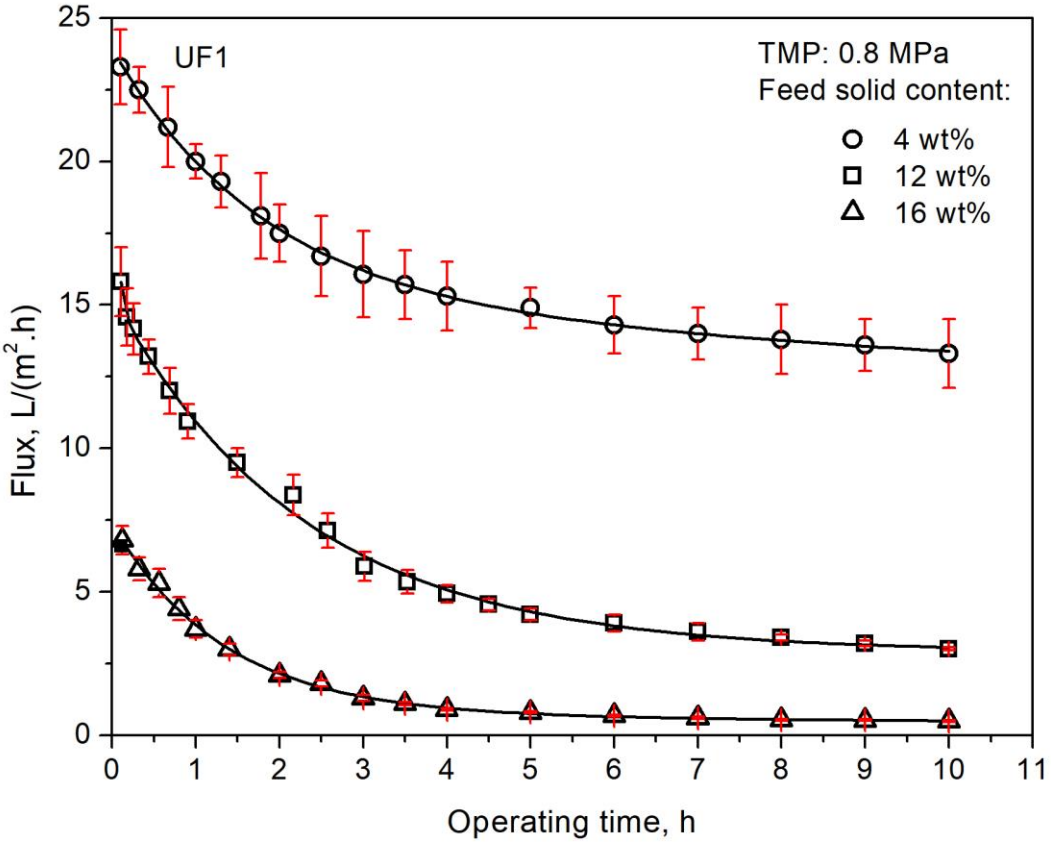

Figure E.1 Total flux during concentration of dairy solutions using UF1 membrane at different feed solid contents. TMP 0.8 MPa. Temperature 22 ˚C.